THE MECHANISM OF COBALAMIN ADENOSYLATION BY THE ENZYMES COBA AND EUTT

by

THEODORE CARLTON MOORE

(Under the Direction of Jorge C. Escalante-Semerena)

ABSTRACT

Cobalamin is an essential cofactor for many organisms across the three domains of life. Cobalamin is comprised of a central cobalt ion in an octahedral complex, ligated along the equatorial by the tetrapyrollic corrin ring. There are several biologically active varieties of cobalamin, each defined by the identities of their axial ligands. Among the most studied is adenosylcobalamin (AdoCbl, Coenzyme B_{12}), which has a lower (α) ligand of 5,6-dimethylbenzimidazole (DMB) and an upper (β) ligand of 5'-deoxyadenosine. This adenosyl ligand is used to generate a radical Ado· species for use by isomerase enzymes.

Cobalamin is only synthesized by bacteria and archaea, yet all organisms that use AdoCbl must be capable of synthesizing the α ligand. They do this through the use of ATP:Co(I)rrinoid adenosyltransferase (ACAT) enzymes, which overcome a thermodynamically difficult barrier to first reduce and then adenosylate a bound cobalamin molecule. There are three distinct ACAT families, CobA, EutT and PduO. CobA is regarded as the "housekeeping" ACAT in the model organism *Salmonella enterica*, and can catalyze adenosylation of cobalamin and several of its precursors. The first section of this work describes a structure-function analysis of a CobA crystal structure in complex with a cobalamin substrate and proposes a mechanism of action.

Of the three ACAT families, little is known about EutT. In *S. enterica*, it participates in ethanolamine catabolism. The second section of this work describes biochemical studies of homogeneous EutT. EutT appears to be unique among the ACATs in that its activity is dependent on a divalent metal cation as a cofactor, which is likely used for proper orientation of the substrate in the active site.

The third section of this work examines two proteins of unknown function in the *eut* operon, which were suspected of interacting with EutT. This hypothesis was incorrect, yet EutP and EutQ were shown to be a novel class of acetate kinase. Additionally, a phenotype was described for a *eutQ* strain of *S. enterica* growing anaerobically on ethanolamine. These data suggest that EutP and EutQ are important for substrate-level phosphorylation, cofactor recycling, carbon flux, or some combination of the three.

INDEX WORDS: Cobalamin, ATP:Co(I)rrinoid adenosyltransferases, cobalt reduction, metal cofactors, ethanolamine metabolism, acetate kinases, *Salmonella enterica*

THE MECHANISM OF COBALAMIN ADENOSYLATION BY THE ACAT ENZYMES COBA AND EUTT

by

THEODORE CARLTON MOORE

BA, The College of Wooster, 2009

A Dissertation Submitted to the Graduate Faculty of The University of Georgia in Partial Fulfillment of the Requirements for the Degree

DOCTOR OF PHILOSOPHY

ATHENS, GEORGIA

2015

THE MECHANISM OF COBALAMIN ADENOSYLATION BY THE ACAT ENZYMES COBA AND EUTT

by

THEODORE CARLTON MOORE

Major Professor:	Jorge C. Escalante-Semerena
Committee:	Michael Adams
	Harry Dailey
	Michael Johnson

Electronic Version Approved:

Suzanne Barbour
Dean of the Graduate School
The University of Georgia
August 2015

ACKNOWLEDGEMENTS

I would like to thank my committee advisors at the University of Wisconsin-Madison, Dr. Jorge C. Escalante-Semerena Dr. Ivan Rayment, Dr. Thomas Brunold, Dr. Diana Downs, and Dr. Michael Thomas for their valuable advice. Likewise, thanks to Dr. Michael Johson, Dr. Michael Adams, and Dr. Harry Dailey for serving on my committee at the University of Georgia. Special thanks to Drs. Rayment and Brunold, as well as to Dr. Sean Newmister from the Rayment lab and Ivan Pallares and Dr. Kiyoung Park from the Brunold lab for fruitful collaborations and insightful discussions. I am also grateful to Dr. Thomas and his lab for hosting me for a time between UW and UGA, and to Dr. Laura Kiessling and the CBIT program for providing financial and professional support.

I am indebted to many members of the Escalante Lab for scientific and moral support. Dr. Paola Mera was instrumental in helping to get my project off the ground. Dr. Chi-Ho Chan, Dr. Heidi Crosby, Dr. Alex Tucker, Norbert Taveres, Kristy Hentchel and Chelsey VanDrisse have been excellent resources to help with scientific problems, and great people to share a drink or a laugh with. Thanks also to the friends and colleagues I have made throughout grad school.

Lastly, I would like to acknowledge my family. My mother and father have been a great source of comfort these past several years. My soon-to-be wife, Lauren Zasadil, has been incredibly supportive, and her patience, optimism, and scientific rigor have been an inspiration to me.

TABLE OF CONTENTS

LIST OF TABLES

Page

LIST OF FIGURES

Page

CHAPTER 1

INTRODUCTION AND LITERATURE REVIEW

1.1 Corrinoids — The Magnificent Macrocycles

Corrinoids are organometallic molecules that belong to the cyclic tetrapyrrole family, which also includes hemes, chlorophylls and factor F_{430} (1). The major difference amongst the aforementioned molecules is the type of metal ion chelated in the center of the tetrapyrrole ring. Corrinoids contain cobalt, while heme has iron, chlorophyll has magnesium, and factor F_{430} has nickel. The degree of macrocycle reduction is another important distinction between the cyclic tetrapyrroles, with the corrinoids possessing six double-bonds. Additionally, corrinoids lack a carbon spanning the bridge from ring A to D, resulting in a unique puckering when compared to the square planar rings of heme and other cyclic tetrapyrroles (Figure 1.1A).

The tetrapyrrole of the corrinoids is specifically referred to as the corrin ring, referencing its position at the "core" of the structure. The corrin ring is also defined by the methyl and amide decorations bound to the pyrrole moieties (Figure 1.1A). Notably, corrinoids also possess two axial ligands, referred to as *Co*α ("lower") and *Co*β ("upper"). The chemical reactivity of corrinoids depends the identity of these ligands, as does the naming convention, both of which are expanded on below.

1.2 Complete and Incomplete Corrinoids

All corrinoids can be characterized as either complete or incomplete. The difference between the two is the presence or absence of the nucleotide loop, a structure that tethers a base

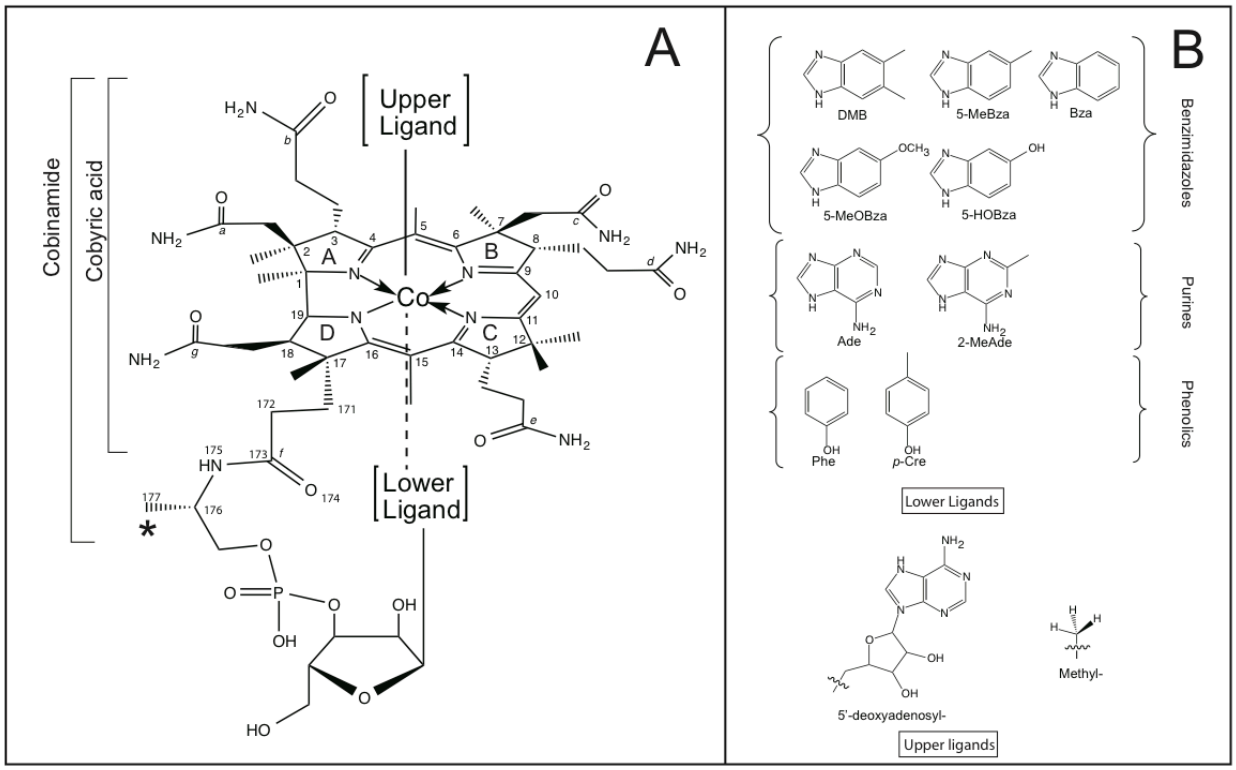

Figure 1.1. The structure of cobamides. A) General structure of a cobamide. Brackets indicate which portion of the molecule constitute the precursors cobinamide and cobyric acid. Removal of the starred methyl group results in a nor-cobamide. B) Non-exhaustive list of cobamide ligands, which determine the naming conventions of cobamides. The cobalt-carbon covalent bond is represented on upper ligands by a wavy line. Adapted from Moore and Escalante (2015, in press).

that acts as the lower ligand to the corrinoid's cobalt ion in most cases. Such complete corrinoids are also referred to as cobamides (Cba). In cases where the nucleotide base acts as a ligand, the base is a nitrogenous benzimidazole or purine derivative that contains unpaired nitrogen electrons that ligate the cobalt ion. Cobalamin (Cbl, also known as B_{12}), the most studied cobamide, contains a 5,6-dimethlybenzimidazole (DMB) lower ligand. Certain cobamides have a cyclic aromatic base, such as phenol or *para*-cresol, which is incapable of binding the cobalt ion. These phenolyl-cobamides, most notably synthesized by *Sporomusa ovata* (2,3), are "base-off," meaning that their nucleotide base is displaced from the ligand position found in a nitrogenous-base cobamide. In such base-off cobamides, a water molecule or other free nucleophile occupies the Coα position.

Incomplete corrinoids, which lack the lower nucleotide loop, are typically precursors to cobamides. As their nucleotide loop is not fully synthesized, a water molecule ligates to their cobalt ions. In addition to being part of the *de novo* synthesis pathway for cobamides, certain incomplete cobamides can be scavenged and/or remodeled by organisms lacking the *de novo* synthesis pathway, as will be discussed later in the chapter.

1.3 Cobamide Upper Ligands and Cobamide-Dependent Chemistry

While most of the diversity of cobamides is due to differences among the lower ligand, the chemical reactivity of cobamides is defined by the upper ligand. Arguably the most well-known cobamide, Vitamin B_{12} (cyanocobalamin, CNCbl), is an artifact of the industrial production process. The *Co*β position is ligated by a strong-field cyanide ion present in trace amounts on the activated charcoal used in the purification. Vitamin B_{12} is biologically inactive until the CN^- ligand can be removed *in vivo*, as discussed later in the chapter. Adenosylcobamides, exemplified by adenosylcobalamin (AdoCbl, coenzyme B_{12}), possess a

biologically-unique covalent bond between the cobalt ion and the upper ligand, 5'-deoxyadenosine. This cobalt-carbon bond can undergo homolysis to form a reduced cobamide (Co^{3+} -> Co^{2+}) and an adenosyl radical. The radical species can be harnessed by enzymes like ethanolamine-ammonia lyase and diol dehydratase to perform carbon-skeleton rearrangements by abstracting an electron from a vicinal hydrogen (Fig 1.2A,). The adenosyl radical can also be used to catalyze reductions via a thiyl intermediate, as in ribonucleotide reductase (Fig 1.2B,(4)).

In addition to the one-electron mechanism of adenosylcobamides, cobamides can also perform two-electron reactions, as in the case of the methyltransferases. Methionine synthase and other methyltransferase enzymes bind cobalamin in a "base-off, his-on" conformation, substituting a histidine residue for DMB in the lower ligand position. The bound cobalamin cofactor is in a "super reduced" state (Co^{1+}) and abstracts a methyl group off another methyl carrier, such as tetrahydrofolate or tetrahydromethanopterin, via a concerted 2-electron attack and transfers it to a substrate. This regenerates the super reduced cob(I)alamin (Fig 1.2C). Methylcobalamin (MeCbl) is often referred to as the cofactor in this reaction, it is more correct to say that cob(I)alamin is the cofactor as it is only transiently methylated in its enzyme-bound state.

A third category of reaction mechanisms is reserved for the cobamides used by organohalide reductases, although little is known about their catalytic mechanisms. Both Cob(I) and Cob(II)alamin have been shown to catalyze reductive dehalogenations in the absence of an enzyme (5-8). Because of this, it has been proposed that there may be multiple pathways for cobalamin to catalyze dehalogenations, be it by a two-electron mechanism similar to methionine synthase (9,10), or a one-electron mechanism more similar to ethanolamine ammonia lyase (11,12). These pathways are not shown in Figure 1.2 due to their undetermined nature, but are

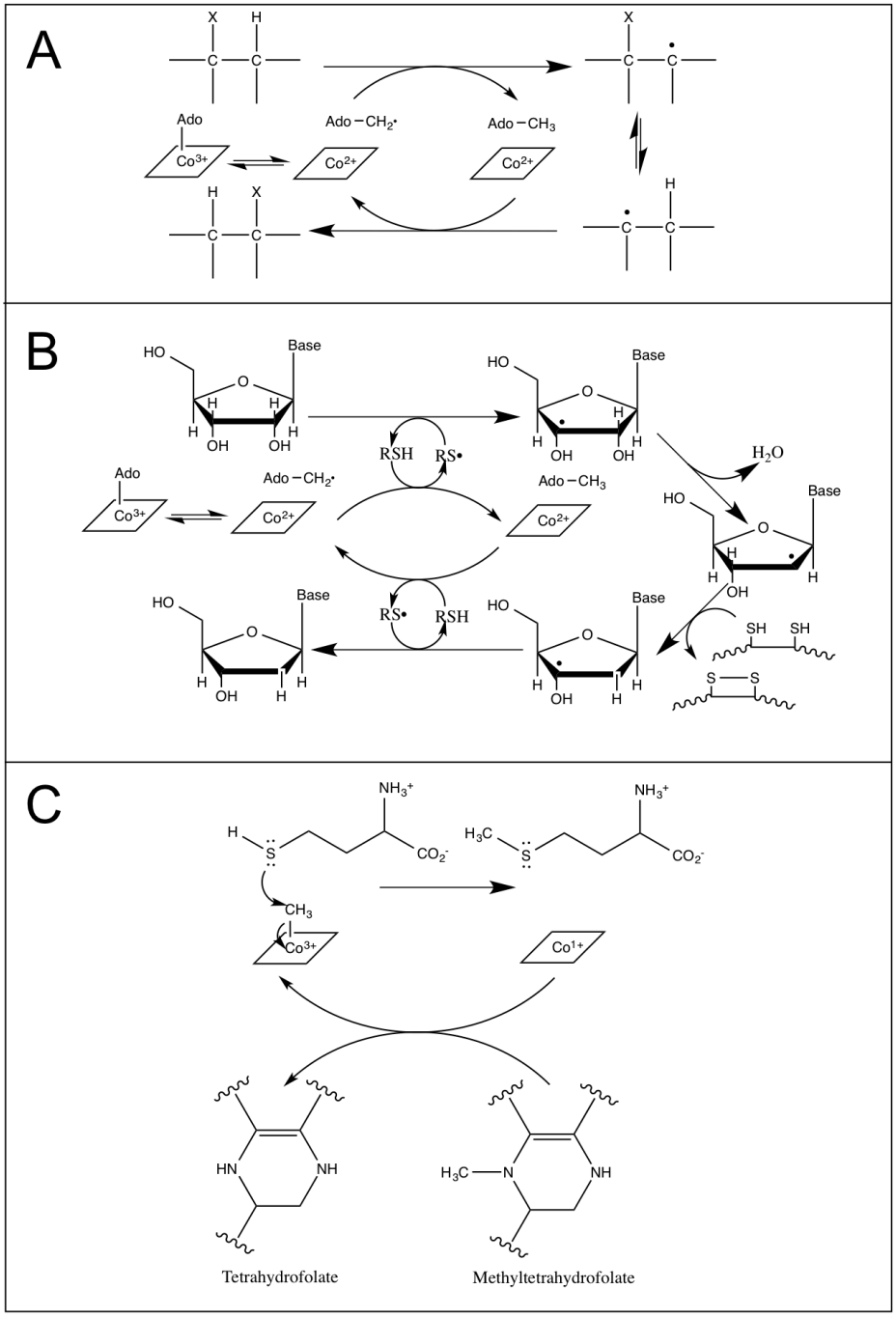

Figure 1.2. Types of cobalamin-dependent enzymatic reactions. A) AdoCbl-dependent carbon-skeleton rearrangements, examples: diol dehydratase (EC 4.2.1.28), ethanolamine-ammonia lyase (EC 4.3.1.7), methylmalonyl-CoA mutase (EC 5.4.99.2). B) AdoCbl-dependent ribonucleotide reductions (EC 1.17.4.1). C) Cobalamin-dependent methionine synthesis (EC 2.1.1.13)

reviewed in several places (13,14), and recently-solved structures of organohalide reductases may be instrumental in deciphering cobalamin-dependent dehalogenation (15,16).

1.4 Cobamide Synthesis

The synthesis of cobalamin, the most studied corrinoid, has been reviewed extensively. Such reviews cover the *de novo* synthesis of cobalamin (17-20), the corrinoid-scavenging pathways (21), and the chemical properties and synthesis of cobalamin (22-26). This collection provides an overview of our knowledge related to the construction of this complex cofactor.

De novo Cbl synthesis has only been observed in the bacteria and the archaea (27), despite an obligate need of this cofactor by many eukaryotes. Eukaryotes must obtain Cbl through diet, as humans do, or through commensal or symbiotic organisms, as in cows and algae (28,29). Some cobamide-requiring bacteria and archaea are also unable to synthesize cobamides *de novo*. These organisms typically possess a corrinoid-scavenging pathway that can import incomplete corrinoids, i.e. corrinoids lacking the nucleotide loop assembly (NLA) and lower ligand. These incomplete corrinoids can enter the later steps of cobamide synthesis and be converted to whichever cobamide the organisms requires. Many organisms that are capable of synthesizing cobamides *de novo* also maintain a corrinoid scavenging pathway, to save on the considerable energy required to synthesize the corrin ring.

1.5 Cobamide Adenosylation

All organisms that utilize adenosylcobalamin or other adenosylcorrinoids must be capable of attaching an adenosyl moiety to the β-position of the corrin ring. This is as true for organisms capable of *de-novo* synthesis and corrinoid scavenging (such as *S. enterica*) as it is for organisms dependent on exogenous cobamides (such as humans). One potential reason for this is that the Co-C bond between corrinoid and adenosine is relatively fragile, and can be

dissociated under environmental conditions by light, acidity, and reducing equivalents (30,31). As mentioned earlier in the chapter, industrial purification of cobalamin from *Propionibacterium shermanii* or *Pseudomonas denitrificans* results in CNCbl, as the cobalamin is ligated by cyanide impurities in activated-charcoal columns used for separation (32).

It has been proposed that corrinoids are reduced upon cellular import to a Co(II) state, which results in upper ligand dissociation (33). The reason for this is not entirely known, although the upper ligand of many environmental cobamides is likely to be inactive, such as in Vitamin B_{12}. Removing an inactive upper ligand is the first step towards generation of an adenosylcobamide.

The synthesis of adenosylcobalamin is dependent on reduction of the corrinoid to a Co(I) "supernucleophilic" state (34). This reduced form is capable of attacking the 5'C of ATP in a two-electron mechanism, resulting in adenosylcobalamin and triphosphate. The redox couple between Co(II)/Co(I) has a E_o' value of -610 mV (35). This exceedingly low value is beyond that of most known biological reductants in cobalamin-synthesizing organisms, including ferredoxin (-432 mV), NADH (-320 mV) and $FADH_2$ (-220 mV) (36). Therefore, an enzymatic mechanism must exist for raising the redox midpoint potential to within the range of biological reductants. The discovery of these enzymes, the ATP:Co(I)rrinoid adenosyltransferases (ACATs), is discussed in the next few sections.

1.6 CobA

The first ACAT was identified in 1990 by a genetic screen in *S. enterica*. CobA was found to be required for both *de novo* synthesis of cobalamin and scavenging of the cobalamin precursors cobinamide and cobyric acid (37). A *cobA*$^-$ variant was able to grow on adenosylated corrinoids, which led to the hypothesis that CobA could overcome the thermodynamic barrier of

Co(II)/Co(I) reduction and facilitate adenosylation. Subsequent studies characterized the biochemical properties of CobA and confirmed that it enzymatically generated adenosylcorrinoids (38-40), and could use cobyric acid, cobinamide, and cobalamin as substrates. It had the highest specificity and activity with cobinamide.

Biochemical characterization initially relied on chemically reducing the corrinoid substrate to a Co(I) state before reacting it with CobA, a process which required CobA to only bind substrate in proximity to ATP and not have to facilitate its reduction. A biological reducing system, FldA and Fpr, was identified that allowed CobA to reduce Co(II) corrinoids, presumably by accepting an electron from the FldA flavoprotein once it had bound Co(II). Generation of the Co(II) substrate from a Co(III) corrinoid was proposed to be accomplished nonenzymatically and nonspecifically by cytosolic reducing equivalents in *S. enterica* (33). However, proteins that selectively bind and reduce Co(III) corrinoids to a Co(II) state using glutathione have been identified in several organisms, including *B. melitensis* and humans (41,42). These proteins are thought to mediate direct delivery of Co(II) corrinoid to their corresponding ACATs.

An initial crystal structure of CobA was published in 2002 (Fig 1.3, (43)). The homodimeric structure crystallized with hydroxycobalamin and MgATP, the latter binding in a unique, inverted P-loop structure. It was presumed that the ATP would be bound very near cobalamin, since cob(I)alamin is very reactive and could easily be quenched by water molecules or a stray side chain if not positioned to attack ATP. However, the hydroxycobalamin appeared to bind CobA very far from where MgATP was bound, >6 Å from Co(III) to the 5' C of ribose. This is beyond the range of nucleophilic attack. Additionally, hydroxycobalamin is a

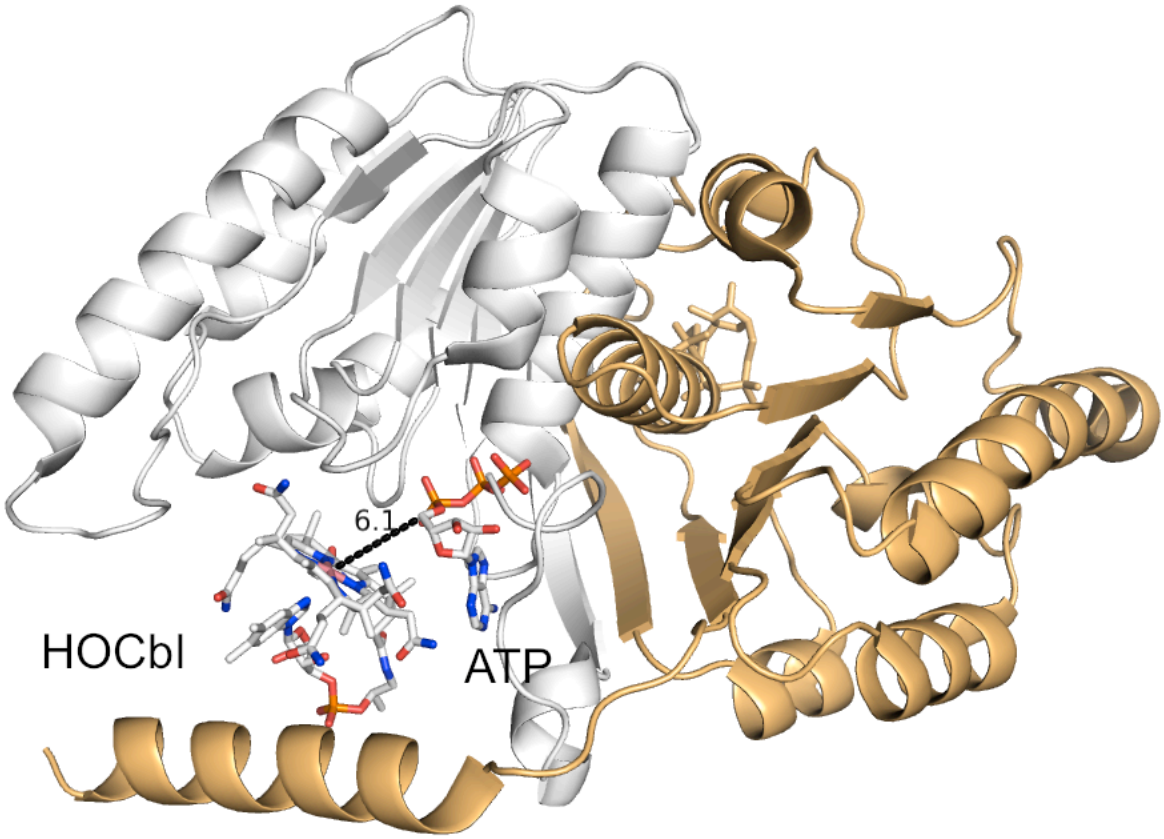

Figure 1.3. The crystal structure of *S. enterica* CobA in complex with MgATP and HOCbl. The cosubstrates are bound in the active site of the monomer colored in white. Distance between the cobalt center of HOCbl and the 5'C of ATP is labeled by the black dotted line. PDB: 1G64.

Co(III)corrinoid, which CobA is incapable of adenosylating. Therefore it was assumed that this corrinoid was forced into the active site in a non-natural conformation.

Subsequent biochemical characterization of CobA determined that it had broad specificity for its nucleotide substrate, capable of using ATP, inosine triphosphate, cytosine triphosphate, uridine triphosphate and guanosine triphosphate (40). Additionally, CobA requires the 2'-OH group of the nucleotide triphosphate (NTP) to catalyze the reaction, and it was proposed that this hydroxyl was important for positioning of the NTP. In contrast to many ATPases, CobA attacks the 5' carbon of ATP and releases triphosphate (PPP_i) as a product. The inverted p-loop of the CobA crystral structure, which results in ATP bound in a reversed orientation compared to regular p-loop enzymes, was proposed to help facilitate attack on the 5' carbon. Interestingly, PPP_i was not cleaved to orthophosphate and diphosphate in the CobA reaction, which is unique among the few enzymes that cleave between the α-phosphate and 5'C of ATP.

Based on the crystal structure, computer modeling was used to generate a co-structure of CobA and FldA, and important arginine residues were identified at the interface (44). Variation of these residues to alanines resulted in a CobA incapable of reducing Co(II) to Co(I). However, this variant CobA could still generate adenosylcorrinoid from chemically-reduced Co(I) substrates, thus supporting the importance of these residues in facilitating electron transfer to the substrate.

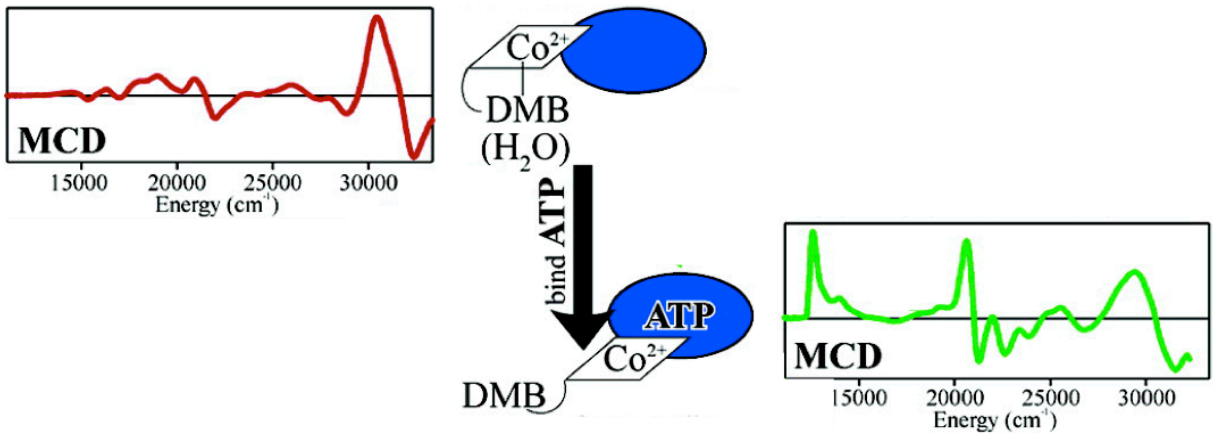

Figure 1.4. 4-coordinate and 5-coordinate cobamides. Typical MCD spectrum of 4c and 5c corrinoids (adapted from Stitch et al., 2004)

1.7 The Four-Coordinate (4c) Corrinoid Intermediate

The mechanism by which ACATs overcame the thermodynamic barrier to Co(I) reduction was solved using spectroscopic methods (45). Using magnetic circular dichroism (MCD) spectroscopy, Stich and coworkers were able to monitor transition energy changes in the ligand field of a Co(II) corrinoid substrate upon binding CobA. Upon binding to CobA, Co(II) corrinoids undergo conversion to a unique paramagnetic species, easily visualized on an MCD spectrum (Fig 1.4). Using electron paramagnetic resonance (EPR) and density functional theory (DFT) calculations as complimentary techniques, this unique species was interpreted as being essentially 4c, with the lower DMB ligand removed from its position coordinating the cobalt ion. The 4c corrinoid form was interpreted as having a more stabilized cobalt $3d_z^2$ molecular orbital (MO) when compared to its five-coordinate (5c) analog The $3d_z^2$ orbital contains the redox-active electron in Co(II) corrinoids, and this MO stabilization was determined to be the mechanism by which CobA effectively lowers the thermodynamic barrier to Co(I) reduction.

The MCD techniques described above provided a technique that is uniquely suited to assessing the functionality of ACATs. 4c corrinoid signals are easily distinguishable from 5c signals, and the amount of 4c corrinoid can be quantified. MCD, when coupled with biochemical assays, allows us to determine whether the lack of activity in an ACAT variant is due to difficulties in generating the 4c intermediate. This technique has been employed in many major ACAT studies since its initial discovery (46-52).

1.8 Other ACAT Families

1.8.1 PduO

In addition to the CobA adenosyltransferase, two other ACAT families exist: PduO and EutT. PduO is named after its role in *Salmonella*, where it is part of the *pdu* operon that is

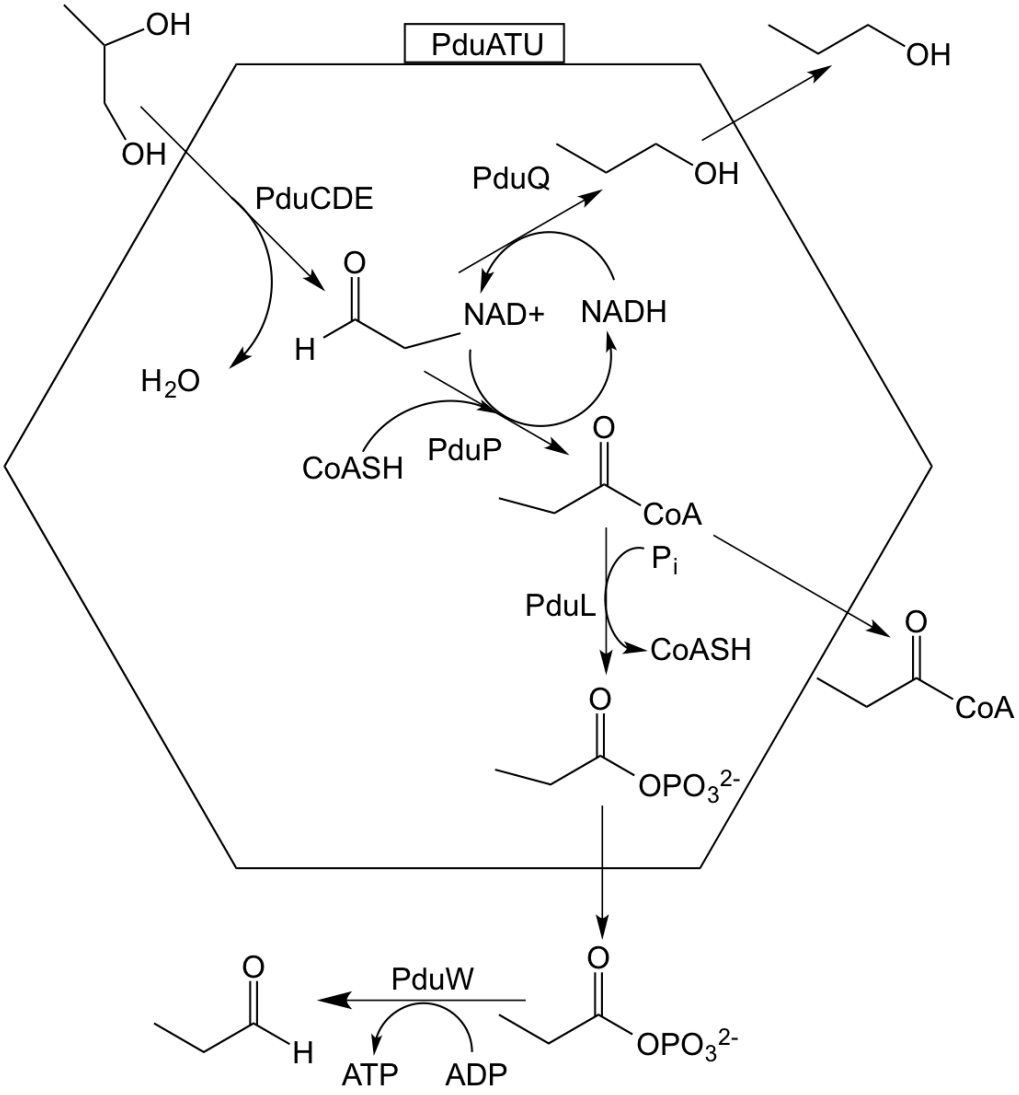

Figure 1.5. The propanediol metabolosome. The pathway of propanediol catabolism as a source of carbon and energy.

responsible for 1,2-propanediol (1,2-PD) catabolism. 1,2-PD degradation is a cobalamin-dependent process, in which diol dehydratase (PduCD) catalyzes the dehydration of 1,2-propanediol to propionaldehyde (53). The catabolism of propionaldehyde is contained within a ~100 nm proteinaceous organelle, also called a metabolosome or bacterial microcompartment (BMC) (Fig 1.5)(54,55). The purpose of this metabolosome is to contain and concentrate the volatile, toxic propionaldehyde intermediate. Propionaldehyde is converted to propionyl-CoA and propionyl-phosphate by additional Pdu proteins downstream of the PduCD reaction.

pduO is required for aerobic growth of *S. enterica* on 1,2-PD when Cbl is supplied, but a Δ*pduO* strain can grow when provided AdoCbl (56,57). PduO is not homologous to CobA, yet both are capable of generating the 4c corrinoid intermediate critical to adenosylation (47). A cobalamin-specific reductase, PduS, was identified as providing Co(II) corrinoid substrate to PduO (58-60). Some publications have speculated that PduS can generate a Co(I) corrinoid substrate, but this view is contentious as no 4c MCD spectra have been detected in a PduS-corrinoid complex. One of the shell proteins of the BMC, PduT, was shown to have an iron-sulfur center transversing its central axis. This iron-sulfur center has been proposed to be capable of shuttling electrons from the cytoplasm to the BMC lumen, where they could specifically be used by PduS or PduO to reduce Co(III) to Co(II) or Co(II) to Co(I), respectively.

The reason the *pdu* operon contains a specialized ACAT is thought to be due both to the isolation of PduCD from the cytoplasm, and the relatively high error rate of that enzyme. PduCD undergoes irreversible suicide inhibition via occasional side reactions with glycerol or oxygen, which results in a nonfunctional alkylated or hydroxylated cobalamin complex (54,61). The PduGH reactivation factor removes this suicide inhibitor in an ATP-dependent mechanism, and PduS/PduO supply a new AdoCbl cofactor. The PduO-dependent recycling mechanism is

the most efficient way to supply AdoCbl cofactor to PduCD, as it avoids transporting the bulky AdoCbl cofactor through the metabolosome shell. However, this latter mechanism does occur *in vivo* as a Δ*pduO* strain can still grow on 1,2-PD if exogenous AdoCbl is added.

PduO is one of the most widely-distributed ACATs, appearing both alone and in conjunction with the *pdu* BMC. Interestingly, humans use a PduO homolog, hATR, to catalyze AdoCbl needed for methylmalonyl-CoA mutase, the only AdoCbl-dependent enzyme in our species (62,63). Some organisms, such as *Lactobacillus reuteri*, appear to use it in place of CobA, as the ACAT involved in *de novo* cobalamin synthesis. The *L. reuteri* PduO was successfully purified and crystallized, as solubility issues precluded similar studies of *S. enterica* PduO (64,65). The resulting structure, a trimer of alpha-helix bundles co-crystallized with MgATP and Co(II)Cbl, differed significantly from the dimeric, alpha/beta-structured CobA. Whereas the ATP of CobA was bound in a reverse P-loop motif, MgATP in PduO was not bound by a specific motif but by a network of backbone oxygens and nitrogens. Additionally, the active site was located in a deep cleft between the PduO subunits, as opposed to CobA in which the active site was cupped centrally in each monomer.

Remarkably, the PduO structure co-crystallized with Co(II)Cbl in the 4c intermediate state. This was accomplished by providing the crystallization solution for *Lr*PduO with a biological reductant capable of reducing Co(III)Cbl to Co(II)Cbl, but incapable of interacting with *Lr*PduO. This resulted in the arrest of the catalytic cycle of PduO after substrate binding, and the capture of 4c Co(II)Cbl. Notably, an aromatic residue, F112, displaced the nucleotide tail of the 4c Cbl (Fig 1.6). F112 occupied the location that is normally occupied by the DMB lower ligand in in 5c Cbl. The use of a hydrophobic, aromatic residue to displace DMB was

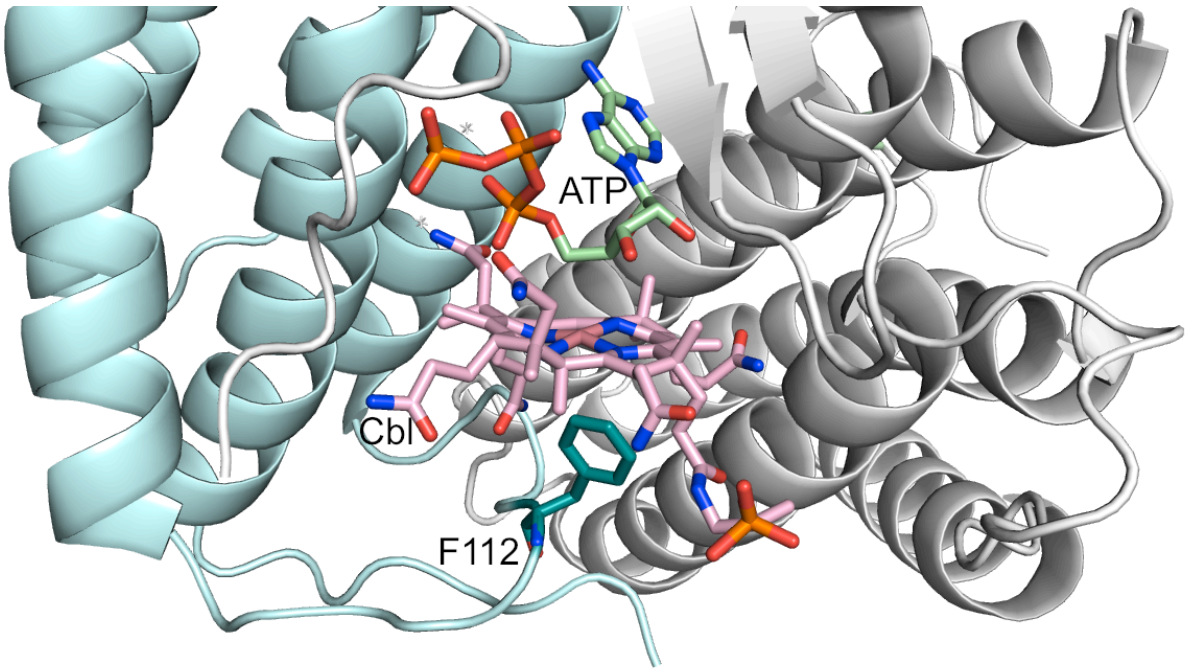

Figure 1.6. The active site of *Lr*PduO. Zoomed-in view of the PduO active site cleft between two of the three subunits. ATP is colored green, Cbl is colored pink, and the Phe112 residue is colored blue. The DMB group of Cbl is not visualized due to to the nucleotide tail being swung into solution. PDB: 3CI1

theorized to be significant, as the large-size and hydrophobic nature could repel ligands attached to the Co(II) ion (66). Those same physical properties could also prevent the residue from ligating to the Co(II) ion itself. This was tested by a series of PduO variants at the 112th position. F112A was incapable of forming 4c Cbl as shown by crystallography and spectroscopy, as expected since it lacked a residue of sufficient size and/or hydrophobicity to displace DMB. A F112H variant emphasized the importance of the hydrophobicity in addition to the bulk of the residue. Although F112H was capable of displacing the DMB lower ligand from Cbl, the residue ligated to the Co(II) ion itself via unpaired nitrogen electrons on its imidazole moiety (50,66). In chapter 2 of this document, I examine a crystal structure of CobA to determine if the active site adopts a similar conformation as PduO to make 4c Cbl.

The combination of data from CobA and PduO studies informed a general scheme for ACAT mechanisms (Fig. 1.7). Upon binding ATP and 5c Co(II) corrinoid, the ACAT displaces the lower ligand of the corrinoid to form a 4c intermediate. This intermediate, shielded from side reactions in the ACAT active site, is positioned close to the 5' C of the ATP cosubstrate. The ACAT accepts an electron from an external source, such as reduced FldA, and uses it to generate a 4c Co(I) corrinoid. The reduced Co(I) corrinoid attacks the ATP cosubstrate which results in an adenosylated Co(III) corrinoid. The Ado corrinoid is subsequently released into solution or to a recipient protein.

1.8.2 EutT

EutT is analogous to PduO, but the two enzymes are not homologous. Both are specialized ACATs in *S. enterica*, and both act within BMCs. Whereas much has been published on the biochemistry of PduO, relatively little is known about how EutT catalyzes its reaction. EutT is named after its role in *S. enterica*, and as part of the 17-gene *eut* operon it participates in

the catabolism of ethanolamine, a substrate that *S. enterica* can use as a carbon, nitrogen, and energy source (67,68). Expression of the *eut* operon results in the formation of a proteinaceous microcompartment similar to the *pdu* BMC, although there are morphological differences between the two (55,69). The *eut* BMC contains and conserves the toxic aldehyde intermediate resulting from the removal of ammonia from ethanolamine. Ethanolamine-ammonia lyase, EutBC, is cobalamin-dependent, like the analogous PduCD (70-72). Aldehyde can be turned into acetyl-CoA, acetyl-phosphate or ethanol by other enzymes from the *eut* operon (Fig. 1.8)(73).

A genetic screen in a *cobA*$^-$ strain suggested the presence of an ethanolamine-specific adenosyltransferase. Mutant strains compensated for the loss of *cobA* by upregulating the *eut* BMC, suggesting that an alternative ACAT was contained therein (74). *eutT* had previously be proposed to fulfill this role, based on its co-occurrence with EutBC in several organisms (75). A *eutT*$^-$ *cobA*$^-$ strain could not grow on ethanolamine without exogenous AdoCbl. Interestingly, either *eutT* or *cobA* could complement this phenotype if nonadenosylated Cbl is provided. Additionally, a *eutT*$^-$ strain in a *cobA*$^+$ background grows with only a slight defect under standard laboratory conditions (74). The reason for this apparent redundancy has yet to be elucidated.

One of the major differences between the physiology of *eut* and *pdu* is that there is no system in the *eut* operon analogous to the PduS cobalamin reductase and the PduT Fe-S containing shell protein. Without an apparent source of electrons with which to reduce its substrate, the ACAT mechanism of EutT has been subject to much debate. Initial enrichment of EutT from cell lysate resulted in ACAT activity that was labile to both oxygen and iron-specific chelators (74). These data, coupled with the presence of a conserved cysteine and histidine-rich motif, indicated that ferrous iron could be directly involved in the EutT reaction, potentially as an electron shuttle. This hypothesis is examined in Chapter 3 of this document.

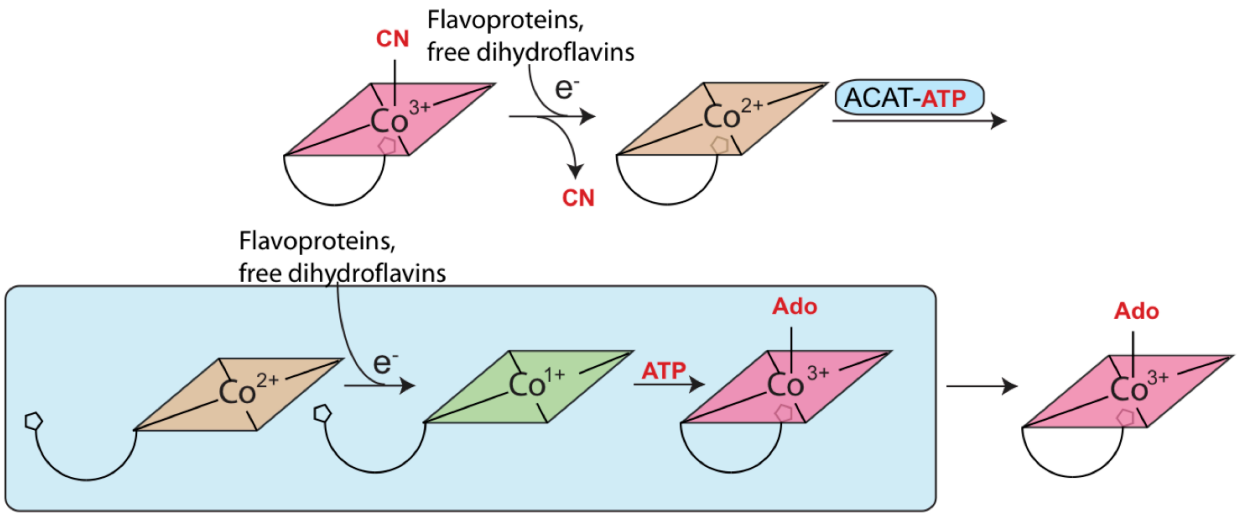

Figure 1.7. General mechanism for ACAT enzymes. Scheme describing the adenosylation of corrinoids with relation to the coordination number and oxidation state of the organometallic substrate. The corrin ring is represented by a parallelogram, and the nucleotide loop containing the lower base is represented by a curved line with a pentagon. The ACAT is represented by a by the blue box, and the ACAT-catalyzed steps of the reaction occurs within the box. Note that while this scheme depicts a complete cobamide, ACATs can also use incomplete cobamides. In the latter, case, the nucleotide loop would be replaced with a water molecule.

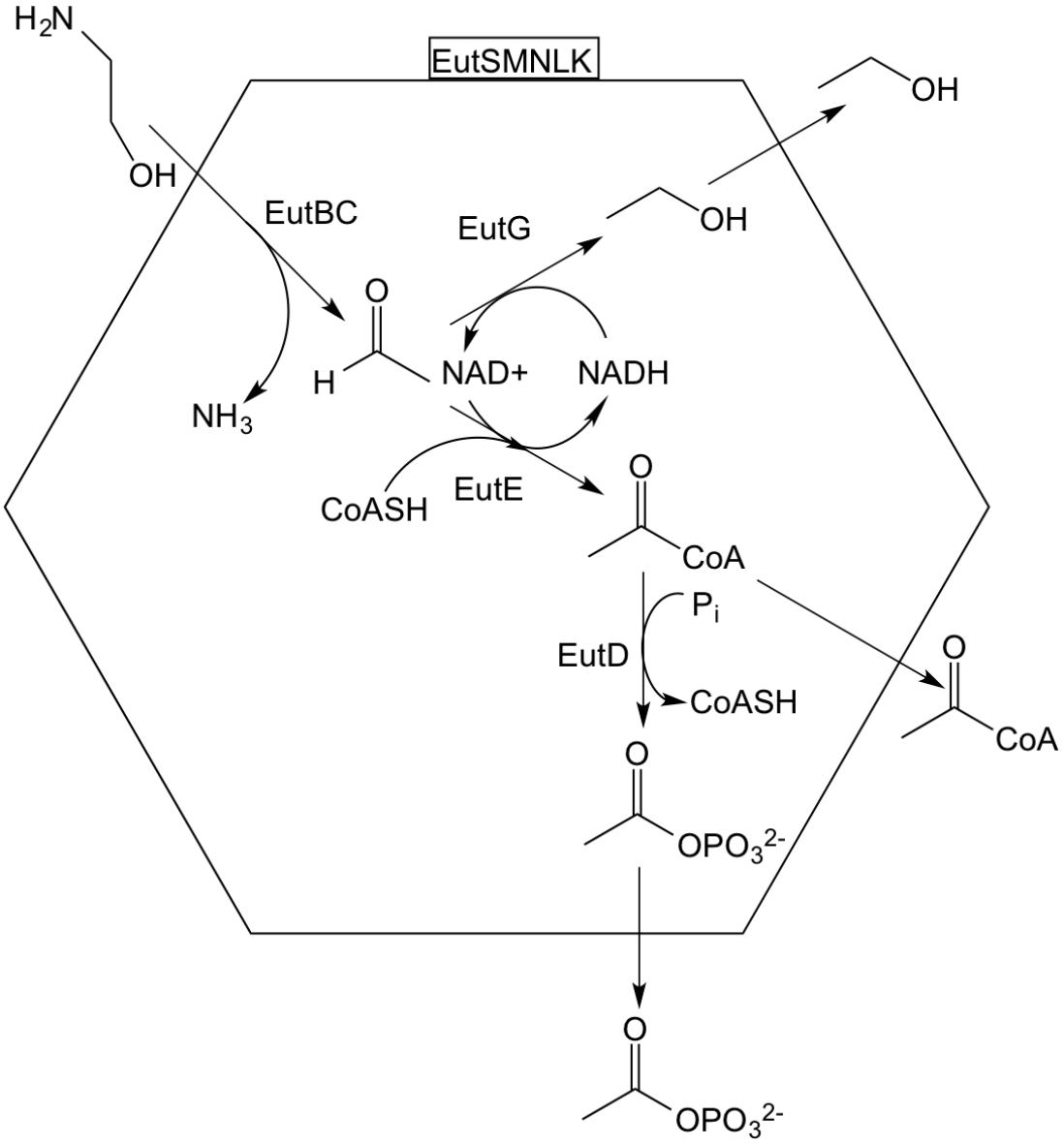

Figure 1.8. The ethanolamine metabolosome. The pathway of ethanolamine catabolism as a source of carbon, nitrogen and energy. The metabolite output shown here is likely transported through selectively permeable shell proteins (80).

MCD spectra (76) indicated that EutT generates 4c corrinoids, similar to CobA and PduO. Very little is known about how EutT generates 4c corrinoids, as no crystal structure exists. More in-depth spectroscopic studies have been hampered by the absence of a protocol to purify homogeneous EutT, the previous biochemical studies being performed with cell lysate (74) and detergent-enriched EutT from cell lysate (77). Biochemical characterization of homogenous EutT is addressed in Chapter 3, and is an important first step for in-depth study of EutT and its substrates by MCD and electron paramagnetic resonance (EPR) (I. Pallares et al., manuscript in preparation).

1.9 Unanswered Questions in Ethanolamine Metabolism

Ethanolamine catabolism, specifically in *S. enterica*, is of great interest to researchers beyond its relevance in AdoCbl synthesis. Biotechnologists in particular have been attempting to understand the assembly of the metabolosome. The overall goal of these studies is to encapsulate industrially-relevant reactions within a modified BMC. The BMC could serve to enhance the efficiency of these reactions, by either concentrating the reagents or sequestering toxic products. A N-terminal peptide on several proteins in the *eut* and *pdu* systems was proposed by Fan et al. to be a signal peptide for targeting to the BMC lumen (78). Fusion of this peptide to recombinant proteins allows the protein to be translocated into the BMC lumen. This effect is especially clear when fusing the signal peptide to green fluoresecent protein (78). This strategy could potentially be used to encapsulate entire reactions into a BMC.

Despite this advance in understanding protein transport into the BMC, most *eut* proteins do not contain the signal peptide, and the mechanism of translocation is also unclear (79). Recent publications have shown that pores in certain shell proteins comprising the BMC are selectively permeable to substrates such as ethanolamine . However, these pores are too small to

allow proteins to pass through, and thus it is likely that transport of protein to the lumen may happen prior to the full assembly of the metabolosome (80,81).

In addition to potential biotechnology applications, the *eut* BMC has recently been recognized as a virulence factor in *S. enterica*. Ethanolamine is a plentiful carbon and nitrogen source in mammalian intestines, as it is a breakdown product of phosphatidylethanolamine, a phospholipid commonly found in eukaryotic membranes. However, the gut environment is essentially anoxic, and under these conditions *S. enterica* cannot respire ethanolamine to generate ATP. Alternative electron acceptors were tested, including fumarate, dimethylsulfoxide, and trimethylamine, but only one, tetrathionate, supported *S. enterica* growth on ethanolamine under anoxic conditions (82). The significance of this electron acceptor was elucidated recently by studying *S. enterica* in a mouse model system (83). Their studies showed that virulent *S. enterica* induce intestinal inflammation via type-three secretion systems, triggering an immune response by phagocytes. The macrophages release oxidants into the gut, which oxidize ambient hydrogen sulfide to tetrathionate (84). Respiration of the tetrathionate allows the virulent *S. enterica* to utilize an energy source unavailable to its microbial competitors. Knocking out the tetrathionate reductase system in *S. enterica* resulted in cells that no longer were able to utilize ethanolamine, and therefore did not thrive in the gut environment of mice models.

As evident in figure 1.8, most of the pathways in the *eut* system have a defined role. However, our picture of this system is not complete. There are three genes of unknown function, *eutJ, eutP,* and *eutQ*. There have been no published phenotypes for these genes, although slight inferences can be made from their homology to other proteins. EutJ is homologous to the chaperone DnaK. It is unknown how *eut* proteins without the N-terminal localization tag enter

the BMC, a chaperone-mediated entry that could "grab" a tagged protein and an untagged protein could be one way to facilitate transport. DnaK contains two domains, a nucleotide-binding, N-terminal regulatory domain and a substrate-binding C-terminal domain, the latter being responsible for binding and stabilizing unfolded protein. However, EutJ is approximately one-half the size of DnaK, and is homologous only to the regulatory N-terminal domain. This apparently excludes the possibility that EutJ can act as a chaperone, at least without help from another undefined partner.

There is less known about EutQ and EutP than EutJ. EutP has a Ras-like NTP-binding domain, and there is no further published information on this protein. Multiple crystal structures exist for EutQ (2PYT, 4AXO). EutQ belongs to the cupin superfamily of proteins, a diverse group named after the characteristic beta-barrel fold formed at the core of the cupin domin (85). Cupins can range from carbohydrate-binding isomerases to flavonoid-binding diooxygenases to nuclear factors regulating apoptosis (86-88). Therefore, assigning a function to EutQ based on structure alone is very difficult. The majority of cupins are metal-binding proteins, with 18 out of 22 cupin structures co-crystallizing with a metal ion. The consensus metal-binding motif in cupins involves two or three histidine and one glutamate residue (85). However, the EutQ family does not have these metal-binding ligands, with hydrophobic residues occupying the position of the metal-binding motif. There are two acidic residues, Glu 172 and Asp 175 (numbering in *S. enterica* EutQ) in place of the metal-binding motif at the bottom of a negatively-charged cleft proposed to be the active site. These residues could potentially interact with a small substrate that could fit into this active site (89).

There are several putative functions for EutP and EutQ. One such role could be as a cobalamin chaperone. Certain systems, such as methylmalonyl-CoA mutase (MMCM) in

Methylobacterium extorquens use a GTP-binding chaperone called MeaB to control the transfer of AdoCbl from the ACAT to MMCM (90,91). MeaB accomplishes this by binding to MMCM and opening the cobalamin-binding domain in a GTP-dependent manner, allowing MMCM to accept a cofactor. As EutP is predicted to bind a NTP, it is possible that it might fulfill such a role with respect to EutBC and EutT. A recent structure of *Clostridium dificile* EutQ modeled an acetate ion into the active site, to provide a size scale. The choice of ion was probably due to the fact that EutQ was crystallized in the presence of acetate. However, the paper may have touched upon one potential role for EutQ. The *pdu* system contains a propionate kinase, PduW, but no such homolog exists in *eut* (92). As EutD generates acetyl-phosphate, an acetyl kinase in the metabolosome could serve to enhance ATP production via substrate-level phosphorylation or to aid recycling of CoA by increasing flux through EutD. Unfortunately, no evidence for these pathways exists, beyond the observation that acetate can fit in the putative EutQ active site.

1.10 Summary

Although cobalamin metabolism has been studied for decades, significant gaps in our understanding remain, specifically with regard to the role and mechanism of ACATs. It is understood that ACATS must generate a 4c corrinoid intermediate in order to overcome the thermodynamically-difficult reduction of Co(II) to Co(I). Out of the three distinct ACAT families, we only have a thorough understanding of how PduO catalyzes the 4c formation. It is unknown if the other two ACATs, CobA and EutT, use a similar mechanism, or as their lack of homology might suggest, use a novel method to generate 4c.

The EutT ACAT is particularly intriguing, as early biochemical work indicates that it is reliant on a metallic cofactor, most likely iron (77). This makes EutT unique among all known ACATs. However, the nature of this metallic cofactor is unknown. Several examples in the

literature exist for mononuclear nonheme iron facilitating electron transfer. As EutT catalyzes a one-electron reduction of its substrate, this is an attractive hypothesis. It is also possible that this ion is playing a structural role, or perhaps it is helping to position the substrate in the active site. The need for the EutT cofactor within the context of ethanolamine catabolism is also unknown; whether or not the cofactor is needed for interaction with other *eut* proteins or is an evolutionary holdover from an earlier form of EutT.

Aside from the role of EutT within the *eut* BMC, there are several other mysteries related to ethanolamine metabolism. EutP, Q and J all are proteins of unknown function. EutJ is homologous to the chaperone DnaK, but does not have homology to the DnaK domain that binds unfolded protein. EutP is a predicted NTP-binding protein and EutQ is a cupin hypothesized to be capable of binding small substrates. EutP and/or EutQ could be involved in an NTP-dependent reaction, such as mediated transfer of AdoCbl to EutBC, or possess acetate kinase activity.

1.11 Dissertation Outline

The work presented in this thesis focuses on the mechanisms of the CobA and EutT ACATs in *S. enterica*, as well as a study of a protein involved in ethanolamine metabolism, EutQ. Previous studies have determined that ACATs generate Co(I) corrinoids via a planar, 4c intermediate, which is positioned in close proximity to ATP to facilitate adenosylation. However, little is known about how CobA and EutT generate this critical intermediate. This work identifies the mechanism by which CobA catalyzes cobalamin adenosylation via the 4c intermediate, and identifies a metallic cofactor in EutT that is required for activity. Additionally, I discuss some work with EutQ, another protein in the ethanolamine operon that I have identified as having acetate kinase activity, which might potentially generate a source of ATP for EutT.

In Chapter 2, I describe the mechanism by which *S. enterica* CobA generates 4c cob(II)alamin. Crystallography with MgATP and cob(II)alamin allowed us to visualize CobA binding both 4c and 5c cobalamin. By comparing the differences in the active sites, we were able to identify two hydrophobic, aromatic amino acids that were responsible for displacing the lower ligand of cobalamin and generating the 4c intermediate. The function of these residues was verified by site-directed mutagenesis. This work highlighted interesting differences and similarities to the nonhomologous PduO. Although they both use hydrophobic amino acids to displace the lower ligand, their active sites are structured very differently, indicating that their mechanisms are instances of convergent evolution.

Chapter 3 discusses the purification of *S. enterica* EutT and the subsequent identification of its metallic cofactor. This is the first known case of an ACAT being dependent on a cofactor. Oddly, the cofactor, which is assumed to be ferrous iron *in vivo*, is not used for electron transfer as non-redox divalent cations like zinc can be substituted with little effect on activity. Neither is the cofactor used in a major structural role, as the circular dichroism (CD) spectrum of Apo EutT is the same as Holo EutT. This work also identifies the binding site for this cofactor, and describes effects of different metal cations on EutT activity *in vivo* and *in vitro*. The techniques and information on the metal cofactor provide important groundwork for EutT crystallography and mechanism studies.

Chapter 4 describes unpublished work I have begun on EutQ, the putative acetate kinase of the ethanolamine system. I show that EutQ has acetate kinase activity under *in vitro* conditions. I also describe a complementable *eutQ* phenotype when growing anaerobically on ethanolamine and tetrathionate, which is also complementable by other acetate kinases. A *eutQ*$^-$ strain also excretes less acetate than wild-type, a trait similar to a strain lacking *ack*, the

housekeeping acetate kinase. I discuss some potential reasons why an acetate kinase might be transcribed from the *eut* operon, including recycling of Coenzyme A, increase substrate-level phosphorylation, and generation of ATP for use as a substrate by EutT and EutA.

In Chapter 5, I provide some concluding remarks and some ideas for future work on the CobA, EutT and EutQ projects. The appendix is a review on cobalamin synthesis and community use by organohalide-respiring organisms.

1.12 References

1. Battersby, A. R. (2000) Tetrapyrroles: the pigments of life. *Nat. Prod. Rep.* **17**, 507-526.

2. Stupperich, E., Eisinger, H. J., and Kräutler, B. (1989) Identification of phenolyl cobamide from the homoacetogenic bacterium *Sporomusa ovata*. *Eur. J. Biochem.* **186**, 657-661.

3. Stupperich, E., and Eisinger, H. J. (1989) Biosynthesis of *para*-cresolyl cobamide in *Sporomusa ovata*. *Arch. Microbiol.* **151**, 372-377.

4. Licht, S., Gerfen, G. J., and Stubbe, J. (1996) Thiyl radicals in ribonucleotide reductases. *Science* **271**, 477-481.

5. Krone, U. E., Thauer, R. K., and Hogenkamp, H. P. C. (1989) Reductive dehalogenation of chlorinated C1-hydrocarbons mediated by corrinoids. *Biochemistry* **28**, 4908-4914.

6. Krone, U. E., Thauer, R. K., Hogenkamp, H. P. C., and Steinbach, K. (1991) Reductive formation of carbon monoxide from carbon tetrachloride and FREONS 11, 12, and 13 catalyzed by corrinoids. *Biochemistry* **30**, 2713-2719.

7. Gantzer, C. J., and Wackett, L. P. (1991) Reductive dechlorination catalyzed by bacterial transition-metal coenzymes. *Environmental science & technology* **25**, 715-722.

8. McCauley, K. M., Pratt, D. A., Wilson, S. R., Shey, J., Burkey, T. J., and van der Donk, W. A. (2005) Properties and reactivity of chlorovinylcobalamin and vinylcobalamin and their implications for vitamin B12-catalyzed reductive dechlorination of chlorinated alkenes. *J. Am. Chem. Soc.* **127**, 1126-1136.

9. Wohlfarth, G., and Diekert, G. (1997) Anaerobic dehalogenases. *Curr. Opin. Biotechnol.* **8**, 290-295.

10. Banerjee, R., and Ragsdale, S. W. (2003) The many faces of vitamin B12: catalysis by cobalamin-dependent enzymes. *Annu. Rev. Biochem.* **72**, 209-247.

11. Glod, G., Angst, W., Holliger, C., and Schwarzenbach, R. P. (1996) Corrinoid-mediated reduction of tetrachloroethene, trichloroethene, and trichlorofluoroethene in homogeneous aqueous solution: Reaction kinetics and reaction mechanisms. *Environ. Sci. Technol.* **31**, 253-260.

12. Schumacher, W., Holliger, C., Zehnder, A. J., and Hagen, W. R. (1997) Redox chemistry of cobalamin and iron-sulfur cofactors in the tetrachloroethene reductase of *Dehalobacter restrictus*. *FEBS Lett.* **409**, 421-425.

13. Wohlfarth, G., and Diekert, G. (1999) Reductive dehalogenases. in *Chemistry and Biochemistry of B12.* (Banerjee, R. ed.), John Wiley & Sons, Inc., New York. pp 871-893.

14. Renpenning, J., Keller, S., Cretnik, S., Shouakar-Stash, O., Elsner, M., Schubert, T., and Nijenhuis, I. (2014) Combined C and Cl Isotope Effects Indicate Differences between Corrinoids and Enzyme (Sulfurospirillum multivorans PceA) in Reductive Dehalogenation of Tetrachloroethene, But Not Trichloroethene. *Environ. Sci. Technol.* **48**, 11837-11845.

15. Payne, K. A. P., Quezada, C. P., Fisher, K., Dunstan, M. S., Collins, F. A., Sjuts, H., Levy, C., Hay, S., Rigby, S. E. J., and Leys, D. (2015) Reductive dehalogenase structure suggests a mechanism for B12-dependent dehalogenation. *Nature* **517**, 513-516.

16. Bommer, M., Kunze, C., Fesseler, J., Schubert, T., Diekert, G., and Dobbek, H. (2014) Structural basis for organohalide respiration. *Science* **346**, 455-458.

17. Lawrence, J. G., and Roth, J. R. (1995) The cobalamin (coenzyme B12) biosynthetic genes of *Escherichia coli*. *J. Bacteriol.* **177**, 6371-6380.

18. Roth, J. R., Lawrence, J. G., and Bobik, T. A. (1996) Cobalamin (coenzyme B12): synthesis and biological significance. *Annu. Rev. Microbiol.* **50**, 137-181.

19. Warren, M. J., Raux, E., Schubert, H. L., and Escalante-Semerena, J. C. (2002) The biosynthesis of adenosylcobalamin (vitamin B12). *Nat. Prod. Rep.* **19**, 390-412.

20. Moore, S. J., and Warren, M. J. (2012) The anaerobic biosynthesis of vitamin B12. *Biochem. Soc. Trans.* **40**, 581-586.

21. Escalante-Semerena, J. C. (2007) Conversion of cobinamide into adenosylcobamide in bacteria and archaea. *J. Bacteriol.* **189**, 4555-4560.

22. Woodward, R. B. (1973) The total synthesis of vitamin B_{12}. *Pure Appl. Chem.* **33**, 145-177.

23. Eschenmoser, A., and Wintner, C. E. (1977) Natural product synthesis and vitamin B_{12}. *Science* **196**, 1410-1420.

24. Lexa, D., and Saveant, J. M. (1983) The Electrochemistry of vitamin-B12. *Acc. Chem. Res.* **16**, 235-243.

25. Brown, K. L. (2005) Chemistry and enzymology of vitamin B_{12}. *Chem. Rev.* **105**, 2075-2149.

26. Randaccio, L., Geremia, S., Demitri, N., and Wuerges, J. (2010) Vitamin B12: unique metalorganic compounds and the most complex vitamins. *Molecules* **15**, 3228-3259

27. Blanche, F., Thibaut, D., Debussche, L., Hertle, R., Zipfel, F., and Muller, G. (1993) Paralleles and decisive differences in vitamin B12 biosynthesis. *Angew. Chem. Int. Ed. Engl.* **32**, 1651-1653.

28. Rodionov, D. A., Vitreschak, A. G., Mironov, A. A., and Gelfand, M. S. (2003) Comparative genomics of the vitamin B_{12} metabolism and regulation in prokaryotes. *J. Biol. Chem.* **278**, 41148-41159.

29. Stabler, S. P., and Allen, R. H. (2004) Vitamin B12 deficiency as a worldwide problem. *Annu. Rev. Nutr.* **24**, 299-326.

30. Weissbach, H., Ladd, J. N., Volcani, B. E., Smyth, R. D., and Barker, H. A. (1960) Struture of the adenylcobamide coenzyme: degradation by cyanide, acid, and light. *J. Biol. Chem.* **235**, 1462-1473.

31. Pailes, W. H., and Hogenkamp, H. P. C. (1968) Photolability of Co-alkylcobinamides. *Biochemistry* **7**, 4160-4166.

32. Martens, J. H., Barg, H., Warren, M. J., and Jahn, D. (2002) Microbial production of vitamin B_{12}. *Appl. Microbiol. Biotechnol.* **58**, 275-285.

33. Fonseca, M. V., and Escalante-Semerena, J. C. (2000) Reduction of cob(III)alamin to cob(II)alamin in *Salmonella enterica* Serovar Typhimurium LT2. *J. Bacteriol.* **182**, 4304-4309.

34. Vitols, E., Walker, G. A., and Huennekens, F. M. (1966) Enzymatic conversion of vitamin B-12s to a cobamide coenzyme, alpha-(5,6-dimethylbenzimidazolyl)deoxyadenosylcobamide (adenosyl-B-12). *J. Biol. Chem.* **241**, 1455-1461.

35. Lexa, D., and Saveant, J.-M. (1983) The electrochemistry of vitamin B12. *Acc. Chem. Res.* **16**, 235-243.

36. Hoover, D. M., Jarrett, J. T., Sands, R. H., Dunham, W. R., Ludwig, M. L., and Matthews, R. G. (1997) Interaction of *Escherichia coli* cobalamin-dependent methionine synthase and its physiological partner flavodoxin: binding of flavodoxin leads to axial ligand dissociation from the cobalamin cofactor. *Biochemistry* **36**, 127-138.

37. Escalante-Semerena, J. C., Suh, S. J., and Roth, J. R. (1990) *cobA* function is required for both de novo cobalamin biosynthesis and assimilation of exogenous corrinoids in *Salmonella typhimurium*. *J. Bacteriol.* **172**, 273-280.

38. Suh, S. J., and Escalante-Semerena, J. C. (1993) Cloning, sequencing and overexpression of *cobA* which encodes ATP:corrinoid adenosyltransferase in *Salmonella typhimurium*. *Gene* **129**, 93-97.

39. Suh, S., and Escalante-Semerena, J. C. (1995) Purification and initial characterization of the ATP:corrinoid adenosyltransferase encoded by the *cobA* gene of *Salmonella typhimurium*. *J. Bacteriol.* **177**, 921-925.

40. Fonseca, M. V., Buan, N. R., Horswill, A. R., Rayment, I., and Escalante-Semerena, J. C. (2002) The ATP:co(I)rrinoid adenosyltransferase (CobA) enzyme of *Salmonella enterica* requires the 2'-OH Group of ATP for function and yields inorganic triphosphate as its reaction byproduct. *J. Biol. Chem.* **277**, 33127-33131.

41. Koutmos, M., Gherasim, C., Smith, J. L., and Banerjee, R. (2011) The structural basis of multifunctionality in a vitamin B12-processing enzyme. *J. Biol. Chem.* **286**, 29780-29787.

42. Lawrence, A. D., Taylor, S. L., Scott, A., Rowe, M. L., Johnson, C. M., Rigby, S. E., Geeves, M. A., Pickersgill, R. W., Howard, M. J., and Warren, M. J. (2014) FAD binding, cobinamide binding and active site communication in the corrin reductase CobR. *Biosci. Rep.* **34**, e00120.

43. Bauer, C. B., Fonseca, M. V., Holden, H. M., Thoden, J. B., Thompson, T. B., Escalante-Semerena, J. C., and Rayment, I. (2001) Three-dimensional structure of ATP:corrinoid adenosyltransferase from *Salmonella typhimurium* in its free state, complexed with MgATP, or complexed with hydroxycobalamin and MgATP. *Biochemistry* **40**, 361-374.

44. Buan, N. R., and Escalante-Semerena, J. C. (2005) Computer-assisted docking of flavodoxin with the ATP:Co(I)rrinoid adenosyltransferase (CobA) enzyme reveals residues critical for protein-protein interactions but not for catalysis. *J. Biol. Chem.* **280**, 40948-40956.

45. Stich, T. A., Buan, N. R., Escalante-Semerena, J. C., and Brunold, T. C. (2005) Spectroscopic and computational studies of the ATP:Corrinoid adenosyltransferase (CobA) from *Salmonella enterica*: Insights into the mechanism of adenosylcobalamin biosynthesis. *J. Am. Chem. Soc.* **127**, 8710-8719.

46. Stich, T. A., Yamanishi, M., Banerjee, R., and Brunold, T. C. (2005) Spectroscopic evidence for the formation of a four-coordinate Co(2+)cobalamin species upon binding to the human ATP:Cobalamin adenosyltransferase. *J. Am. Chem. Soc.* **127**, 7660-7661.

47. Park, K., Mera, P. E., Escalante-Semerena, J. C., and Brunold, T. C. (2008) Kinetic and spectroscopic studies of the ATP:corrinoid adenosyltransferase PduO from *Lactobacillus reuteri*: substrate specificity and insights into the mechanism of Co(II)corrinoid reduction. *Biochemistry* **47**, 9007-9015.

48. St Maurice, M., Mera, P., Park, K., Brunold, T. C., Escalante-Semerena, J. C., and Rayment, I. (2008) Structural characterization of a human-type corrinoid adenosyltransferase confirms that coenzyme B_{12} is synthesized through a four-coordinate intermediate. *Biochemistry* **47**, 5755-5766.

49. Liptak, M. D., Fleischhacker, A. S., Matthews, R. G., Telser, J., and Brunold, T. C. (2009) Spectroscopic and computational characterization of the base-off forms of cob(II)alamin. *J. Phys. Chem. B* **113**, 5245-5254.

50. Park, K., Mera, P. E., Escalante-Semerena, J. C., and Brunold, T. C. (2012) Spectroscopic characterization of active-site variants of the PduO-type ATP:Corrinoid adenosyltransferase from *Lactobacillus reuteri*: Insights into the mechanism of four-coordinate Co(II)corrinoid formation. *Inorg. Chem.* **51**, 4482-4494.

51. Park, K., and Brunold, T. C. (2013) Combined spectroscopic and computational analysis of the vibrational properties of Vitamin B12 in its Co3+, Co2+, and Co1+ oxidation states. *J. Phys. Chem. B* **117**, 5397–5410.

52. Pallares, I. G., Moore, T. C., Escalante-Semerena, J. C., and Brunold, T. C. (2014) Spectroscopic studies of the *Salmonella enterica* adenosyltransferase enzyme *Se*CobA: Molecular-level insight into the mechanism of substrate cob(II)alamin activation. *Biochemistry* **53**, 7969-7982.

53. Bobik, T. A., Xu, Y., Jeter, R. M., Otto, K. E., and Roth, J. R. (1997) Propanediol utilization genes (*pdu*) of *Salmonella typhimurium*: three genes for the propanediol dehydratase. *J. Bacteriol.* **179**, 6633-6639.

54. Bobik, T. A., Havemann, G. D., Busch, R. J., Williams, D. S., and Aldrich, H. C. (1999) The propanediol utilization (*pdu*) operon of *Salmonella enterica* serovar Typhimurium LT2 includes genes necessary for formation of polyhedral organelles involved in coenzyme B_{12}-dependent 1, 2-propanediol degradation. *J. Bacteriol.* **181**, 5967-5975.

55. Yeates, T. O., Jorda, J., and Bobik, T. A. (2013) The shells of BMC-type microcompartment organelles in bacteria. *J. Mol. Microbiol. Biotechnol.* **23**, 290-299.

56. Walter, D., Ailion, M., and Roth, J. (1997) Genetic characterization of the *pdu* operon: use of 1,2-propanediol in *Salmonella typhimurium*. *J. Bacteriol.* **179**, 1013-1022.

57. Johnson, C. L., Buszko, M. L., and Bobik, T. A. (2004) Purification and initial characterization of the *Salmonella enterica* PduO ATP:Cob(I)alamin adenosyltransferase. *J. Bacteriol.* **186**, 7881-7887.

58. Sampson, E. M., Johnson, C. L., and Bobik, T. A. (2005) Biochemical evidence that the *pduS* gene encodes a bifunctional cobalamin reductase. *Microbiology* **151**, 1169-1177.

59. Cheng, S., and Bobik, T. A. (2010) Characterization of the PduS cobalamin reductase of *Salmonella* and its role in the Pdu microcompartment. *J. Bacteriol.* **192**, 5071-5080.

60. Parsons, J. B., Lawrence, A. D., McLean, K. J., Munro, A. W., Rigby, S. E., and Warren, M. J. (2010) Characterisation of PduS, the *pdu* metabolosome corrin reductase, and evidence of substructural organisation within the bacterial microcompartment. *PLoS ONE* **5**, e14009.

61. Toraya, T. (2000) Radical catalysis of B_{12} enzymes: structure, mechanism, inactivation, and reactivation of diol and glycerol dehydratases. *Cell Mol. Life Sci.* **57**, 106-127.

62. Yamanishi, M., Vlasie, M., and Banerjee, R. (2005) Adenosyltransferase: an enzyme and an escort for coenzyme B12? *Trends Biochem. Sci.* **30**, 304-308.

63. Fan, C., and Bobik, T. A. (2008) Functional characterization and mutation analysis of human ATP:Cob(I)alamin adenosyltransferase. *Biochemistry* **47**, 2806-2813.

64. St Maurice, M., Mera, P. E., Taranto, M. P., Sesma, F., Escalante-Semerena, J. C., and Rayment, I. (2007) Structural characterization of the active site of the PduO-type ATP:Co(I)rrinoid adenosyltransferase from *Lactobacillus reuteri*. *J. Biol. Chem.* **282**, 2596-2605.

65. Mera, P. E., Maurice, M. S., Rayment, I., and Escalante-Semerena, J. C. (2007) Structural and functional analyses of the human-type corrinoid adenosyltransferase (PduO) from *Lactobacillus reuteri*. *Biochemistry* **46**, 13829-13836.

66. Mera, P. E., St Maurice, M., Rayment, I., and Escalante-Semerena, J. C. (2009) Residue Phe112 of the human-type corrinoid adenosyltransferase (PduO) enzyme of *Lactobacillus reuteri* is critical to the formation of the four-coordinate Co(II) corrinoid substrate and to the activity of the enzyme. *Biochemistry* **48**, 3138-3145.

67. Roof, D. M., and Roth, J. R. (1988) Ethanolamine utilization in *Salmonella typhimurium*. *J. Bacteriol.* **170**, 3855-3863.

68. Kofoid, E., Rappleye, C., Stojiljkovic, I., and Roth, J. (1999) The 17-gene ethanolamine (*eut*) operon of *Salmonella typhimurium* encodes five homologues of carboxysome shell proteins. *J. Bacteriol.* **181**, 5317-5329.

69. Yeates, T. O., Crowley, C. S., and Tanaka, S. (2010) Bacterial microcompartment organelles: protein shell structure and evolution. *Annu. Rev. Biophys.* **39**, 185-205.

70. Babior, B. M. (1970) The mechanism of action of ethanolamine ammonia-lyase, a B12-dependent enzyme. VII. The mechanism of hydrogen transfer. *J. Biol. Chem.* **245**, 6125-6133.

71. Chang, G. W., and Chang, J. T. (1975) Evidence for the B12-dependent enzyme ethanolamine deaminase in *Salmonella*. *Nature* **254**, 150-151.

72. Blackwell, C. M., Scarlett, F. A., and Turner, J. M. (1976) Ethanolamine catabolism by bacteria, including *Escherichia coli*. *Biochem. Soc. Trans.* **4**, 495-497.

73. Brinsmade, S. R., Paldon, T., and Escalante-Semerena, J. C. (2005) Minimal functions and physiological conditions required for growth of *Salmonella enterica* on ethanolamine in the absence of the metabolosome. *J. Bacteriol.* **187**, 8039-8046

74. Buan, N. R., Suh, S. J., and Escalante-Semerena, J. C. (2004) The *eutT* gene of *Salmonella enterica* encodes an oxygen-labile, metal-containing ATP:corrinoid adenosyltransferase enzyme. *J. Bacteriol.* **186**, 5708-5714.

75. Johnson, C. L., Pechonick, E., Park, S. D., Havemann, G. D., Leal, N. A., and Bobik, T. A. (2001) Functional genomic, biochemical, and genetic characterization of the *Salmonella pduO* gene, an ATP:cob(I)alamin adenosyltransferase gene. *J. Bacteriol.* **183**, 1577-1584.

76. Park, K., Mera, P. E., Moore, T. C., Escalante-Semerena, J. C., and Brunold, T. C. (2015) Unprecedented Mechanism Employed by the Salmonella enterica EutT ATP:CoIrrinoid Adenosyltransferase Precludes Adenosylation of Incomplete CoIIrrinoids. *Angew. Chem. Int. Ed.* **54**, 7158-7161.

77. Buan, N. R., and Escalante-Semerena, J. C. (2006) Purification and initial biochemical characterization of ATP:Cob(I)alamin adenosyltransferase (EutT) enzyme of *Salmonella enterica*. *J. Biol. Chem.* **281**, 16971-16977.

78. Fan, C., Cheng, S., Liu, Y., Escobar, C. M., Crowley, C. S., Jefferson, R. E., Yeates, T. O., and Bobik, T. A. (2010) Short N-terminal sequences package proteins into bacterial microcompartments. *Proc. Natl. Acad. Sci. U S A* **107**, 7509-7514.

79. Held, M., Quin, M. B., and Schmidt-Dannert, C. (2013) Eut bacterial microcompartments: insights into their function, structure, and bioengineering applications. *J. Mol. Microbiol. Biotechnol.* **23**, 308-320.

80. Thompson, M. C., Cascio, D., Leibly, D. J., and Yeates, T. O. (2015) An allosteric model for control of pore opening by substrate binding in the EutL microcompartment shell protein. *Protein Sci.* **26** 956-975.

81. Chowdhury, C., Chun, S., Pang, A., Sawaya, M. R., Sinha, S., Yeates, T. O., and Bobik, T. A. (2015) Selective molecular transport through the protein shell of a bacterial microcompartment organelle. *Proc. Natl. Acad. Sci. U S A* **112**, 2990-2995.

82. Price-Carter, M., Tingey, J., Bobik, T. A., and Roth, J. R. (2001) The alternative electron acceptor tetrathionate supports B12-dependent anaerobic growth of *Salmonella enterica* serovar Typhimurium on ethanolamine or 1,2-propanediol. *J. Bacteriol.* **183**, 2463-2475.

83. Thiennimitr, P., Winter, S. E., Winter, M. G., Xavier, M. N., Tolstikov, V., Huseby, D. L., Sterzenbach, T., Tsolis, R. M., Roth, J. R., and Bäumler, A. J. (2011) Intestinal inflammation allows Salmonella to use ethanolamine to compete with the microbiota. *Proc. Natl. Acad. Sci. U S A* **108**, 17480-17485.

84. Winter, S. E., Thiennimitr, P., Winter, M. G., Butler, B. P., Huseby, D. L., Crawford, R. W., Russell, J. M., Bevins, C. L., Adams, L. G., Tsolis, R. M., Roth, J. R., and Baumler, A. J. (2010) Gut inflammation provides a respiratory electron acceptor for *Salmonella*. *Nature* **467**, 426-4269.

85. Dunwell, J. M., Purvis, A., and Khuri, S. (2004) Cupins: the most functionally diverse protein superfamily? *Phytochemistry* **65**, 7-17.

86. Trazzi, S., Bernardoni, R., Diolaiti, D., Politi, V., Earnshaw, W. C., Perini, G., and Della Valle, G. (2002) In vivo functional dissection of human inner kinetochore protein CENP-C. *J. Struct. Biol.* **140**, 39-48.

87. Privalle, L. S. (2002) Phosphomannose Isomerase, a Novel Plant Selection System. *Ann. NY Acad. Sci.* **964**, 129-138.

88. Fusetti, F., Schröter, K. H., Steiner, R. A., van Noort, P. I., Pijning, T., Rozeboom, H. J., Kalk, K. H., Egmond, M. R., and Dijkstra, B. W. (2002) Crystal Structure of the Copper-Containing Quercetin 2,3-Dioxygenase from Aspergillus japonicus. *Structure* **10**, 259-268.

89. Pitts, A. C., Tuck, L. R., Faulds-Pain, A., Lewis, R. J., and Marles-Wright, J. (2012) Structural insight into the *Clostridium difficile* ethanolamine utilisation microcompartment. *PLoS One* **7**, e48360.

90. Padovani, D., Labunska, T., and Banerjee, R. (2006) Energetics of interaction between the G-protein chaperone, MeaB, and B12-dependent methylmalonyl-CoA mutase. *J. Biol. Chem.* **281**, 17838-17844.

91. Padovani, D., and Banerjee, R. (2009) A G-protein editor gates coenzyme B12 loading and is corrupted in methylmalonic aciduria. *Proc. Natl. Acad. Sci. U S A* **106**, 21567-21572.

92. Palacios, S., Starai, V. J., and Escalante-Semerena, J. C. (2003) Propionyl coenzyme A is a common intermediate in the 1,2-propanediol and propionate catabolic pathways needed for expression of the *prpBCDE* operon during growth of *Salmonella enterica* on 1,2-propanediol. *J. Bacteriol.* **185**, 2802-2810.

CHAPTER 2

STRUCTURAL INSIGHTS INTO THE MECHANISM OF FOUR-COORDINATE COB(II)ALAMIN FORMATION IN THE ACTIVE SITE OF THE *SALMONELLA ENTERICA* ATP:CO(I)RRINOID ADENOSYLTRANSFERASE (COBA) ENZYME: CRITICAL ROLE OF RESIDUES PHE91 AND TRP93[1]

[1] Theodore C. Moore, Sean A. Newmister, Ivan Rayment, and Jorge C. Escalante-Semerena. 2012. *Biochemistry*. 51:9647-9657.

Abbreviations: ACAT, ATP:Co(I)rrinoid adenosyltransferase; Cbl, cobalamin; Coα, cobalamin α-ligand; Coβ, cobalamin β-ligand; DMB, 5,6-dimethylbenzimidazole; Cbl, cobalamin; Cbi, cobinamide; AdoCbl, adenosylcobalamin; CoB_{12}, Coenzyme B_{12}; HOCbl, hydroxycobalamin; ATP, adenosine triphosphate; PPPi, tripolyphosphate; *Lr*PduO, *Lactobacillus reuteri* PduO; Tris-HCl, tris(hydroxymethyl)aminomethane hydrochloride; TCEP, *tris*-(2-carboxyethyl)phosphine; rTEV, recombinant tobacco etch virus, NTA, nitrilotriacetic acid; FAD, flavin adenine dinucleotide; FldA, flavodoxin A; Fpr, ferredoxin (flavodoxin):NADPH reductase; NADH, reduced nicotinamide adenine dinucleotide; MES, 2-(*N*-morpholino)ethanesulfonic acid.

2.1 Abstract

ATP:Co(I)rrinoid adenosyltransferases (ACATs) are enzymes that catalyze the formation of adenosylcobalamin (AdoCbl, coenzyme B_{12}) from cobalamin and ATP. There are three families of ACATs, namely CobA, EutT and PduO. In *Salmonella enterica*, CobA is the housekeeping enzyme that is required for *de novo* AdoCbl synthesis and for salvaging incomplete precursors and cobalamin from the environment. Here, we report the crystal structure of CobA in complex with ATP, four-coordinate cobalamin, and five-coordinate cobalamin. This provides the first crystallographic evidence for the existence of cob(II)alamin in the active site of CobA. The structure suggests a mechanism in which the enzyme adopts a closed conformation and two residues, Phe91 and Trp93, displace 5,6-dimethylbenzimidazole (DMB), the lower nucleotide ligand base of cobalamin, to generate a transient four-coordinate cobalamin, which is critical in the formation of the AdoCbl Co-C bond. In vivo and in vitro mutational analysis of Phe91 and Trp93 emphasize the important role of bulky hydrophobic side chains in the active site. The proposed manner in which CobA increases the redox potential of the cob(II)alamin/cob(I)alamin couple to facilitate formation of the Co-C bond appears to be analogous to that utilized by the PduO-type ACATs, where in both cases the polar coordination of the lower ligand to the cobalt ion is eliminated by placing that face of the corrin ring adjacent to a cluster of bulky hydrophobic sidechains.

2.2 Introduction

Cobalamin (Cbl, vitamin B_{12}) is one of the largest cofactors in biology, and is utilized by organisms across all domains of life (1,2). Cobalamin features a cobalt ion coordinated equatorially by the nitrogen atoms of a cyclic tetrapyrrole known as the corrin ring. The lower (*Coα*) axial ligand of Cbl is the purine analog base 5,6-dimethylbenzimidazole (DMB), which is tethered to the corrin ring by a phosphodiester bond between an aminopropanol substituent of the ring and the phosphoryl moiety of the DMB-ribotide (3).

In adenosylcobalamin (AdoCbl, coenzyme B_{12} or CoB_{12}), the upper (*Coβ*) ligand is a 5'-deoxyadenosyl moiety covalently bound to the cobalt ion of the ring, forming a weak Co-C bond. Homolysis of the Co-C bond of AdoCbl results in five-coordinate cob(II)alamin and a 5'-deoxyadenosyl radical critical to the initiation of intramolecular rearrangements catalyzed by a variety of enzymes, such as ethanolamine ammonia-lyase (4), diol dehydratase (5) and methylmalonyl-CoA mutase (6), among others.

AdoCbl is synthesized by a family of enzymes known as ATP:co(I)rrinoid adenosyltransferases (ACATs). There are three non-homologous types of ACATs, CobA, PduO and EutT, which were named based on their function in the enterobacterium *Salmonella enterica* (7-9). In this bacterium, CobA is the housekeeping ACAT involved in *de novo* AdoCbl synthesis and incomplete corrinoid salvaging (7). CobA has the broadest substrate specificity of the three ACAT types, and recognizes both complete and incomplete corrinoids (10).

Corrinoid adenosylation proceeds via a reactive nucleophilic Co^{1+} species which is generated through a series of consecutive one-electron transfers to reduce the Co^{3+} ion (11). The bacterial cytoplasm has sufficient reducing power for reduction of Co^{3+} to Co^{2+}, an event that removes the β-ligand (12). Further reduction to Co^{1+} is thermodynamically difficult, since the $Co^{2+/1+}$ redox

couple in solution (-610 mV) is beyond the reach of known biological reductants (13,14). ACATs raise the redox potential of the $Co^{2+/1+}$ couple by generating a four-coordinate cob(II)alamin species in the active site (15-17). In such species, the redox-active $3d_z^2$ orbital of cobalt is stabilized resulting in an increase of ≥250 mV (18). In such an environment, cob(II)alamin can accept an electron from reduced flavodoxin A (FldA), to generate cob(I)alamin (12,19,20). Generation of cob(I)alamin is followed by a nucleophilic attack by Co^{1+} on the 5'-carbon of the ATP co-substrate, forming AdoCbl and releasing tripolyphosphate (PPP_i) (21). This is accomplished in *Lactobacillus reuteri* PduO ACAT (hereafter *Lr*PduO) by placing the lower ligand coordination site of the cobalt ion in a hydrophobic environment (*35*). In *Lr*PduO Phe112 displaces DMB from its coordination bond with the cobalt ion to generate the four-coordinate intermediate (22). It was unknown whether this mechanism is shared by other non-homologous ACATs, or whether each ACAT has a distinct mechanism for achieving a four-coordinate cob(II)alamin.

CobA is capable of generating the four-coordinate intermediate (18), however such an intermediate has not been observed in the active site of CobA so that the mechanism for the conversion of five- to four-coordinate cob(II)alamin in CobA was unknown. In earlier structural studies, prior to understanding the importance four-coordinate cob(II)alamin intermediates, CobA was crystallized in complex with HO-cob(III)alamin (HOCbl) (23). In that structure the cobalt ion of HOCbl is not in a suitable position for nucleophilic attack since it is located too far (>6Å) from the 5'-carbon of ATP (23). Significantly, HOCbl is a Co^{3+} species that is not encountered by the enzyme in vivo (12).

To address the mechanism by which four-coordinate Cbl formation is supported in CobA we have determined the structure of CobA in complex with cob(II)alamin and MgATP at 2.0Å

resolution. This revealed four-coordination for the cobalt ion and provided insight into how this is accomplished in this class of ACATs. The structure was used to guide an investigation in vivo and in vitro of the components of the active site that appear critical for function.

2.3 Materials and Methods

Strains, Culture Media and Chemicals. Strains used in this study are listed in Table 2.1. Primers used for PCR-based site-directed mutagenesis are listed in Table 2.2. Chemicals were purchased from Sigma and were used without further purification.

Minimal medium (24) containing ethanolamine as carbon, energy and nitrogen source was used to assess AdoCbl biosynthesis via the adenosylcobalamin-dependent expression of the ethanolamine utilization (*eut*) operon of *S. enterica* sv. Typhimurium strain LT2 as described (7). The culture medium was supplemented with ethanolamine (90 mM), glycerol (0.5 mM), methionine (2 mM), $MgSO_4$ (1 mM), arabinose (0.5 mM) and trace minerals (25). AdoCbl precursors dicyanocobinamide [$(CN)_2$Cbi, 100 nM], and 5,6-dimethylbenzimidazole (DMB, 300 μM) were also added to the medium. Lysogenic broth (LB) (26,27) and Nutrient Broth (Difco Laboratories) medium were used as complex media.

Protein Overexpression and Overproduction. Overexpression and purification of tagless, wild-type CobA ($CobA^{WT}$) protein was performed as described (23). $CobA^{WT}$ was concentrated (10,000 MWCO centrifugal filter, Millipore) to 20 mg/mL as determined by A_{280} using the calculated molar extinction coefficient (23,950 M^{-1} cm^{-1}, ExPASy (28)). The protein was flash-frozen in liquid nitrogen and stored at -80 °C until used.

To facilitate overproduction and purification of CobA variants, the *S. enterica* $cobA^+$ allele was cloned into a pTEV5 vector to direct synthesis of CobA proteins fused to a N-terminal, rTEV

Table 2.1: Strains and plasmids used over the course of this study

Strain ID	Genotype	Plasmid	Allele	Protein encoded	Source
E. coli strains					
JE3892	BL21 (λ*DE3*)				Laboratory collection
JE15023	BL21 (λ*DE3*) *btuR*::Tn1000				
Derivatives of DH5á					Laboratory collection
JE16446		pCOBA102	*cobA1475*	$CobA^{F91A}$	
JE16116		pCOBA89	*cobA1475*	H_6CobA^{F91A}	
JE16024		pCOBA88	*cobA1476*	$CobA^{F91W}$	
JE15827		pCOBA81	*cobA1476*	H_6CobA^{F91W}	
JE16312		pCOBA96	*cobA1477*	$CobA^{F91H}$	
JE15828		pCOBA82	*cobA1477*	H_6CobA^{F91H}	
JE16313		pCOBA97	*cobA1478*	$CobA^{F91Y}$	
JE15834		pCOBA83	*cobA1478*	H_6CobA^{F91Y}	
JE16447		pCOBA103	*cobA1479*	$CobA^{F91D}$	
JE15835		pCOBA84	*cobA1479*	H_6CobA^{F91D}	
JE16022		pCOBA86	*cobA1480*	$CobA^{W93A}$	
JE15836		pCOBA85	*cobA1480*	H_6CobA^{W93A}	
JE16314		pCOBA99	*cobA1481*	$CobA^{W93F}$	
JE16444		pCOBA100	*cobA1481*	H_6CobA^{W93F}	
JE16023		pCOBA87	*cobA1482*	$CobA^{W93H}$	
JE16307		pCOBA91	*cobA1482*	H_6CobA^{W93H}	
JE16314		pCOBA98	*cobA1483*	$CobA^{W93Y}$	
JE16308		pCOBA92	*cobA1483*	H_6CobA^{W93Y}	
JE16448		pCOBA104	*cobA1484*	$CobA^{W93D}$	
JE16309		pCOBA93	*cobA1484*	H_6CobA^{W93D}	
JE16449		pCOBA105	*cobA1485*	$CobA^{F91A,W93A}$	
JE16310		pCOBA94	*cobA1485*	$H_6CobA^{F91A,W93A}$	
JE16311		pCOBA95	*cobA1486*	$CobA^{F91W,W93F}$	
JE16445		pCOBA101	*cobA1486*	$H_6CobA^{F91W,W93F}$	
S. enterica strains					
JE1096	*metE205 ara-9 cobA343::*MuD*J*				
Derivatives of JE1096					Laboratory collections
JE13249		pBAD24		Vector control	
JE8057		pCOBA70		$CobA^{WT}$	
JE16490		pCOBA102	*cobA1475*	$CobA^{F91A}$	
JE16491		pCOBA88	*cobA1476*	$CobA^{F91W}$	
JE16492		pCOBA96	*cobA1477*	$CobA^{F91H}$	
JE16493		pCOBA97	*cobA1478*	$CobA^{F91Y}$	
JE16494		pCOBA103	*cobA1479*	$CobA^{F91D}$	
JE16495		pCOBA86	*cobA1480*	$CobA^{W93A}$	
JE16498		pCOBA98	*cobA1481*	$CobA^{W93F}$	
JE16497		pCOBA87	*cobA1482*	$CobA^{W93H}$	
JE16498		pCOBA98	*cobA1483*	$CobA^{W93Y}$	
JE16499		pCOBA104	*cobA1484*	$CobA^{W93D}$	
JE16500		pCOBA105	*cobA1485*	$CobA^{F91A,W93A}$	
JE16501		pCOBA95	*cobA1486*	$CobA^{F91W,W93F}$	

Table 2.2 Primers used for mutagenesis in this study			
Protein, variation	Template	5’ Primer	Resulting Plasmid
$CobA^{WT}$	pCOBA70	5'-ggtgatggcaacgggagctacctgggagacgcaa-3'	pCOBA102
$CobA^{F91A}$	pCOBA80	5'-ggtgatggcaacgggagctacctgggagacgcaa-3'	pCOBA89
$CobA^{F91W}$	pCOBA70	5'-gtgatggcaacgggatatacctgggagacg-3	pCOBA88
$CobA^{F91W}$	pCOBA80	5'-gtgatggcaacgggatatacctgggagacg-3	pCOBA81
$CobA^{F91H}$	pCOBA70	5'-ggtgatggcaacgggacatacctgggagacgcaa-3'	pCOBA96
$CobA^{F91H}$	pCOBA80	5'-ggtgatggcaacgggacatacctgggagacgcaa-3'	pCOBA82
$CobA^{F91Y}$	pCOBA70	5'-gtgatggcaacgggatatacctgggagacg-3	pCOBA97
$CobA^{F91Y}$	pCOBA80	5'-gtgatggcaacgggatatacctgggagacg-3	pCOBA83
$CobA^{F91D}$	pCOBA70	5'-ggtgatggcaacgggagatacctgggagacgcaa-3’	pCOBA103
$CobA^{F91D}$	pCOBA80	5'-ggtgatggcaacgggagatacctgggagacgcaa-3’	pCOBA84
$CobA^{W93A}$	pCOBA70	5'-ggcaacgggatttaccgcggagacgcaaaatcgc-3'	pCOBA86
$CobA^{W93A}$	pCOBA80	5'-ggcaacgggatttaccgcggagacgcaaaatcgc-3'	pCOBA85
$CobA^{W93F}$	pCOBA70	5'-ggcaacgggatttaccttcgagacgcaaaatcgcga-3'	pCOBA98
$CobA^{W93F}$	pCOBA80	5'-ggcaacgggatttaccttcgagacgcaaaatcgcga-3'	pCOBA100
$CobA^{W93H}$	pCOBA70	5'-gatggcaacgggatttacccatgagacgcaaaatcgcgagg-3'	pCOBA87
$CobA^{W93H}$	pCOBA80	5'-gatggcaacgggatttacccatgagacgcaaaatcgcgagg-3'	pCOBA91
$CobA^{W93Y}$	pCOBA70	5'-gatggcaacgggatttacccatgagacgcaaaatcgcgagg-3'	pCOBA98
$CobA^{W93Y}$	pCOBA80	5'-gatggcaacgggatttacccatgagacgcaaaatcgcgagg-3'	pCOBA92
$CobA^{W93D}$	pCOBA70	5'-gatggcaacgggatttaccgatgagacgcaaaatcgcgagg-3'	pCOBA104
$CobA^{W93D}$	pCOBA80	5'-gatggcaacgggatttaccgatgagacgcaaaatcgcgagg-3'	pCOBA93
$CobA^{F91A,W93A}$	pCOBA70	5'-tcaggtgatggcaacgggagctaccgcggagacgcaaaatcgcg-3'	pCOBA105
$CobA^{F91A,W93A}$	pCOBA80	5'-tcaggtgatggcaacgggagctaccgcggagacgcaaaatcgcg-3'	pCOBA94
$CobA^{F91W,W93F}$	pCOBA70	5'-caggtgatggcaacgggatggaccttcgagacgcaaaatcgcgag-3'	pCOBA95
$CobA^{F91W,W93F}$	pCOBA80	5'-caggtgatggcaacgggatggaccttcgagacgcaaaatcgcgag-3'	pCOBA101

Table 2.3. Calculated ε_M for CobA protein variants[a]	
Protein, variation	ε_M (M^{-1} cm^{-1})
$CobA^{WT}$	24075
$CobA^{F91A}$	23950
$CobA^{F91W}$	29450
$CobA^{F91H}$	23950
$CobA^{F91Y}$	25440
$CobA^{F91D}$	23950
$CobA^{W93A}$	18450
$CobA^{W93F}$	18450
$CobA^{W93H}$	18450
$CobA^{W93Y}$	19940
$CobA^{W93D}$	18450
$CobA^{F91A,W93A}$	18450
$CobA^{F91W,W93F}$	24075

[a]Calculated using the ProtParam too, ExPASy

protease-cleavable H_6 tag (29). Mutant *cobA* alleles were constructed using the QuickChange II site-directed mutagenesis kit (Stratagene). The presence of the desired mutations was confirmed using BigDye® Terminator DNA sequencing protocols (ABI PRISM); reaction mixtures were resolved at the University of Wisconsin-Madison Biotechnology Center. Plasmids directing the synthesis of the CobA variants were moved by electroporation into a strain of *E. coli* BL21(λDE3) carrying a null allele of *btuR*, the *cobA* homologue in this bacterium (Table 2.1). Strains expressing different *cobA* alleles were inoculated into 2L of LB containing ampicillin (100 μg/mL), and grown with shaking at 37 °C to OD_{600} nm of ~0.6. At that point, the incubator temperature was dropped to 15 °C for 30 min before overnight induction with 1 mM IPTG. Cells were harvested (9,000 x*g* for 15 min at 4 °C) and stored at -80 °C for at least 3 days. Cell pellets were resuspended in 100 mM *tris*-(hydroxymethyl)aminomethane hydrochloride buffer (Tris-HCl) (pH 8 at 4 °C) with 500 mM NaCl, 70 mM imidazole, 1 mM *tris*-(2-carboxyethyl)phosphine (TCEP) and protease inhibitor cocktail (Sigma) at 3 mL of buffer per gram of cell pellet. Resuspended cells were lysed by two passages through a French pressure cell (10.3 MPa) at 4 °C. The insoluble fraction was removed by centrifugation (44,000 x *g*, 45 min at 4 °C) followed by filtration through a 0.45 μm filter (Millipore). Clarified lysate was applied over a Ni-activated nitrilotriacetic acid (NTA) column (5mL HisPur resin, Thermo). After loading, the column was washed with 5 bed volumes of buffer A [100 mM Tris-HCl (pH 8 at 4 °C)] containing 500 mM NaCl, 70 mM imidazole and 1 mM TCEP. CobA protein bound to the resin was eluted using 5 bed volumes of buffer B (buffer A containing 500 mM imidazole) and collected in 3 mL fractions. The location of CobA was established by SDS-PAGE analysis of fractions. Fractions containing CobA of highest purity (12 mL) were combined and dialyzed (10000 MWCO, Pierce) with His_7-tagged recombinant tobacco etch virus (His7-rTEV) protease

(1 mg/mL, 1:50 v/v) to cleave the His_6-tag. His_7-tagged rTEV was prepared as described elsewhere (30). The combined fractions were dialyzed against buffer C (buffer A containing 20 mM imidazole) with three buffer changes at 4 °C. The first and second dialyses lasted 3 h and the third dialysis lasted 10 h. The dialyzed fractions were loaded onto a fresh Ni-NTA column and washed with 5 bed volumes of buffer A; the flow-through was collected in 3 mL fractions. The protein content of these fractions was analyzed by SDS-PAGE, those containing CobA of the highest purity were pooled (9 mL) and dialyzed against one liter of 50 mM Tris-HCl (pH 8.0 at 4 °C), 500 mM NaCl, 1 mM TCEP, and 10% v/v glycerol at 4 °C. Three changes of dialysis buffer were used at 4°C. The first and second lasted 3 h, the third lasted 10 h. The final dilution factor of the dialyzable material was 7.2×10^{-7}. Proteins were concentrated (10,000 MWCO centrifugal filter, Millipore), concentration was measured by A_{280} using the calculated molar extinction coefficients (Table 2.3, ExPASy), and the proteins were flash-frozen in liquid N_2 and stored at -80 °C. Flavodoxin A (FldA) and ferredoxin (flavodoxin):$NADP^+$ reductase (Fpr) were produced and purified as described (12).

Crystallography. Crystallization conditions were analyzed using a 144-condition sparse matrix screen developed in the Rayment laboratory. All crystals of tag-less CobA were grown by hanging-drop vapor diffusion in an anoxic chamber (Coy) at 20-25 °C. CobA was thawed and dialyzed three times against 1L of 20mM Tris-HCl (pH 8.0 at 25 °C) for 30 min each at 25 °C to remove glycerol. A reaction mixture containing 20 μg/mL Fpr, 20 mM NADH, 3 mM ATP, 4.5 mM $MgCl_2$, and 2 mM HOCbl was constituted at room temperature inside an anoxic chamber (90% N_2/10% H_2) to reduce HO-cob(III)alamin to cob(II)alamin. The reduction was performed inside the anoxic chamber to avoid the rapid oxidation of cob(II)alamin back to cob(III)alamin. Anoxic CobA was added to the reaction mixture after 20 min of pre-incubation at 25 °C. The

final concentration of CobA in the mixture was 10 mg/mL. CobA was co-crystallized with MgATP and cob(II)alamin by mixing 2 μL of the reaction mixture with 2 μL of well solution composed of 100 mM 2-(*N*-morpholino)ethanesulfonic acid (MES) (pH 6.0, 320 mM NaCl, and 19.6% w/v polyethylene glycol 4000 (PEG4000).

Brown, orthorhombic crystals (0.1 x 0.5 mm) were observed after 48 h. The crystals were incrementally transferred in two steps to a cryoprotectant solution which contained 22.5% w/v PEG4000, 13.8% v/v ethylene glycol, 100 mM MES (pH 6.0), 240 mM NaCl], 0.5 mM HOCbl, 20 μg/mL Fpr, 10 mM NADH, 1 mM ATP, 1.5 mM $MgCl_2$ in acrylic batch plates inside the anaerobic chamber. The plates containing the crystals were moved into an O_2-free argon bath for ease of manipulation before freezing. The crystals were briefly exposed to oxygen (≤ 1 s) during flash freezing in liquid nitrogen. Tagless CobA in complex with MgATP and cob(II)alamin crystallized in the space group $P2_12_12_1$ with unit cell dimensions of a = 59.7 Å, b = 74.2 Å, c = 92.4 Å with one homodimer of CobA per asymmetric unit. Each chain contained ATP, while one chain contained four-coordinate cob(II)alamin and the other contained five-coordinate cob(II)alamin.

X-ray Data Collection and Structure Refinement. X-ray data for the CobA/cob(II)alamin/MgATP complex were collected at 100°K on the Structural Biology Center beamline 19BM at the Advanced Photon Source in Argonne, IL. Diffraction data were integrated and scaled with HKL3000 (31). Data collection statistics are given in Table 2.4. The structure of the CobA/cob(II)alamin/MgATP complex was determined using the *apo* form of CobA (PDB entry 1G5R) (23) as a molecular replacement search model in the program Molrep (32). The final

Table 2.4. Data collection and refinement statistics

complex	CobA·ATP·B12
pdb ID	
space group	$P2_12_12_1$
wavelength	0.979 Å
resolution range	50–1.95 (1.98–1.95)[a]
reflections: measured	647369
reflections: unique	30580
redundancy	4.7 (4.8)
completeness (%)	98.4 (99.8)
average I/σ	29.4 (3.6)
R_{merge} (%)[b]	9.1 (73.2)
R_{work}	17.8
R_{free}	23.0
protein atoms	2769
ligand atoms	225
water molecules	332
average B factors (Å^2)	33.989
Ramachandran (%)	--
most favored	97.8%
allowed	2.2%
disallowed	0.0%
rms deviations	--
bond lengths (Å)	0.020
bond angles (deg)	2.657

[a]Values in parentheses are for the highest resolution shell

[b]$R_{merge} = \Sigma| I_{(hkl)} - I | \times 100 / \Sigma| I_{(hkl)} |$, where the average intensity I is taken over all symmetry equivalent measurements and $I_{(hkl)}$ is the measured intensity for a given observation.

[c]$R_{factor} = \Sigma| F_{(obs)} - F_{(calc)} | \times 100 / \Sigma| F_{(obs)} |$, where R_{work} refers to the R_{factor} for the data utilized in the refinement and R_{free} refers to the R_{factor} for 5% of the data that were excluded from the refinement.

model was generated with alternate cycles of manual model building and least-squares refinement using the programs Coot (33) and Refmac (34). Refinement statistics are presented in Table 2.4.

In vivo Assessment of CobA Variant Function. Mutant *cobA* alleles encoding specific CobA variants were constructed on the plasmid pCOBA70 (Table S2) using the QuickChangeII site-directed mutagenesis kit (Stratagene). Plasmids carrying mutant *cobA* alleles were moved by electroporation into a strain harboring a null allele of *cobA* (JE15023, Table S1). The functionality of CobA variants was assessed in vivo for their ability to restore AdoCbl synthesis in a Δ*cobA* strain during growth on ethanolamine as the sole source of carbon, energy and nitrogen. Strains were grown to full density overnight in Nutrient Broth plus ampicillin (100 μg/mL). A 20 μL sample was used to inoculate fresh minimal medium containing ethanolamine, $(CN)_2$Cbi, and DMB (1:40, v/v) in 96-well plates; each culture was analyzed in triplicate. Growth behavior was monitored for 48 h using a BioTek ELx808 Ultra microplate reader. Data were collected at 630 nm every 1800 s at 30 or 37 °C. Plates were shaken for 1795 s between readings.

In vitro Assessment of CobA Variant Function. Continuous spectrophotometric assays of CobA activity were performed using either cob(II)alamin or cob(I)alamin substrate as described (22,35), with the following modifications. All reaction mixtures contained 0.2 M Tris-HCl (pH 8 at 37 °C), 1.5 mM $MgCl_2$, 0.5-50 μM HOCbl, and 1-1000 μM ATP. Two assays were used to quantify CobA activity: i) the Co^{1+} assay, in which 0.5 mM Ti(III)citrate was used to reduce cob(III)alamin to cob(I)alamin; and ii) the Co^{2+} assay. The reaction mixture of this assay included 44 μg/mL Fpr, 300 μg/mL FldA, and 1 mM NADH to reduce cob(III)alamin to

cob(II)alamin (36). CobA-dependent formation of AdoCbl was monitored using a Perkin-Elmer Lambda 45 UV/Vis spectrophotometer.

2.4 Results and Discussion

Evidence for the Existence of Four-coordinate Cob(II)alamin in the Active Site of CobA. CobA was crystallized under anoxic conditions in the presence of cob(II)alamin in an effort to generate a structure of the enzyme with the physiologically-relevant substrate in its active site. The structure of the CobA/cob(II)alamin/MgATP complex was determined at 2.0 Å resolution where the overall fold is shown in Figure 2.1. The protein crystallized with a dimer in the asymmetric unit. The electron density is well defined for both subunits in the dimer. The final model extends continuously from amino acids Tyr6 - Tyr196 for subunit A and Arg28 - Tyr196 for subunit B. The polypeptide chain exhibits a similar α/β fold to that seen in RecA, F_1ATPase, and adenosylcobinamide kinase/adenosylcobinamide guanylyltransferase (*22*) where a P-loop is located at the end of the first β-strand. Both active sites contain unequivocal electron density for MgATP and a corrinoid (Figure 2.2). As noted in the original structure for CobA, MgATP is oriented in a unique manner in the opposite direction across the P-loop compared to that seen in other enzymes with this fold (*22*). In this way the γ-phosphate resides at the location normally occupied by the α-phosphate in other nucleotide hydrolases. This facilitates transfer of the 5'-carbon of the ribose to the cobalt ion.

The earlier structure of the CobA/hydroxycob(III)alamin/MgATP complex also crystallized with a molecular dimer in the crystallographic asymmetric unit, where both active sites contained MgATP but only one bound cob(III)alamin. In the latter case, the N-terminal section of the

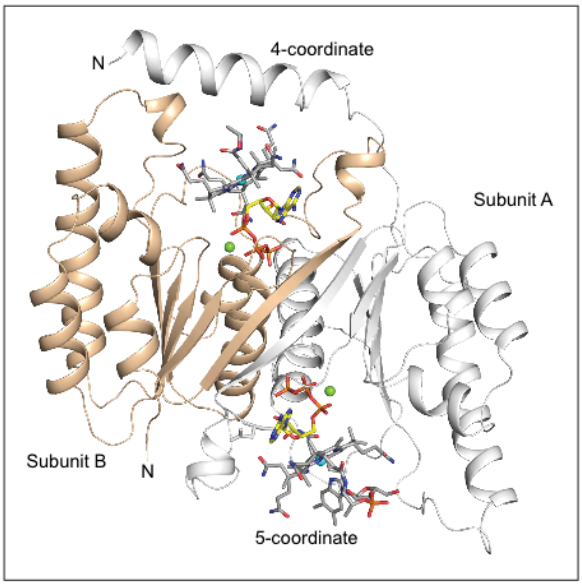

Figure 2.1. Cartoon representation of the *S. enterica* CobA homodimer. Each subunit binds one molecule of MgATP and one molecule of cob(II)alamin. Subunit (B) depicted in wheat binds a four-coordinate cob(II)alamin whereas subunit (A) colored in white binds a five-coordinate cob(II)alamin. The N-terminal helix of subunit A extends over the active site of subunit B, while the N-terminal helix of subunit B is disordered. Figures 2.1-2.5 were prepared with the program Pymol (*47*).

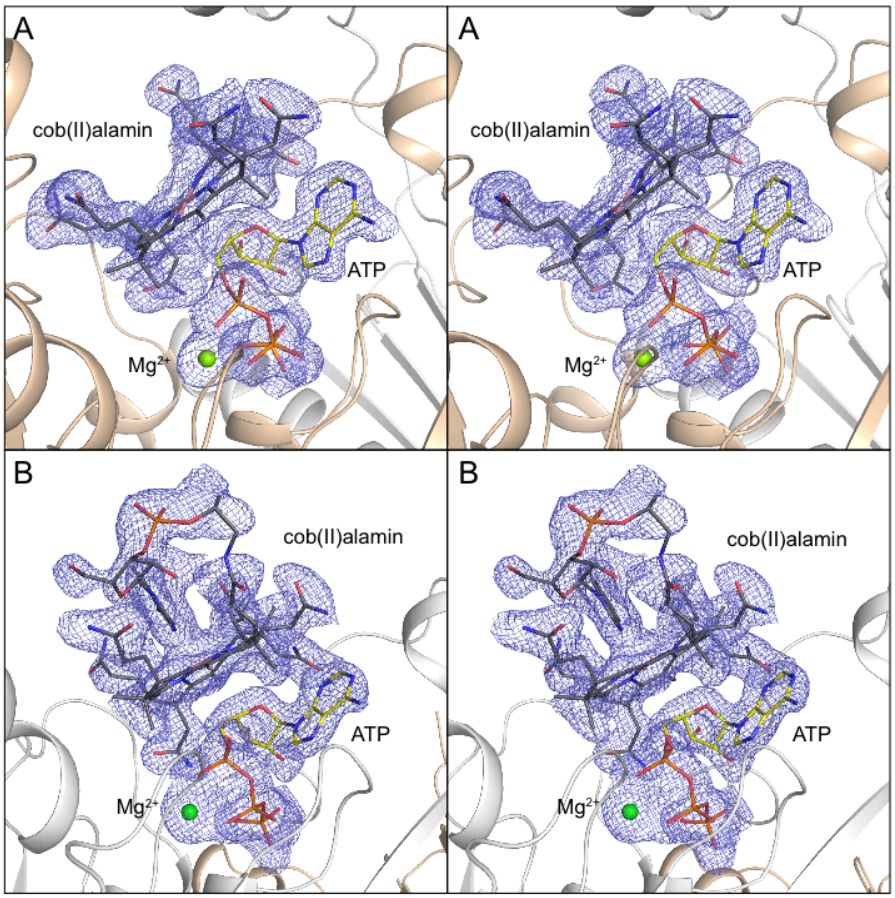

Figure 2.2 Stereo view of the electron density for four-coordinate cob(II)alamin (A), five-coordinate cob(II)alamin (B), and MgATP. Electron density (2.0 σ for four-coordiante cob(II)alamin and MgATP, 1.5 σ for five-coordinate cob(II)alamin) was calculated from coefficients of the form $F_o - F_c$ where cob(II)alamin and MgATP were omitted from phase calculation and refinement. The electron density was not as well defined in the five-coordinate active site.

polypeptide chain from the symmetry related subunit folded over the cobalamin and DMB remained bound to the central cobalt ion. In this way, the active site was formed by sections from both subunits of the dimer. Conversely the corresponding section of the opposing polypeptide chain was disordered in the active site that lacked hydroxycob(III)alamin. In the present crystal structure there is also a dimer in the asymmetric unit but here both active sites include cob(II)alamin and MgATP, but even here there is asymmetry in the molecular dimer, as described below.

In the structure of the CobA/cob(II)alamin/MgATP complex one site is occupied by four-coordinate cob(II)alamin, whilst the other site is occupied by five-coordinate cob(II)alamin. In the active site that contains the four-coordinate cob(II)alamin (subunit B) the N-terminal helix of subunit A folds over the corrin ring and contributes to the displacement of the lower ligand (DMB). In this active site there is no electron density visible for the aminopropanol linkage, nucleotide loop, or DMB, but the remainder of the corrin ring is well defined (Figure 2.2a). Presumably the missing segments of cob(II)alamin are solvent exposed and do not contribute to substrate binding. This observation is consistent with the broad specificity of CobA and its role as a corrinoid salvaging enzyme. The square-planar structure of the Co(II) ion and its four nitrogen ligands from the corrin ring together with the lack of axial ligands reveal the presence of four-coordinate cob(II)alamin. A similar structure was observed in the active site of the *Lactobacillus reuteri* PduO (*Lr*PduO) ACAT (22).

In contrast the other active site (subunit A) contains a five-coordinate cob(II)alamin. Here, the DMB ligand remains coordinated via N3 to the central Co(II) ion. Additionally, the N-terminal helix from opposing subunit B is disordered and could not be modeled due to low electron density. The electron density in this active site is somewhat lower than that of the four-

coordinate site suggesting a lower occupancy. Nevertheless, the density for DMB is well defined, although that for the aminopropanol arm and nucleotide loop is less continuous suggesting conformational flexibility in the absence of the N-terminal helix from the opposing subunit (Figure 2.2b).

Interactions of the Corrin Ring with Side Chains in the Active Site. The protein cores of the two subunits in the asymmetric unit are highly similar and show a root mean square difference of only 0.19 Å between 129 structurally equivalent α-carbon atoms. The only significant differences occur in the regions that interact with the corrin ring and relate to differences between the four- and five-coordination of cob(II)alamin. These differences are discussed later. Overall the corrin ring binds in a similar location in both active sites but is shifted ~0.7 Å further into the binding pocket in the case of the four-coordinate cob(II)alamin (Figure 2.3). In both active sites the corrin ring lies on top of the MgATP so that most of the interactions occur around the periphery of the corrinoid. The four-coordinate cob(II)alamin experiences more interactions than the five-coordinate cob(II)alamin as a consequence of the displacement of DMB and the small movement further into the active site. However the interactions in the five-coordinate species are also found in the four-coordinate site.

There are a very limited number of direct polar interactions to the corrin ring. In the both coordination states there is a hydrogen bond between the carbonyl oxygen of Asp195 and the acetamide group on the β-face of pyrrole ring B, and a hydrogen bond between Oγ of Thr68 and the propionamide group on the α-face of pyrrole ring B (Figure 2.4). The interaction between Asp195 and the acetamide group on the β-face of pyrrole ring B was present in the previously reported structure (23). In the four-coordinate state there are several additional polar interactions, which include hydrogen bonds between the α-face propionamide of pyrrole ring C and the

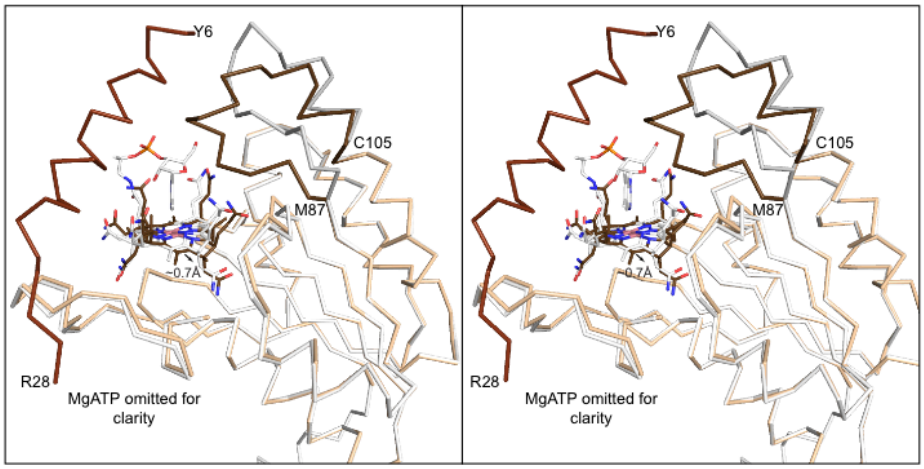

Figure 2.3. Comparison of the polypeptide chain and cob(II)alamin for the four- and five-coordinate states. This shows a stereo ribbon representation of the superposition of the four- and five-coordinate states. The four-coordinate state is depicted in wheat and brown and is denoted as the "closed" conformation of the protein. The five coordinate species is colored in white and light gray and is denoted as the "open" conformation of the protein. The protein fold is essentially identical for both subunits except for the N-terminal helix that is ordered in subunit A and a loop between Met87 and Cys105 (depicted in brown and gray in the closed and open states respectively). This loop is well ordered in both active sites, but rotates to exclude DMB in the four-coordinate state. MgATP was excluded from this figure for clarity.

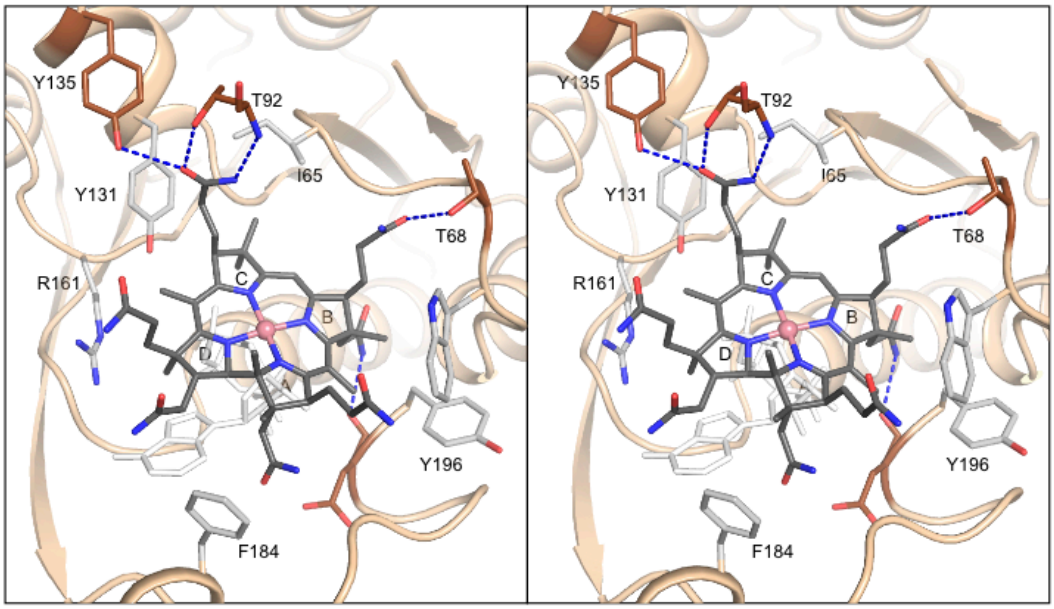

Figure 2.4. Stereoview of the corrin binding site for four-coordinate cob(II)alamin. The corrin ring sits across the MgATP and interacts with a constellation of polar and hydrophobic side chains around the periphery of the corrin ring. The large hydrophobic side chains are colored in gray (*22*). The loop that extends over the corrin ring and displaces DMB in the five-coordinate state (Ala88 - Asn97) was removed for clarity.

hydroxyl of Tyr135, Oγ of Thr92, and amide hydrogen of Thr92. A hydrogen bond is also formed between the amide hydrogen of Thr68 and the α-face propionamide of pyrrole ring B. Apart from these specific interactions there are numerous water-mediated interactions with the remaining polar groups on the corrin ring. It is likely that this ensemble of polar interactions provides conformational specificity, but most of the binding energy is probably derived from the hydrophobic components of the binding site.

The corrin ring is surrounded by a constellation of hydrophobic residues and hydrophobic components of polar side chains (Figure 2.4). The hydrophobic nature of the binding site was noted in the earlier structure of CobA complexed with cob(III)alamin, though most of those residues were not in contact with the corrinoid because the cobalt ion was positioned ~6.1Å from the 5'-carbon of ATP. In the present structure the corrin ring is nestled more deeply in the binding pocket and is in close proximity to Ile65, Trp69, Arg161, Phe184, and Tyr196. This serves to bring the Co(II) ion significantly closer to the MgATP. In the current structure the Co(II) ion is 3.1 Å away from its target and is well-positioned to initiate nucleophilic attack once it is reduced to cob(I)alamin. This closer positioning of the corrin ring to MgATP seen in the Co(II) state compared to the Co(III) state is solely due to the reduction of the cobalt ion and not due to displacement of the lower ligand to attain the four-coordinate state because five-coordinate cob(II)alamin adopts a similar position (Figure 2.3).

Structural Basis for the Formation of Four-coordinate Cob(II)alamin. In the four-coordinate state the lower ligand (DMB) and entire nucleotide arm are displaced by Phe91 and Trp93 and the N-terminal helix from the opposing subunit (Figure 2.5). This yields a closed active site or conformation for the enzyme. Relative to the five-coordinate cob(II)alamin state this displacement involves a conformational change in the loop that extends from Met87 to

Cys105 and includes the a change in the orientation of Phe91 and Trp93. The structure of this loop in the five-coordinate state is essentially identical to that seen in the substrate free and MgATP bound forms reported earlier (Figure 2.5) (*22*). In this case the active site adopts an open conformation. This suggests that the active site can adopt two stable conformational states, the first of which (open) arises in the absence of substrate, presence of MgATP, and in the five-coordinate state. The second conformation (closed) only occurs with four-coordinate cob(II)alamin. Examination of the crystal lattice for the current structure indicates that the active site that carries the five-coordinate cob(II)alamin complex is maintained in the open state by crystal packing forces and thus neither implies nor excludes negative cooperativity between the active sites.

As shown in Figure 2.5, Phe91 and Trp93 move a considerable distance during the transition from the open to closed conformation. The α-carbons of these residues move 7.1 and 5.1 Å respectively whereas the side chains themselves move ~12.1 and 7.5 Å respectively (Figure 2.5). Interestingly, these side chains are mostly buried in both the open and closed conformations suggesting that there is a small difference in hydrophobic stabilization between states. Thus in the closed state the Co(II) is placed in a hydrophobic environment that serves to eliminate water from the α-face of the corrin ring which would quench the cob(I)alamin nucleophile (37).

The N-terminal helix of the adjacent subunit provides additional hydrophobic cover to the α-face of the corrin ring. The side chains of Val13 and Val17 abut the face of Trp93, whereas Val21 contacts the hydrophobic component of the α-propionamide on pyrrole ring A (Figure 2.5).

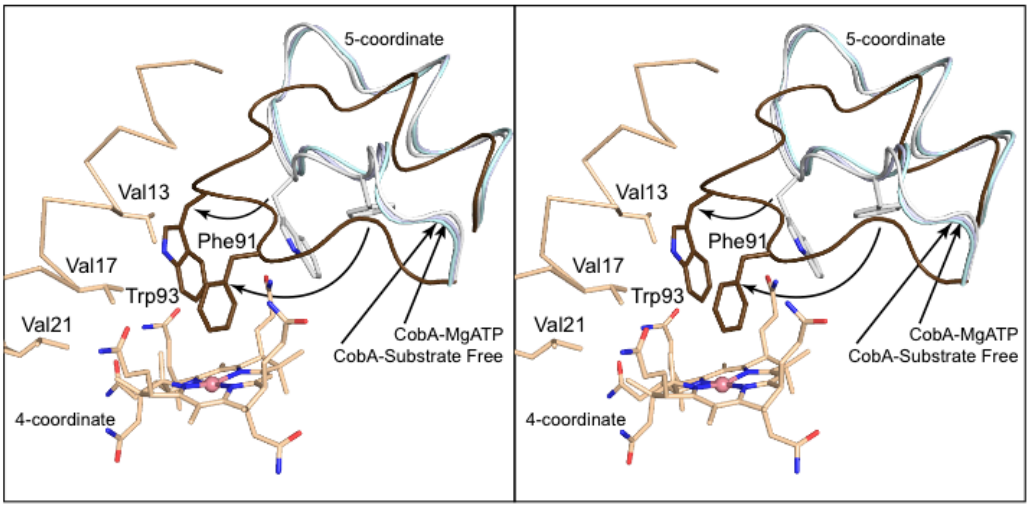

Figure 2.5. Stereo view of the conformational change between the open and closed state of CobA for the loop between Met87 and Cys105. This shows a superposition of the four-coordinate cob(II)alamin closed state and the open state observed in the five coordinate complex. The closed state is depicted in wheat and brown whereas the open state of the cob(II)alamin complex is depicted in white. The conformation of Met87-Cys105 is also seen in the MgATP and substrate free CobA determined earlier (*22*). The loops for these structures are depicted in light cyan and blue respectively. In the closed state Phe91 and Trp93 rotate and translate from a partially buried location within the loop to a stacking position ~4 Å above the corrin ring. The side chains for Phe91 and Trp93 move by ~12.1 and 7.5 Å respectively. The ordered N-terminal helix from the opposing helix is shown in wheat for the closed complex. This contributes three hydrophobic side chains to the corrin binding pocket. The coordinates for the structures of MgATP and substrate free CobA were taken from the RCSB with accession numbers 1G5T and 1G5R respectively.

The structure of the four-coordinate substrate suggests that Phe91 and Trp93 play a critical role in CobA function. This role was tested by site-directed mutagenesis. Both in vitro and in vivo analyses were performed, as each provided unique information about the contribution of these residues to adenosyltransferase activity. The in vivo analysis is a sensitive test for the ability of a variant to produce adenosylated corrinoid, as only small amounts are needed for growth. However, the in vivo analysis cannot distinguish between problems of protein expression and folding versus lack of enzymatic activity. The biochemical analysis provides insight into the molecular consequences of a mutation, but does not necessarily indicate how it might influence the biological fitness of its host. The effect of mutations on in vivo function are described first.

Residues Phe91 and Trp93 are Critical for Function of CobA in vivo. A series of mutant *cobA* alleles were constructed and placed under the control of an inducible promoter for expression, and the resulting variant proteins were tested for their ability to restore AdoCbl synthesis in a Δ*cobA* strain in vivo. *S. enterica* cannot synthesize de novo AdoCbl under aerobic conditions (*1*), but can scavenge incomplete corrinoids. AdoCbl is required for induction of the *eut* operon in *S. enterica*, which allows the strain to catabolize ethanolamine as a carbon, nitrogen, and energy source (*39*). The precursor Cbi was added to the medium instead of Cbl to prevent false positives via the Cbl-specific ACAT, EutT. CobA is capable of adenosylating Cbi and Cbl (*7*). Adenosylated Cbi proceeds via *S. enterica*'s corrinoid salvaging pathway to become AdoCbl (*1*).

Variant CobA proteins with conservative substitutions at these positions (i.e. F91Y, W93F, W93Y) retained sufficient activity to support AdoCbl synthesis at 37ºC resulting in wild-type growth of the Δ*cobA* strain (Figure 2.6A, Group 1). Interestingly, a variant in which residues Phe91 and Trp93 were switched (i.e. $CobA^{F91W, W93F}$) also retained sufficient activity to support

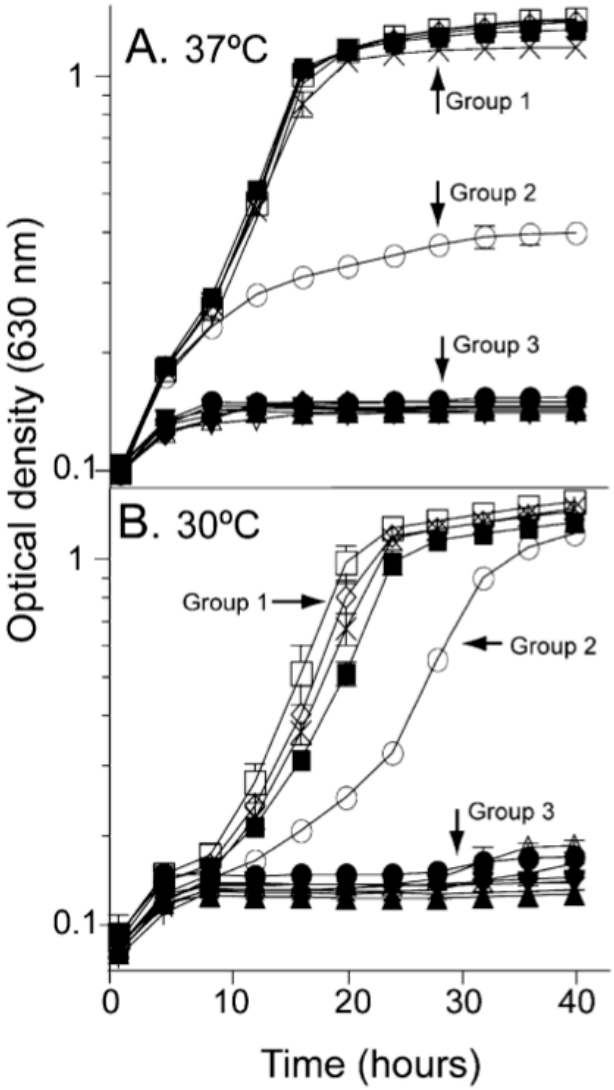

Figure 2.6. Representative growth of *cobA*$^{-}$ strains expressing variant CobA proteins on a plasmid. The medium contained ethanolamine as the sole source of carbon, nitrogen, and energy and was supplemented with $(CN)_2$Cbi and DMB at 37 (A) and 30°C (B), respectively. Strains synthesizing variant CobAs are grouped according to the maximal OD reached under these conditions. Group 1: CobA^{WT} (closed squares), CobA^{F91Y} (open squares), CobA^{W93F} (open triangles), CobA^{W93Y} (crosses), and CobA^{F91W,W93F} (bars). Group 2: CobA^{W93H} (open circles). Group 3: vector control (closed triangles), CobA^{F91A} (inverted closed triangles), CobA^{F91W} (closed diamonds), CobA^{F91H} (closed circles), CobA^{F91D} (open triangles), CobA^{W93A} (plus sign), and CobA^{F91A,W93A} (asterisks).

AdoCbl synthesis at 37ºC (Figure 2.6A, Group 1). Notably, variant CobA^{W93H} only partially restored growth of the Δ*cobA* strain at 37°C (Figure 2.6A, Group 2). When the growth temperature was lowered to 30 °C, CobA^{W93H} supported growth of the Δ*cobA* strain to full density after a short lag and at a slightly slower growth rate (Figure 2.6B, Group 2). In contrast, alanine substitutions at residues Phe91 or Trp93 abolished growth (Figure 2.6B; Group 3).

Residues Phe91 and Trp93 are Needed to Displace the Lower Ligand of Five-coordinate Cob(II)alamin. In general, CobA variants that synthesized enough AdoCbl to support growth of a Δ*cobA* strain on ethanolamine had specific activities similar to that of the wild-type enzyme (Figure 2.7B) with two exceptions that are discussed below. All CobA variants that supported growth of the Δ*cobA* strain on ethanolamine had substitutions that retained aromatic side chains. On the basis of the structure reported here, and extensive analysis of the mechanism of the *Lr*PduO ACAT, we suggest that hydrophobic side chains at positions 91 and 93 play a role in the conversion of five- to four-coordinate cob(II)alamin to allow the formation of the cob(I)alamin nucleophile. In support of this hypothesis, alanine substitutions at either Phe91 or Trp93 resulted in variant enzymes unable to produce sufficient AdoCbl for growth on ethanolamine.

Consistent with the in vivo data, substitutions at Trp93 did not have a major effect on the activity of the enzyme, where the CobA^{W93F}, CobA^{W93Y}, and CobA^{W93H} variants retained ≥78% the specific activity of CobA^{WT}. The effect of a W93H substitution is noteworthy. Even though the in vitro specific activity of the CobA^{W93H} variant with cob(II)alamin was only slightly lower (<10%) than CobA^{WT}, the CobA^{W93H} variant only partially supported growth of the Δ*cobA* strain on ethanolamine (Figure 2.6A, Group 2). To clarify this issue, a Co^{1+} assay was used to measure the combined rate of adenosylation and product release independently of those factors needed to generate the four-coordinate state. The variant CobA^{W93H} only has 58% specific activity relative

to wild type in this assay, yet this value is still higher than several other CobA variants capable of complementation (Figure 2.7A). It is likely that the CobA^{W93H} variant has a detrimental effect in vivo that is not evident in the in vitro assay. Further work is required to elucidate the effects of this variant on corrinoid adenosylation.

The effects of substitutions at position Phe91 were more severe than those at Trp93, which might be expected based on the closer proximity of its side chain to the corrin ring. CobA^{F91A}, CobA^{F91H} and CobA^{F91D} variants lost >95% of their activity relative to CobA^{WT} in the Co^{2+} assay. Surprisingly, a CobA^{F91Y} variant retained sufficient enzymatic activity (85% of CobA^{WT}) to support growth of the Δ*cobA* strain on ethanolamine.

The effect of histidine in the variant CobA^{F91H} was very similar to that reported for the *Lr*PduO ACAT, where replacement of critical Phe112 residue by histidine inactivated the enzyme by mimicking the effect of the coordination of the imidazole ring of DMB with the cobalt ion (22). It is unknown whether the imidazole side chain of the CobA^{F91H} variant interacts with the cobalt ion, but the predicted proximity of the side chain makes this likely.

Kinetic Analyses of CobA Variants. As described above, two assays were used to evaluate CobA activity in vitro. The first assay (referred to as the Co^{2+} assay), used a flavoprotein reductase (Fpr) and NADH to reduce cob(III)alamin to cob(I)alamin via reduced flavodoxin A (FldA). The latter is an electron transfer protein specifically recognized by CobA (12,19). Reduced FldA supplies the electron needed to reduce cob(II)alamin to cob(I)alamin in the active site of CobA. Since the Co^{2+} assay measures the rates of reduction and adenosylation, we consider this assay to be more reflective of what happens in vivo.

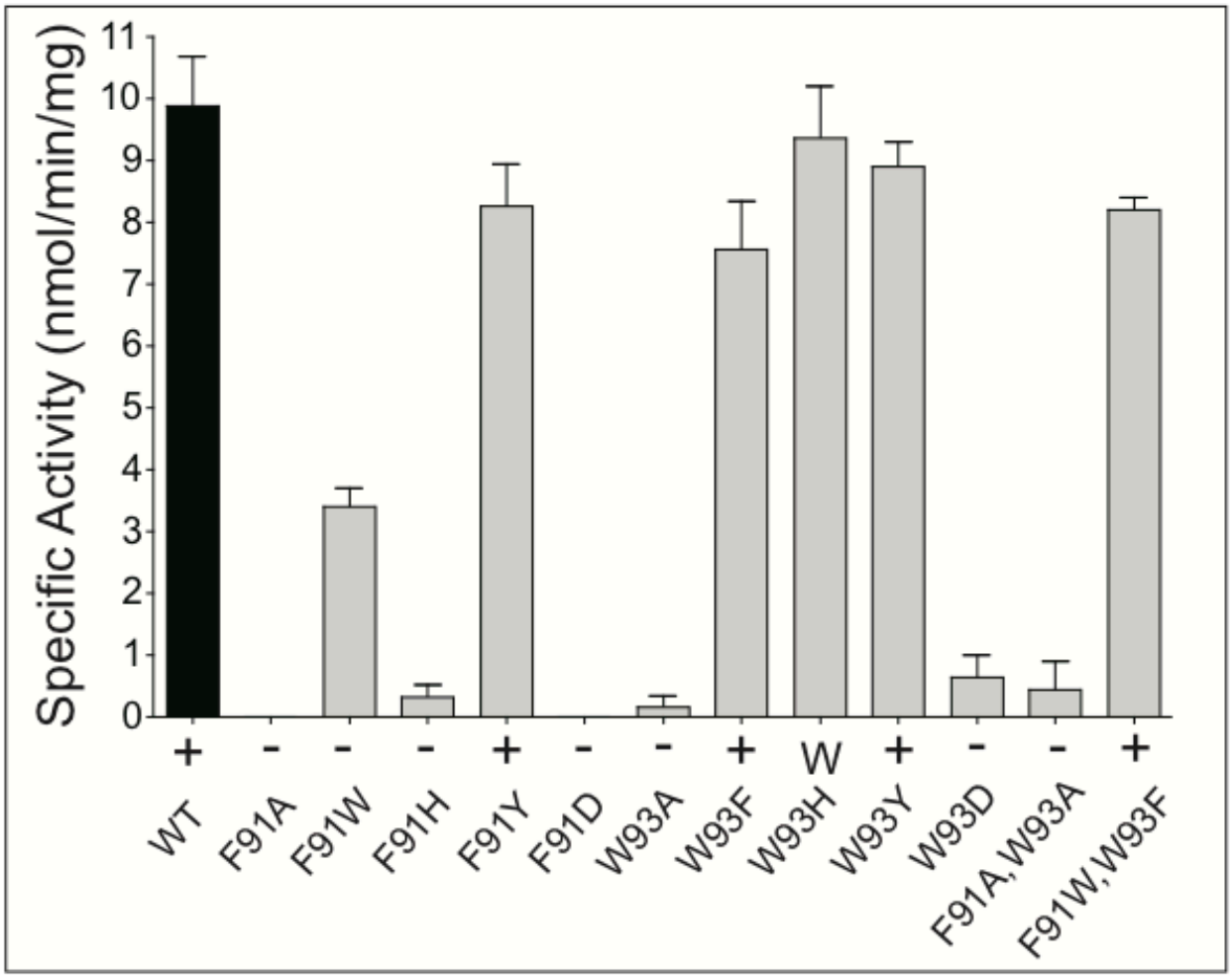

Figure 2.7. In vitro and in vivo assessment of CobA variant function. Histogram represents specific activity when cob(I)alamin (A) or cob(II)alamin (B) was the substrate. Plus and minus signs indicate whether or not a D*cobA* strain synthesizing a plasmid-encoded CobA variant could reach $OD_{630} \geq 0.2$ after 24 h of incubation on ethanolamine medium at 37 °C. The W symbol indicates a Δ*cobA* strain synthesizing a plasmid-encoded CobA variant could not reach $OD_{630} \geq 1.0$ after 24 hours of incubation on ethanolamine medium at 37 °C.

The second assay (referred to as the Co^{1+} assay) bypasses the need for the Fpr/FldA system by chemically reducing cob(III)alamin to cob(I)alamin using Ti(III)citrate(19). Cob(I)alamin is four-coordinate in solution(38) and needs only to be positioned adjacent to ATP to perform a nucleophilic attack on the 5'-carbon of ATP to yield adenosylcobalamin and tripolyphosphate (21).With the exception of $CobA^{F91D}$, all CobA variants had detectable activity with the Co^{1+} assay (Figure 2.7A, Table 2.5). Furthermore, the K_M values of all other variant proteins were <5 fold different than $CobA^{WT}$ with respect to cob(I)alamin and ATP. The reason for the lack of activity in the $CobA^{F91D}$ variant is unknown, although placement of a polar, charged side chain in close proximity to several hydrophobic groups may be detrimental to protein function. Interestingly, the $CobA^{W93D}$ retains ~40% specific activity relative to WT in the Co^{1+} assay, further indicating a greater tolerance for amino acid variation in this position.

In contrast to the Co^{1+} assay, the Co^{2+} assay showed a much greater variation in kinetic parameters among variants with ≥30% $CobA^{WT}$ activity (Table 2.6). The apparent Michaelis constant (K_M) values are higher for $CobA^{F91W}$, $CobA^{W93H}$, and $CobA^{F91W,W93F}$ relative to $CobA^{WT}$, indicating that such substitutions affect the ability of the enzyme to bind substrate under saturating conditions. Surprisingly, the cob(II)alamin K_M values of $CobA^{F91Y}$, $CobA^{W93F}$ and $CobA^{W93Y}$ were 3-, 4-, and 8-fold lower than the that of $CobA^{WT}$.

Turnover (k_{cat}) values were relatively unchanged across all variants, with the exception of 2- and 10- fold enhancements for $CobA^{F91Y}$ with respect to cobalamin and ATP, respectively and a >10- fold decrease with respect to cob(II)alamin for $CobA^{F91W}$. Notable exceptions are discussed below.

While the specific activity of $CobA^{WT}$ increased >30 fold when provided with cob(I)alamin as a substrate, other variants increased only a few fold over their specific activity with

Table 2.5: Kinetic parameters of wild-type CobA and variants using the Co^{1+} assay[a]

	Cob(I)alamin			ATP		
Protein	K_M(μM)	k_{cat} (s^{-1})	k_{cat} / K_M (M^{-1} s^{-1})	K_M(μM)	k_{cat} (s^{-1})	k_{cat} / K_M (M^{-1} s^{-1})
$CobA^{WT}$	4 ± 1	(8 ± 1) x 10^{-2}	(2 ± 0.3) x 10^{4}	7 ± 2	(8 ± 1) x 10^{-2}	(1 ± 0.2) x 10^{4}
$CobA^{F91A}$	5 ± 1	(2 ± 0.1) x 10^{-2}	(4 ± 1) x 10^{3}	9 ± 4	(2 ± 0.1) x 10^{-2}	(2 ± 0.5) x 10^{3}
$CobA^{F91W}$	5 ± 2	(8.0 ± 1) x 10^{-2}	(2 ± 0.3) x 10^{4}	9 ± 2	(8 ± 1) x 10^{-3}	(9 ± 1) x 10^{2}
$CobA^{F91H}$	3 ± 1	(2 ± 1) x 10^{-2}	(5 ± 1) x 10^{3}	3 ± 0.4	(2 ± 0.5) x 10^{-2}	(6 ± 1) x 10^{3}
$CobA^{F91Y}$	1 ± 1	(5 ± 0.3) x 10^{-2}	(5 ± 2) x 10^{4}	0.3 ± 0.1	(5 ± 0.4) x 10^{-2}	(2 ± 0.4) x 10^{5}
$CobA^{F91D}$	ND[b]			ND[b]		
$CobA^{W93A}$	11 ± 4	(5 ± 0.5) x 10^{-2}	(4 ± 1) x 10^{3}	3 ± 0.5	(4 ± 0.2) x 10^{-2}	(2 ± 0.3) x 10^{4}
$CobA^{W93F}$	12 ± 5	(9 ± 1) x 10^{-3}	(8 ± 0.5) x 10^{2}	30 ± 9	(1 ± 0.1) x 10^{-2}	(3 ± 0.5) x 10^{2}
$CobA^{W93H}$	2 ± 0.3	(8 ± 0.5) x 10^{-2}	(4 ± 0.5) x 10^{4}	26 ± 10	(7 ± 0.3) x 10^{-2}	(3 ± 1) x 10^{3}
$CobA^{W93Y}$	16 ± 7	(9 ± 1) x 10^{-3}	(6 ± 2) x 10^{2}	2 ± 0.4	(1 ± 0.1) x 10^{-1}	(7 ± 1) x 10^{3}
$CobA^{W93D}$	2 ± 0.4	(5 ± 0.1) x 10^{-2}	(2 ± 0.3) x 10^{4}	3 ± 1	(5 ± 0.2) x 10^{-2}	(2 ± 0.3) x 10^{4}
$CobA^{F91A,W93A}$	3 ± 1	(1 ± 0.2) x 10^{-2}	(5 ± 1) x 10^{3}	2 ± 0.6	(8 ± 1) x 10^{-3}	(5 ± 1) x 10^{3}
$CobA^{F91W,W93F}$	9 ± 4	(4 ± 0.3) x 10^{-3}	(4 ± 1) x 10^{2}	6 ± 2	(1 ± 0.1) x 10^{-2}	(2 ± 1) x 10^{3}

[a]The cob(I)alamin was generated chemically using Ti(III)citrate as reductant
[b]Not determined due to low activity

cob(II)alamin (Figure 2.7). Kinetic parameters indicated that many of the variants with <10% of the CobA^{WT} activity also had 10 to 15-fold lower catalytic efficiencies with respect to ATP (Table 2.5). Explanations for these observations are not obvious from available data and need to be investigated further.

Effect of a F91W Substitution on CobA Activity. The formation of four-coordinate cob(II)alamin requires a hydrophobic residue of sufficient bulk to displace the α-ligand base. Given that the activity of the CobA^{F91W,W93F} variant was similar to CobA^{WT} in the Co^{2+} assay (Figures 2.5, 2.6), we hypothesized that CobA^{F91W} might also exhibit high levels of activity. Surprisingly, the CobA^{F91W} variant had a >10-fold decrease in k_{cat} values and >10-fold increase in K_M for cob(II)alamin relative to CobA^{WT}. The CobA^{F91W} variant also failed to support growth of a Δ*cobA* strain (Figure 2.5A). In contrast, K_M values for ATP were lower than those of CobA^{F91W} and the turnover number was only a few fold lower than CobA^{WT} in the Co^{2+} assay. Collectively, these data suggest that the F91W replacement affects cob(II)alamin binding or the formation of four-coordinate cob(II)alamin. Kinetic data obtained using the Co^{1+} assay (Table 2.5) support the possibility that lower ligand base displacement is the process affected by this replacement, since the kinetic values for CobA^{F91W} did not differ significantly from CobA^{WT}. This information suggests that binding of cob(I)alamin to CobA^{F91W} is not impaired, but since cob(I)alamin is a four-coordinate species, the reaction can occur as efficiently as in CobA^{WT}.

F91Y Substitution Makes the *S. enterica* CobA a Better Enzyme in vitro. Strikingly, one CobA variant was a better enzyme than CobA^{WT} in vitro in both the Co^{1+} and Co^{2+} assays. In the Co^{1+} assay, the CobA^{F91Y} variant had a ~4 fold lower K_M for cob(I)alamin, a ~20-fold lower K_M with for ATP. In the more physiologically relevant Co^{2+}, the CobA^{F91Y} variant displayed a ~3-

fold higher k_{cat} and ~10 fold higher catalytic efficiency (k_{cat} / K_M) than $CobA^{WT}$. These results were surprising since, based on the structure, it would be predicted that the additional polar hydroxyl group might interfere with ligand binding, coordinate with the cobalt ion, or slow product formation or release. Bioinformatic analysis (39) shows that residue Phe91 is conserved among the CobA family (Figure 2.8). Several species of the genus *Ralstonia* have a tyrosine in place of phenylalanine in the equivalent residue of their putative CobA proteins. Several species, including the plant pathogen *R. solanacearum,* contain the complete suite of AdoCbl biosynthetic genes, several B_{12}-dependent enzymes, and additional ACATs (40). To the best of our knowledge, this is the only variation of this residue tolerated in nature, but this does not explain why this variant has improved kinetic parameters or why it is not seen more frequently.

2.5 Conclusions

The structure and mutational and kinetic analyses of the housekeeping CobA ACAT of *S. enterica* in complex with cob(II)alamin and MgATP offers new insights into its mechanism of catalysis. The structure also revealed how the catalytically important four-coordinate cob(II)alamin intermediate binds to the active site of the enzyme. Although CobA- and PduO-type ACATs are structurally dissimilar, both types of enzymes use similar mechanisms to accomplish corrinoid adenosylation. In CobA, lower ligand base displacement appears to be the result of a coordinated effect of residues Phe91 and Trp93, neither of which can coordinate to the cobalt ion of the ring, bringing the redox potential of the Co^{2+}/Co^{1+} pair within reach of the $FMNH_2$ cofactor of flavodoxin A (FldA). The importance of residues Phe91 and Trp93 was confirmed in vitro and in vivo.

```
Bm_CobA      ------------MLEHRLQKKQHGCKLKFKEKEVFRLKDK------------------RGLTLIYTGDGKGKTTAALGLALRAT
Pp_CobA      ----------------------------------MKN--------------------GLLQVYTGDGKGKTTAAFGMAFRAH
Pm_CobA      MKNKITKEDSRLNKLDKSAERIGMGGNLIPNMTEEKYKERMQKRKEVQTQRLKERKKEKGLIIVNTGQGKGKTTAALGMGLRTI
Se_CobA      -------------MSDERYQQR-----------QQKVKDRVDARVAQAQE-------ERGIIIVFTGNGKGKTTAAFGTAARAV
Af_CobA      ----------------------------------MPVPSR--------------------LLVNTGDGKGKSSAAFGVMGRAW
Ta_CobA      ----------------------------------MESPRRVKPYTKPSGE-------RRGLLIVYTGDGKGKSTAAFGLALRAH
Sp_CobA      ------------------------------------MQGTN-----------------KPLILLYTGNGKGKTTAAMGQLMRAF
Ca_CobA      -----------MSDETTTPVEPGLSPEAKERRKAVRASHTP-----------------KGLVIVNTGNGKGKTTAALGILLRAW
Rs_CobA      ------------MKTDPAAHQR---------MTERR-KAGFEKKKAAATG-------EKGLLIVHTGTGKGKSSAAFGMGLRVV

Bm_CobA      GRGQKVLMIQFIKS--PQRTYGEKLMFDRMG---IEMIQTGVGFTWT-KTPP---EHRDALQKAWALTKEKVFSNEYDVVILDE
Pp_CobA      GRGFKVGVVQFMKT----RATGEVMLAQTLENFFVKRIDTSPKFTWD-MNEAELVELKATIREGFFLICELVKAAEYDMLILDE
Pm_CobA      GHNHNVAIIQFIK---GGWEPGESLAFKIFG-DKLKFHACGEGFTWE---TQDRNRDINLVKSSWRKAVSYIKDPNYKLIILDE
Se_CobA      GHGKNVGVVQFIK---GTWPNGERNLLEPH---GVEFQVMATGFTWE---TQNREADTAACMAVWQHGKRMLADPLLDMVVLDE
Af_CobA      ARGWTVLVVQFLKS--GTWKVGERKLAEHL---GIEFYALGDGFTWE---STDLERTAELGREAWAFAAERLASGAYDLVILDE
Ta_CobA      GRGLRVRIFQFLKH--QGARFGEHRALARL---GIPIEGLGDGFTWK---SRDLEASAQMAREGWARAKEAILSGAYDLVVLDE
Sp_CobA      GHGAKCAVAQFIKDDPEKLDIGEYRTAKTLG---VAWKNFGCGFTWE---GDNDKVNAELAKKGWEQVKRWISTGAFEMIVLDE
Ca_CobA      GRDMRVGGVQFIKH--EQANFGELRALKRMG---ITLTPMGDGFTWT---SRNLDETQARALHGWEVAKQQIAGGDYDVFLLDE
Rs_CobA      GHGMRLGVVQFIK---GALHTAERDLLGRF--DNCDFLTMGEGYTWN---TQDRDADIATARQGWAEARRMIESGDYAMVILDE

Bm_CobA LNNALAIEKFPIDDVSPLHEVIDLIQKRPEH---MHLVITGRSAKKEVMDAADLVTEMKPHKHYY-DEGIPAVKGIEF
Pp_CobA FN------HIIVQGFVTKEEVLELIDAKPDT---MEIVMTGRNAPDWLMERADLVTEMKCIKHPF-DKGIPARVGIEK
Pm_CobA II------VAIKLGYIDEDEIINGINLRPEL---THIVLTGRGASEKLINSADLVTEMKLIHHPFREQGIKAQEGIEY
Se_CobA LT------YMVAYDYLPLEEVISALNARPGH---QTVIITGRGCHRDILDLADTVSELRPVKHAF-DAGVKAQMGIDY
Af_CobA LT------YPVRYGWVSEDAVVEALRSRPSR---TNVIVTGRGAPEGVVELADTVTEMRKVKHAY-DQGIRARKGIEY
Ta_CobA AT------YPLRYGWILLEEFLEALKARPSH---VHVVVTGRGAPEPLLALADTVTEMRKVKHAF-DLGVPAQKGIEH
Sp_CobA FT------YALSLGYLDTEQVCIWIEDHKGKNDFPHLVITGRDAPPRLLAIADMVSEIVEIKHHLTRTGRKSEAMIEF
Ca_CobA FT------YVMHYGWVPASEVVAWLRAHKPP--MLHLIITGRYAPSELIEYADLVTEMHEVKHPFRDQGIRAQPGIEY
Rs_CobA LN------IVLKYDYLPLDEVLAVLAARPAA---LHVVITGRHAPEALVEAADLVTEMRLVKHPYREQGIKAQRGVEY
```

Figure 2.8. Multiple sequence alignment of bacterial CobA proteins. Conserved active site residues are highlighted. Yellow residues are strictly conserved, green is partially conserved. Organism codes are as follows: Bm; *Bacillus megaterium*, Pp; *Paludibacter propionicigenes* WB4, Pm;n *Prochlorococcus mariunus* str. NATL2A, Se; *Salmonella enterica* sv. Typhimurium str. LT2, Am; *Acidimicrobium ferrooxidans* DSM 10331, Ta; *Thermus aquaticus* Y51MC23, Sp; *Sphaerochaeta pleomorpha* str. Grapes, Ca; *Chloroflexus aggregans* DSM 9485, Rs; *Rastonia solanacearum* GMI1000

2.6 References

1. Warren, M. J., Raux, E., Schubert, H. L., and Escalante-Semerena, J. C. (2002) The biosynthesis of adenosylcobalamin (vitamin B12), *Nat. Prod. Rep.* **19**, 390-412.

2. Randaccio, L., Geremia, S., Demitri, N., and Wuerges, J. (2010) Vitamin B12: unique metalorganic compounds and the most complex vitamins, *Molecules* **15**, 3228-3259.

3. Lenhert, P. G., and Hodgkin, D. C. (1961) Structure of the 5,6-dimethylbenzimidazolylcobamide coenzyme, *Nature* **192**, 937-938.

4. Babior, B. M. (1970) The mechanism of action of ethanolamine ammonia-lyase, a B12-dependent enzyme. VII. The mechanism of hydrogen transfer, *J. Biol. Chem.* **245**, 6125-6133.

5. Toraya, T. (2002) Enzymatic radical catalysis: coenzyme B12-dependent diol dehydratase, *Chem. Rec.* **2**, 352-366.

6. Banerjee, R., and Vlasie, M. (2002) Controlling the reactivity of radical intermediates by coenzyme B(12)-dependent methylmalonyl-CoA mutase, *Biochem. Soc. Trans.* **30**, 621-624.

7. Escalante-Semerena, J. C., Suh, S. J., and Roth, J. R. (1990) *cobA* function is required for both de novo cobalamin biosynthesis and assimilation of exogenous corrinoids in *Salmonella typhimurium*, *J. Bacteriol.* **172**, 273-280.

8. Johnson, M. G., and Escalante-Semerena, J. C. (1992) Identification of 5,6-dimethylbenzimidazole as the *Coα* ligand of the cobamide synthesized by *Salmonella typhimurium*. Nutritional characterization of mutants defective in biosynthesis of the imidazole ring, *J. Biol. Chem.* **267**, 13302-13305.

9. Buan, N. R., Suh, S. J., and Escalante-Semerena, J. C. (2004) The *eutT* gene of *Salmonella enterica* encodes an oxygen-labile, metal-containing ATP:corrinoid adenosyltransferase enzyme, *J. Bacteriol.* **186**, 5708-5714.

10. IUPAC-IUB Commission on Biochemical Nomenclature. (1974) The nomenclature of corrinoids (1973 recommendations). *Biochemistry* **13**, 1555-1560.

11. Mera, P. E., and Escalante-Semerena, J. C. (2010) Multiple roles of ATP:cob(I)alamin adenosyltransferases in the conversion of B(12) to coenzyme B (12), *Appl. Microbiol. Biotechnol.* **88**, 41-48.

12. Fonseca, M. V., and Escalante-Semerena, J. C. (2001) An in vitro reducing system for the enzymic conversion of cobalamin to adenosylcobalamin, *J. Biol. Chem.* **276**, 32101-32108.

13. Olteanu, H., Wolthers, K. R., Munro, A. W., Scrutton, N. S., and Banerjee, R. (2004) Kinetic and thermodynamic characterization of the common polymorphic variants of human methionine synthase reductase, *Biochemistry* **43**, 1988-1997.

14. Lexa, D., and Saveant, J.-M. (1983) The electrochemistry of vitamin B12, *Acc. Chem. Res.* **16**, 235-243.

15. Stich, T. A., Brooks, A. J., Buan, N. R., and Brunold, T. C. (2003) Spectroscopic and computational studies of Co(3+)-corrinoids: spectral and electronic properties of the B(12) cofactors and biologically relevant precursors., *J. Am. Chem. Soc.* **125**, 5897-5914.

16. Stich, T. A., Buan, N. R., and Brunold, T. C. (2004) Spectroscopic and computational studies of Co(2+)corrinoids: spectral and electronic properties of the biologically relevant base-on and base-off forms of Co(2+)cobalamin., *J. Am. Chem. Soc.* **126**, 9735-9749.

17. Park, K., Mera, P. E., Escalante-Semerena, J. C., and Brunold, T. C. (2008) Kinetic and spectroscopic studies of the ATP:corrinoid adenosyltransferase PduO from *Lactobacillus reuteri*: substrate specificity and insights into the mechanism of Co(II)corrinoid reduction, *Biochemistry* **47**, 9007-9015.

18. Stich, T. A., Buan, N. R., Escalante-Semerena, J. C., and Brunold, T. C. (2005) Spectroscopic and computational studies of the ATP:Corrinoid adenosyltransferase (CobA) from *Salmonella enterica*: Insights into the mechanism of adenosylcobalamin biosynthesis., *J. Am. Chem. Soc.* **127**, 8710-8719.

19. Buan, N. R., and Escalante-Semerena, J. C. (2005) Computer-assisted docking of flavodoxin with the ATP:Co(I)rrinoid adenosyltransferase (CobA) enzyme reveals residues critical for protein-protein interactions but not for catalysis, *J. Biol. Chem.* **280**, 40948-40956.

20. Hoover, D. M., Jarrett, J. T., Sands, R. H., Dunham, W. R., Ludwig, M. L., and Matthews, R. G. (1997) Interaction of *Escherichia coli* cobalamin-dependent methionine synthase and its physiological partner flavodoxin: binding of flavodoxin leads to axial ligand dissociation from the cobalamin cofactor, *Biochemistry* **36**, 127-138.

21. Fonseca, M. V., Buan, N. R., Horswill, A. R., Rayment, I., and Escalante-Semerena, J. C. (2002) The ATP:co(I)rrinoid adenosyltransferase (CobA) enzyme of *Salmonella enterica* requires the 2'-OH Group of ATP for function and yields inorganic triphosphate as its reaction byproduct, *J. Biol. Chem.* **277**, 33127-33131.

22. Bauer, C. B., Fonseca, M. V., Holden, H. M., Thoden, J. B., Thompson, T. B., Escalante-Semerena, J. C., and Rayment, I. (2001) Three-dimensional structure of ATP:corrinoid adenosyltransferase from *Salmonella typhimurium* in its free state, complexed with MgATP, or complexed with hydroxycobalamin and MgATP, *Biochemistry* **40**, 361-374.

23. Mera, P. E., St Maurice, M., Rayment, I., and Escalante-Semerena, J. C. (2009) Residue Phe112 of the human-type corrinoid adenosyltransferase (PduO) enzyme of *Lactobacillus reuteri* is critical to the formation of the four-coordinate Co(II) corrinoid substrate and to the activity of the enzyme, *Biochemistry* **48**, 3138-3145.

24. Ratzkin, P., and Roth, J. R. (1978) Cluster of genes controlling proline degradation in Salmonella typhimurium, *J. Bacteriol.* **133**, 744-754.

25. Balch, W. E., and Wolfe, R. S. (1976) New approach to the cultivation of methanogenic bacteria: 2-mercaptoethanesulfonic acid (HS-CoM)-dependent growth of *Methanobacterium ruminantium* in a pressurized atmosphere, *Appl. Environ. Microbiol.* **32**, 781-791.

26. Bertani, G. (1951) Studies on lysogenesis. I. The mode of phage liberation by lysogenic *Escherichia coli*., *J. Bacteriol.* **62**, 293-300.

27. Bertani, G. (2004) Lysogeny at mid-twentieth century: P1, P2, and other experimental systems., *J. Bacteriol.* **186**, 595-600.

28. Gasteiger, E., Gattiker, A., Hoogland, C., Ivanyi, I., Appel, R. D., and Bairoch, A. (2003) ExPASy: The proteomics server for in-depth protein knowledge and analysis, *Nucleic Acids Res.* **31**, 3784-3788.

29. Rocco, C. J., Dennison, K. L., Klenchin, V. A., Rayment, I., and Escalante-Semerena, J. C. (2008) Construction and use of new cloning vectors for the rapid isolation of recombinant proteins from *Escherichia coli*, *Plasmid* **59**, 231-237.

30. Blommel, P. G., and Fox, B. G. (2007) A combined approach to improving large-scale production of tobacco etch virus protease, *Protein Expr. Purif.* **55**, 53-68.

31. Otwinowski, Z., and Minor, W. (1997) Processing of X-ray diffraction data collected in oscillation mode., *Method. Enzymol.* **276**, 307-326.

32. Vagin, A., and Teplyakov, A. (2000) An approach to multi-copy search in molecular replacement, *Acta Crystallogr. D Biol. Crystallogr.* **56**, 1622-1624.

33. Emsley, P., and Cowtan, K. (2004) Coot: model-building tools for molecular graphics., *Acta Crystallogr. D. Biol. Crystallogr.* **60**, 2126-2132.

34. Murshudov, G. N., Vagin, A. A., Lebedev, A., Wilson, K. S., and Dodson, E. J. (1999) Efficient anisotropic refinement of macromolecular structures using FFT, *Acta Crystallogr. D. Biol. Crystallogr.* **55** *(Pt 1)*, 247-255.

35. St Maurice, M., Mera, P., Park, K., Brunold, T. C., Escalante-Semerena, J. C., and Rayment, I. (2008) Structural characterization of a human-type corrinoid adenosyltransferase confirms that coenzyme B_{12} is synthesized through a four-coordinate intermediate, *Biochemistry* **47**, 5755-5766.

36. Fonseca, M. V., and Escalante-Semerena, J. C. (2000) Reduction of cob(III)alamin to cob(II)alamin in *Salmonella enterica* Serovar Typhimurium LT2., *J. Bacteriol.* **182**, 4304-4309.

37. Ouyang, L., Rulis, P., Ching, W. Y., Nardin, G., and Randaccio, L. (2004) Accurate redetermination of the X-ray structure and electronic bonding in adenosylcobalamin, *Inorg. Chem.* **43**, 1235-1241.

38. Marsh, E. N., and Harding, S. E. (1993) Methylmalonyl-CoA mutase from *Propionibacterium shermanii*: characterization of the cobalamin-inhibited form and sububit-cofactor interactions studied by analytical ultracentrifugation., *Biochem. J.* **290**, 551-555.

39. Roof, D. M., and Roth, J. R. (1992) Autogenous regulation of ethanolamine utilization by a transcriptional activator of the *eut* operon in *Salmonella typhimurium*. *J. Bacteriol.* **174**, 6634-6643.

40. Liu, D., Williamson, D. A., Kennedy, M. L., Williams, T. D., Morton, M. M., and Benson, D. R. (1999) Aromatic side chain-porphyrin interactions in designed hemoproteins, *J. Amer. Chem. Soc.* **121**, 11798-11812.

41. Wirt, M. D., Sagi, I., and Chance, M. R. (1992) Formation of a square-planar cobalt(I) B-12 intermediate: implication for enzyme catalysis., *Biophys. J.* **63**, 412-417.

42. Altschul, S. F., Gish, W., Miller, W., and Myers, E. W. (1990) Basic local alignment search tool., *J. Mol. Biol.* **215**, 403-410.

43. Rodionov, D. A., Vitreschak, A. G., Mironov, A. A., and Gelfand, M. S. (2003) Comparative genomics of the vitamin B_{12} metabolism and regulation in prokaryotes, *J. Biol. Chem.* **278**, 41148-41159.

44. Padovani, D., Labunska, T., and Banerjee, R. (2006) Energetics of interaction between the G-protein chaperone, MeaB, and B12-dependent methylmalonyl-CoA mutase, *J. Biol. Chem.* **281**, 17838-17844.

45. Padovani, D., Labunska, T., Palfey, B. A., Ballou, D. P., and Banerjee, R. (2008) Adenosyltransferase tailors and delivers coenzyme B12, *Nat. Chem. Biol.* **4**, 194-196.

46. Padovani, D., and Banerjee, R. (2009) A G-protein editor gates coenzyme B12 loading and is corrupted in methylmalonic aciduria, *Proc. Natl. Acad. Sci. U S A* **106**, 21567-21572.

47. DeLano, W.L. (2002) The Pymol Molecular Graphics System. DeLano Scientific, USA.

CHAPTER 3

THE EUTT ENZYME OF *SALMONELLA ENTERICA* IS A UNIQUE ATP:COB(I)ALAMIN ADENOSYLTRANSFERASE METALLOPROTEIN THAT REQUIRES FERROUS IONS FOR MAXIMAL ACTIVITY[2]

[2] Moore T.C., Mera P.E. and J.C. Escalante-Semerena. 2014. *J. Bacteriol*. 196:903-910.
Reprinted here with permission from the publisher

3.1 Abstract

ATP:co(I)rrinoid adenosyltransferase (ACAT) enzymes convert vitamin B_{12} to coenzyme B_{12}. EutT is the least understood ACAT. We report the purification of EutT to homogeneity and show that, in vitro, free dihydroflavins drive the adenosylation of cob(II)alamin bound to EutT. Results of chromatography analyses indicate that EutT is dimeric in solution, and unlike other ACATs, EutT catalyzes the reaction with sigmoidal kinetics indicative of positive cooperativity for cob(II)alamin. Maximal EutT activity was obtained after metalation with ferrous ions. EutT/Fe(II) protein lost all activity upon exposure to air and H_2O_2, consistent with previously reported results indicating that EutT was an oxygen-labile metalloprotein containing a redox-active metal. Results of in vivo and in vitro analyses of single-amino-acid variants affecting a $HX_{11}CCXXC_{83}$ motif conserved in EutT proteins showed that residues His67, Cys80, and Cys83 were required for EutT function in vivo, while Cys79 was not. Unlike that of other variants, the activity of the EutTC80A variant was undetectable in vitro, suggesting that Cys80 was critical to EutT function. Results of circular dichroism studies indicate that the presence or absence of a metal ion does not affect protein folding. EutT can now be purified in the presence of oxygen and reactivated with ferrous ions for maximal activity.

3.2 Introduction

Coenzyme B_{12} (adenosylcobalamin, AdoCbl, CoB_{12}) is an essential nutrient for animals, lower eukaryotes, and many prokaryotes. The unique organometallic bond of AdoCbl, between the cobalt ion of the corrinoid and the carbon of the 5'-deoxyadenosyl group, lies at the center of its reactivity. The formation of this bond is catalyzed by ATP:cob(I)alamin adenosyltransferase (ACAT) enzymes (1). There are three types of ACAT enzymes, namely, CobA, PduO, and EutT (2–8). They do not share sequence similarity at the nucleotide level or at the amino acid level,

making them a good example of convergent evolution. All three ACAT types were discovered in Salmonella enterica, and they serve distinct growth requirements. The CobA type is the housekeeping ACAT, whereas PduO and EutT are specialized enzymes needed for growth on 1,2-propanediol and ethanolamine, respectively (7, 9).

Extensive work has been done to understand the mechanism of corrinoid adenosylation performed by the CobA and PduO type ACATs. These two types of enzymes facilitate the thermodynamically unfavorable reduction of cob(II)alamin to cob(I)alamin by generating a cob(II)alamin four-coordinate intermediate in the active site of the enzyme (10–12). Both CobA and PduO use conserved aromatic side chains located directly below the cobalt ion to displace the lower ligand of Cbl and generate the four-coordinate species (5, 13). The reduction potential of the cobalt ion in this intermediate is raised enough so that free or protein-bound dihydroflavins can reduce cob(II)alamin to cob(I)alamin (5). Unlike the CobA and PduO type ACAT enzymes, nothing is known about the mechanism of how the thermodynamically unfavorable reduction to cob(II)alamin is facilitated when EutT type ACAT enzymes adenosylate Cbl. In fact, the EutT type enzyme is the least understood of the three types of ACATs because it has not been isolated to homogeneity.

We previously reported a method for enriching a sample with EutT using detergents (6). We proposed that the EutT type ACAT enzyme contained a metal cofactor because the protein contains an $HX_{11}CCXXC_{83}$ motif that resembles those found in Fe/S-containing proteins and inferred that the metal cofactor was labile to oxidation and could be extracted from the protein by metal chelators (6). Problems with the isolation of EutT hindered its biochemical characterization.

In this study, we successfully purified wild-type EutT to homogeneity in the absence of detergents. Herein, we report the initial kinetic characterization of EutT and show that the enzyme requires a divalent, transition state metal ion and is most active when in complex with ferrous ions. Results from experiments using homogeneous EutT demonstrate that free dihydroflavins can reduce cob(II)alamin, suggesting that EutT, similar to CobA and PduO, facilitates the unfavorable reduction of cob(II)alamin. This is the first known example of an ACAT requiring an inorganic cofactor for activity.

3.3 Materials and Methods

Construction of expression vectors. To generate a recombinant construct of EutT with an N-terminal hexahistidine (H6) tag and a maltose- binding protein (MBP) tag in tandem, the *S. enterica eutT* allele was PCR amplified from the *S. enterica* strain JE6583 (see Table 3.1). The primers used for the amplification were 5'-GTAG GTACCATGAACGATTTCATCACCGAAAC-3' (forward) and 5'ATCA AGCTTTCATGGCTTCTCTCCCAACC-3' (reverse). The PCR fragment and the vector pTEV6 (14) were cut with restriction enzymes KpnI and HindIII and then ligated, yielding plasmid pEUT76 (see Table 3.1). Plasmid pEUT76 directed the synthesis of a recombinant H6-MBP-EutT protein whose tags were removed using recombinant tobacco etch virus (rTEV) protease (15). Tagless EutT protein contained two residues (Gly-Thr) upstream of its N-terminal methionine; such residues did not block enzyme function.

Table 3.1: Strains and plasmids used over the course of this study

Strain ID	Genotype	Plasmid	Allele	Protein encoded	Source
***E. coli* strains**					
JE3892	BL21 (λ*DE3*)				Laboratory collection
DH5α	*fhuA2* Δ*(argF-lacZ)U1(* *phoA glnV44 Φ80* Δ*(lacZ)M15 gyrA96 recA1 relA1 endA1 thi-* *hsdR17*				
Derivatives of DH5α					Laboratory collection
JE11332		pEUT76	*eutT*$^{+}$	H_6-MBP-EutT^{WT}	
JE17480		pEUT98	*eutT1193*	H_6-MBP-EutT^{H67A}	
JE11814		pEUT81	*eutT1187*	H_6-MBP-EutT^{C79A}	
JE11815		pEUT82	*eutT1188*	H_6-MBP-EutT^{C80A}	
JE11894		pEUT83	*eutT1189*	H_6-MBP-EutT^{C83A}	
JE11816		pEUT84	*eutT1190*	H_6-MBP-EutT^{C79A,C80A}	
JE11846		pEUT86	*eutT1191*	H_6-MBP-EutT^{C79A,C80A,C83A}	
JE7095		pEUT7	*eutT*$^{+}$	EutT^{WT}	
JE17480		pEUT95	*eutT1192*	EutT^{H67A}	
JE8117		pEUT36	*eutT1187*	EutT^{C79A}	
JE8119		pEUT37	*eutT1188*	EutT^{C80A}	
JE8121		pEUT38	*eutT1189*	EutT^{C83A}	
***S. enterica* strains**[1]					
JE6583	*metE205 ara-9*				Laboratory collection
JE13176	*metE205 ara-9* Δ*eut1141,* Δ*pduO523, cobA343*::MudJ				
Derivatives of JE13176					Laboratory collection
JE13253		pBAD24		Vector control	
JE13199		pEUT7	*eutT*$^{+}$	EutT^{WT}	
JE17482		pEUT95	*eutT1194*	EutT^{H67A}	
JE131200		pEUT36	*eutT1187*	EutT^{C79A}	
JE131201		pEUT37	*eutT1188*	EutT^{C80A}	
JE131202		pEUT38	*eutT1189*	EutT^{C83A}	

[1]All *S. enterica* strains were derivatives of *S. enterica* sv Typhimurium strain LT2

eutT alleles encoding variant EutT proteins were generated using the QuikChange XL site-directed mutagenesis kit (Stratagene). The pEUT76 plasmid was used as the template for the PCR-based site-directed mutagenesis in accordance with the manufacturer's instructions. Mutations were confirmed by DNA sequencing using nonradioactive BigDye (ABI-Prism) protocols. DNA sequencing reactions were resolved at the Biotechnology Center of the University of Wisconsin-Madison.

EutT protein overproduction and purification. Escherichia coli strain BL21(DE3) was used to overproduce wild-type and variant EutT proteins. Strains were grown at 37°C with 200-rpm agitation in Super Broth (SB) medium supplemented with ampicillin (100 μg/ml). After the culture reached an optical density at 650 nm (OD650) of 0.7, the inducer isopropyl-β-D-thiogalactopyranoside (IPTG; 1 mM) was added to the medium. Cells were grown an additional 12 h at 15°C and harvested by centrifugation at 12,000 x g (15 min) using a Beckman/Coulter Avanti J-25I centrifuge equipped with a JLA-16.250 rotor. Cell pellets were frozen at 80°C until used.

The purification steps described below were performed inside an anoxic chamber (Coy Laboratories) at 25°C; anoxic conditions during centrifugation steps were maintained using stainless steel tubes fitted with lids fitted with expandable O rings. Cell pellets obtained from a 1-liter culture (5 g of wet cell paste) were thawed and resuspended in 30 ml of piperazine-N,N'-bis(2-ethanesulfonic acid) (PIPES) buffer (0.1 M, pH 7.0 at 25°C) containing the protease inhibitor phenylmethanesulfonyl fluoride (PMSF; 1 mM), DNase (25 μg/ml), lysozyme (1 μg/ml), imidazole (20 mM), tris(2-carboxyethyl)phosphine (TCEP; 1 mM), and NaCl (0.5 M). The high salt concentration was included to maintain EutT solubility. The resuspended cell paste

was loaded into a French pressure cell at 4°C under a stream of O2-free nitrogen to create an anoxic environment. The cell suspension was passed through the French press once at 103 MPa. The cell lysate was collected and sealed while being flushed with O2-free nitrogen gas. Cell debris was removed by centrifugation at 4°C for 45 min at 45,000 xg. The resulting supernatant was filtered (0.45 μm; Nalgene), and proteins were resolved from crude lysate using an ÄKTA Purifier fast protein liquid chromatograph equipped with a 5-ml HisTrap column (GE Healthcare).

The column was washed with 25 ml of buffer A (PIPES; 0.1 M, pH 7.0 at 25°C), imidazole (70 mM), TCEP (1 mM), and NaCl (0.5 M). H6-MBP-EutT was eluted with 25 ml buffer B (PIPES [0.1 M, pH 7.0 at room temperature], imidazole [0.5 M], TCEP [1 mM], and NaCl [0.5 M]). Purified rTEV protease (15) (1 mg/ml) was mixed with H6-MBP-EutT (1:50 [vol/vol]). ATP (1 mM) was added to buffer B for stability. The buffer of this mixture was exchanged using PD-10 desalting columns (packed with Sephadex G-25; GE Healthcare) equilibrated with buffer C (PIPES buffer [0.1 M, pH 7.0 at 25°C], imidazole [20 mM], and NaCl [0.5 M]).

Untagged EutT protein was separated from the cleaved H6-MBP tag on a 5-ml HisTrap column over 25 ml of buffer C. The column flowthrough was collected, and the buffer was exchanged for storage buffer (PIPES [0.2 M, pH 7.0 at 25°C] containing NaCl [0.25 M], and TCEP [1 mM]). The untagged EutT protein mixture was loaded onto a column packed with 5 ml of amylose resin (New England BioLabs) to resolve EutT from trace amounts of the H6-MBP tag. The column flowthrough was collected over 25 ml. Protein concentration was determined by measuring the absorbance at 280 nm using the calculated molar extinction coefficient (24980; ExPASy [16]). Glycerol was added to a final concentration of 50% (vol/vol), and additional ATP (0.25 mM) was added. Tagless EutT protein was stored in sealed anoxic vials at 20°C for up to

6 months without loss of activity. In vitro adenosyltrasferase activity assays. The Co^{1+} and Co^{2+} continuous assays were performed as described previously (5, 17) with the following modification: the reaction buffer for the enzyme assay was changed to PIPES (50 mM, pH 7.0 at 37°C) to optimize EutT activity. The reaction buffer was treated with Chelex 100 resin (Bio-Rad) to remove trace metals. The extinction coefficient (ε) for AdoCbl at 525 nm in this buffer was determined to be 0.0074 M^{-1} cm^{-1} using pure AdoCbl standards. The calculated molar extinction coefficient for AdoCbl was consistent with values reported in the literature (18). In the Co^{2+} assay, cob(II)alamin was chemically reduced to cob(I)alamin using Ti(III)citrate (19), whereas in the Co2 assay cob(II)alamin was reduced in the active site of EutT by free or protein-bound dihydroflavins as described previously (20). The optimal concentration of free dihydroflavins in the Co^{2+} assay was found to be 20 μM, and reduced flavin adenine dinucleotide ($FADH_2$) was used as the electron donor in the kinetic assays. A preincubation step (15 to 20 min) was sufficient for the reduced dihydroflavins to completely reduce hydroxycob(III)alamin to cob(II)alamin. The flavin reductase Fre (0.005 mg/ml) and NADH (1 mM) were included to maintain the pool of reduced dihydroflavins. These assays were performed under anoxic conditions at 37°C; MgATP was added to a final concentration of 1 mM. Assays in relation to ATP were not performed due to the presence of ATP added to EutT to enhance its stability.

In vitro metalation of EutT. Purified EutT was dialyzed three times for 20 min each into HEPES buffer (50 mM, pH 7.0), TCEP (1 mM), and EDTA (1 mM) using D-tube dialyzers (10,000 molecular weight cutoff [MWCO]; Novagen) to remove bound metals from the protein. EutT was dialyzed three times for 20 min each time into PIPES (50 mM, pH 7) and TCEP (1 mM) to remove EDTA. The dilution factor for each individual dialysis was 1:7,000. All dialyses were performed using anoxic buffers inside an anoxic chamber. All buffers were treated with

Chelex 100 resin (Bio-Rad) to remove trace metals. Demetalated EutT was incubated anoxically for 1 h on ice with one of several divalent metal cations (1 mM) in PIPES (50 mM, pH 7) and TCEP (1 mM). EutT was also incubated with the divalent metals in the presence of oxygen and H_2O_2 (0.3%). H_2O_2 was quenched by addition of catalase (550 units/ml; Sigma) after the first 5 min of incubation. Specific activity was evaluated using the Co2 assay.

Elemental analysis of EutT protein. Inductively coupled plasma optical emission spectroscopy (ICP-OES) was performed on EutT protein samples at the University of Wisconsin-Madison Soil Testing Laboratory (Verona, WI). Samples of EutT protein that was 99% homogeneous were concentrated to 6 μM in 10 ml storage buffer containing PIPES (50 mM, pH 7.0 at 25°C) and TCEP (0.5 mM) supplemented with nitric acid (1% [vol/vol]) to enhance metal solubility. Additional replicates were run at the University of Georgia Chemical Analysis Laboratory (Athens, GA) using the same protocol described above.

Iron-binding assays. EutT was demetalated in an anaerobic chamber as described above and incubated with 1 molar equivalent of Fe^{2+} for 1 h on ice. The protein was precipitated by addition of urea and removed from solution by centrifugation. A colorimetric iron assay kit (Sigma) was used to quantify the amount of Fe^{2+} remaining in the solution in comparison to standards.

Circular dichroism spectroscopy. Circular dichroism (CD) spectroscopy was performed on a model 202SF circular dichroism spectrophotometer (Aviv Biomedical) at the University of Wisconsin-Madison Biophysics Instrumentation Facility (Madison, WI). EutT was demetalated as described above and incubated with either zinc or a buffer control after dialysis into phosphate buffer (10 mM, pH 7). Scans were run from 190 to 310 nm using a 0.1-mm diameter cuvette at 37°C.

Oligomeric determination of EutT. Size exclusion chromatography inside an anoxic chamber was used to determine the oligomeric state of wild-type EutT and its variants in the absence or presence of ATP. EutT samples were dialyzed against 500 ml of phosphate buffer (50 mM, pH 7) containing 0.15 M NaCl for 30 min to remove any trace of ATP. Two more 30-min dialyses were subsequently repeated with fresh buffer. A subset of the EutT samples were incubated with a 10 molar excess of ATP on ice for 30 min prior to being resolved on the gel permeation column. EutT was resolved using a 25-ml Superose 12 (10/300 GL) column (GE Healthcare) developed at a flow rate of 0.5 ml/min with phosphate buffer (50 mM, pH 7 at room temperature) containing NaCl (0.15 M). The buffer contained ATP (1 mM) when EutT samples previously incubated with ATP were analyzed. Gel filtration standards (Bio-Rad) were used to generate a standard curve for retention times on the column. The standard components were as follows: thyroglobulin (670 kDa), g-globulin (158 kDa), ovalbumin (44 kDa), myoglobin (17 kDa), and vitamin B_{12} (1.35 kDa). Additional standards of chicken egg white lysozyme (14.3 kDa; Sigma), bovine pancreas DNase I (31 kDa; Sigma), and bovine serum albumin (66 kDa; Promega) were used to increase the accuracy of the standard curve.

Native PAGE was performed to assess the stability of EutT variant proteins. A sample containing 5 µg of protein was loaded on a 10% acrylamide gel and developed at 4°C (3 h, 95 V). The set of molecular mass markers comprised bovine serum albumin (66 kDa/monomer), *S. enterica* CobB (25 kDa), and lysozyme (14.3 kDa).

In vivo assessment of function. To assess cobalamin adenosylation in vivo, a strain (JE13176 *cobA*343::MudJ *eut*114 *pduO*523) lacking the housekeeping ACAT enzyme (CobA), the 1,2-propanediol degradation ACAT (PduO), and EutT was used as an indicator strain for growth on minimal medium. No-carbon essential (NCE) minimal medium (21, 22) was supplemented with

ethanolamine (90 mM), methionine (0.5 mM), NH_4Cl (30 mM), MgSO4 (1 mM), L-(+)-arabinose (500 mM), glycerol (0.5 mM), and trace minerals (23). Strain JE13176 (see above) can use ethanolamine as a source of carbon and energy as long as AdoCbl is provided in the medium. Plasmids used for in vivo analysis were previously constructed (6). Plasmids carrying the *eutT*^{WT} and mutant alleles were under the control of the arabinose-inducible P_{ara}*BAD* promoter in plasmid pBAD24 (24).

3.4 Results and Discussion

Isolation of EutT to homogeneity. Our previous approach to the isolation of EutT yielded enriched, partially homogeneous preparations of the protein (70% homogeneity). Under such purification conditions, EutT activity was oxygen labile and was insoluble in the absence of detergent (6, 7). More importantly, the use of detergent prevented the isolation of EutT to homogeneity. By fusing the maltose binding protein (MBP) to EutT, we bypassed the need for detergent, and the protein remained soluble after removal of the tag. This new approach yielded homogeneous EutT (Fig. 3.1). Unexpectedly, EutT remained active in the presence or absence of oxygen, a result that was inconsistent with previous observations (6). Reasons for this inconsistency were identified and are discussed below. The specific activity of homogeneous EutT did not decrease over 6 months when kept at 20°C in 50% glycerol, nor did it decrease over 4 h when removed from 20°C and kept on ice.

EutT can use free dihydroflavins to drive the adenosylation of cob(II)alamin. Our laboratory has shown that PduO ACAT enzymes can use free dihydroflavins to drive the adenosylation of cob(II)alamin (20) and that enzyme activity depended on the generation of a four-coordinate cob(II)alamin species in the active site. The redox potential of free dihydroflavins is not low enough to drive the reduction of free cob(II)alamin to cob(I)alamin in solution, yet it is low

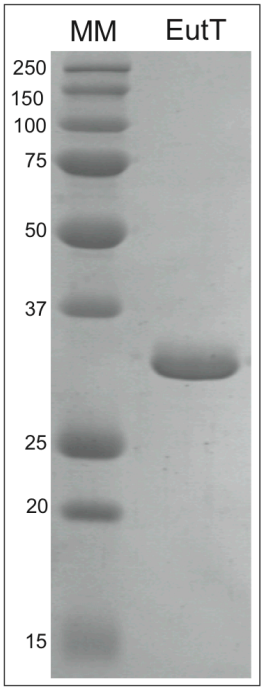

Figure 3.1. Homogeneous *S. enterica* EutT protein. Denaturing polyacrylamide gel electrophoresis (SDS-PAGE) [(1)] of commercially available molecular mass standards and homogeneous EutT protein. A sample containing 10 μg of protein was electrophoresed using a 15% (w/v) gel for 1 h at 200 V, followed by staining with Coomassie Brilliant Blue R. Numbers on the left of the figure refer to the molecular masses of standards described under Materials and Methods.

enough to reduce the four-coordinate cob(II)alamin bound in the active sites of PduO ACATs. The total concentration of free dihydroflavins in S. enterica is unknown, although in E. coli it has been estimated at 4 μM (25). Similar to findings for PduO, free dihydroflavins also reduced cob(II)alamin in the active site of EutT, leading to the formation of AdoCbl (Fig. 3.2). The specific activity of EutT when cob(II)alamin was the substrate was unaffected by the choice of reduced dihydroflavins. That is, incubation with reduced flavin mononucleotide ($FMNH_2$) resulted in specific activity of 15.8 ± 0.2 nmol/min/mg, incubation with $FADH_2$ resulted in specific activity of 16.3 ± 0.4 nmol/min/mg, and incubation with dihydroriboflavin resulted in specific activity of 15.5 ± 0.4 nmol/min/mg. The fact that even dihydroriboflavin, the vitamin form of flavin mononucleotide (FMN) and flavin adenine dinucleotide (FAD) can serve as an electron donor suggested that the 4-coordinate cob(II)alamin species in the active site of EutT could be reached by free reduced flavins without the assistance of a protein. Subsequent work was performed using $FADH_2$ assays. Together, these results suggested that EutT facilitated the unfavorable reduction of cob(II)alamin and that an electron transfer protein might not be necessary for EutT function given the level of reduced dihydroflavins in the cell.

EutT loses activity in the absence of ATP. Initial preparations of EutT enzyme lost catalytic activity over time, even when the enzyme was kept under anoxic conditions on ice. The Co^{2+} assay described in Materials and Methods showed that the activity left after 2h dropped to less than 65% (see Fig. 3.3). This loss of activity was avoided by the addition of MgATP (1 mM) to the buffer. Therefore, subsequent purifications of EutT included MgATP in the buffer used after nickel affinity chromatography.

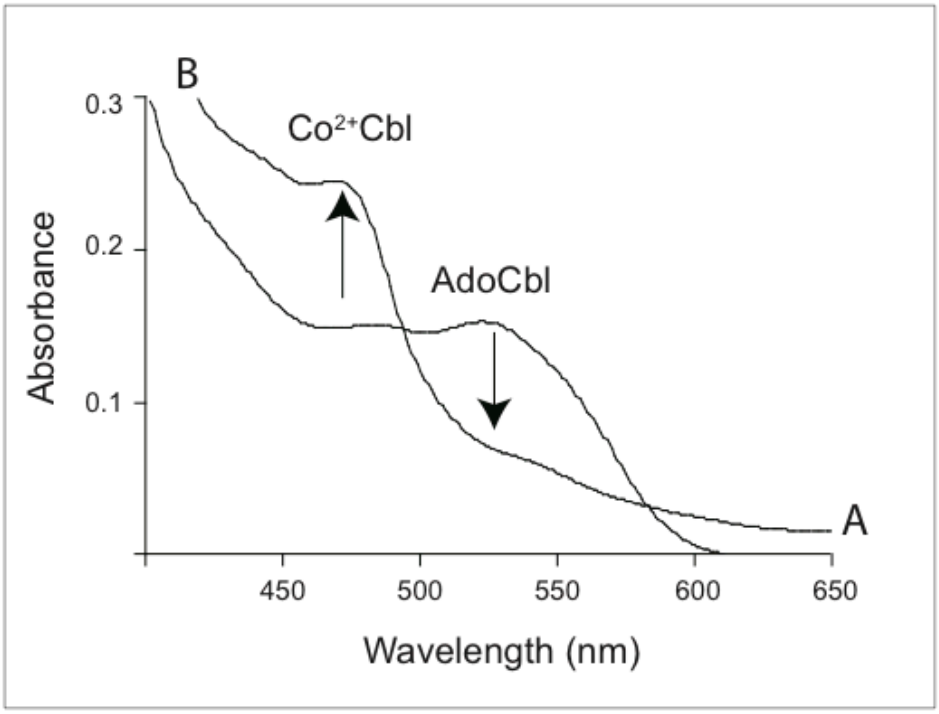

Figure 3.2. UV-visible spectrum of the EutT product with cob(II)alamin as substrate and dihydroflavins as reductant. Curve A represents the product of incubating EutT with ATP, cob(II)alamin and $FADH_2$. The absorbance maximum at 525 nm corresponds to AdoCbl. Curve B represents the product of incubating EutT with ATP, cob(II)alamin and $FADH_2$ after exposing the product of the reaction mixture to a tungsten lamp for 10 min inside an anoxic cuvette. The absorbance maximum at 473 nm corresponds to cob(II)alamin. Arrows represent spectral changes associated with photolysis of AdoCbl. No peaks corresponding to flavins were observed, as the concentration of $FADH_2$ was 5-fold lower than that of cobalamin, and was likely too low to be detected.

To gain insights into how MgATP affected the catalytic activity of EutT, we performed size exclusion chromatography analysis of EutT in the absence and presence of MgATP (see Fig. 3.4). The retention time of EutT protein corresponded to 60 kDa, while the predicted molecular mass of a EutT monomer is 30.3 kDa; thus, we concluded that EutT was a dimer in solution. The dimeric state of EutT was unaffected by MgATP treatment, which led us to conclude that MgATP did not influence the quaternary structure of EutT. The mechanism by which MgATP stabilizes EutT activity cannot be surmised from this study and remains an open question.

EutT copurifies with Zn(II) ions. A previous report from our laboratory, in which EutT was enriched from lysates, suggested that EutT contained a redox-active metal (6). The chief reason for suggesting that EutT was a metalloprotein was based on (i) the presence of a conserved $HX_{11}CCXXC_{83}$ motif, similar to motifs found in Fe/S-containing proteins (26), and (ii) the lability of EutT activity to oxygen and to the metal chelator bathophenanthroline (6). Our previous work suggested that residue His75 was part of this motif, but bioinformatics comparisons of EutT sequences showed that His75 was not conserved. We replaced His75 with alanine and determined that the activity of the resulting variant was unaffected in vitro and in vivo (data not shown), indicating that His75 was not critical for EutT function.

Bathophenanthroline, the metal chelator used in our previous study of enriched EutT (6), did not significantly affect the activity of enzyme purified in the absence of detergent. When homogeneous EutT was incubated with a 5x molar excess chelator, the enzyme retained 95% of

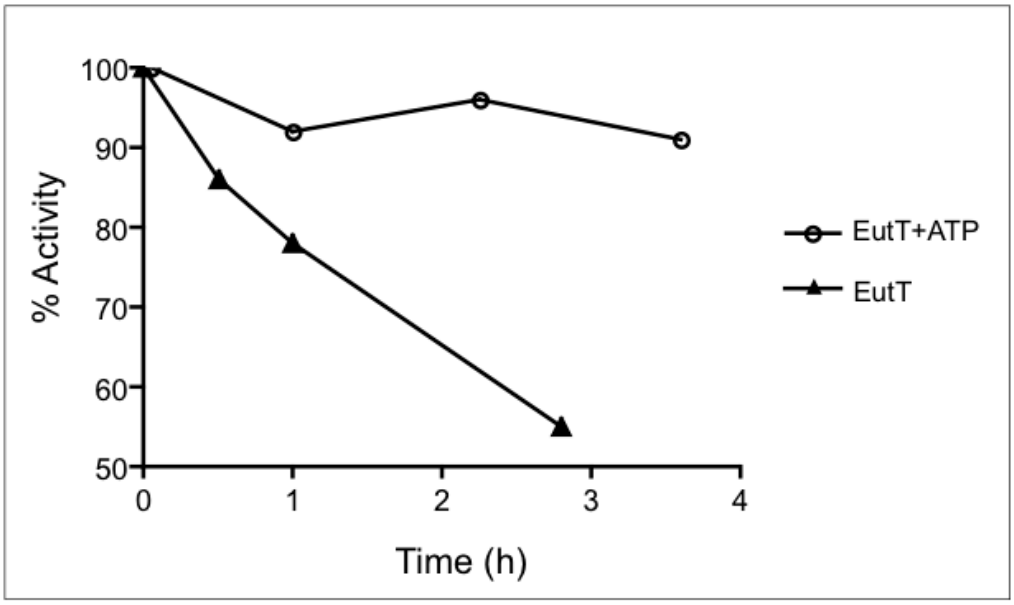

Figure 3.3. Stability of EutT activity as a function of ATP. Specific activities were measured using the Co^{1+} assay described under Material and Methods. Briefly, EutT samples in Tris-HCl buffer (100 mM, pH 8) were incubated with or without ATP at 25°C for the time indicated. The formation of AdoCbl was monitored at 525 nm.

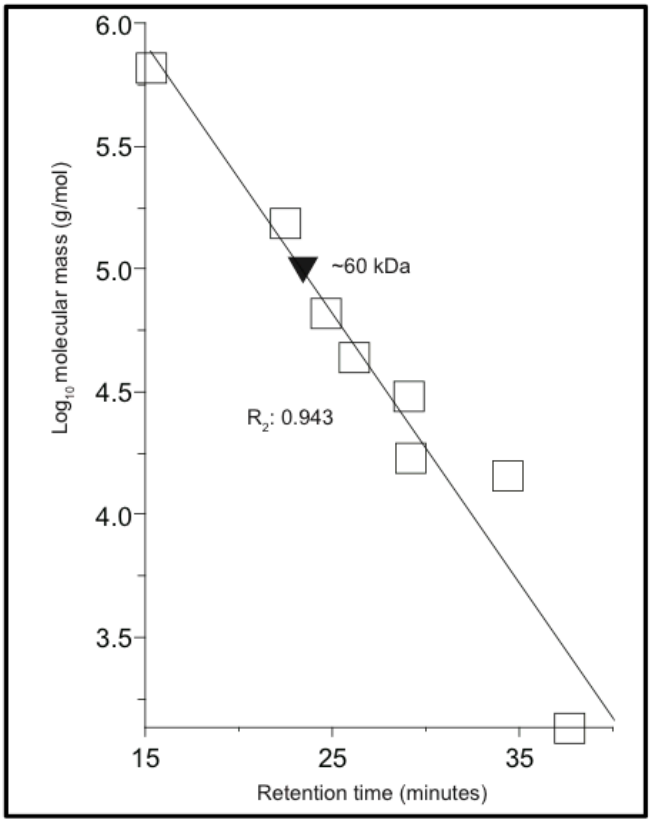

Figure 3.4. Molecular mass of EutT in solution. Size-exclusion chromatography of EutT (25 mL Superose 12 column). The black triangle represents EutT. Squares represent molecular mass standards. Names and molecular masses of standards are as follows: thyroglobulin (670 kDa), γ-globulin (158 kDa), ovalbumin (44 kDa), myoglobin (17 kDa), vitamin B_{12}, (1.35 kDa), chicken egg white lysozyme (14.3 kDa), bovine pancrease deoxyribonuclease I (31 kDa), and bovine serum albumin (66 kDa). The molecular mass of EutT did not change with the addition of MgATP.

its activity relative to that of the enzyme incubated in the absence of bathophenanthroline for the same time (30 min at 37°C; data not shown). To reconcile previous and past results, we posited that the metal originally bound by enriched EutT was lost in the purification process for homogeneous EutT.

When we used the new protocol to purify EutT, the activity of the enzyme was unaffected by oxygen. This result prompted us to look for an explanation to our previous observations made with enriched EutT. To this end, we performed metal ion analysis using ICP-OES on EutT protein samples to determine whether or not metal ions were present in our 99% homogeneous EutT preparations and, if so, which ions were present. Surprisingly, the wildtype Eut ($EutT^{WT}$) protein contained Zn(II) ions in approximately a 1:2 Zn(II)/EutT molar ratio (Table 3.2). We substituted alanine for each of the conserved residues in the aforementioned $HX_{11}CCXXC_{83}$ motif of EutT and measured the metal content in each variant. We found that $EutT^{C79A}$ and $EutT^{H67A}$ contained Zn(II) at an approximately 1:3 Zn(II)/EutT molar ratio, but Zn(II) was undetectable in the $EutT^{C80A}$ and $EutT^{C83A}$ variants. On the basis of these data, we suggested that the $HX_{11}CCXXC_{83}$ motif was involved in the acquisition of a metal cofactor.

EutT requires Fe(II) ions for optimal activity. Classifying EutT as a Zn(II)-binding metalloenzyme did not explain the observed bathophenanthroline and oxygen sensitivities of EutT-enriched cell-free lysates. To us it made sense that EutT/Zn(II) was not sensitive to either effector, since Zn(II) is not redox active and thus would not be inactivated by oxygen. The metal chelator bathophenanthroline has been used since the 1960s as a reagent for detection of Fe(II) in biological and environmental samples and likely did not chelate Zn(II) bound to EutT (27, 28).

Table 3.2. Elemental analysis results.						
A		$EutT^{WT}$	$EutT^{C79A}$	$EutT^{H67A}$	$EutT^{C80A}$	$EutT^{C83A}$
	[EutT] (μM)	6 ± 0.2	12 ± 0.8	12 ± 1	10 ± 0.6	15 ± 0.9
	[Zn] (μM)	3 ± 0.1	4.5 ± 0.5	4 ± 0.6	<1	1 ± 0.4
B		$EutT^{WT}$	$EutT^{C79A}$	$EutT^{H67A}$	$EutT^{C80A}$	$EutT^{C83A}$
	[EutT] (μM)	15.2	15.5	12.4	13.0	19.1
	[Fe] (μM)	8.0 ± 0.3	4.6 ± 0.6	4.3 ± 0.5	UD	UD

A. Zn(II) ions detected using ICP-OES. Assays were done in sextuplicate between two separate analytical labs with no change in the ratios detected. ***B***. Ferrous ions bound to EutT detected by colorimetric analysis with a colorimetric assay. Assays were performed in triplicate.

To test the effect of different divalent metal cations on EutT activity, we used EDTA to demetalate EutT before incubating it with a 10x molar excess of divalent metal cations under aerobic and anaerobic conditions. The results shown in Fig. 3.5 indicated that there was a clear requirement for metal cations and that several transition state metals could fulfill such a need. Notably, the highest EutT activity was observed after metalation of EutT with Fe(II) ions. Not surprisingly, the activity of EutT/Fe(II) was abolished under oxic conditions, likely due to the oxidation of Fe(II) to Fe(III). Zn(II) ions provided the second-highest activity, but the activity of EutT/Zn(II) was insensitive to molecular oxygen and hydrogen peroxide. Co(II), Ni(II), and Mn(II) ions also stimulated EutT activity but to levels lower than those measured with EutT/Zn(II) and EutT/Fe(II). The activity of EutT/Zn(II) and EutT/Fe(II) was lost upon exposure to EDTA, indicating that activity was reliant on the concentration of available metal ions (see Fig. 3.6).

We did not detect iron bound to EutT using ICP-OES. We used a colorimetric assay specific for ferrous iron to investigate Fe(II) binding to EutT (Table 3.2). From these experiments we found that demetalated EutT bound Fe(II) in the same monomer/ion ratio at which it bound Zn(II). The physiological significance of this ratio is unknown. One possibility is that the binding site for the metal is at the subunit interface of the EutT dimer. Alternatively, the EutT monomers might exist in two different conformations and only one is capable of binding metal at a time. Determination of the specific EutT ligands binding transition state metal ions by magnetic circular dichroism is an ongoing area of study and will be discussed in a separate study.

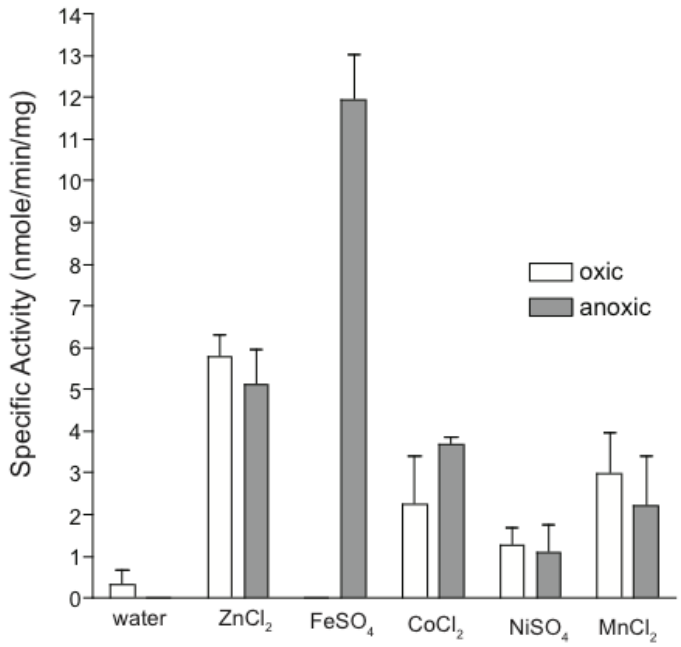

Figure 3.5. EutT activity as a function of metal ions and oxygen. Specific activity was measured using the Co2+ assay described under Materials and Methods. Briefly, de-metallated EutT (40 μM) was incubated with either a 1mM metal ion solution or buffer for one hour on ice. AdoCbl generation was monitored by absorbance at 525 nm. Assays were performed in triplicate (mean ± SD).

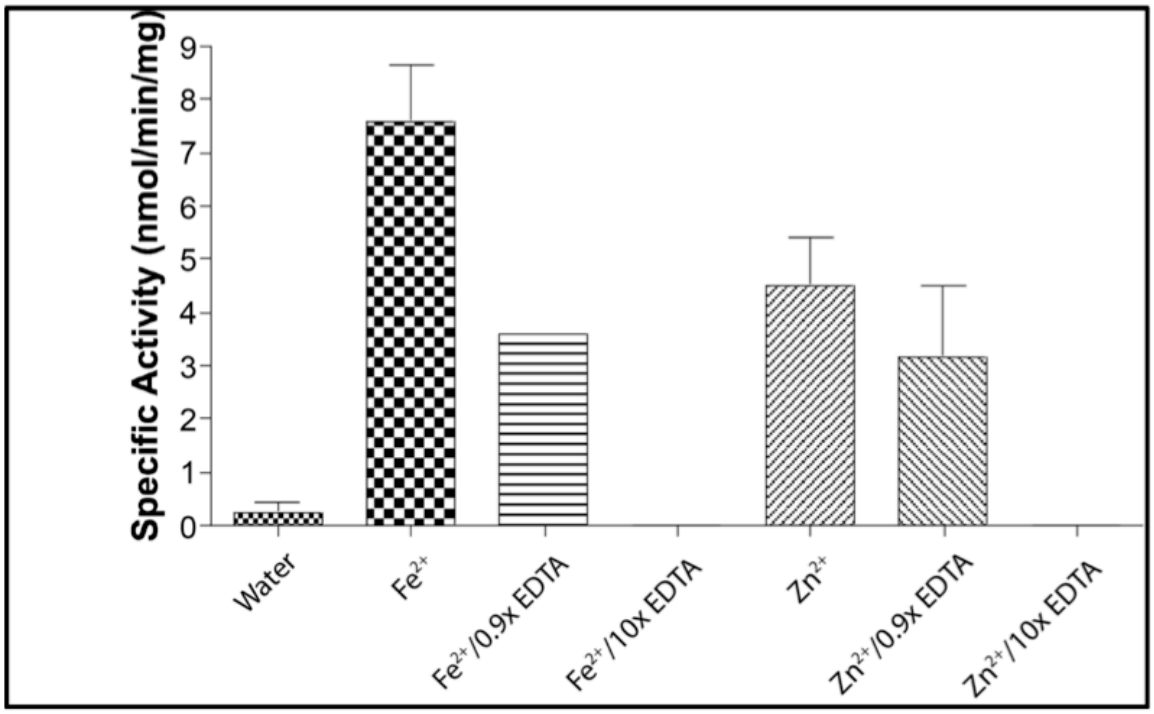

Figure 3.6. Re-metallated EutT enzyme activity as a function of chelator concentration. The specific activity of the EutT enzyme was measured using the Co^{2+} assay described under *Material and Methods*. The concentration of EDTA used was relative to the molar concentration of the metal ion incubated with EutT.

Possible roles for the metal ion in EutT function. The role of the metal cofactor is unclear. One potential function could be to promote proper enzyme folding. To investigate this possibility, we used CD spectroscopy to examine the folding of demetalated EutT and EutT/Zn(II) enzymes. We could not test EutT/Fe(II) because anoxic conditions could not be set up for this analysis. The CD spectra of demetalated EutT and EutT/ Zn(II) were virtually identical (see Fig. 3.7), suggesting that the lack of the metal ion did not cause the enzyme to misfold.

Precedent in the literature. Our results were similar to those reported by others, who determined that metalloenzymes previously thought to be Zn(II)-binding proteins exhibited higher activity with ferrous iron (29). In light of this precedent, we propose that, even though EutT can bind Zn(II) and retain some of its activity after losing Fe(II) to oxidation or diffusion, the higher specific activity of EutT/Fe(II) suggests that, in vivo, EutT might be a ferroprotein. Iron and zinc are the two most abundant transition state metals in E. coli (30) and probably in S. enterica. Mn(II) ions are typically imported under oxidative stress or iron shortage (31), while Ni(II) is imported only under anaerobic growth (32). It should also be noted that Zn(II) is a common contaminant in the laboratory setting (33, 34). Our protocol for EutT purification is substantially longer than the protocol for EutT enrichment from lysates. The protocol in this paper involves three chromatography steps, whereas the previous enrichment method involved no chromatography or dialyses. Thus, there is a greater chance that EutT would lose its native cofactor in the purification than in the enrichment and a strong likelihood that apo-EutT would bind Zn(II) present in solution.

EutT exhibits non-Michaelis-Menten kinetics. $EutT^{WT}$ kinetics did not exhibit Michaelis-Menten behavior. Rather, the kinetics of the reaction manifested as a sigmoidal curve (Fig. 3.8).

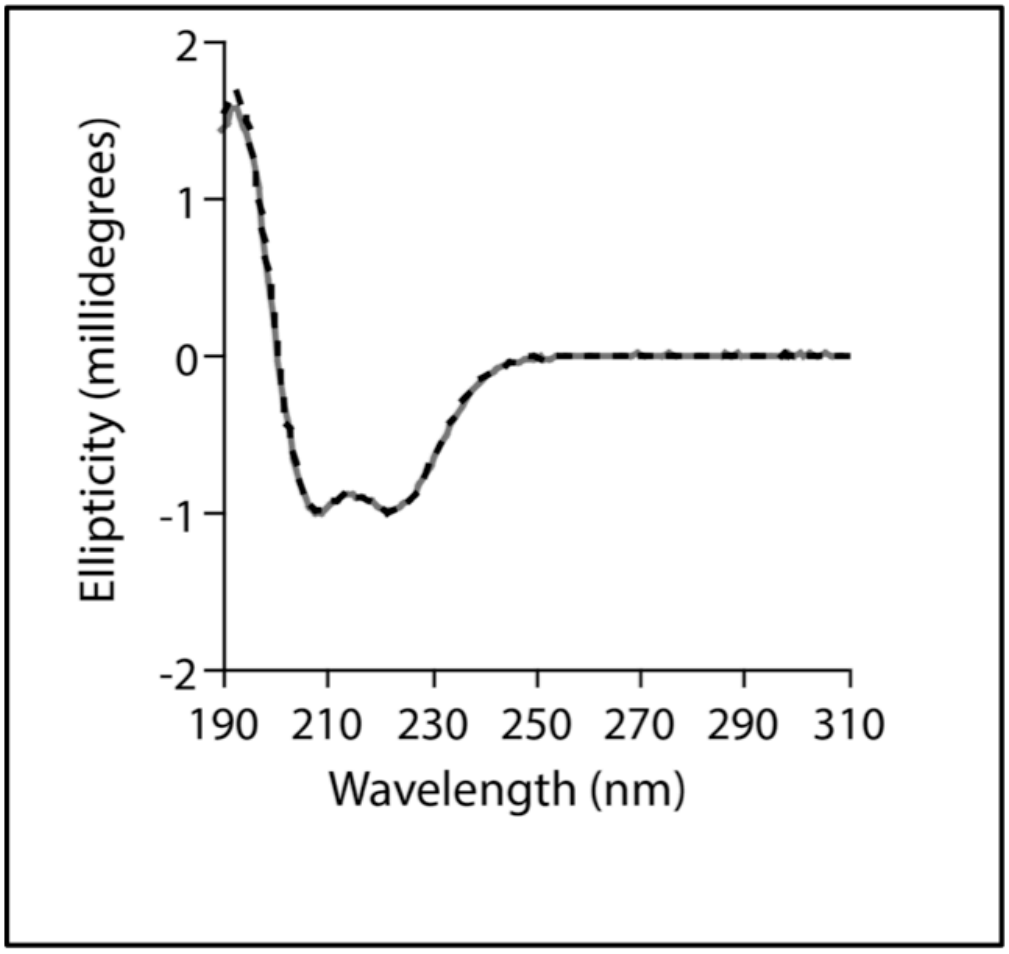

Figure 3.7. CD spectroscopy of EutT protein. De-metallated EutT protein (grey solid) and protein incubated with Zn(II) ions (black dashed line) at 37°C. Protein concentration was at 13 mM in a 0.1 mm light path diameter. Scans were performed in triplicate and averaged with the baseline subtracted.

At concentrations of $K_{0.5}$ (where $K_{0.5}$ is the substrate concentration at half the maximal velocity), the kinetics were concave but returned to a linear range before the rate plateaued due to substrate saturation. Although a variety of mechanisms could cause this effect, the simplest explanation would be cooperativity. For the purpose of this study we report the constants pertaining to cooperativity (Table 3.3). Given the dimeric nature of the protein and a Hill coefficient of ~2 (Fig. 3.8), the data suggested that EutT was positively cooperative. This is the first ACAT enzyme to display such cooperativity. The role of cooperativity within the context of ethanolamine catabolism is unknown, although it may increase the efficiency of scavenging cob(II)alamin at low concentrations.

Kinetic analyses were performed on Fe(II)-reconstituted $EutT^{WT}$ and individual variants of the $HX_{11}CCXXC_{83}$ motif using the Co^{2+} assay (Table 3.3. The assay employed in these experiments provided EutT with cob(II)alamin as the substrate, the cobalamin species that EutT encounters in the cell (20, 35). Previously reported kinetic parameters of $EutT^{WT}$ were determined with cob(I)alamin as the substrate; the value for apparent affinity was lower (Km of 4 μM) and that for turnover higher (kcat of 0.06 s^{-1}) than the values reported herein (6). The reported differences can be explained by the fully reduced nature of cob(I)alamin, which eliminates the need for the formation and reduction of the four-coordinate intermediate. Thus, kinetics parameters for cob(I)alamin solely reflect the rate of binding and rate of the nucleophilic attack on ATP, whereas those for cob(II)alamin reflect the rates of binding, reduction, and the nucleophilic attack.

The kinetic parameters of EutT variants with altered $HX_{11}CCXXC_{83}$ motifs differed significantly depending on the purification method. Variants with individual Cys-to-Ala variations were shown to have substantially less (≤20%) activity than $EutT^{WT}$ when purified with detergents (6).

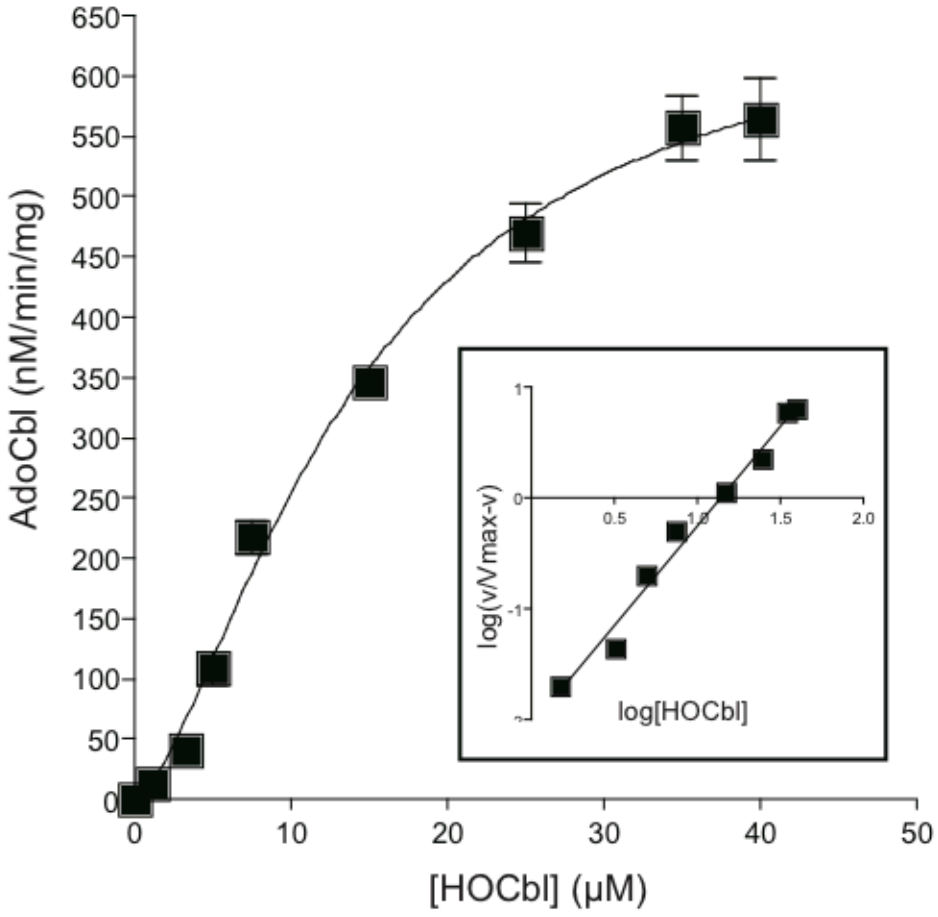

Figure 3.8. Kinetic analysis of cob(II)alamin adenosylation by EutT. The concentration of ATP was held at 1 mM as the [HOCbl] varied. Demetalated EutT was incubated with Fe^{2+} (10x molar amount) for at least 1 h on ice before assay. The inset shows the Hill plot. Assays were performed in triplicate, error in standard deviation from the mean.

Table 3.3. Kinetic constants for EutT using the Co^{2+} assay[a]				
Protein variant	**$K_{0.5}$ (Cbl, mM)**	**k_{cat} (s^{-1})**	**k_{cat} / $K_{0.5}$ (M^{-1} s^{-1})**	***h***
$EutT^{WT}$	13 ± 1.8	(2.2 ± 0.2) x 10^{-2}	(1.7 ± 0.1) x 10^{3}	1.9 ± 0.1
$EutT^{H67A}$	42 ± 5.0	(8.3 ± 1.0) x 10^{-3}	(2.0 ± 0.1) x 10^{2}	2.4 ± 0.5
$EutT^{C79A}$	17 ± 1.5	(4.2 ± 0.3) x 10^{-3}	(2.5 ± 0.1) x 10^{2}	2.4 ± 0.3
$EutT^{C80A}$	UD[b]	UD[b]	UD[b]	UD[b]
$EutT^{C83A}$	39 ± 4.2	(2.2 ± 0.2) x 10^{-3}	5.6 ± 0.1) x 10^{1}	2.0 ± 0.2

[a] Assays were run in triplicate. Values were calculated using nonlinear regressions in Prism4 (2003, GraphPad software v. 4.0a)
[b] Undetermined due to extremely low activity

However, EutT variants purified without detergents behaved differently. For example, $EutT^{C79A}$ had no significant effect on $K_{0.5}$ relative to hydroxycobalamin (HOCbl) but displayed a 5-fold decrease in kcat, and the catalytic efficiency (kcat/$K_{0.5}$) was 1 order of magnitude lower than that of $EutT^{WT}$. $EutT^{C83A}$ had a 10-fold-lower kcat than $EutT^{WT}$, a 3-fold-higher $K_{0.5}$, and a 30-fold decrease in catalytic efficiency. Although we did not detect any metals bound to this variant, it is possible that the concentration of metal was below the detection limit of the method used, but metalation of $EutT^{C83A}$ still promoted measureable activity. Variant $EutT^{H67A}$, which had not been kinetically analyzed before, displayed a 3-fold-higher $K_{0.5}$, a 3-fold-lower kcat, and a 10-fold-lower catalytic efficiency than $EutT^{WT}$. However, the most dramatic effect was observed with the $EutT^{C80A}$ variant, which had no detectable activity, indicating a critical function for this residue.

To determine the effects of substitutions on variant protein stability, we performed native PAGE (see Fig. 3.9). $EutT^{WT}$, $EutT^{C79A}$, $EutT^{C80A}$, and $EutT^{C83A}$ proteins migrated primarily as a broad band between the 50- and 66-kDa molecular mass markers and were considered to be dimers. There was an additional high-molecular-mass species in the 66- to 132-kDa range and one more at 132 kDa. The $EutT^{H67A}$ variant was detectable primarily in the 66- to 132-kDa range, with a smaller proportion existing as a dimer. This $EutT^{H67A}$ dimer appeared to have a slightly smaller size than $EutT^{WT}$. These data suggested that the kinetic effects observed in $EutT^{H67A}$ might be due to structural changes to the enzyme. Taken together, our data suggest the likelihood that the $HX_{11}CCXXC_{83}$ motif may be involved in binding a metal ion. Elemental analysis indicated that EutT could not bind metals without Cys80 and Cys83, while Cys79 and His67 bound metal ions at a reduced capacity. Interestingly, the kinetic data indicated that $EutT^{C80A}$ and $EutT^{C83A}$ had a much lower in vitro activity relative to

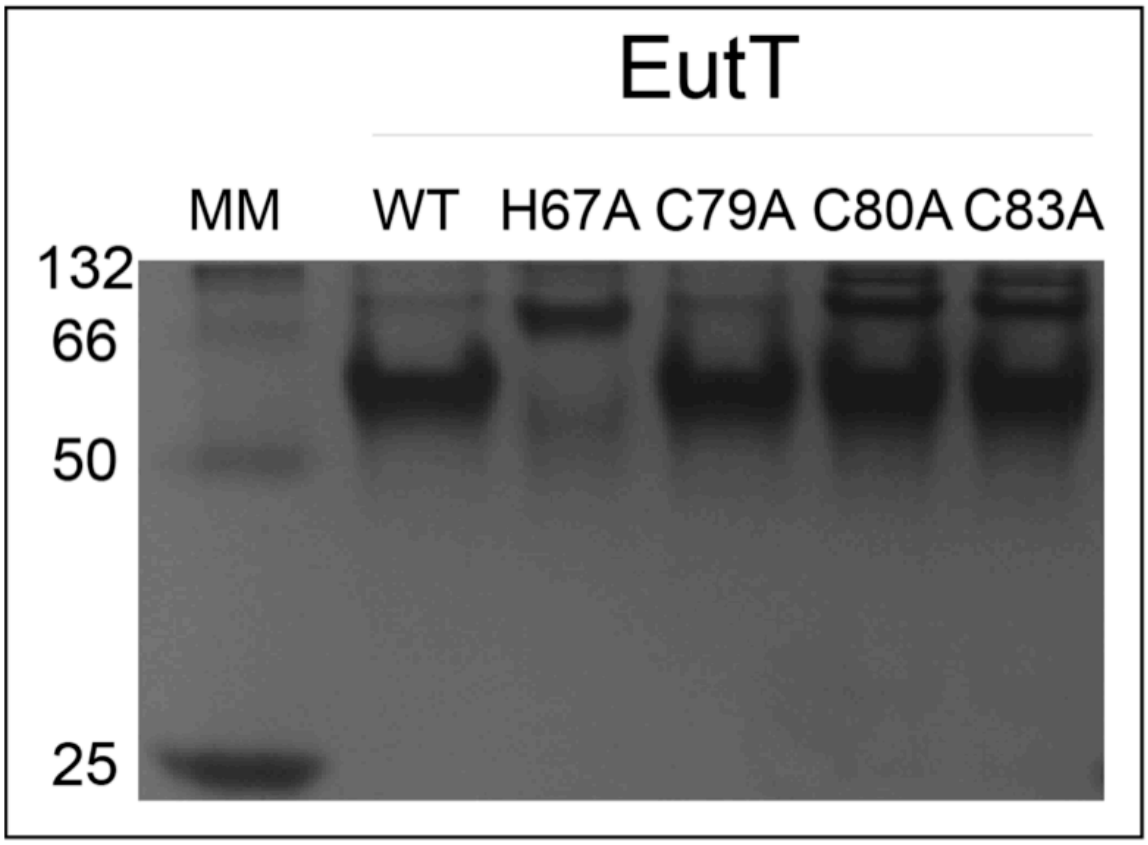

Figure 3.9. Native PAGE of EutT^{WT}, EutT^{H67A}, EutT^{C79A}, EutT^{C80A} and EutT^{C83A}. A sample containing 5 μg of protein was loaded on a 10% acrylamide gel and run for 3 hours at 95 V and 4°C. The molecular weight marker was comprised several proteins of known mass, including bovine serum albumin (monomer at 66 kDa, dimer at 132 kDa), *S. lividans* TK74 EFD68037 (50 kDa) and *S. enterica* CobB (25 kDa)

that of EutT^{WT} than EutT^{C79A} and EutT^{H67A}, although EutT^{H67A} may disrupt oligomerization. On the basis of this information we suggest that the conserved HX^{11}CCXXC^{83} motif is involved in binding or maintaining a metal ion for activity, with the Cys80 and Cys83 residues likely to be most critical for this purpose.

In vivo effects of substitutions in the $HX_{11}CCXXC_{83}$ motif on EutT activity. The effect of changes at positions His67, Cys79, Cys80, and Cys83 were assessed in an *S. enterica* AdoCbl auxotroph (strain JE13176). The allele coding for EutT^{C79A} complemented almost as well as that coding for EutT^{WT} during growth on ethanolamine as the carbon and energy source when the medium was supplemented with HOCbl (Fig. 3.10). In contrast, alleles coding for EutT^{H67A}, EutT^{C80A}, and EutT^{C83A} did not restore growth of the AdoCbl auxotroph (strain JE13176) under the same conditions. Although EutT^{H67A} and EutT^{C83A} variants produced AdoCbl in vitro (Table 3.3), they did so at significantly lower rates than EutT^{WT}, and we concluded that EutT^{H67A} and EutT^{C83A} could not produce sufficient AdoCbl to support growth on ethanolamine. Interestingly, the EutT^{H67A}, EutT^{C79A}, and EutT^{C80A} variants had kcat values at least 3-fold lower than that of EutT^{WT}, but EutT^{C79A} had a $K_{0.5}$ similar to that of EutT^{WT}, whereas EutT^{H67A} and EutT^{C83A} had at least 3-fold-higher $K_{0.5}$ values than EutT^{WT} (Table 3.2). Since the allele encoding EutT^{C79A} supported growth of a Δ*eutT* strain but alleles encoding EutT^{H67A} and EutT^{C83A} did not, we speculate that the affinity for the cobalamin substrate has a greater in vivo effect than the rate at which EutT can produce AdoCbl. Collectively, these in vivo data mirror the in vitro data, highlighting the need for residues His67, Cys80, and Cys83 for EutT function.

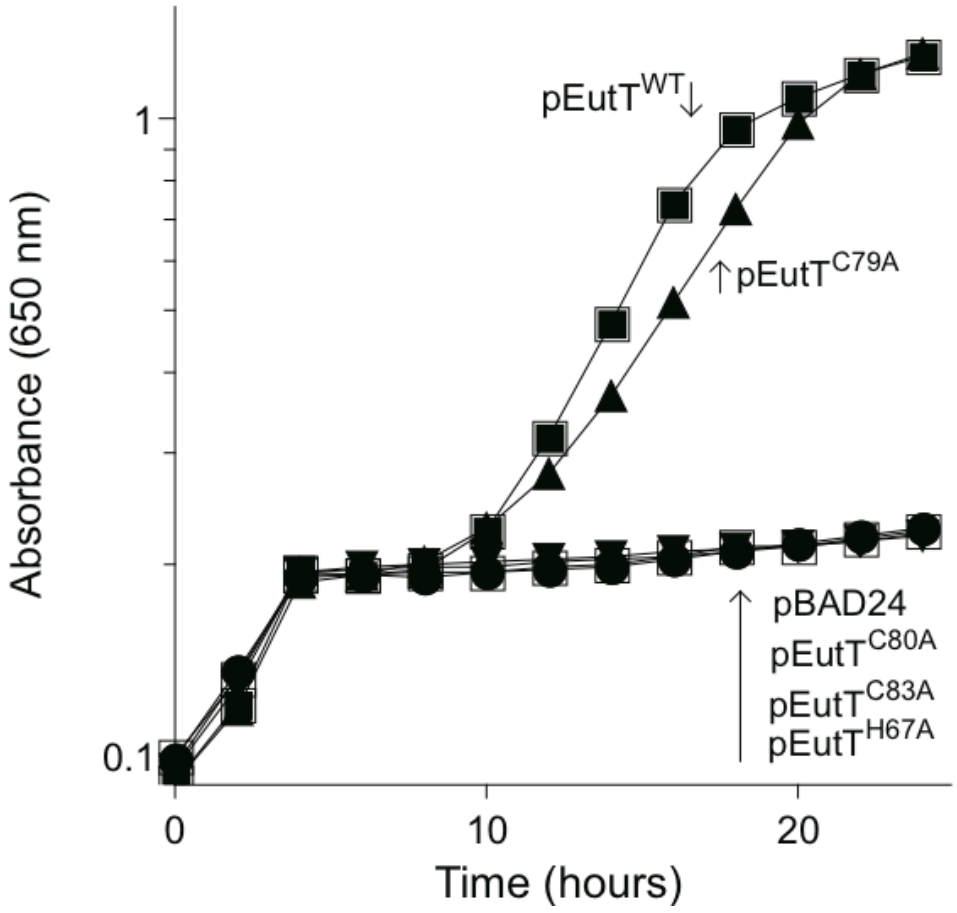

Figure 3.10. ***In vivo*** **assessment of EutT^{H67A}, EutT^{C79A}, EutT^{C80A}, and EutT^{C83A} function.** A strain devoid of all ACATs (*cobA* Δ*eutT* Δ*pduO*, JE13176), and harboring a plasmid encoding one of the above-mentioned EutT variants was grown on minimal medium with ethanolamine as the sole source of carbon and energy. Other supplements to the medium are described under Material and Methods. The plasmid expressing each EutT variant is indicated on the graph

Reconciling previous and present findings. As mentioned above, our previous isolation procedure for the isolation of EutT rendered its activity sensitive to oxygen and metal chelation (6, 7). Considering EutT a ferroprotein would explain both observations. In sharp contrast, considering EutT a Zn(II) protein would not explain our previous findings. Thus, we suggest that the new means of isolating EutT results in loss of Fe(II) and its replacement by Zn(II) ions, yielding active enzyme, although not as active as EutT/Fe(II), but insensitive to oxygen inactivation. One additional advantage to the new purification protocol is that it simplifies the isolation of active EutT enzyme (i.e., no need for anoxic conditions), and using a simple procedure we can exchange Fe(II) for Zn(II), with a concomitant increase in the activity of the enzyme.

Concluding remarks. The results reported herein lead us to conclude that the S. enterica ACAT EutT enzyme binds a divalent transition state metal ion that is important for its activity. EutT is the first example of an ACAT that requires a metal ion for function. The likelihood that this metal is Fe(II) is high since enzyme activity is highest when EutT is in complex with Fe(II) ions. It is proposed that residues within the conserved $HX_{11}CCXXC_{83}$ motif interact with the metal ion. However, the identity of the metal ion bound to EutT in vivo has not been confirmed, nor has the specific mechanistic effect of the metal ion on EutT activity been discerned. Growth of *S. enterica* in medium supplemented with ^{59}Fe and subsequent immunoprecipitation of EutT could help deter- mine if iron is the in vivo cofactor of EutT. Spectroscopic studies of EutT, which will be published elsewhere, analyze the effects of the putative metal ion cofactor and the conserved $HX_{11}CCXXC_{83}$ motif on enzyme function. The role of EutT cooperativity with regard to ethanolamine catabolism remains a topic for future research. Increased sensitivity to substrate may allow it to respond more quickly to the metabolic needs of a cell switching to growth on

ethanolamine. The study of orthologous EutT may help determine how widespread this positive cooperativity is and may shed more light on its contribution to ACAT-dependent physiology.

3.5 Acknowledgements

We declare that no competing interests exist. We thank Ivan Pallares, Kiyoung Park, and Thomas Brunold for stimulating discussions and critical reading of the manuscript. This work was supported by USPHS grant R37 GM40313 to J.C.E.-S. T.C.M. was supported in part by Chemistry and Biology Interface Training grant T32 GM008505, and P.E.M. was supported in part by NIH Grant NRSA F31 GM081979. CD data were obtained at the University of Wisconsin-Madison Biophysics Instrumentation Facility, which was established with support from the University of Wisconsin-Madison and grants BIR-9512577 (NSF) and S10 RR13790 (NIH).

3.6 References

1. Mera, P. E., Escalante-Semerena, J. C. (2010) Multiple roles of ATP: cob(I)alamin adenosyltransferases in the conversion of B(12) to coenzyme B(12). *Appl. Microbiol. Biotechnol*. **88**, 41– 48.

2. Escalante-Semerena, J. C., Suh, S. J., Roth, J. R. (1990) *cobA* function is required for both *de novo* cobalamin biosynthesis and assimilation of exogenous corrinoids in *Salmonella typhimurium*. *J. Bacteriol.* **172**, 273–280.

3. Suh, S., Escalante-Semerena, J. C. (1995) Purification and initial characterization of the ATP:corrinoid adenosyltransferase encoded by the *cobA* gene of Salmonella typhimurium. *J. Bacteriol.* **177**, 921–925.

4. Mera, P.E., Maurice, M.S., Rayment, I., Escalante-Semerena, J. C. (2007) Structural and functional analyses of the human-type corrinoid adenosyltransferase (PduO) from *Lactobacillus reuteri*. *Biochemistry.* **46**, 13829 –13836.

5. Mera, P. E., St. Maurice, M., Rayment, I., Escalante-Semerena, J.C. (2009) Residue Phe112 of the human-type corrinoid adenosyltransferase (PduO) enzyme of Lactobacillus reuteri is critical to the formation of the four-coordinate Co(II) corrinoid substrate and to the activity of the enzyme. *Biochemistry.* **48**, 3138 –3145.

6. Buan, N. R., Escalante-Semerena, J. C. (2006) Purification and initial bio- chemical characterization of ATP:cob(I)alamin adenosyltransferase (EutT) enzyme of Salmonella enterica. *J. Biol. Chem.* **281**, 16971–16977.

7. Buan, N. R., Suh, S. J., Escalante-Semerena, J. C. (2004) The *eutT* gene of Salmonella enterica encodes an oxygen-labile, metal-containing ATP: corrinoid adenosyltransferase enzyme. *J. Bacteriol*. **186**, 5708 –5714.

8. Johnson, C. L., Buszko, M. L., Bobik, T. A. (2004) Purification and initial char- acterization of the Salmonella enterica PduO ATP:Cob(I)alamin adenosyltransferase. *J. Bacteriol.* **186**, 7881–7887.

9. Johnson, C. L., Pechonick, E., Park, S. D., Havemann, G. D., Leal, N. A., Bobik, T. A. (2001) Functional genomic, biochemical, and genetic characterization of the Salmonella pduO gene, an ATP:cob(I)alamin adenosyltransferase gene. *J. Bacteriol.* **183**, 1577–1584.

10. Stich, T. A., Yamanishi, M., Banerjee, R., Brunold, T.C. (2005) Spectroscopic evidence for the formation of a four-coordinate Co(2+)cobalamin species upon binding to the human ATP:cobalamin adenosyltransferase. *J. Am. Chem. Soc.* **127**, 7660 –7661.

11. Stich, T. A., Buan, N. R., Escalante-Semerena, J. C., Brunold, T. C. (2005) Spectroscopic and computational studies of the ATP:corrinoid adenosyltransferase (CobA) from Salmonella enterica: insights into the mechanism of adenosylcobalamin biosynthesis. *J. Am. Chem. Soc*. **127**, 8710 – 8719.

12. Park, K., Mera, P. E., Escalante-Semerena, J. C., Brunold, T. C. (2008) Kinetic and spectroscopic studies of the ATP:corrinoid adenosyltransferase PduO from Lactobacillus reuteri: substrate specificity and insights into the mechanism of Co(II)corrinoid reduction. *Biochemistry* **47**, 9007–9015.

13. Moore, T. C., Newmister, S. A., Rayment, I., Escalante-Semerena, J. C. (2012) Structural insights into the mechanism of four-coordinate cob(II)alamin formation in the active site of the Salmonella enterica ATP:co(I)rrinoid adenosyltransferase (CobA) enzyme: critical role of residues Phe91 and Trp93. *Biochemistry* **51**, 9647–9657.

14. Rocco, C. J., Dennison, K. L., Klenchin, V. A., Rayment, I., Escalante-Semerena, J. C. (2008) Construction and use of new cloning vectors for the rapid isolation of recombinant proteins from Escherichia coli. *Plasmid* **59**, 231–237.

15. Blommel, P. G., Fox, B. G. (2007) A combined approach to improving largescale production of tobacco etch virus protease. *Protein Expr. Purif*. **55**, 53– 68.

16. Gasteiger, E., Gattiker, A., Hoogland, C., Ivanyi, I., Appel, R. D., Bairoch, A. (2003) ExPASy: the proteomics server for in-depth protein knowledge and analysis. *Nucleic Acids Res*. **31**, 3784 –3788.

17. St. Maurice, M., Mera, P. E., Taranto, M. P., Sesma, F., Escalante-Semerena, J. C., Rayment, I. (2007) Structural characterization of the active site of the PduO-type ATP:Co(I)rrinoid adenosyltransferase from Lactobacillus reuteri. *J. Biol. Chem*. **282**, 2596 –2605.

18. Hogenkamp, H. P. C., Pailes, W. H., Brownson, C. (1971) Preparation of 5'-deoxyadenosylcobalamin and analogs containing modified nucleosides, p 57–71. In McCormick DB, Wright LD (ed), *Vitamins and coenzymes,* vol 18C. Academic Press, Inc., New York, NY.

19. Zehnder, A. J., Wuhrmann K. (1976) Titanium (III) citrate as a nontoxic oxidation-reduction buffering system for the culture of obligate anaerobes. *Science* **194**, 1165–1166.

20. Mera, P. E., Escalante-Semerena J. C. (2010) Dihydroflavin-driven adenosylation of 4-coordinate Co(II) corrinoids: are cobalamin reductases enzymes or electron transfer proteins? *J. Biol. Chem.* **285**, 2911–2917.

21. Vogel, H. J., Bonner, D. M. (1956) Acetylornithinase of *Escherichia coli*: partial purification and some properties. *J. Biol. Chem*. **218**, 97–106.

22. Berkowitz, D., Hushon, J. M., Whitfield, H. J., Jr, Roth, J., Ames, B.N. (1968) Procedure for identifying nonsense mutations. *J. Bacteriol*. **96**, 215–220.

23. Balch, W. E., Wolfe, R. S. (1976) New approach to the cultivation of methanogenic bacteria: 2-mercaptoethanesulfonic acid (HS-CoM)-dependent growth of Methanobacterium ruminantium in a pressurized atmosphere. *Appl. Environ. Microbiol.* **32**, 781–791.

24. Guzman, L. M, Belin, D., Carson, M. J, Beckwith, J. (1995) Tight regulation, modulation, and high-level expression by vectors containing the arabinose PBAD promoter. *J. Bacteriol*. **177**, 4121– 4130.

25. Wilson, A. C., Pardee, A. B. (1962) Regulation of flavin synthesis by *Escherichia coli. J. Gen. Microbiol.* **28**, 283–303.

26. Brindley, A. A, Raux, E., Leech, H. K, Schubert, H. L, Warren, M. J. (2003) A story of chelatase evolution: identification and characterization of a small 13-15-kDa "ancestral" cobaltochelatase (CbiXS) in the archaea. *J. Biol. Chem.* **278**, 22388 –22395.

27. Tetlow, J. A, Wilson, A. L. (1964) The absorptiometric determination of iron in boiler feedwater. Part III. Method for determining the total iron content. *Analyst* 89:442– 452.

28. Torrance JD, Bothwell TH. (1968) A simple technique for measuring storage iron concentrations in formalinised liver samples. *South Afric. J. Med. Sci*. **33**, 9 –11.

29. Sobota, J. M., Imlay, J. A. (2011) Iron enzyme ribulose-5-phosphate 3-epimerase in Escherichia coli is rapidly damaged by hydrogen peroxide but can be protected by manganese. *Proc. Natl. Acad. Sci.* U. S. A. **108**, 5402– 5407.

30. Rouf, M. A. (1964) Spectrochemical analysis of inorganic elements in bacteria. *J. Bacteriol*. **88**, 1545–1549.

31. Kehres, D. G., Janakiraman A., Slauch J. M., Maguire, M. E. (2002) Regulation of *Salmonella enterica* serovar Typhimurium *mntH* transcription by H_2O_2, Fe^{2+}, and Mn^{2+}. *J. Bacteriol*. **184**, 3151–3158.

32. Rowe, J. L., Starnes, G. L., Chivers, P. T. (2005) Complex transcriptional control links NikABCDE-dependent nickel transport with hydrogenase expression in Escherichia coli. *J. Bacteriol*. **187**, 6317– 6323.

33. Gagnon, P. (2006) Practical strategies for protein contaminant detection by high performance ion exchange chromatography, p. 67–79. In Rodribuez- Diaz R, Wehr T, Tuck S (ed), *Analytical techniques for biopharmaceutical development*. Marcel Dekker, New York, NY.

34. Kay, A. (2004) Detecting and minimizing zinc contamination in physiological solutions. *BMC Physiol*. **4**,4.

35. Fonseca, M. V., Escalante-Semerena, J. C. (2001) An in vitro reducing system for the enzymic conversion of cobalamin to adenosylcobalamin. *J. Biol. Chem*. **276**, 32101–32108.

36. Laemmli, U. K. (1970) Cleavage of structural proteins during the assembly of the head of bacteriophage T4. *Nature* **227**, 680 – 685.

37. Sasse, J. (1991) *Detection of proteins*, p 10.16.11–10.16.18. In Ausubel FA, Brent R, Kingston RE, Moore DD, Seidman JG, Smith JA, Struhl K (ed), Current protocols in molecular biology, vol 1. Wiley Interscience, New York, NY.

CHAPTER 4

THE EUTQ PROTEIN IS A NOVEL ACETATE KINASE INVOLVED IN ETHANOLAMINE CATABOLISM[3]

[3] Theodore C. Moore and Jorge C. Escalante-Semerena. To be submitted to *J. Biol. Chem.*

4.1 Abstract

The catabolism of ethanolamine by *Salmonella enterica* can serve as a source of carbon, nitrogen and energy for the bacterium, and is important for pathogenesis. Ethanolamine breakdown occurs in a proteinaceous microcompartment encoded by the 17-gene *eut* operon. Of these 17 genes, the function of *eutQ* and *eutP* are uncharacterized. Here we provide phenotypic and biochemical evidence that EutQ is an acetate kinase. EutQ is required when growing anaerobically on ethanolamine with tetrathionate as a terminal electron acceptor, and alternative acetate kinases can complement *eutQ* strains. Formation of ATP was detected by HPLC and ^{31}P NMR when EutQ was supplied with ADP, Mg and acetyl-phosphate. Coupling EutQ to the phosphotransacetylase EutD indicated that it could generate acetyl-phosphate when supplied with ATP and acetate. EutP is also shown to have acetate kinase activity under the same biochemical conditions as EutQ. However, *eutP* strains lack any detectable phenotypes under the conditions used for *eutQ* strains. EutQ and EutP represent a novel class or classes of acetate kinase, and we propose that they play an important role in energy generation or balancing carbon flux when *S. enterica* grows on ethanolamine.

4.2 Introduction

Salmonella enterica is a facultative anaerobic bacterium that is capable of using ethanolamine as a carbon, nitrogen and energy source (1-3) (Figure 4.1). Ethanolamine is a breakdown product of phosphatidylethanolamine, a major component of eukaryotic membranes. Ethanolamine is abundant in the intestines due to frequent turnover of eukaryotic cells.

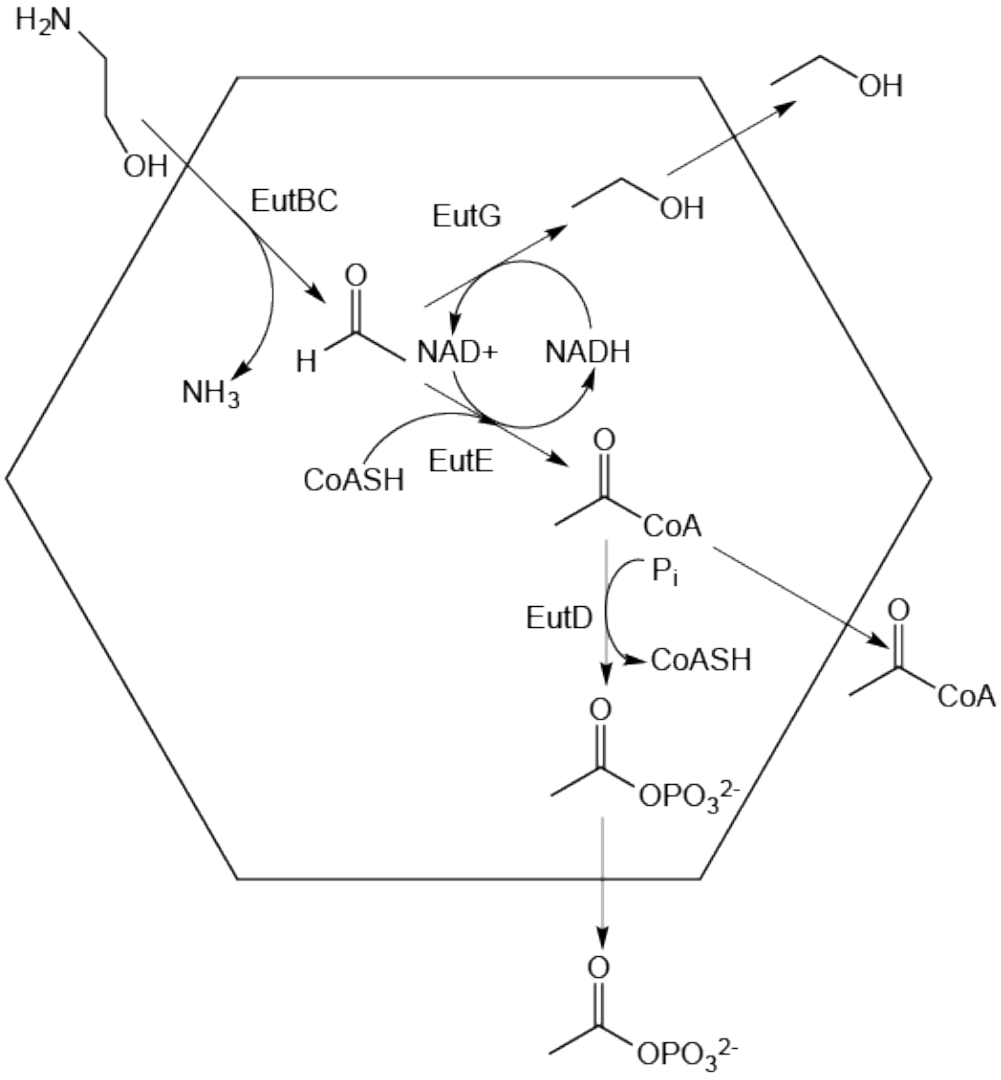

Figure 4.1. The ethanolamine catabolic pathway. The ethanolamine metabolosome, made of EutSMNLK, is represented as a hexagonal shell. The enzymes required to catalyze the breakdown of ethanolamine are shown within the shell.

Most organisms require oxygen as a terminal electron acceptor to use this plentiful energy source, which is not available in the mostly-anaerobic environment of the intestine. *S. enterica* sidesteps this problem by using tetrathionate as a terminal electron acceptor when growing on ethanolamine. Access to this nutrition source gives *S. enterica* a competitive advantage over other intestinal microbes (4). Additionally, when *S. enterica* triggers intestinal inflammation and white blood cells are recruited to the infection site, the reactive oxygen species released generate tetrathionate by oxidizing ambient hydrogen sulfide in the gut (5). Generating tetrathionate via the inflammatory response is therefore important for *S. enterica* pathogenesis. This was shown recently in a mouse model system, where pathogenic *S. enterica* strains lacking inflammatory type-three secretion systems were unable to utilize ethanolamine to colonize the gut (6).

Ethanolamine catabolism is contained within a metabolosome, also known as a bacterial microcompartment (BMC or MCP) (7-9). The metabolosome is a proteinaceous icosahedron assembled from the 17-gene *e*thanolamine *ut*ilization operon, its expression is induced by the presence of ethanolamine and coenzyme B_{12} (10). It is thought that the metabolosome serves several barrier functions: to prevent the toxic aldehyde intermediates from damaging the cell, to prevent carbon loss from volatilization of aldehyde, and to conserve and recycle cofactors used in catabolism. All of the proteins expressed from the operon have assigned functions, except for EutQ, EutP and EutJ.

Previous studies were unable to assign roles to the *eut* genes of unknown function, as strains carrying deletions in those genes grew like wild-type on ethanolamine as a carbon and energy source (11-13). Penrod and Roth (14) observed that *eutP* and *eutQ* strains excreted more acetaldehyde than wild-type when growing on glycerol with ethanolamine as a nitrogen source. EutQ belongs to the cupin superfamily, which includes a wide variety of enzymes such as carbohydrate-binding isomerases, flavonoid-binding diooxygenases and nuclear factors (15).

EutP contains a predicted nucleotide triphosphate binding site. It was not possible to hypothesize functions of these enzymes given the scant experimental and bioinformatics data.

Given the importance of tetrathionate to pathogenic *S. enterica*, we decided to examine these genes of unknown function under anaerobic conditions with tetrathionate as a terminal electron acceptor. The results suggest that *eutQ* plays a critical role when *S. enterica* grows anaerobically on tetrathionate and ethanolamine, yet is note necessary when growing aerobically. *In vitro* and complementation studies suggest that EutQ is an acetate kinase, and likely is involved in balancing substrate-level phosphorylation and carbon utilization. EutP can also generate acetate kinase *in vitro*, although we were unable to detect a phenotype for *eutP*.

4.3 Materials and Methods

Construction of expression and complementation vectors. To generate a recombinant construct of EutQ with a cleavable *N*-terminal hexahistidine (H_6) tag, the *S. enterica eutQ*$^+$ allele was PCR amplified from the *S. enterica* strain JE6583 (Table 4.1). The primers used for the amplification were 5'- NNGCTCTTCNTTCGTGAAAAAACTTATCACAGCTAACGA -3' (forward) and 5'-NNGCTCTTCNTTATCATACGGATTGCCAGTTTG -3'. The PCR fragment and the vector pTEV18 (VanDrisse et al., in preparation)(16) were cut with the restriction enzyme BspQI and ligated, yielding plasmid pEUT112. pEUT112 directed the synthesis of a recombinant H_6-EutQ whose tag was removed using recombinant tobacco etch virus (rTEV) protease. Tagless EutQ contained two residues (Gly-Thr) upstream of the *N*-terminal Met residue, these residues did not inhibit enzyme function. This method was also used to generate pTEV18 constructs containing

Table 4.1: Strains and plasmids used over the course of this study				
Strain ID	Genotype	Plasmid	Protein encoded	Source
E. coli strains				
JE3892	BL21 (λ*DE3*)			Laboratory collection
JE8833	XL10 Gold	pEUT56	EutQ^{WT}	Laboratory collection
JE19891 (DH5a) backround	*fhuA2 Δ(argF-lacZ)U169 phoA glnV44 Φ80 Δ(lacZ)M15 gyrA96 recA1 relA1 endA1 thi-1 hsdR17*	pACK7	AckA^{WT}	Laboratory collection
S. enterica strains				
JE6814	*metE205* ara-9 *prpC114*::MudJ	pTDCD1	TdcD^{WT}	Laboratory collection
JE5304 (formerly JR501)	*hsdSA29 hsdSB121 hsdL6 metA22 metE551 trpC2 ilv-452 rpsL120 xyl-404 galE719 H1-b H2-e, n,x) fla-66 nm*			Laboratory collection
Derivatives of JE5304				
JE20869		pEUT112	EutQ^{WT}	This paper
JE5912		pPDU1	PduW^{WT}	Laborator collection
JE8816	*metE205* ara-9 Δ*eutQ1183*			Laboratory collection
Derivatives of JE8816				
JE14190		pBAD24	Vector control	Laboratory collection
JE14116		pEUT56	EutQ^{WT}	This paper
JE21131		pACK7	AckA	This paper
JE21167		pPDU1	PduW	This paper
JE21168		pTDCD1	TdcD	This paper

EutP (pEUT110) and EutPQ (pEUT129) alleles. For EutP, the following primers were used: 5'- NNGCTCTTCNTTCATGAAACGTATTGCTTTTGTCG -3' (forward) and 5'-NNGCTCTTCNTTATTAGCTGTGATAAGTTTTTTCACCTG -3' (reverse). pEUT129 was generated using the EutP forward primer and the EutQ reverse primer. *eutQ* alleles encoding variant EutQ proteins were generated using the QuikChange XL site-directed mutagenesis kit (Stratagene). The pEUT112 and the pEUT56 plasmids were used as templates for the PCR-based site-directed mutagenesis according to the manufacturer's instructions. Mutations in the *eutQ* sequence were confirmed by sequencing with BigDye protocols (ABI-Prism). Plasmid sequences were determined at the Georgia Genomics Facility at the University of Georgia-Athens.

Protein overexpression and purification. Plasmids expressing EutP or EutQ were transformed into *Escherichia coli* BL21 via heat-shock. Overnight cultures were inoculated 1:100 (v/v) into 2L Terrific Broth supplemented with ampicillin (100 μg/mL). Cultures were grown to OD600 ~0.7 at 37°C with shaking. Protein expression was induced with isopropyl β-D-1 thiogalactopyranoside (IPTG, 0.5 mM) and shaken overnight at 10°C. Cell pellets were harvested at 12,000 x g using a Beckman/Coulter Avanti J-25I centrifuge equipped with a JLA-16.250 rotor. Cell pellets were frozen at -80°C until used.

Cell pellets were resuspended in buffer A (4-(2-hydroxyethyl)-1-piperazineethanesulfonic acid (HEPES , 50 mM, pH 7), Sodium Chloride (NaCl, 500 mM), imidazole (70 mM) and tris(2-carboxyethyl)phosphine (TCEP, 0.25 mM)), at a ratio of 5 mL per 1g cell paste. The resuspended cell pellet was lysed by two passes through a French pressure cell at 103 MPa and 4°C. Cellular debris was removed from solution by centrifugation (45,000 x g for 45 min) and filtering (0.45 μm pore).

His-tagged proteins were separated from crude lysate using an AKTA Purifier fast protein liquid chromatograph equipped with a 5 mL HisTrap column (GE Healthcare). The column was washed with 40 mL buffer A, and tagged protein was eluted over a 50 mL gradient to 100% buffer B (buffer A containing 500 mM imidazole). Recombinant H_7-tobacco etch virus (TEV) protease (1 mg/mL) was added to the elutate in a 1:50 ratio (v/v) to cleave the H_6-tag from the protein of interest. H_7-rTEV was prepared as described elsewhere (17). The tagged protein/protease mixture was dialyzed three times into buffer A (1L each), once for 1 hour, once overnight, and once for 3 hours, all at 4°C.

The protein of interest was loaded onto a fresh HisTrap column and eluted with 25 mL buffer A to remove the cleaved his-tag and H_7-rTEV. The protein was dialyzed into buffer C (buffer A with no imidazole and 10% glycerol) three times as described above. The protein was flash-frozen in liquid N_2 and stored at -80°C until use. Protein purity was assessed by sodium dodecyl-sulfate polyacrylamide gel electrophoresis (SDS-PAGE).

In vivo *assessment of function.* To assess the role of EutQ *in vivo*, a strain (JE8816, *metE205 ara*-9 Δ*eutQ1182*) was tested for deleterious phenotypes when grown on minimal medium. No-carbon essential (NCE) minimal medium (18,19) was supplemented with ethanolamine (30 mM), methionine (0.5 mM), NH_4Cl (30 mM), $MgSO_4$ (1 mM) L-(+)-arabinose (500 mM), glycerol (0.5 mM), and trace minerals (20). When growth curves were performed under anaerobic conditions, tetrathionate (40 mM) was supplied as an electron acceptor. Anoxic medium was degassed in an anoxic chamber (Coy) for 24 hours and stirred for 1 hour prior to the growth curve to remove all oxygen. Anaerobic growth curves using tetrathionate were run for 24 hours or less due to precipitation of sulfur granules after prolonged growth (21). Plasmids used for *in*

vivo analyses were constructed as described above and in table 4.1. Plasmids carrying the *eutQ*$^{+}$ and mutant alleles were under the control of the arabinose-inducible P_{araBAD} promoter in plasmid pBAD24 (22).

Determination of excreted acetate during growth on ethanolamine. Acetate excretion of *S. enterica* strains growing on ethanolamine was assessed as described previously (23). Overnight cultures of *S. enterica* were inoculated into NCE minimal medium in Klett flasks containing ethanolamine as the sole carbon and nitrogen source. The cultures were grown at 37°C with shaking (160 RPM). Optical density was determined using a Klett colorimeter with a red filter, and samples (1mL) were removed.

500 µL samples of *S. enterica* were centrifuged and the supernatant was filtered through a 0.45 µm SpinX column before being acidified by 2.5 µL of 5M H_2SO_4. 200 µL of these samples were loaded onto a Shimadzu HPLC system equipped with an LC-20AT pump, a SIL-20AC autosampler, a CTO-20AC heater and a SPD-M20A prominence photodiode detector. Samples were run over an Aminex HPX-87H organic acid analysis column (300 x 7.8 mm, BioRad) at 45°C with a 0.6 mL/min flow rate. Peaks were detected at 210 nm. Identity of the acetate peak was determined by comparison to a NaOAc control. Under these conditions, the acetate peak eluted at 15.1 minutes. Area under the peaks was quantified using the Shimadzu LabSolutions software to determine the concentration of acetate in the sample.

Spectrophotometric acetate kinase assay. To measure the kinetics of homogeneous EutQ, we used a modified version of a previously-described acetate kinase coupled assay (24). Each reaction contained HEPES buffer (84 mM), Sodium Acetate (NaOAc, made fresh, variable concentration), $MgCl_2$ (6.6 mM), NADH (1.1 mM), Pyruvate kinase/lactate dehydrogenase (1-

1.6/1.6-2.3 U, respectively), myokinase (0.66 U), PEP (1.9 mM, made fresh) and ATP (variable concentration). Reactions were set up in a 96-well plate and initiated with the addition of EutQ or EutP (2 μM). The reaction was monitored at 340 nm on a Spectramax Plus (Molecular Devices). Reactions were performed at 40°C.

HPLC determination of EutQ and EutP reaction products. Products of the EutP and EutQ reactions were analyzed via a Partisil-10 SAX column (250 x 4.6 mm, Phenomenex) equipped with an NH_2 SecurityGuard cartridge (Phenomenex). A gradient of potassium phosphate (monobasic) was run from 0.05 to 1 M over 35 minutes at a flow rate of 1 mL/min at 25°C. Reaction products were detected at 254 nm. Prior to running, all reactions were incubated at 37°C for 2 hours and filtered through Spin-X columns (Costar, 0.45 μm).

Reactions using EutP and/or EutQ to generate ATP were prepared in PIPES buffer (20 mM, pH 7). The reaction mixture contained EutQ and/or EutP (0.7 μM each), ADP (1mM), Acetyl-phosphate (1mM) and $MgCl_2$ (1 mM).

For reactions using EutD to generate acetyl-phosphate for EutP and/or EutQ, acetyl-phosphate in the above reaction was replaced with EutD (0.7 μM), acetyl-CoA (0.5 mM), and KH_2PO_4 (1mM).

Reactions using EutP and/or EutQ to generate acetyl-phosphate for EutD contained EutD (0.7 μM), EutP and/or EutQ (0.7 μM), ATP (1 mM), acetate (1 mM), $MgCl_2$ (1 mM), and coenzyme A (0.5 mM).

^{31}P NMR Spectroscopy. For ^{31}P NMR analysis, reaction mixtures were prepared as described for HPLC analysis. Reactions were brought to a final volume of 600 μL in D_2O (16.6%).

Proton-decoupled ^{31}P Spectra were obtained using a Varian Unity Inova500 500 mHz spectrometer (Chemical Sciences Magnetic Resonance Facility, University of Georgia). Chemical shifts were referenced to H_3PO_4 (85%) set to 0.0 ppm.

4.4 Results

High levels of EutQ *expression from a plasmid when growing aerobically results in a growth defect on ethanolamine and acetate*

Previous results have been unable to identify aerobic phenotypes for *eutQ* strains growing aerobically on ethanolamine (12). Our results were similar to the earlier studies, although we note that *eutQ* strains provide a slight increase to growth rate (52% faster than WT) and maximum density of the cell culture when growing on 30 mM ethanolamine at 40°C (Figure 4.2A). However, expression of EutQ from the pBAD24 vector decreased both growth rate (163% slower than WT) and maximal cell density and effectively prevents growth at low concentrations of ethanolamine and high concentrations of inducer. In order see if other Eut proteins produce a similar phenotype under these conditions, we overexpressed the EutE acetaldehyde dehydrogenase *in trans* and observed similar growth enhancement. This was also observed when we expressed the analogous propanealdehyde dehydrogenase in the 1,2-propandiol metabolosome, PduP (Figure 4.3).

We overexpressed EutQ in a WT background when growing on acetate (60 mM) and observed a reduction in the maximal OD compared to the positive control (Figure 4.2B). No phenotype was observed when EutQ was overexpressed on glycerol or glucose carbon sources (data not shown).

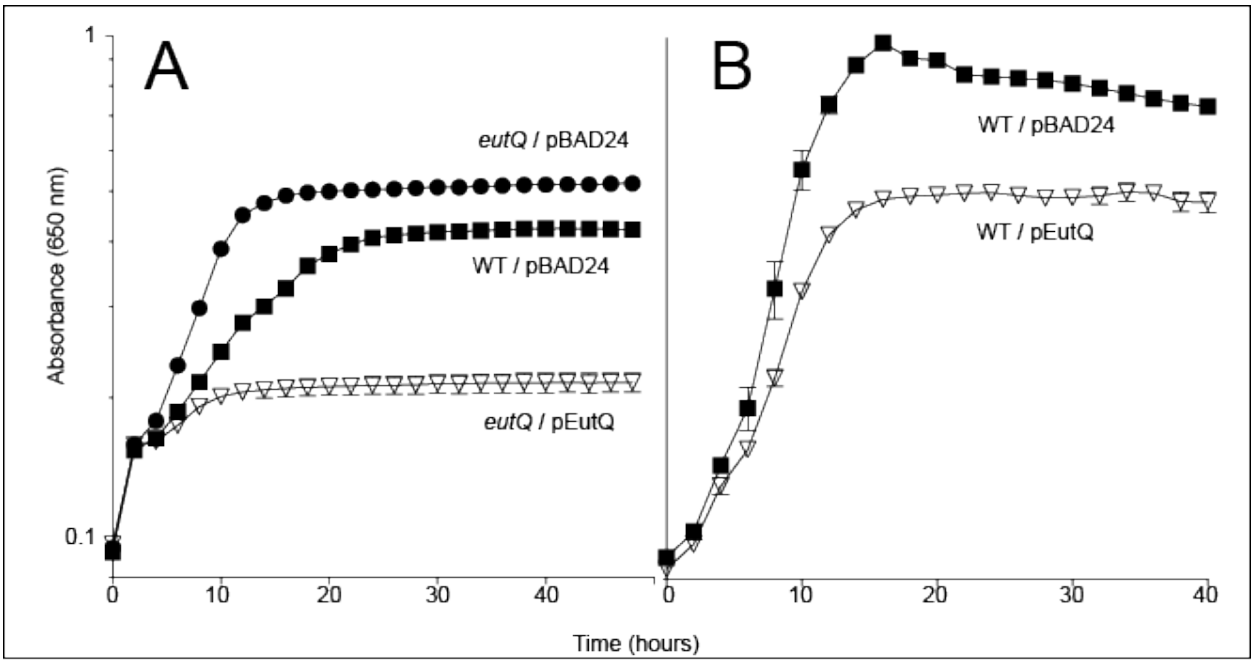

Figure 4.2. Aerobic phenotypes of eutQ- strains and strains overexpressing pEutQ. A) Strains grown on minimal medium supplemented with ethanolamine (30 mM) as a carbon and energy source and arabinose inducer (1 mM), 40°C. B) Strains grown on minimal medium supplemented with acetate (60 mM) as a carbon and energy source and arabinose inducer (1 mM), 40°C.

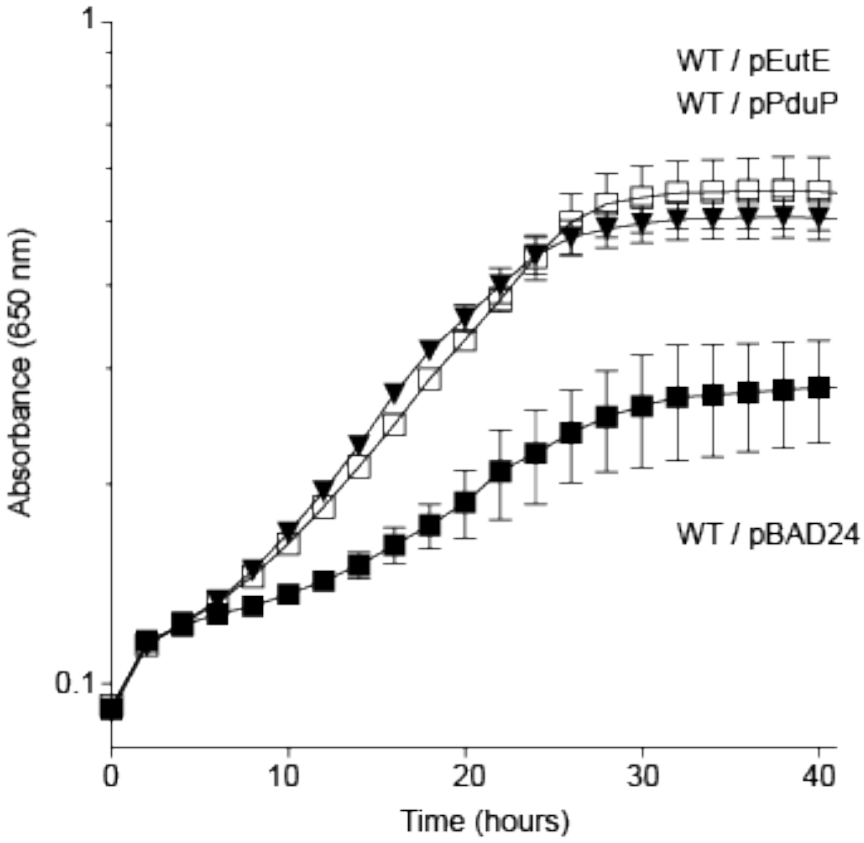

Figure 4.3. Overexpression of EutE and PduP *in trans* enhance growth of *S. enterica* on ethanolamine at 40°C. Strains grown on minimal medium supplemented with ethanolamine (30 mM) as a carbon and energy source with arabinose inducer (1 mM), 40°C.

A eutQ *strain excretes less acetate than wild-type when growing on ethanolamine*

As the aerobic growth curves indicated that EutQ overexpression has deleterious effects on both acetate and ethanolamine media, we investigated the effect of *eutQ* on acetate excretion. WT, *eutQ* and *eutD* strains were grown aerobically on ethanolamine as the sole carbon, nitrogen and energy source (Figure 4.4). WT accumulates 5 mM acetate before reuptake occurs. The *eutD* strain acts as a negative control, as *eutD* is required to export acetate when growing on ethanolamine (23). The *eutQ* strain exports about half the amount of acetate as the WT strain before reuptake. This phenotype is very similar to a previously-observed phenotype of an *ackA* strain growing under the same conditions, where AckA is the housekeeping acetate kinase (23).

A eutQ *strain has a severe growth defect when growing anaerobically on ethanolamine and tetrathionate*

To determine if a *eutQ* strain has an anaerobic phenotype, we grew the strain on ethanolamine (30 mM) utilizing tetrathionate (40 mM) as a terminal electron acceptor (Figure 4.5). The *eutQ* strain grows significantly slower than wild-type under these conditions, and its maximal OD is ~0.8 units lower than WT. Complementation by EutQ expressed from a plasmid restores growth to near-WT levels. The housekeeping acetate kinase, AckA, complemented the *eutQ* strain to near-WT levels. The kinases PduW and TdcD (25-27), both capable of phosphorylating acetate, complemented at a similar level as AckA.

An *ackA* strain has a significant growth defect on ethanolamine and tetrathionate, which is complementable by *eutQ* (Figure 4.6). In contrast to this result, *ackA* strains only have a slight growth defect when growing aerobically on ethanolamine (23). *eutQ* was unable to complement an *ackA* strain growing aerobically on acetate (data not shown), indicating that its acetate kinase activity is specialized to anaerobic conditions on ethanolamine.

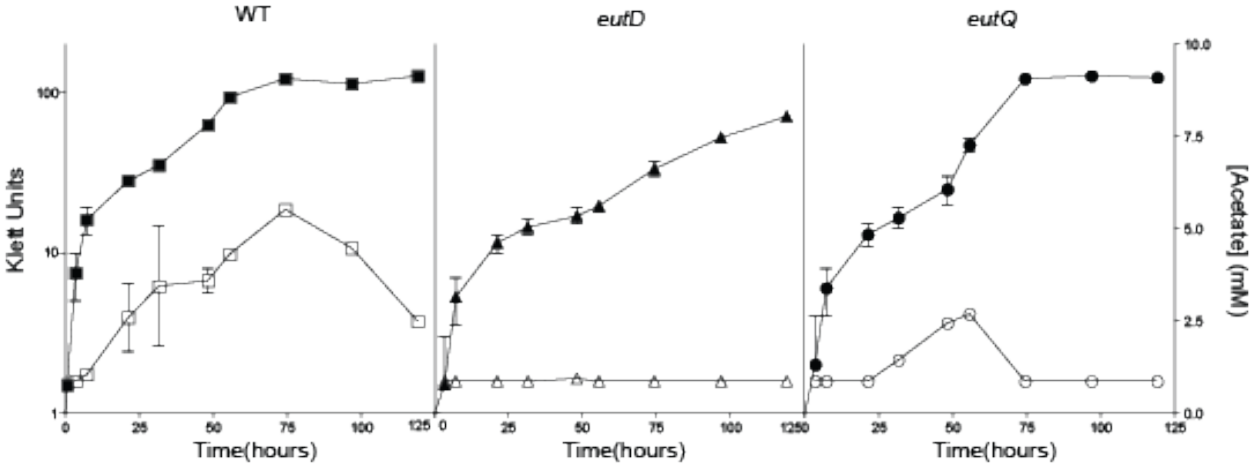

Figure 4.4. Acetate excretion and growth curves. Strains were grown on minimal medium supplemented with ethanolamine (30 mM) in Klett flasks equipped with a red filter. Closed symbols represent growth (left Y axis), open symbols represent acetate excretion (right Y axis).

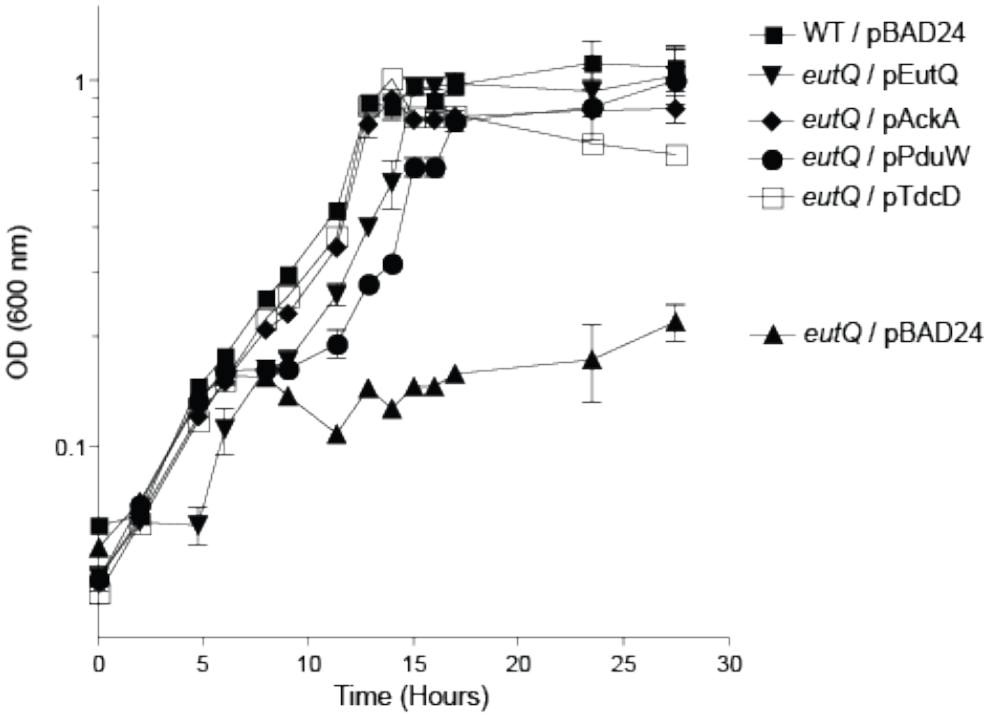

Figure 4.5. Complementation of a *eutQ* phenotype by acetate kinases. Strains were grown anaerobically on minimal medium supplemented with ethanolamine (30 mM), NH_4Cl (30 mM), tetrathionate (40 mM) and arabinose (0.05 mM) at 37°C.

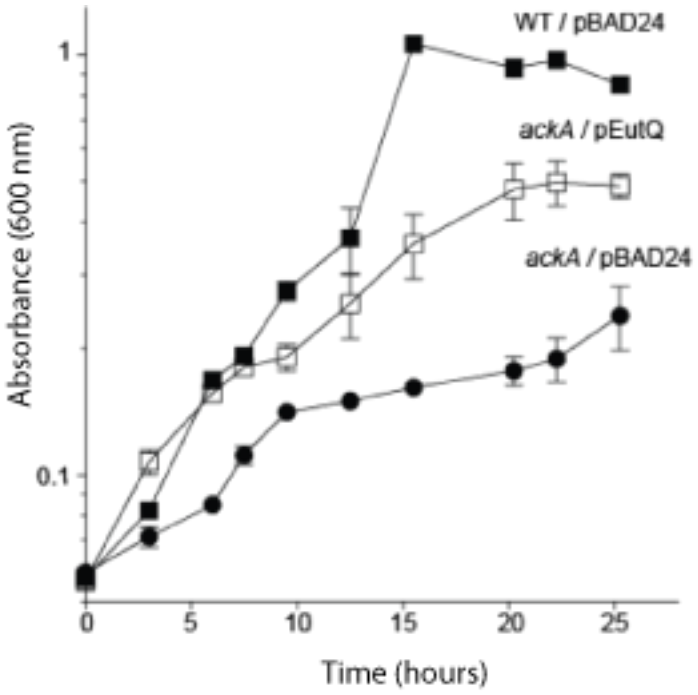

Figure 4.6. Complementation of an *ackA* phenotype by acetate kinases. Strains were grown anaerobically on minimal medium supplemented with ethanolamine (30 mM), NH_4Cl (30 mM), tetrathionate (40 mM) and arabinose (0.05 mM) at 37°C.

Although EutQ complements a *eutQ* phenotype at low levels of induction, it fails to do so when expressed at high levels (1 mM arabinose), potentially due to the same toxicity observed under aerobic conditions. However, this toxicity is rescued by the addition of pantothenate, a precursor to coenzyme A (CoA) (Figure 4.7).

EutQ has acetate kinase activity in vitro

EutQ was assayed for acetate kinase activity by analyzing the products of its reaction on an HPLC system. As acetyl phosphate is very labile and difficult to detect in low amounts, we ran the reaction in the opposite direction, supplying acetyl-phosphate and ADP to make ATP (Figure 4.8). The formation of ATP was confirmed using ^{31}P NMR in comparison to a standard and no-enzyme control (Figure 4.9). Similar results were obtained when coupling EutQ to EutD, the phosphotransacetylase in the *eut* operon. EutD generates acetyl phosphate from acetyl-CoA and orthophosphate. When these reagents are added to the EutQ reaction in place of acetyl-phosphate, ATP is still generated (Figure 4.10A-D). This reaction can also be run in reverse, with the acetyl-phosphate generated by EutQ being used by EutD acetylate coenzyme A (Figure 4.10E-H). Interestingly, the amount of acetyl-CoA converted to CoA by EutD is increased by co-incubation of EutQ (by 15%) or EutP (by 44%).

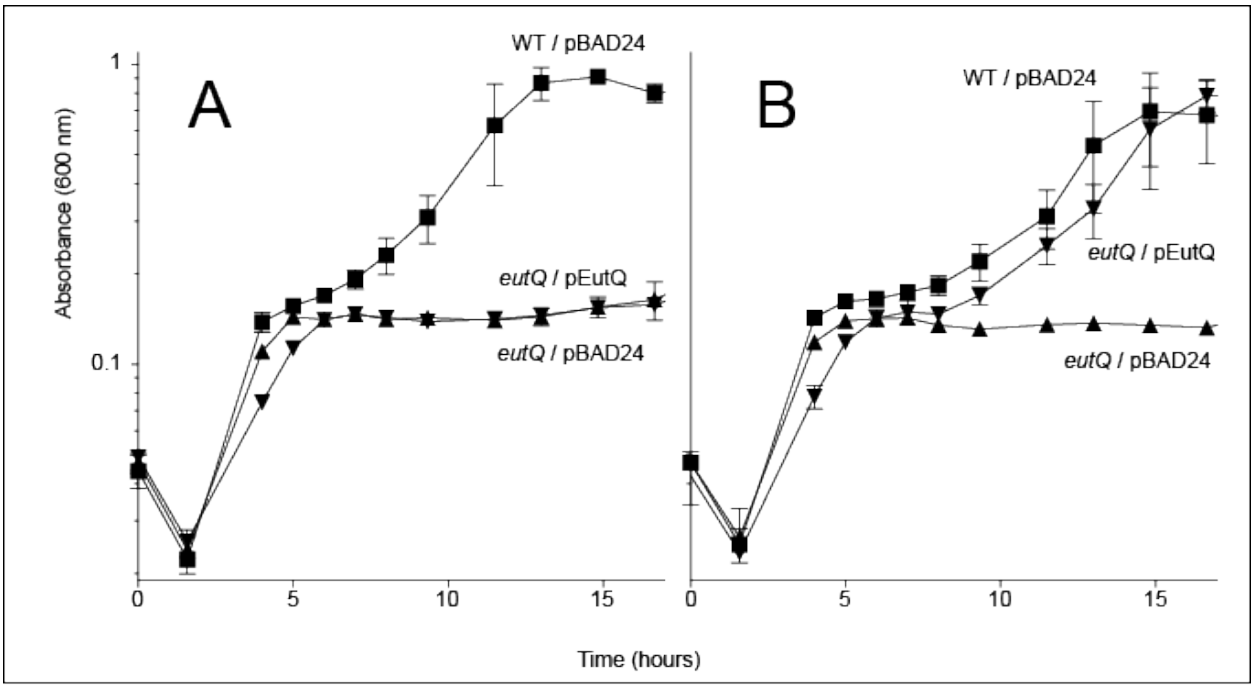

Figure 4.7 Exogenous pantothenate rescues strains expressing high levels of EutQ. A) Strains overexpressing EutQ from a plasmid growing anaerobically on minimal medium supplemented with ethanolamine (30 mM), NH_4Cl (30 mM), tetrathionate (40 mM) and arabinose (1 mM). B) Same conditions as A, but with the addition of pantothenate (20 μM)

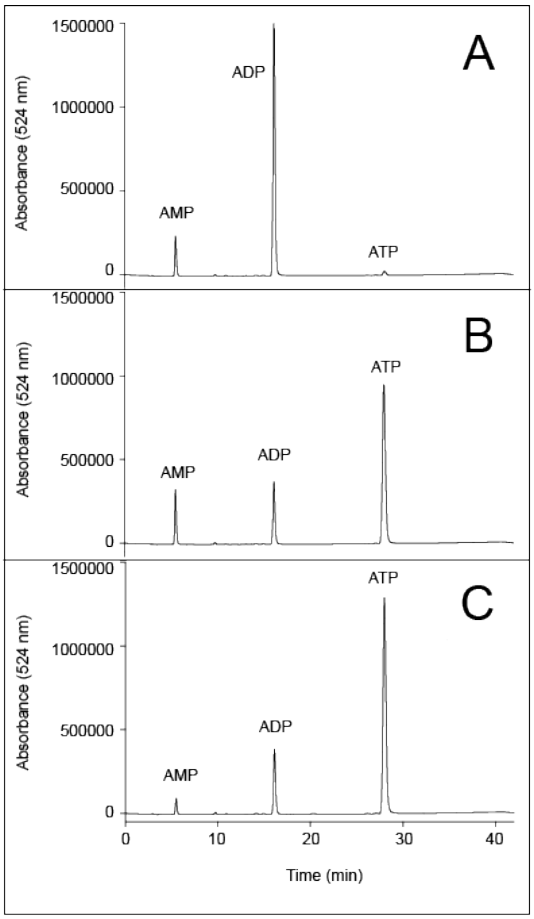

Figure 4.8. HPLC spectra of the EutQ and EutP acetate kinase reactions, detecting the generation of ATP from ADP and acetyl-phosphate. Assays (20 mM HEPES pH 7, ADP (1mM), Acetyl-phosphate (1mM) and $MgCl_2$ (1 mM)) were incubated at 37°C for 1 hour with our without enzyme (0.7 µM each). A) No-enzyme control, B) EutQ, C) EutP

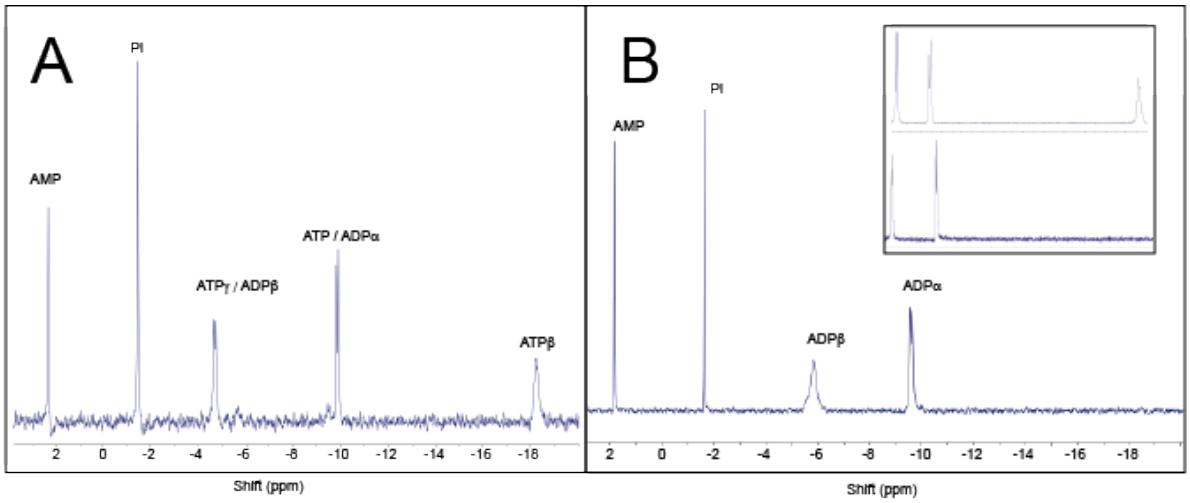

Figure 4.9. ^{31}P NMR of EutQ with ADP and acetyl-phosphate. A) EutQ generating ATP from ADP and acetyl-phosphate. B) No-enzyme control of reaction A. Inset: pure standards of ATP (top) and ADP (bottom)

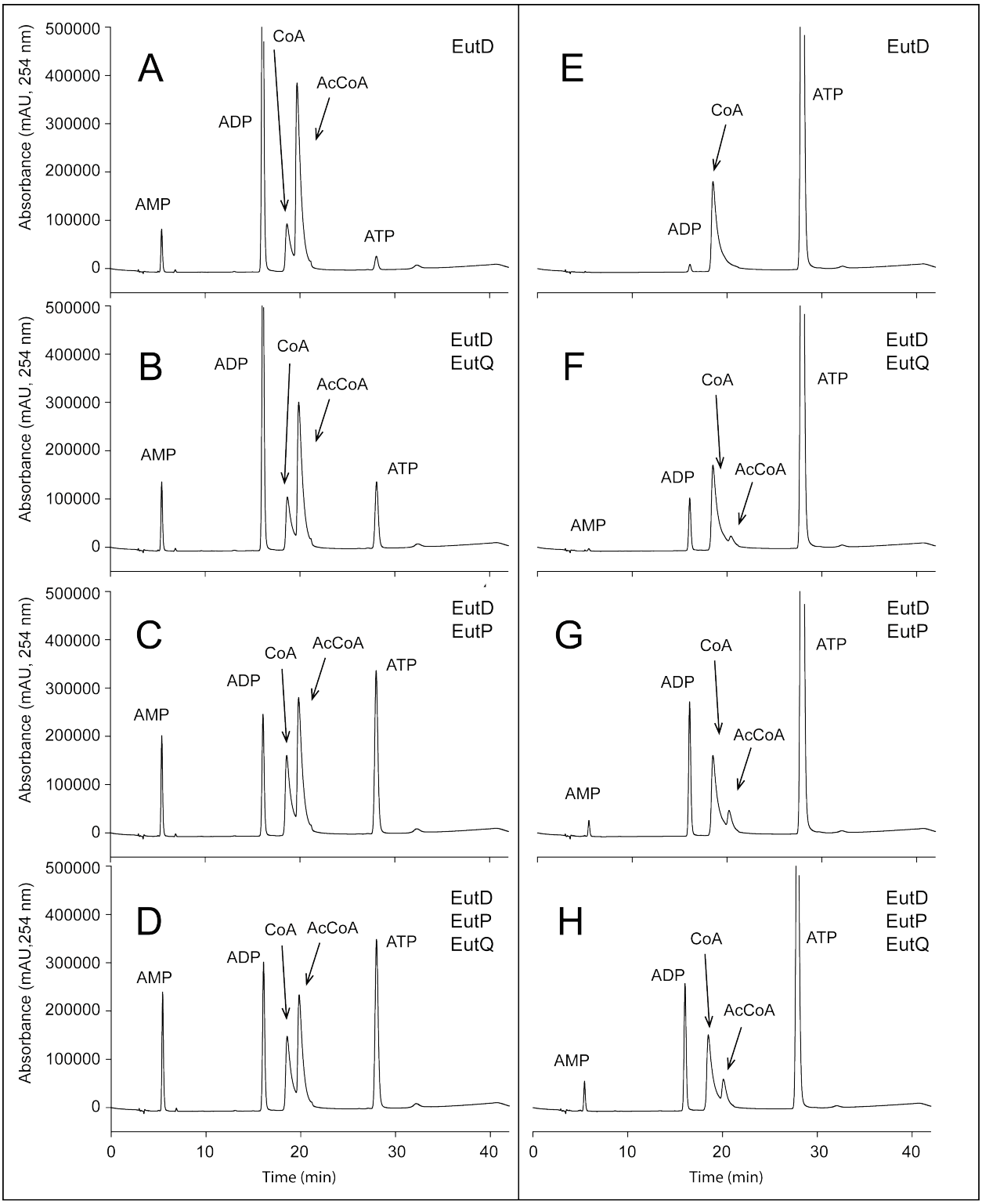

Figure 4.10. HPLC spectra of EutQ and/or EutP reactions coupled to EutD, monitored at 254 nm. Enzymes included in the reaction are denoted in the upper right of each spectrum. A-D) EutD supplies acetyl-phosphate to EutQ and/or EutP, which generates ATP from ADP. E-H) EutQ and/or P supplies acetyl-phosphate to EutD, which generates acetyl-CoA from CoA.

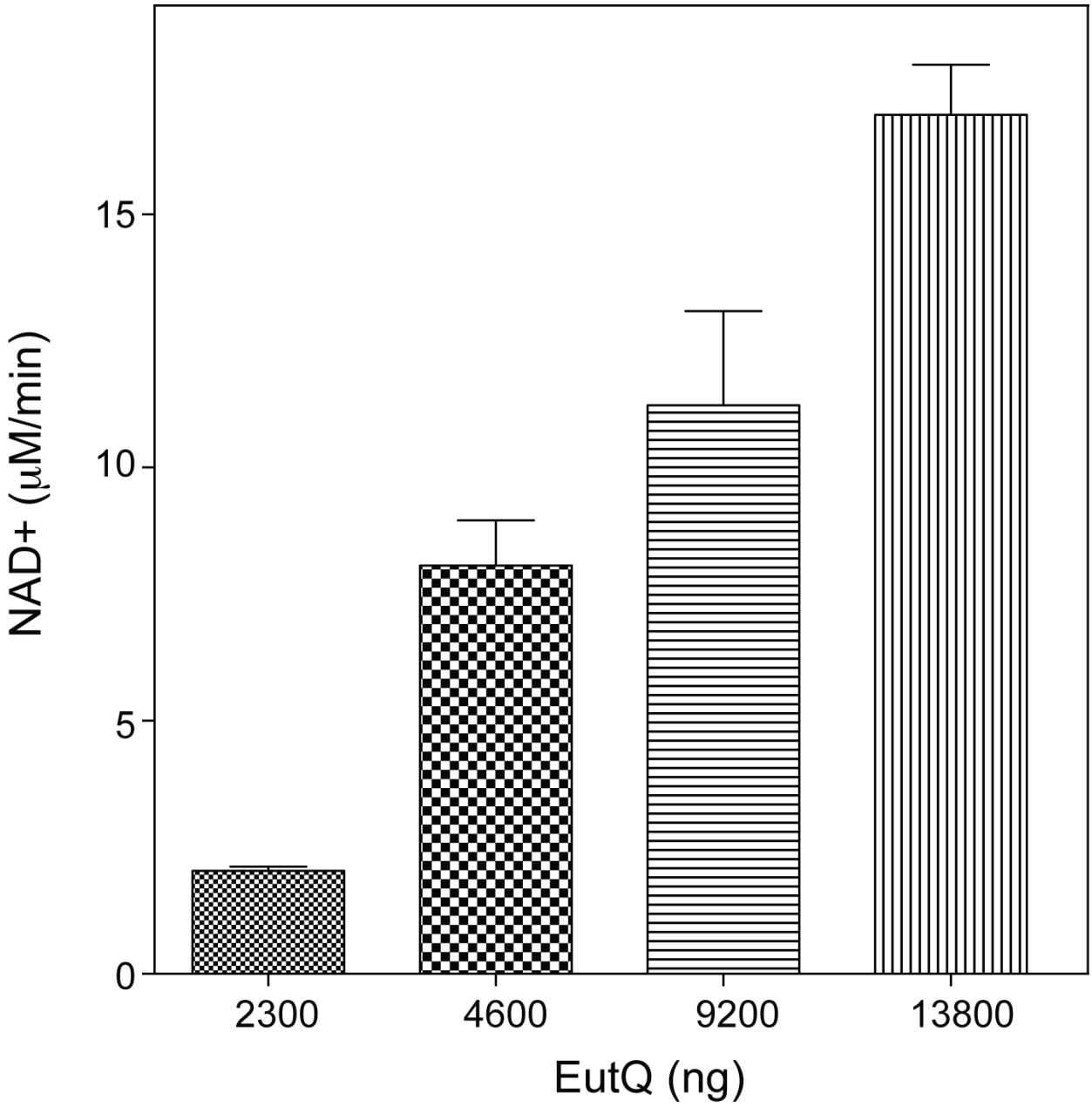

Figure 4.11. Activity of EutQ in a coupled assay. Indirect EutQ activity was observed spectrophotometrically at 340 nm in a coupled assay with pyruvate kinase and lactate dehydrogenase.

EutQ was also assayed for acetate kinase activity in a continuous spectrophotometric assay that ultimately measured the disappearance of NADH from the reaction (See materials and methods). The reaction rate was dependent on the concentration of EutQ (Figure 4.11). Addition of a nonhydrolyzable ATP analog, AMP-PCP, in place of ATP resulted in complete loss of activity. Dialysis of EutQ with EDTA (buffer A with no imidazole and 2 mM EDTA, 3 buffer changes for 2 hours each) did not result in any loss of activity compared to controls. EutQ was able to use guanosine triphosphate (GTP) at a 45% slower specific activity compared to ATP. No activity was detected in when cytidine triphosphate (CTP) or thymidine triphosphate (TTP) was used in place of ATP.

Table 4.2 presents the kinetics of EutQ as determined by the lactate dehydrogenase/pyruvate kinase coupled assay. These differ slightly from published values for the housekeeping *S. enterica* acetate kinase AckA (28). In comparison, EutQ has a tenfold-lower K_M (70 μM) for ATP and a twofold higher K_M (1.2 mM) for acetate.

EutQ belongs to the cupin superfamily, and many members of this superfamily bind transition-state metals to catalyze a variety of reactions. However, EutQ belongs to a minority of cupins that lacks a metal-binding motif (15). In place of one of the conserved histidines of the metal binding motif is an aspartate residue (D175), which has been proposed to form an acidic pair with a nearby glutamate (E173). These two residues are located deep within a negatively-charged cleft, as seen in a crystallized EutQ from *Clostridium difficile*. This cleft was proposed to be the active site. Remarkably, Pitts et al. modeled an acetate molecule deep within the site, demonstrating a feasible acetate-binding active site (29). However, changing either of these two residues to alanine does not impact the ability of EutQ to complement a *eutQ* phenotype. Changing both of the residues to alanine results in a slight growth defect, compared to complementation by WT (data not shown).

Table 4.2. EutQ and EutP kinetics				
Enzyme	Substrate:	Km (mM)	Vmax (μM/min)	Kcat (s-1)
EutQ	Acetate	0.7 ± 0.2	6.3 ± 0.3	317.6
	ATP	0.5 ± 0.1	8.6 ± 0.5	433.6
EutP	Acetate	0.7 ±0.2	9.5 ± 0.7	545.1
	ATP	0.5 ± 0.2	11.5 ± 1.2	657.1

EutP *has acetate kinase activity in vitro, but a eutP strain does not have a phenotype*

The *eutP* gene is immediately upstream of *eutQ* in the *eut* operon, and the start codon of *eutQ* overlaps with the coding sequence of *eutP*. Although we have been unable to find a phenotype for *eutP* under conditions in which *eutQ* has a phenotype, we hypothesized that EutP and EutQ may interact based on their proximity. Surprisingly, EutP demonstrated acetate kinase activity independently of EutQ, and is capable of generating ATP from ADP and acetyl-phosphate and acetyl-phosphate from ATP and acetate (Figures 4.8, 4.10). Similarly to EutQ, it does not have activity with AMP-PCP, CTP, or TTP, but has a 28% lower specific activity with GTP compared to ATP. Dialysis with EDTA has no effect on the EutP specific activity. Kinetics indicated that EutP is a slightly faster enzyme than EutQ, with near-identical K_M rates and a k_{cat} value approximately 30-40% higher than EutQ for either acetate or ATP (Table 4.2).

4.5 Discussion

EutQ belongs to a novel class of acetate kinase

The discovery of conditions that require *eutQ* for growth is a first in the literature. An analog to EutQ exists in the *pdu* operon, which encodes a similar metabolosome for the catabolism of 1,2 propanediol (7,27). The PduW propionate kinase is 87% identical to the *S. enterica* AckA housekeeping acetate kinase (30). There is no observed phenotype for a *pduW* strain growing either aerobically on anaerobically with tetrathionate (10mM) on 1,2-propanediol (82 mM) (25). These growth conditions contain a higher concentration of carbon and a lower concentration of tetrathionate than the conditions in this report. A *pduW* phenotype could possibly be detected if growth conditions are adjusted to more closely match those reported in this paper. Figure 4.12 proposes the location of EutQ and/or EutP to be downstream of EutD, the enzyme that generates acetyl-phosphate in the metabolosome, based on the ability of those

enzymes to use the product of EutD. There is no data on the location of EutQ relative to the exterior or lumen of the metabolosome, the figure places EutQ inside as it probably exists in close proximity to the other *eut* enzymes. However, acetyl-phosphate is capable of passing through the metabolosome shell, as *eutQ* can be complemented by cytoplasmic acetate kinases.

Bioinformatic searches via BLAST do not indicate any significant similarity between EutQ and other acetate kinases (31). However, given the biochemical activity tested and the ability of alternative acetate kinases to complement *eutQ,* we believe that EutQ belongs to a novel family of acetate kinase. The dual beta-barrel fold of the EutQ cupin domain is widespread across many different types of enzymes, and is insufficient to predict activity. The active site of EutQ was proposed to be located deep within a negative cleft of each beta-barrel, and a conserved aspartate and glutamate residue were hypothesized to be important for activity (29). These residues occupy the position of histidines conserved among cupins that bind metal cofactors. EutQ does not seem to require metal cofactors, as dialysis with EDTA had no effect on activity. Varying either of the two conserved residues to alanine did not affect the ability of EutQ to complement, and varying both to alanine resulted in only a slight growth defect. Therefore, the location and nature of the active site remains uncertain.

Maintenance of the energy charge (The ratio of ATP +1/2 ADP : ATP + ADP + AMP) is another important function of acetate kinases (45). In *E. coli*, this charge is maintained at ~0.9 during log phase, with growth arrest occurring if the charge drops below ~0.5 (46). Quantification of energy charge difference in *eutQ*$^{+}$ and *eutQ* mutant strains would help determine if the ATP generated by EutQ via substrate-level phosphorylation is important to maintain the energy pool of *S. enterica*.

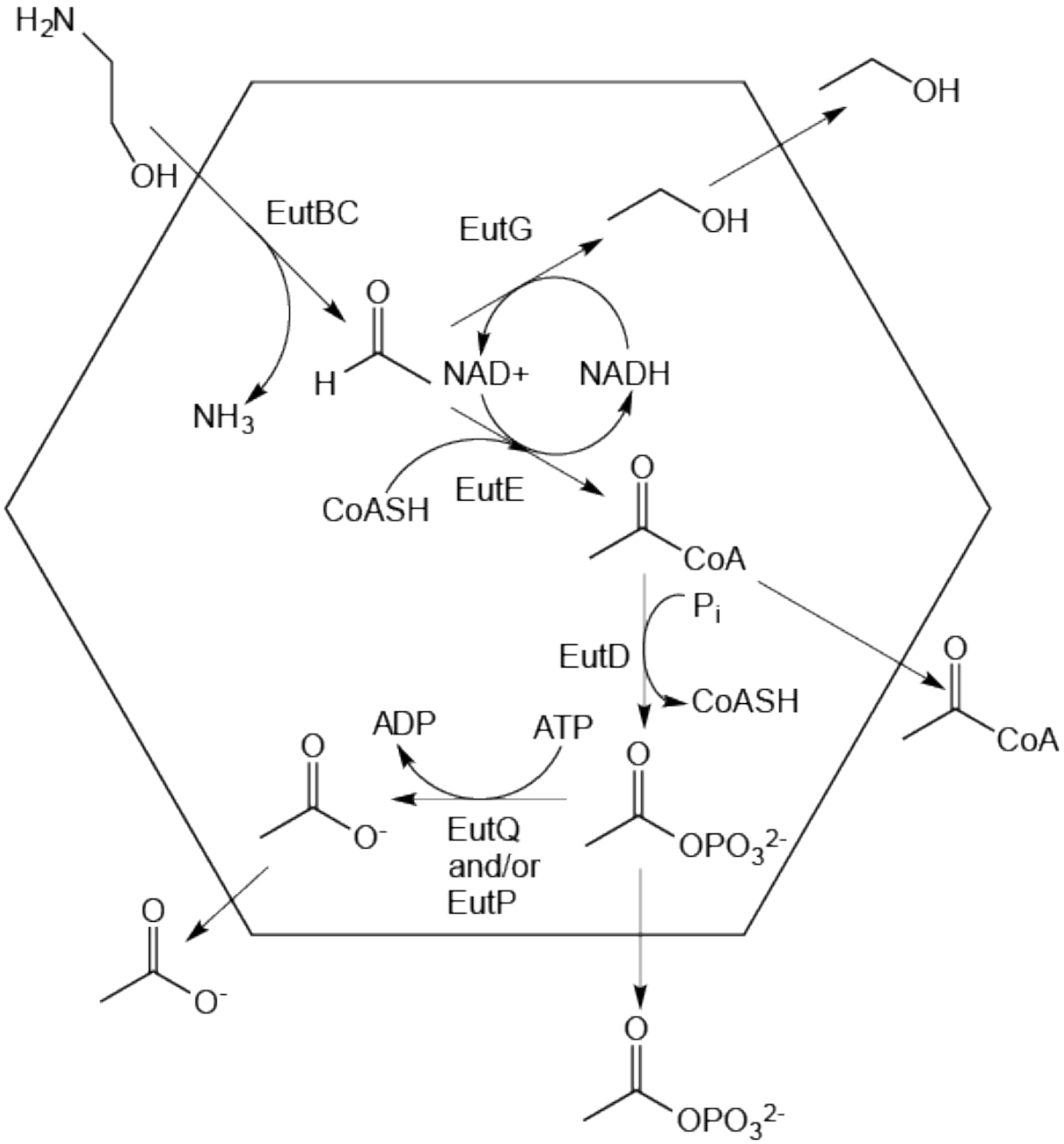

Figure 4.12. Proposed location of EutQ with regards to ethanolamine catabolism.

EutP has acetate kinase activity in vitro

EutP has observable acetate kinase activity under the same conditions as EutQ. Given the data presented within this report, it is possible that EutP and EutQ are two halves of an acetate kinase heterodimer. The lack of phenotypes for *eutP* strains would indicate that EutQ is the more important half of this putative heterodimer, although kinetics indicate that EutP is a slightly more efficient enzyme. EutQ may be important for reasons other than enzyme activity, such as facilitating protein-protein interactions.

Across organisms with *eut* operons, EutP and EutQ are not always present together, nor are their genes always adjacent. The *Nocardiodes, Listeriaceae*, and *Entercoccaceae eut* operons only have *eutQ*, and *Clostridiaciae,* and *Fusobacterium nucleatum* do not have *eutP* and *eutQ* located next to one another (32). Numerous other genomes do not have either *eutP* or *eutQ*, although these organisms often have minimal *eut* operons lacking the shell and most other *eut* proteins except for EutBC.

Despite only observing the *eutQ* phenotype growing anaerobically on tetrathionate, the presence of *eutQ* and *eutP* is not necessarily linked to the ability to respire tetrathionate. Many ethanolamine-catabolizing organisms such as *Klebsiella pneumoniae, Escherichia coli* and *Shigella flexneri* encode copies of *eutQ* and *eutP* yet are incapable of respiring tetrathionate (33). Therefore, it seems that EutQ and EutP are not directly involved in tetrathionate respiration. A requirement for *eutQ* or *eutP* has yet to be tested in other organisms.

EutQ may be important for increasing flux through EutD

The enzyme upstream of EutQ in the catabolic pathway, EutD converts acetyl-CoA to acetyl-phosphate and CoA (47). The CoA precursor pantothenate can rescue EutQ overexpression-induced toxicity during anaerobic growth. The negative growth phenotype could

conceivably be caused by excess EutQ increasing the rate of EutD, resulting in a depletion of acetyl-CoA needed for central metabolism (Figure 4.12). This is supported by the *in vitro* tests of EutD coupled to EutQ and EutP. EutQ, EutP, or both in combination enhanced the EutD-catalyzed conversion of acetyl-CoA to CoA. An increased concentration of CoA precursors may have increased the flux through EutE, resulting in higher acetyl-CoA levels and compensating for the increase in EutD activity.

Related to the above hypothesis, the *eutQ* phenotype could be due to increased concentrations of acetaldehyde, which is can be toxic to *S. enterica* (48). If EutQ and EutP enhance upstream EutD reaction as proposed above, their absence would result in a less-active EutD, which could in turn result in a less active EutE aldehyde dehydrogenase. With less flux through EutE, the acetaldehyde produced by EutBC could accumulate to a higher level. This hypothesis is consistent with an earlier observation that *eutQ* and *eutP* mutant strains excrete more acetaldehyde than wild-type (14). If this hypothesis is correct, expressing aldehyde dehydrogenases in *eutQ* strains should correct the phenotype. These experiments are ongoing in our lab.

EutQ may balance substrate-level phosphorylation with carbon assimilation when growing anaerobically on ethanolamine

The standard oxidation/reduction potential of tetrathionate/thiosulfate is +170 mV, compared to +815 for oxygen/water (34,35). If NADH acts as electron donor, the Nernst equation indicates that -94.6 kJ/mol is possible for respiration to tetrathionate as a terminal electron acceptor, compared to the -219 kJ/mol possible for respiration to oxygen. This lower free energy may result in fewer ATPs produced during oxidative phosphorylation, which would place a greater importance on substrate-level phosphorylation. EutQ might be important for

energy generation under these conditions, which could explain why *eutQ* strains, as well as *ackA* strains, grow poorly on ethanolamine with tetrathionate.

Another possibility is that EutQ is important for recycling ATP within the metabolosome, assuming EutQ is located inside the metabolosome. EutA requires ATP to regenerate EutBC, and EutT uses ATP to adenosylate cobalamin to coenzyme B_{12} (36,37). Several enzymes have recently been identified as being important for cofactor recycling within both the *eut* and *pdu* metabolosomes, respectively. EutD, EutE and EutG have been proposed to recycle CoA and NAD+ within the *eut* metabolosome, while PduP, PduQ and PduL have been proposed to fulfill the same role in the *pdu* metabolosome (38-40). EutT and PduO are thought to be responsible for recycling cobalamin (13,41-43). ATP is the only shared cosubstrate whose regeneration is not accounted for in the metabolosome, and EutQ/EutP could be responsible for keeping concentrations sufficiently high within the lumen.

Aerobic growth conditions may enable a eutQ *strain to tolerate higher acetaldehyde concentrations*

The lack of a deleterious phenotype for *eutQ* when growing aerobically is puzzling, given its essential nature when growing anaerobically using tetrathionate. However, if the *eutQ* phenotype slows the activity of EutE as proposed above, aerobic growth may be able to tolerate the resulting increased concentration of aldehyde. The concentration of the detoxifying tripeptide glutathione (GSH) is four times higher during aerobic growth than anaerobic growth in the related bacterium *Escherichia coli* (44). Additionally, aerobic growth provides *S. enterica* with more energy to divert to expression of proteins to detoxify acetaldehyde, such as aldehyde dehydrogenase (AdhE). The presence of additional detoxifying factors may prevent the increased acetaldehyde from damaging proteins and DNA.

Alternatively, if EutQ is required for substrate-level phosphorylation anaerobically, it could be that energy generation via this route is not required for aerobic growth on ethanolamine, as more energy would be available through oxidative phosphorylation. Thus, no negative phenotype would be seen. This however does not explain the slight growth enhancement in aerobic *eutQ* strains, as discussed below.

In strains growing aerobically on ethanolamine, a slight growth enhancement was observed in *eutQ* strains at 40°C. This could be due to less acetyl-CoA being consumed by EutD, increasing the amount of that molecule available to central metabolism. Another possibility is that the excess aldehyde produced in *eutQ* strains is able to diffuse out of the metabolosome at 40°C and become accessible to cytoplasmic aldehyde dehydrogenases capable of generating acetyl-CoA. 40°C is slightly higher than the 37°C used in most studies of the *eut* metabolosome. It is conceivable that the higher temperature causes greater volatility in the aldehyde intermediates or instability in the metabolosome shell, resulting in aldehyde being released from the shell's lumen. This is supported by the significant growth enhancements observed expressing EutE and PduP aldehyde dehydrogenases *in trans* at 40°C. In addition to removing excess acetaldehyde, these enzymes produce acetyl-CoA that can enter central metabolism and enhance cell growth.

Strains overexpressing EutQ on a plasmid show significant growth defects on ethanolamine, both respiring aerobically and anaerobically on tetrathionate. This may be due to aggregation or interference with the *eut* metabolosome. However, it may also be due to depletion of acetyl-CoA via increased flux through EutD. Correction of anaerobic EutQ-overexpression toxicity by pantothenate could stimulate greater flux through EutE and decrease the accumulation of acetaldehyde. The aerobic phenotype cannot be rescued by pantothenate

under the conditions tested, indicating that EutQ-overexpression toxicity may have multiple causes.

EutQ and P may require specific protein-protein interactions in the metabolosome

The inability of EutQ and/or EutP to complement an *ackA* phenotype growing aerobically on acetate is not well understood. AckA and other acetate kinases complement a *eutQ* phenotype to near-WT levels. It could be that EutQ and P require specific interactions only present within the *eut* metabolosome to function *in vivo*. Similarly, we are unsure why the overexpressing EutQ results in a lower maximal OD when growing on acetate, although it may also be related to indirect depletion of acetyl-CoA or other interference with metabolite levels in the TCA cycle.

4.6 Conclusion

This work provides the first evidence for phenotypes and biochemical activity related to EutQ in *S. enterica*, as well as biochemical activity for EutP. These enzymes compose a novel class of acetate kinase, and are active when coupled to the physiologically-relevant EutD phosphotransacetylase. EutQ is required for growth of *S. enterica* on ethanolamine when utilizing tetrathionate as a terminal electron acceptor, but is not required when growing aerobically. This finding is significant as tetrathionate is much more likely to be utilized than oxygen by *S. enterica* when growing on ethanolamine in a host system. Our initial results indicate that EutQ, and potentially EutP, are important for maintaining optimum acetaldehyde and acetyl-CoA concentrations during ethanolamine metabolism

The role of EutP *in vivo* remains unexplained. Whereas its ability to generate ATP *in vitro* parallels that of EutQ, *eutP* strains have no observable phenotype under aerobic or anaerobic conditions. EutP's activity remains an area of active study in our lab.

4.7 Acknowledgements

We would like to thank Dongtao Cui at the University of Georgia Chemical Sciences Magnetic Resonance facility for her technical assistance.

4.8 References

1. Chang, G. W., and Chang, J. T. (1975) Evidence for the B12-dependent enzyme ethanolamine deaminase in *Salmonella*. *Nature* **254**, 150-151.

2. Roof, D. M., and Roth, J. R. (1988) Ethanolamine utilization in *Salmonella typhimurium*. *J. Bacteriol.* **170**, 3855-3863.

3. Roof, D. M., and Roth, J. R. (1989) Functions required for vitamin B12-dependent ethanolamine utilization in *Salmonella typhimurium*. *J. Bacteriol.* **171**, 3316-3323.

4. Price-Carter, M., Tingey, J., Bobik, T. A., and Roth, J. R. (2001) The alternative electron acceptor tetrathionate supports B12-dependent anaerobic growth of *Salmonella enterica* serovar Typhimurium on ethanolamine or 1,2-propanediol. *J. Bacteriol.* **183**, 2463-2475.

5. Winter, S. E., Thiennimitr, P., Winter, M. G., Butler, B. P., Huseby, D. L., Crawford, R. W., Russell, J. M., Bevins, C. L., Adams, L. G., Tsolis, R. M., Roth, J. R., and Baumler, A. J. (2010) Gut inflammation provides a respiratory electron acceptor for *Salmonella*. *Nature* **467**, 426-4269.

6. Thiennimitr, P., Winter, S. E., Winter, M. G., Xavier, M. N., Tolstikov, V., Huseby, D. L., Sterzenbach, T., Tsolis, R. M., Roth, J. R., and Bäumler, A. J. (2011) Intestinal inflammation allows Salmonella to use ethanolamine to compete with the microbiota. *Proc. Natl. Acad. Sci.* **108**, 17480-17485.

7. Bobik, T. A. (2006) Polyhedral organelles compartmenting bacterial metabolic processes. *Appl. Microbiol. Biotechnol.* **70**, 517-525.

8. Cheng, S., Liu, Y., Crowley, C. S., Yeates, T. O., and Bobik, T. A. (2008) Bacterial microcompartments: their properties and paradoxes. *Bioessays* **30**, 1084-1095

9. Yeates, T. O., Thompson, M. C., and Bobik, T. A. (2011) The protein shells of bacterial microcompartment organelles. *Curr .Opin. Struct. Biol.* **21**, 223-231.

10. Held, M., Quin, M. B., and Schmidt-Dannert, C. (2013) Eut bacterial microcompartments: insights into their function, structure, and bioengineering applications. *J. Mol .Microbiol. Biotechnol.* **23**, 308-320.

11. Kofoid, E., Rappleye, C., Stojiljkovic, I., and Roth, J. (1999) The 17-gene ethanolamine (*eut*) operon of *Salmonella typhimurium* encodes five homologues of carboxysome shell proteins. *J. Bacteriol.* **181**, 5317-5329.

12. Stojiljkovic, I., Baumler, A. J., and Heffron, F. (1995) Ethanolamine utilization in *Salmonella typhimurium*: nucleotide sequence, protein expression, and mutational analysis of the *cchA cchB eutE eutJ eutG eutH* gene cluster. *J. Bacteriol.* **177**, 1357-1366.

13. Buan, N. R., and Escalante-Semerena, J. C. (2006) Purification and initial biochemical characterization of ATP:Cob(I)alamin adenosyltransferase (EutT) enzyme of *Salmonella enterica*. *J. Biol. Chem.* **281**, 16971-16977.

14. Penrod, J. T., and Roth, J. R. (2006) Conserving a volatile metabolite: a role for carboxysome-like organelles in *Salmonella enterica*. *J. Bacteriol.* **188**, 2865-2874.

15. Dunwell, J. M., Purvis, A., and Khuri, S. (2004) Cupins: the most functionally diverse protein superfamily? *Phytochemistry* **65**, 7-17.

16. Galloway, N. R., Toutkoushian, H., Nune, M., Bose, N., and Momany, C. (2013) Rapid cloning for protein crystallography using Type IIS restriction enzymes. *Crystal. Growth Des.* **13**, 2833-2839.

17. Rocco, C. J., Dennison, K. L., Klenchin, V. A., Rayment, I., and Escalante-Semerena, J. C. (2008) Construction and use of new cloning vectors for the rapid isolation of recombinant proteins from *Escherichia coli*. *Plasmid* **59**, 231-237.

18. Vogel, H. J., and Bonner, D. M. (1956) Acetylornithinase of Escherichia coli: partial purification and some properties. *J. Biol. Chem.* **218**, 97-106.

19. Berkowitz, D., Hushon, J. M., Whitfield, H. J., Jr., Roth, J., and Ames, B. N. (1968) Procedure for identifying nonsense mutations. *J. Bacteriol.* **96**, 215-220.

20. Balch, W. E., and Wolfe, R. S. (1976) New approach to the cultivation of methanogenic bacteria: 2-mercaptoethanesulfonic acid (HS-CoM)-dependent growth of *Methanobacterium ruminantium* in a pressurized atmosphere. *Appl. Environ. Microbiol.* **32**, 781-791.

21. Price-Carter, M., Fazzio, T. G., Vallbona, E. I., and Roth, J. R. (2005) Polyphosphate kinase protects Salmonella enterica from weak organic acid stress. *J. Bacteriol.* **187**, 3088-3099

22. Wilson, A. C. a. A. B. P. (1962) Regulation of flavin synthesis by *Escherichia coli*. *J. Gen. Microbiol.* **28**, 283-303.

23. Starai, V. J., Garrity, J., and Escalante-Semerena, J. C. (2005) Acetate excretion during growth of Salmonella enterica on ethanolamine requires phosphotransacetylase (EutD) activity, and acetate recapture requires acetyl-CoA synthetase (Acs) and phosphotransacetylase (Pta) activities. *Microbiology* **151**, 3793-3801.

24. Bergmeyer, H. U., Bergmeyer, J., Grassl, M., and Berger, R. (1985) Methods of enzymatic analysis. vol. iv. "enzymes 2: Esterases, glycosidases, lyases, ligases". 3rd Edition. Weinheim; Deerfield Beach, Florida; Basel: Verlag Chemie, 1984. 426 S., 258 DM. *Acta Biotechnol.* **5**, 114-114.

25. Palacios, S., Starai, V. J., and Escalante-Semerena, J. C. (2003) Propionyl coenzyme A is a common intermediate in the 1,2-propanediol and propionate catabolic pathways needed for expression of the *prpBCDE* operon during growth of *Salmonella enterica* on 1,2-propanediol. *J. Bacteriol.* **185**, 2802-2810.

26. Hesslinger, C., Fairhurst, S. A., and Sawers, G. (1998) Novel keto acid formate-lyase and propionate kinase enzymes are components of an anaerobic pathway in Escherichia coli that degrades L- threonine to propionate. *Mol. Microbiol.* **27**, 477-492.

27. Bobik, T. A., Havemann, G. D., Busch, R. J., Williams, D. S., and Aldrich, H. C. (1999) The propanediol utilization (*pdu*) operon of *Salmonella enterica* serovar Typhimurium LT2 includes genes necessary for formation of polyhedral organelles involved in coenzyme B_{12}-dependent 1, 2-propanediol degradation. *J. Bacteriol.* **181**, 5967-5975.

28. Chittori, S., Savithri, H. S., and Murthy, M. R. (2012) Structural and mechanistic investigations on Salmonella typhimurium acetate kinase (AckA): identification of a putative ligand binding pocket at the dimeric interface. *BMC structural biology* **12**, 24.

29. Pitts, A. C., Tuck, L. R., Faulds-Pain, A., Lewis, R. J., and Marles-Wright, J. (2012) Structural insight into the *Clostridium difficile* ethanolamine utilisation microcompartment. *PLoS One* **7**, e48360.

30. Havemann, G. D., and Bobik, T. A. (2003) Protein content of polyhedral organelles involved in coenzyme B12-dependent degradation of 1,2-propanediol in *Salmonella enterica* serovar Typhimurium LT2. *J. Bacteriol.* **185**, 5086-5095.

31. Altschul, S. F., Gish, W., Miller, W., and Myers, E. W. (1990) Basic local alignment search tool. *J. Mol. Biol.* **215**, 403-410.

32. Tsoy, O., Ravcheev, D., and Mushegian, A. (2009) Comparative genomics of ethanolamine utilization. *J. Bacteriol.* **191**, 7157-7164.

33. Barrett, E. L., and Clark, M. A. (1987) Tetrathionate reduction and production of hydrogen sulfide from thiosulfate. *Microbiol. Rev.* **51**, 192-205.

34. Kaprálek, F. (1972) The physiological role of tetrathionate respiration in growing citrobacter. *J. Gen. Microbiol.* **71**, 133-139.

35. Thauer, R. K., Jungermann, K., and Decker, K. (1977) Energy conservation in chemotrophic anaerobic bacteria. *Bacteriol. Rev.* **41**, 100-180.

36. Aaron, M., Charbon, G., Lam, H., Schwarz, H., Vollmer, W., and Jacobs-Wagner, C. (2007) The tubulin homologue FtsZ contributes to cell elongation by guiding cell wall precursor synthesis in *Caulobacter crescentus*. *Mol. Microbiol.* **64**, 938-952.

37. Mori, K., Bando, R., Hieda, N., and Toraya, T. (2004) Identification of a reactivating factor for adenosylcobalamin-dependent ethanolamine ammonia lyase. *J. Bacteriol.* **186**, 6845-6854.

38. Huseby, D. L., and Roth, J. R. (2013) Evidence that a metabolic microcompartment contains and recycles private cofactor pools. *J. Bacteriol.* **195**, 2864-2879.

39. Liu, Y., Jorda, J., Yeates, T. O., and Bobik, T. A. (2015) The PduL phosphotransacylase is used to recycle coenzyme A within the Pdu microcompartment. *J. Bacteriol.* **197**, 2393-2399.

40. Cheng, S., Fan, C., Sinha, S., and Bobik, T. A. (2012) The PduQ enzyme is an alcohol dehydrogenase used to recycle NAD+ internally within the Pdu microcompartment of *Salmonella enterica*. *PLoS One* **7**, e47144.

41. Johnson, C. L., Buszko, M. L., and Bobik, T. A. (2004) Purification and initial characterization of the *Salmonella enterica* PduO ATP:Cob(I)alamin adenosyltransferase. *J. Bacteriol.* **186**, 7881-7887.

42. Sheppard, D. E., Penrod, J. T., Bobik, T., Kofoid, E., and Roth, J. R. (2004) Evidence that a B12-adenosyl transferase is encoded within the ethanolamine operon of *Salmonella enterica*. *J. Bacteriol.* **186**, 7635-7644.

43. Mera, P. E., Maurice, M. S., Rayment, I., and Escalante-Semerena, J. C. (2007) Structural and functional analyses of the human-type corrinoid adenosyltransferase (PduO) from *Lactobacillus reuteri*. *Biochemistry* **46**, 13829-13836.

44. Fahey, R. C., Brown, W. C., Adams, W. B., and Worsham, M. B. (1978) Occurrence of glutathione in bacteria. *J. Bacteriol.* **133**, 1126-1129.

45. Atkinson, D. E. (1968) The energy charge of the adenylate pool as a regulator parameter. Interaction with feedback modifiers. *Biochemistry* **7**, 4030-4034.

46. Chapman, A. G., Fall, L., and Atkinson, D. E. (1971) Adenylate energy charge in *Escherichia coli* during growth and starvation. *J. Bacteriol*. **108**, 1072-1086.

47. Brinsmade, S. R., Escalante-Semerena, J. C. (2004) The eutD gene of Salmonella enterica encodes a protein with phosphotransacetylase enzyme activity. *J. Bacteriol.* 186, 1890-1892

48. Brinsmade, S. R., Paldon, T., and Escalante-Semerena, J. C. (2005) Minimal functions and physiological conditions required for growth of Salmonella enterica on ethanolamine in the absence of the metabolosome. *J. Bacteriol.* **187**, 8039-8046

CHAPTER 5

CONCLUSIONS AND FUTURE DIRECTIONS

5.1 Summary and conclusions

Overview. Cobalamin synthesis has been studied in *S. enterica* for decades, and numerous studies have assembled a near-complete genetic pathway for this process (1-5). However, our knowledge of corrinoid adenosylation, one of the last steps of cobalamin synthesis, is incomplete. Specifically, the method by which ACATs generate 4c corrinoid intermediates is only partially understood. This work identified the mechanism by which the ACAT CobA generates a 4c corrinoid, and thus how it generates adenosylcobalamin. Significant progress was also made in understanding the EutT ACAT, including its unique dependence on a metal cofactor. Chapter 4 investigated the ethanolamine catabolic system that EutT is a member of, and found evidence that EutQ encodes an acetate kinase important for anaerobic growth on ethanolamine. Together, this work has defined surprising similarities and differences among nonhomologous ACAT mechanisms, as well as helping to define a branch of a pathway dependent on AdoCbl usage.

*Identification of the CobA mechanism***.** CobA was the first ACAT identified to use a 4c corrinoid intermediate to raise the redox potential of cob(II)alamin to within range of biological reductants (6). However, the mechanism by which CobA accomplished this reaction was completely unknown. In Chapter 2, we generated an anaerobic crystal structure of *S. enterica* CobA in complex with both 4c and 5c cob(II)alamin. Aromatic, hydrophobic residues were identified as likely catalytic residues, acting to displace the DMB lower ligand in 5c cob(II)alamin to form 4c

cob(II)alamin. The significance of these residues was verified by site-directed mutagenesis and subsequent *in vitro* and *in vivo* tests. This mechanism is similar to that of PduO, a nonhomologous ACAT (7,8), demonstrating an intriguing example of convergent evolution among ACATs.

Novel use of a metal cofactor by EutT. EutT has been the least-understood of the ACAT enzymes, due in part to its difficulty in purification. In Chapter 3, we determine a method to homogeneously purify *S. enterica* EutT and perform biochemical analysis. Previous studies indicated EutT bound an iron-sulfur center (9), however we found evidence that EutT instead binds a mononuclear transition-state cation, likely ferrous iron, which is used in a non-redox role. This is the first known example of an ACAT binding a transition state metal as a cofactor, and it is unclear why EutT has evolved to require this cofactor.

*EutQ is a novel acetate kinase***.** EutQ is one of three enzymes of unknown function in the *eut* operon, which is responsible for the AdoCbl-dependent catabolism of ethanolamine. In Chapter 4, we show that EutQ acts as an acetate kinase that is required for anaerobic growth on ethanolamine and tetrathionate. Biochemical assays also indicate that it has acetate kinase function. EutQ is not required for aerobic growth on ethanolamine, and overexpression of EutQ results in a growth defect. I hypothesize that EutQ is important for either substrate-level phosphorylation, or for regulating the flow carbon through ethanolamine catabolism by exerting a downstream "pull" on the EutD phosphotransacetylase.

5.2 Future directions

Investigation of alternative CobA active sites. One of the differences between the PduO mechanism and the CobA mechanism is that CobA requires 2 aromatic hydrophobic residues, whereas PduO only requires. Work by Ivan Pallares et al. (10) indicates that this is due to a pi-

stacking arrangement of the residues in CobA. Intriguingly, species of *Dehalococcoides* encode multiple CobA isoforms, which are largely like *S. enterica* CobA but only have one of the two required catalytic residues, indicating that *Dehalococcoides* CobA is active without pi-stacking. It would be interesting to determine if *Dehalococcoides* CobA has similar activity and substrate specificity as *S. enterica* CobA, and would perhaps inform us on why pi-stacking is required in *S. enterica*.

During the mutational screening of *S. enterica* CobA, a F91Y variant was determined to be more active than WT. Several *Ralstonia* species contain this single amino acid variation in their WT CobAs. It would be interesting to know if *Ralstonia* CobA is catalytically more active that *S. enterica* CobA, as the possibility exists that *Ralstonia* may be under selective pressure for higher AdoCbl turnover.

Investigation of *Methanosarcina mazei* CobA is another interesting avenue of research. This archaeal CobA lacks the N-terminal α-helix which clamps down over the active site of CobA that binds 4c corrinoid. This α-helix is thought to play an important role in excluding water from the active site. A crystal structure of this enzyme with cob(II)alamin could help determine if *Mm*CobA has an alternative mechanism for protecting the 4c corrinoid from stray nucleophiles.

Determination of the EutT mechanism and elucidation of the cofactor role. The mechanism by which EutT generates 4c-corrinoid is the biggest unknown in the study of ACATs. As indicated by both CobA and PduO, EutT will likely use an aromatic, hydrophobic amino acid residue to displace the lower ligand. However, I predict that the structure of its active site will be different from both other crystallized ACATs. A crystal structure is necessary to address this question. Additionally, a crystal structure will help determine the role of the novel metal cofactor bound by EutT. Unpublished spectroscopy (Pallares et al.) indicates that the cofactor is important for the

positioning of the corrinoid substrate in the active site, and potentially for preventing deleterious side-reactions. An exhaustive variation of crystal screens have already been performed on *Se*EutT, therefore I recommend screening EutT homologs for crystallization suitability.

Studies in collaboration with the Brunold lab indicate that *Se*EutT is very specific for cobalamin, potentially via recognition of the DMB moiety (11)(Pallares et al., manuscript in preparation). Should EutT ultimately fail to crystallize, an alternative approach would be to locate active site residues by performing a mutagenic screen on *eutT*. Specifically, by growing a *cobA pduO eutT S. enterica* aerobically on ethanolamine and supplying cobinamide and DMB you can select for a variant *eutT* allele that is capable of adenosylating Cbi. Identification of residues important for DMB recognition could help determine why $EutT^{WT}$ is so specific for cobalamin.

How do EutQ and EutP function in the metabolosome? The discovery of EutQ as an acetate kinase brings up several intriguing possibilities regarding its role in ethanolamine catabolism. Generation of ATP via substrate-level phosphorylation has been discussed as one of the most likely roles. That ATP could either be used as an energy source by the cell, or as a substrate for EutA and EutT.

Another possibility is that EutQ is important for regulating carbon flux through EutD by consuming the EutD reaction product, acetyl-phosphate. This could bring about the deleterious phenotype observed when overexpressing EutQ, as an over-active EutD would divert too much acetyl-CoA from central metabolism. This is supported by the correction of *eutQ* phenotypes by supplementing with the CoA precursor, pantothenate Similarly, the deleterious phenotype of *eutQ* strains could be caused by a less-active EutD. Without EutD consuming the EutE product, acetyl-CoA, EutE may become less-active and this could lead to a buildup of acetaldehyde. An aerobically-growing cell may be able to handle this stress due to the greater concentration of

glutathione and cytoplasmic dehydrogenases it can synthesize, but an anaerobically-growing cell may be more sensitive. This could be tested anaerobically by expressing aldehyde dehydrogenases *in trans* in a *eutQ* background, as well as supplementing with glutathione.

Curiously, EutP has acetate kinase *in vitro* yet I have failed to detect a *eutP* phenotype under the conditions I've tested for EutQ. Therefore, I hypothesize that EutQ is the more important acetate kinase, and that EutP may enhance eutQ, but cannot replace it. Perhaps *eutP* is required under more stringent growth conditions, such as lower concentrations of ethanolamine or tetrathionate, or when growing at >37°C, as might be experienced in an inflamed intestine. This hypothesis would likely involve the two enzymes acting as a heterodimer. Interestingly, the start codon for *eutQ* is within the +1 frame of *eutP*, and is immediately followed by a string of six adenosine bases. Perhaps there is occasional transcription slippage which results in the synthesis of a single *eutPQ* mRNA. *eutPQ* could be synthesized through recombinant methods fairly easily by deleting the *eutP* stop codon and moving the EutQ start codon into the same frame as *eutP*. The EutPQ protein may have enhanced biochemical activity compared to either EutP or EutQ. It would be worthwhile to compare its kinetics to that of EutP and EutQ alone.

I have proposed that EutQ resides inside the metabolosome, as it would be in closer contact with the other *eut* enzymes and their products, especially EutD and acetyl-phosphate. However, there is no data for this placement, and it would be prudent to obtain EutQ and EutP antibodies and probe whole vs. lysed metabolosomes to determine the location of the acetate kinases. I also think similar treatment should be applied to PduW, the propionate kinase in the propanediol metabolosome. *pduW* was reported not to have an anaerobic phenotype, but in light of the *eutQ* findings I think that should be re-examined. *pduW* should also be probed for its localization relative to the propanediol metabolosome.

5.3 References

1. Jeter, R. M., Olivera, B. M., and Roth, J. R. (1984) *Salmonella typhimurium* synthesizes cobalamin (vitamin B_{12}) de novo under anaerobic growth conditions. *J. Bacteriol.* **159**, 206-213.

2. Jeter, R., Escalante-Semerena, J. C., Roof, D., Olivera, B., and Roth, J. R. (1987) Synthesis and use of vitamin B12. in *Escherichia coli and Salmonella tyhpimurium : cellular and molecular biology* (Neidhardt, F. C., Ingraham, J. L., Low, K. B., Magasanik, B., Schaechter, M., and Umbarger, H. E. eds.), Am. Soc. Microbiol., Washington, D. C. pp 551-556.

3. Escalante-Semerena, J. C., and Roth, J. R. (1987) Regulation of cobalamin biosynthetic operons in *Salmonella typhimurium*. *J. Bacteriol.* **169**, 2251-2258.

4. Escalante-Semerena, J. C., Suh, S. J., and Roth, J. R. (1990) *cobA* function is required for both de novo cobalamin biosynthesis and assimilation of exogenous corrinoids in *Salmonella typhimurium*. *J. Bacteriol.* **172**, 273-280.

5. Debussche, L., Thibaut, D., Cameron, B., Crouzet, J., and Blanche, F. (1993) Biosynthesis of the corrin macrocycle of coenzyme B_{12} in *Pseudomonas denitrificans*. *J. Bacteriol.* **175**, 7430-7440.

6. Stich, T. A., Buan, N. R., Escalante-Semerena, J. C., and Brunold, T. C. (2005) Spectroscopic and computational studies of the ATP:Corrinoid adenosyltransferase (CobA) from *Salmonella enterica*: Insights into the mechanism of adenosylcobalamin biosynthesis. *J. Am. Chem. Soc.* **127**, 8710-8719.

7. Mera, P. E., St Maurice, M., Rayment, I., and Escalante-Semerena, J. C. (2009) Residue Phe112 of the human-type corrinoid adenosyltransferase (PduO) enzyme of *Lactobacillus reuteri* is critical to the formation of the four-coordinate Co(II) corrinoid substrate and to the activity of the enzyme. *Biochemistry* **48**, 3138-3145.

8. Park, K., Mera, P. E., Escalante-Semerena, J. C., and Brunold, T. C. (2012) Spectroscopic characterization of active-site variants of the PduO-type ATP:Corrinoid adenosyltransferase from *Lactobacillus reuteri*: Insights into the mechanism of four-coordinate Co(II)corrinoid formation. *Inorg. Chem.* **51**, 4482-4494.

9. Buan, N. R., Suh, S. J., and Escalante-Semerena, J. C. (2004) The *eutT* gene of *Salmonella enterica* encodes an oxygen-labile, metal-containing ATP:corrinoid adenosyltransferase enzyme. *J. Bacteriol.* **186**, 5708-5714.

10. Pallares, I. G., Moore, T. C., Escalante-Semerena, J. C., and Brunold, T. C. (2014) Spectroscopic studies of the *Salmonella enterica* adenosyltransferase enzyme *Se*CobA: Molecular-level insight into the mechanism of substrate cob(II)alamin activation. *Biochemistry* **53**, 7969-7982.

11. Park, K., Mera, P. E., Moore, T. C., Escalante-Semerena, J. C., and Brunold, T. C. (2015) Unprecedented Mechanism Employed by the Salmonella enterica EutT ATP:CoIrrinoid Adenosyltransferase Precludes Adenosylation of Incomplete CoIIrrinoids. *Angew. Chem. Int. Ed.* **54**, 7158-7161.

APPENDIX A

CORRINOID METABOLISM IN DEHALOGENATING PURE CULTURES AND MICROBIAL COMMUNITIES[4]

[4] Theodore C. Moore and Jorge C. Escalante-Semerena. 2015. In *Organohalide Respiring Bacteria*. Löffer, Frank and Lorenz Adrian, Eds. Manuscript accepted. Reprinted with permission from publisher.

A.1 Abstract

Corrinoid cofactors are critical components of the electron-transport chain for many organohalide-respiring bacteria (OHRB). This chapter examines the synthesis and metabolism of corrinoids, with a focus on studies in bacteria that express reductive dehalogenases (RDases). We discuss the physical characteristics of corrinoids that make them distinct from one another, and provide examples of the various corrinoids isolated from OHRB. We provide a brief review of the synthesis, scavenging, and transport of corrinoids as it is currently understood in non-dehalogenating model organisms. Wherever applicable, we draw parallels to the pathways present in OHRB. We present some recent examples of work studying the metabolism of corrinoids in mixed cultures of OHRB, and discuss how these bacteria may share and modify corrinoids at a community-based level.

A.2 Introduction

What are corrinoids? Corrinoids are complex organometallic compounds that belong to the family of cyclic tetrapyrroles, which are also known as 'The Pigments of Life'. Members of this family of biomolecules include hemes, chlorophylls, and factor F_{430} (1). The most obvious difference amongst cyclic tetrapyrroles is the transition metal ion chelated by the equatorial pyrrolic nitrogen atoms. Hemes contain iron, chlorophylls contain magnesium, factor F_{430} contains nickel, and corrinoids contain cobalt. Also important is the degree of reduction of the macrocycle, with cobamides containing six double bonds. Corrinoids are also set aside from the other cyclic tetrapyrroles by the lack of the methane bridge at position C20. The absence of such a bridge puckers the corrin ring, in contrast to the planarity of heme. Last, but not least, corrinoids are the only natural cyclic tetrapyrroles that contain axial ligands.

The tetrapyrrole ring of corrinoids is referred to as the corrin ring, reflecting the 'core' of the structure. The chemical structure of the corrin ring is the same in all known corrinoids. However, the identity of the upper (beta, *Co*β) and lower (alpha, *Co*α) axial ligands varies. We expand on the nature and proper nomenclature of ligands below.

Classes of corrinoids and distinguishing features. There are two classes of corrinoids: incomplete corrinoids, and complete corrinoids. The difference between incomplete and complete corrinoids is the absence or presence of the nucleotide loop. This loop structure tethers the nucleotide base to the corrin ring via an amide bond formed between the amino group of a 1-amino-2-propanol (AP) moiety with the carboxyl group of a propionyl substituent of ring D (Fig. A.1A). The alcohol group of AP participates in the formation of a phosphodiester bond with the nucleotide. In fact, complete corrinoids are one of only three coenzymes containing a phosphodiester bond. The other two are coenzyme F_{420} (2) and methanopterin (3).

Complete corrinoids can also vary amongst themselves. In this case, the structure that varies is the base of the nucleotide. We note that, although the majority of the bases found in corrinoids are nitrogenous benzimidazoles or purines that can directly interact with the Co ion of the ring via a coordination bond, there are bases, such as phenol and *p*-cresol, which cannot coordinate with Co because they lack unpaired electrons in their structures. Therefore, it is incorrect to refer to phenol or *p*-cresol as ligands. They should simply be referred to as 'bases' since they are still part of the nucleotide loop.

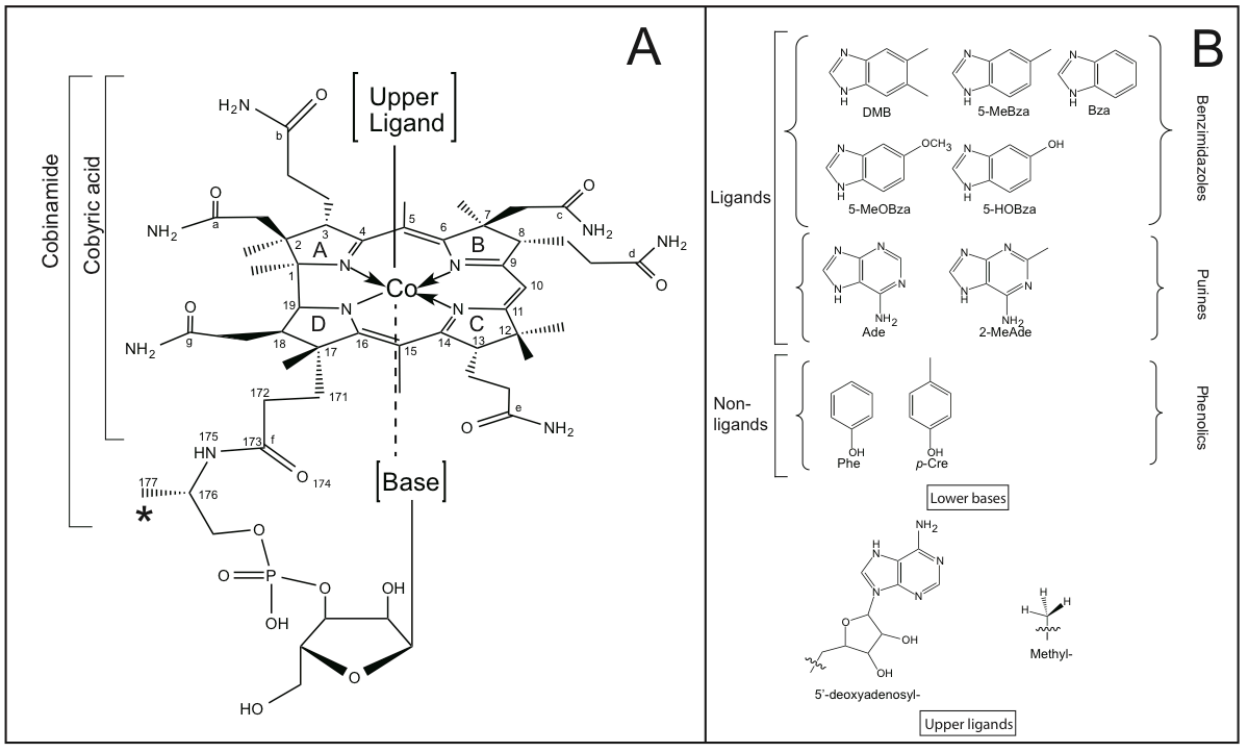

Figure A.1. Structural features of cobamides. (A) Structure of a cobamide. The brackets indicate the common precursors cobinamide and cobyric acid. Individual pyrroles are labeled A-D. Changing the starred methyl group 177 to a hydrogen results in a nor-cobamide. (B) A selection of biologically active axial ligands and bases of cobalamin that are mentioned in this chapter. The brackets around the lower bases indicate which are capable of ligating the Co ion. Abbreviations: DMB, 5,6-dimethylbenzimidazole; 5-MeBza, 5-methylbenzimidazole; Bza, benzimidazole; 5-MeOBza, 5-methoxybenzimidazole; 5-HOBza, 5-hydroxybenzimidazole; Ade, adenine; 2-MeAde, 2-methyladenine; Phe, phenol; *p*-Cre, *para*-cresol. Wavy line denotes the Co-C covalent bond between upper ligands and cobalamin.

Cobamides. The term ‘cobamide’ is used to refer to complete corrinoids, regardless of the base found in the nucleotide loop structure of the molecule. The best-studied cobamide is cobalamin (Cbl), which is the cobamide whose *Co*α (lower axial) ligand is 5,6-dimethylbenzimidazole (DMB) (Fig. A.1B). Also shown in figure A.1 are purine analogues that bacteria and archaea incorporate into cobamides, including adenine, which forms pseudocobalamin, another commonly studied cofactor. The list is not all-inclusive, but encompasses the lower ligands used by OHRB. To date acetogenic bacteria are the only microorganisms known to incorporate phenol or *p*-cresol into their cobamides (4, 5).

In cobamides containing purines or benzimidazoles, the base can be found in the ‘base-on’ (coordinated to the Co ion) or ‘base-off’ conformation. The base-on conformation is made possible by the presence of unpaired electrons in the nitrogen atom of the imidazole ring of the base that is not bonded to the ribosyl moiety of the nucleotide. As noted above, phenolyl cobamides cannot acquire the base-on conformation due to the absence of unpaired electrons in phenolic bases, thus restricting their use by some cobamide-dependent enzymes that require the base-on conformation of the cofactor to function (*e.g.*, ethanolamine ammonia-lyase, EC 4.3.1.7; 1,2-propanediol dehydratase, EC 4.2.1.28) (6, 7).

Cobalamin The literature on cobalamin is extensive, covering many different aspects of this magnificent molecule. Some reviews cover the biosynthesis, metabolism, molecular biology, genetics, enzymology, and structure of cobalamin biosynthetic enzymes (8-13), other reviews focus on the elucidation and chemical synthesis (14-16), yet other reviews focus on chemical properties (17-20). This body of work provides a comprehensive understanding of the most complex coenzyme known and the largest molecule with biological activity that is not a polymer.

Cobalamin is defined by the coordination bond between a nitrogen atom of 5,6-dimethylbenzimidazole (DMB) and the Co ion on the α face of the corrin ring. The coenzymic form of cobalamin is adenosylcobalamin (AdoCbl). AdoCbl possesses a unique Co(III)-C covalent bond between the corrin ring and the *Co*β (upper) ligand (Fig. A.1A). This organometallic bond is pivotal to AdoCbl-dependent chemistry, which proceeds via a homolytic, one-electron mechanism, generating a Co(II) cobalamin species and an adenosyl radical used by dehydratases, lyases, mutases and reductases (21, 22). Conversely, the Co-C bond of methylcobalamin (MeCbl, Fig. A.1B) is exploited in a heterolytic, two-electron mechanism of methyl transfer involving a Co(I) cobalamin intermediate, used primarily in methanogenesis and methionine synthesis (21, 22).

Cobamide biosynthesis. To date, cobamide biosynthesis has only been observed in bacteria and archaea (10, 12), including genera of dehalogenating bacteria (e.g., *Desulfitobacterium, Dehalobacter, Sulfurospirillum*, and *Geobacter*), some of which use organohalides as electron acceptors in cellular respiration (23). Since cobamide-dependent dehalogenases recognize narrow substrate spectra, bacteria encode several distinct dehalogenases to expand their range of useable electron acceptors. Case in point is *Dehalococcoides mccartyi* strain VS, an obligate cobamide-scavenging strain, whose genome encodes the largest number (36) of cobamide-binding proteins known to occur in any prokaryote whose genome has been sequenced (24). Consequently, these microorganisms have a strong selective pressure exerted on them to maintain sufficient levels of cobamides to satisfy their physiological needs.

Some species of OHRB that do not synthesize cobamides *de novo* can scavenge incomplete corrinoids that enter the late steps of the pathway (a.k.a. the nucleotide loop assembly pathway, NLA) yielding cobamides that can meet their physiological needs. In fact, many organisms that

synthesize cobamides *de novo* also maintain scavenging pathways to save considerable energy on synthesis of the corrin ring.

Cobamides encountered in organohalide-respiring bacteria. In OHRB, corrinoid-dependent dehalogenases serve an essential function in the electron transport chain as terminal reductases, and are known as reductive dehalogenases (RDases). The dependence of several RDases on cobamides has been studied biochemically via UV-Vis spectroscopy, electron paramagnetic resonance (EPR), inductively coupled plasma mass-spectrometry (ICP-MS) and alkylating inhibitors which ligate the catalytically-active b-position of cobamides (25-28). However, the identity of the cobamide cofactor in most RDases is unknown. Prominent exceptions are the RDases of *Sulfurospirillum multivorans* (formerly *Dehalospirillum multivorans*). *S. multivorans* synthesizes the unusual cofactor norpseudocobalamin, that is, pseudocobalamin lacking a methyl group at the propionyl linkage of the nucleotide tail (C176, Fig. A.1A) (29). The mechanistic preference of an enzyme for a particular type of cobamide is mostly unknown, both in regards to RDases as well as other cobamide-dependent enzymes.

In vitro analyses of reductive dehalogenases. The cobamide content in representative RDases is not always known. Often the identity of the cobamide is confirmed by optical spectroscopy and alkyl halide inhibitors, which will selectively and reversibly inhibit cobamide activity by ligating to the upper ligand position (30). Most cobamide-dependent RDases bind two 4Fe/4S iron-sulfur centers per molecule of corrinoid, which have been proposed to transfer electrons to the corrinoid cofactor to generate a reduced Co(I) state *in vivo* (31).

Many RDases are translocated through the inner membrane and are subsequently anchored to the membrane via a secondary protein (25, 32, 33). A recent study (34) characterized the effect

of cobalamin on the maturation and localization of the PCE-degrading RDase PceA in *Desulfitobacterium hafniense* strain Y51 (EC 1.97.1.8). The authors found that when PceA was synthesized in the absence of cobalamin, the protein formed aggregates in the cytoplasm, whereas in the presence of cobalamin PceA was translocated to the exoplasmic face of the inner membrane. The study suggests that PceA is formed in a cofactor-free precursor state, prePceA, along with its chaperone PceT. PceT is proposed to keep prePceA in an open conformation, which allows cobalamin and iron-sulfur centers to be post-translationally incorporated into prePceA (35, 36). Reconstitution with cofactors helps complete folding of PceA, which is translocated across the membrane via the Tat pathway.

Part of the barrier to obtaining clearer information on the nature of the cobamide cofactor has been the difficulty in purifying RDases to sufficient yield and homogeneity for structural studies. Recently, the norpseudocobalamin-binding PceA from *Sulfurospirillum multivorans* was crystallized in complex with substrate and substrate analogs (37). Key features include a unique base-off conformation in which the adenine lower ligand has been 'curled' away from the Co(II) ion to generate an apparent four-coordinate corrinoid in complex with the substrate. Additionally, two cubane Fe-S centers are clearly visible in each monomer, and are positioned within a favorable range to transfer electrons to the corrin ring. Another recently-identified and crystallized RDase, RdhA from *Nitratireductor pacificus*, revealed a similar conformation for the bound cobalamin cofactor, as well as two [4Fe-4S] clusters positioned favorably for reduction of cobalamin (38). For an in-depth description of the mechanism of reductive dehalogenases, please refer to chapters 17 and 18 in this book.

A.3 Corrin ring synthesis

Corrin ring biosynthesis has not been studied in OHRB. Most experiments regarding corrin ring assembly have been performed in *Salmonella enterica, Pseudomonas denitrificans*, and

	Transport				Anaerobic Pathway																	Aerobic Pathway																	Miscellaneous						
	BtuB	BtuF	BtuC	BtuD	CbiK	CbiX	CbiL	CbiH	CbiG	CbiF	CbiD	CbiJ	CbiE	CbiT	CbiC	CbiA	CobA[1]	CbiP	CbiB	CobU	CobS[2]	CobT[3]	CobC	CobI	CobG	CobJ	CobM	CobF	CobK	CobL	CobH	CobB	CobN	CobS[4]	CobT[5]	CobR	CobO	CobQ	CobP	CobD	CobA[6]	CbiZ	CbiZ/BtuD	BluB	PduS	PduO	CblS	CblT
R. pomeroyi DSS-3				x																				x	x	x	x	x	x	x	x		x	x	x	x												
R. sp. TM1040	x	x	x	s																				2x	x	x	x		x	x	x		x	x	x	x				x							
P. profundum 3TCK	3x	x	x	x														x	x	2x	x	x												x	x	x					4x			x	x			
Jannaschia sp. CCS1		x	x	x																				x	x	x	x		x	x	x		x	x	x	x	x	x	x							
Abrensia sp. R2A130		x	x	x																				x		x	x		x	x	x		x	x	x	x	x	x	x	x						
S. sediminis	2x	3x			x		x	x	x	x	x	x	x	x	x	x	2x	2x	x	2x	x	x	x																		2x						
Vibrio sp. RC586	x	x	x	4x												x	x	x	x	x	x	x	x																								
Anaeromyxobacter sp. K	x	2x	x	3x																																					x						
A. dehalogenans 2CP-1	x	2x	x	4x																																					x						
A. dehalogenans 2CP-C	x	2x	x	4x																																					x						
Geobacter lovleyi SZ	2x	x	x	5x	x		x	x	x	x	x	x	x	x	x	x	2x	2x	x	x	x	2x	x										x	x							x						
delta proteobacterium NaphS2	x	x	x	5x	x		2x	2x	x	x	x		x	x	x	2x	2x	x	x	x	x	2x	x																		2x						
S. multivorans	x	x	x	x	x		x	x	x	x	x	x	x	x	x	x		x	x	x	x	x	x																								
D. aaccartyi CBDB1		2x	x	x												x	2x	x	3x	x	x	x	x																	2x	x	2x					
D. aaccartyi GT		x	x														x	x	2x	x	x	x	x																	x		2x					
D. aaccartyi BAV1		2x	x	x												x	2x	x	2x	x	x	x	x																			x					
D. aaccartyi 195		3x	2x	2x												x	2x	x	4x	2x	2x	2x	2x																	x		2x					
D. aaccartyi VS		x	x	2x									x			x	x	x	x	x	x	x	x																	x	x						
D. lykanthroporepellens BL-DC-9		2x	2x	6x									x	x		x	x	x	x	x	x	x	x																	2x	x	x					
D. tiedjei			2x	2x		x	x	x	x	x	x	x	x			x	3x	4x	x	x	x	x					x						x			x					x			x			
A. capsulatum	x			2x																																	x											
D. alkaliphilus		2x	2x	6x		x	2x	x	x	x	x	x	x	x	x	x	2x	x	x	x	x	x	x																								
C. difficile 630	x	x	x	x	x		x	x	x	x	x	x	x	x	x	x		x	x	x	x	x	x																			x						
C. difficile R20291	x		2x	3x	x	x	x	x	x	x	x	x	x	x	x	x		x	x	x	x	x	x																			x						
D. hafniense Y51						x	x	x		x	x	x			x	x	4x	x		x	x	x	2x																			x		x		x	x	
D. hafniense DCB-2	x	5x	x				x	x		x	x	x			x	x	3x	x		x	x	x	x																			x	2x		x		x	x	
D. dehalogenans ATCC 51507		x	x	4x		x	x	x	x	x	x	x	x	x	x	2x	3x	x	x	x	x	x	x																			x	x			x	x	
D. dichloroeliminans LMG P-21439		x	x	2x		x	x	x	x	x	x	x	x	x	x	x	3x	x	x	x	x	x	x																			x						
D. restrictus DSM 9455									x	x	x	x	x	x	x	x	x																															
Dehalobacter sp. CF		x	x	x		x	x		2x	x	2x	x	x	x	x	x	x	x	x		x	x	x																			x	x					
M. prima mesG1.Ag.4.2			x	x													x																									x	x					
F. placidus DSM 10642		x	2x	6x			x	x	x	x	x			x	x	x		x	x		x	x														x						x	x			x		

Table A1. Putative cobamide biosynthetic enzymes identified from available sequenced genomes of species containing RDase genes. The proteins are grouped by function, those involved in transport are in light grey, those in the anaerobic, early Co insertion are in medium grey, and those involved in aerobic, late Co insertion are in dark grey. Proteins that are shared among the anaerobic and aerobic pathways, as well as those used as alternatives to parts of those pathways, are grouped under "Miscellaneous." The x indicates copy number. Superscript numbering indicates proteins with duplicate names: 1, ACAT; 2, cobalamin synthase; 3, a-R synthase; 4 and 5, chelators; 6, SUMT. Genes were identified using the SEED [153] and verified by homology to known cobamide-synthesis proteins in *Salmonella enterica*, *Pseudomonas denitrificans*, *Listeria innocua*, *Bacillus megaterium* or *Brucella melitensis*, as applicable, using BLAST [154]. The NCBI taxid numbers for the above strains are as follows: *Rugeria pomeroyi* DSS-3, 246200; *Ruegeria* sp. TM1040, 292414; *Photobacterium profundum* 3TCK, 314280; *Jannaschia* sp. CCS1, 290400; *Ahrensia* sp. R2A130, 744979; *Shewanella sediminis*, 271097; *Vibrio* sp. RC586, 675815; *Anaeromyxobacter* sp. K, 447217; *Anaeromyxobacter dehalogenans* 2CP-1, 455488; *Anaeromyxobacter dehalogenans* 2CP-C, 290397; *Geobacter lovleyi* SZ, 398767; delta proteobacterium NaphS2, 88274; *Sulfurospirillum multivorans*, 66821; *Dehalococcoides mccartyi* CBDB1, 255470; *Dehalococcoides mccartyi* GT, 633145; *D. mccartyi* BAV1, 216389; *Dehalococcoides mccartyi* 195, 243164; *Dehalococcoides mccartyi* VS, 311424; *Dehalogenimonas lykanthroporepellens* BL-DC-9, 552811; *Desulfuomonile tiedjei*, 2358; *Acidobacter capsulatum*, 33075; *Dethiobacter alkaliphilus*, 555088; *Clostridium difficile* 630, ; *Clostridium difficile* R20291*, ; Desulfitobacterium hafniense* Y51, 138119; *Desulfitobacterium hafniense* DCB-2, 272564; *Desulfitobacterium dehalogenans*, 36854; *Desulfitobacterium dichloroeliminans* LMG P-21439, 871963; *Dehalobacter restrictus* DSM 9455, 55583; *Dehalobacter* sp. CF, 1131462; *Mesotoga prima* mesG1.Ag.4.2, 660470; *Ferroglobus placidus* DSM 10642, 589924. This information was reported by [42].

Bacillus megaterium (39-41). Even though biochemical and genetic studies of *de novo* synthesis in OHRB are lacking, inferences can be made from genome sequencing efforts. Relevant parallels to studies in OHRB will be made throughout this section. Table A.1 indicates the distribution of corrinoid synthesis genes in the genomes of species with confirmed RDases (42). Figure A.2 compares the organization of gene clusters related to cobamide synthesis in *Dehalococcoides mccartyi* sp. CBDB1 and *Sulfurospirillum multivorans* to *S. enterica*. Notably, both the *de novo* cobamide synthesizer *S. multivorans* and the cobamide scavenger *D. mccartyi* have cobamide synthetic genes located near genes encoding RDases.

The corrin ring of cobamides is similar to heme, siroheme, chlorophyll and factor F_{430}. Unlike other corrinoids, the ring in cobamides is contracted between C1 and C19 (Fig. A.1) to allow tighter metal binding, and is modified by additional methyl and amide groups. The corrin ring is more reduced than most tetrapyrroles, containing only 6 double bonds, compared to the 11 of heme, 10 of chlorophyll, and 9 of siroheme. Only factor F_{430} is more reduced, with 5 double bonds. Heme, siroheme, corrins, and other tetrapyrroles are all synthesized from the precursor uroporphyrinogen III (10). Uroporphyrinogen III is made up of 4 porphobilinogen moieties, which are each synthesized from the condensation of two molecules of d-aminolevulinic acid (43-45). An *S*-adenosyl-L-methionine:Uroporphyrinogen III MethylTransferase (the SUMT family, CobA in *P. denitrificans*, EC 2.1.1.107) catalyzes methylations of carbons C2 and C7, resulting in precorrin-2 (47). Precorrin-2 refers to the number of methyl group decorations on the nascent corrin ring. At this point, the *de novo* synthesis diverges into one of two pathways, the "anaerobic" (early Co insertion route) or the "aerobic" (late Co insertion route) (Table A.1) (40, 48). Certain enzymes in the two pathways have the same name, such as CobS and CobA. Table A.1 attempts to clarify which pathway these enzymes are involved in.

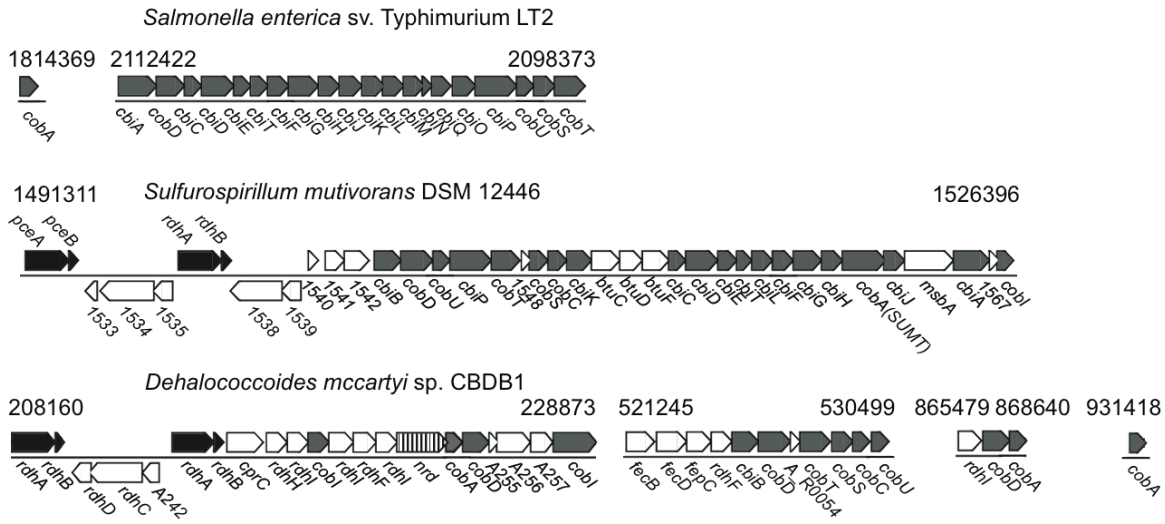

Figure A.2. Genetic organization of cobamide synthesis genes. Gene clusters relating to cobamide synthesis in non-organohalide respiring *S. enterica*, organohalide-respiring *de novo* cobamide producer *S. multivorans*, and organohalide-respiring cobamide auxotroph *D. mccartyi* sp. CBDB1. Genes directly related to cobamide synthesis are colored grey. Genes encoding RDases are colored black. Other cobalamin-dependent genes are colored with vertical stripes. Gene name or locus number is shown above or below cartoon representation. Nucleotide position in the genome is shown above each gene cluster. Annotated gene clusters were downloaded from the Integrated Microbial Genomes database (46)

The aerobic pathway is referred to as such because it utilizes a monooxygenase, CobG in the ring contraction step. After CobI (EC 2.1.1.130) methylates precorrin-2 at C20 to precorrin-3A (49), CobG (EC 1.14.13.83) reacts with precorrin-3A to form a lactone intermediate (precorrin-3B), which is acted upon by the *S*-adenosylmethionine-dependent CobJ (EC 2.1.1.131), catalyzing the ring contraction by releasing an acetic acid moiety when a methyl group attached to carbon C20 of the ring is excised (Fig. A.3A), granting the corrin ring its signature "pucker". The resulting intermediate, precorrin-4, undergoes two subsequent methylations, on C2 by CobM (EC 2.1.1.271) yielding precorrin-5, and on C12 by CobF (EC 2.1.1.152). CobF also deacetylates C1 to produce precorrin-6A.

The NADPH-dependent reductase, CobK (EC 1.3.1.54), reduces a double bond between carbons C18 and C19 on precorrin-6A to produce precorrin-6B. CobL (EC 2.1.1.289/2.1.1.132, PDB 3EO5, 3NJR) methylates the C5 and C15 positions, as well as removing the carboxyl moiety at C12 to form precorrin-8. CobH (EC 5.4.99.61) isomerizes precorrin-8, moving the methyl at C11 to C12, resulting in hydrogenobyrinic acid (50). The CobB amidotransferase uses ATP and glutamine to amidate the acetic acid side chains *a* and *c*, producing hydrogenobyrinic acid *a,c*-diamide. The latter is the substrate for the CobNST cobalt ion chelatase (EC 6.6.1.2), which yields cobyrinic acid *a,c*-diamide upon insertion of the Co ion into the ring.

The anaerobic pathway was initially thought to be due to the inability of anaerobes to use molecular oxygen in the CobG reaction (51). This included obligate anaerobic, cobamide-dependent organohalide-respiring species such as *Desulfitobacterium hafniense*, *Sulfurospirillum multivorans* and others, which contain genes specific to the anaerobic pathway (52). Some OHRB have incomplete anaerobic pathways that lack the ability to attach the nucleotide tail to

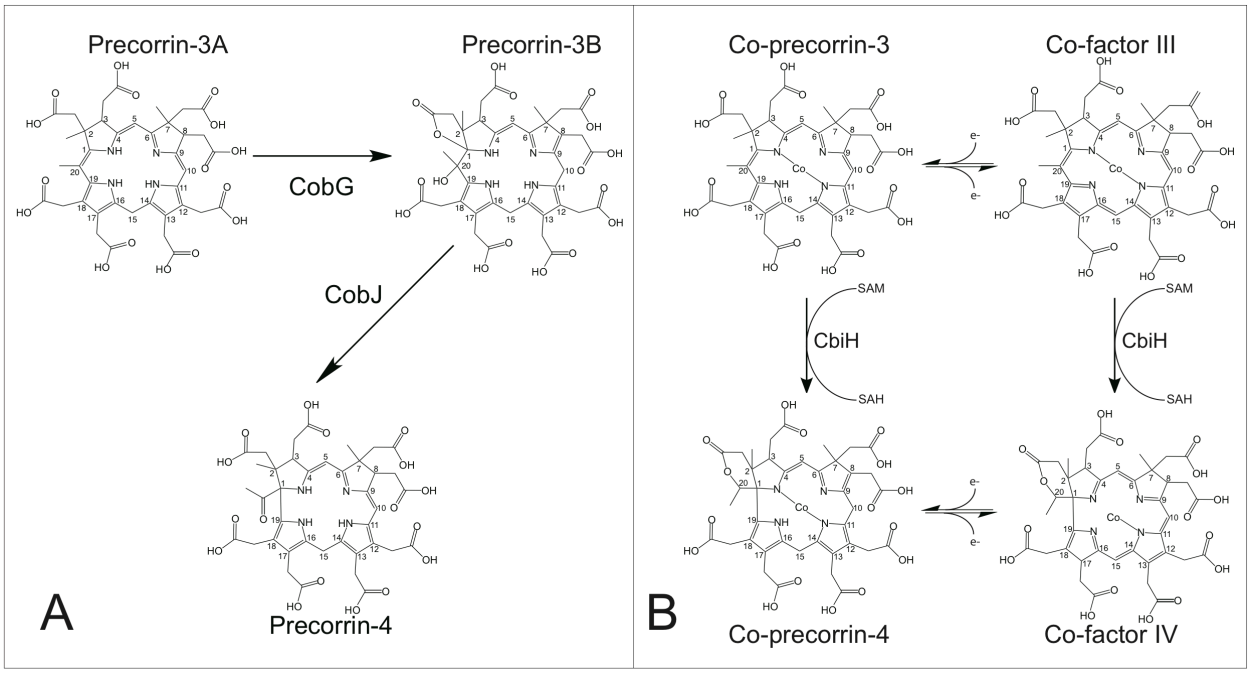

Figure A.3. Pathway for the ring contraction of precorrin-2. (A) Synthesis of the cobamide intermediate Precorrin-4 in the aerobic or 'late Co-insertion' pathway. Precorrin-2 undergoes methylation to precorrin-3A, lactone formation results in precorrin-3B. Subsequent lactone cleavage and extrusion of C20 results in precorrin-4. (B) Synthesis of the cobamide intermediate Co-precorrin-4 in the anaerobic or 'early Co-insertion' pathway. Co-precorrin-3 undergoes SAM-dependent methylation to Co-precorrin-4, resulting in the formation of a lactone moiety and the contraction of the corrin ring. The CbiH methylase can also catalyze the contraction of Co-factor-III; the oxidized form of Co-precorrin-3.

cobamides, such as *Dehalobacter restrictus*. Others species with anaerobic pathways, such as several *Dehalococcoides mccartyi* strains, lack enzymes for insertion of cobalt into the corrin ring (Table A.1). These species are characterized as being incapable of *de novo* corrin ring biosynthesis (53).

In the anaerobic pathway, precorrin-2 is oxidized to factor II by SirC (EC 1.3.1.76, PDB 3dfz). At this point cobalt is inserted by either CbiX (EC 4.99.1.3, PDB 1TJN, 2DJ5, 2XWQ, 2XWS) as in *Bacillus megaterium*, or by CbiK (EC 4.99.1.3, PDB 1QGO, 2XWP) as in *Salmonella typhimurium.* The multifunctional siroheme synthase/ferrochelatase enzyme CysG (EC 1.3.1.76/4.99.1.4, PDB 1PJQ, 1PJS) inserts cobalt in the absence of CbiK (41, 54). This is the reason why the anaerobic pathway is also known as the "early" Co ion insertion pathway. The Co-factor II complex is methylated by the SAM-dependent CbiL (EC 2.1.1.136, PDB 2EOK, 2EON) to produce Co-factor III. This precursor is contracted by extrusion of the carbon atom C20, between the corrin ring C1 and C19. This carbon atom is incorporated into a lactone ring between C1 and C2 (Fig. A.3B). The iron-sulfur protein CbiH (EC 2.1.1.272) catalyzes lactone formation and ring contraction via methyl donation from an *S*-adenosylmethionine (SAM) cofactor to form Co-factor IV. This was determined recently in a *Bacillus* system, where it was noted that CbiH could also act on the Co-precorrin-3, the reduced form of Co-factor III (55). Difficulties in isolating the intermediates delayed our understanding of the steps leading from Co-precorrin-4 to cobyrinic acid. These difficulties were recently overcome (56). CbiF (EC 2.1.1.271, PDB 1CBF, 2CBF) methylates the C11 position of Co-precorrin-4, and the lactone is opened and removed by CbiG (EC 3.7.1.12) to form Co-precorrin-5B. CbiD (EC 2.1.1.195) catalyzes the methylation of carbon C1 using *S*-adenosylmethionine as the methyl donor yielding Co-precorrin-6A. The NADH reductase CbiJ (EC 1.3.1.106) is expected to reduce the double

bond between C18 and C19 in a manner similar to CobK in the aerobic pathway, but to date, the resulting intermediate Co-precorrin-6B has not been detected when the reaction is performed *in vitro*. CbiE (EC 2.1.1.196) and CbiT (EC 2.1.1.289) catalyze two additionally methylation reactions at carbons C5 and C15, along with a deacetylation at C12, resulting in Co-precorrin-8. CbiC (EC 5.4.99.60) converts precorrin-8 to cobyrinic acid by transferring the C11 methyl to C12.

A.4 Final corrin ring amidations and corrinoid adenosylation

The aerobic and anaerobic pathways converge with the production of cobyric acid. Either CobQ (oxically, EC 6.3.5.10) or CbiA and CbiP (anoxically, EC 6.3.5.11, EC 6.3.5.10, respectively) catalyze the final corrin ring amidations to form cobyric acid. All three enzymes belong to the same family of glutamine amidotransferases (57). CobQ acts on cobyrinic acid *a,c*-diamide, and amidates the acetic acid side chains *b,d,e* and *g* in an ATP and glutamine dependent process (58). The substrate of CbiA is cobyrinic acid, which is amidated at side chains *c* and *a*, in that order (57). CbiP is responsible for side chains *b, d, g* and *e*.

Cobyrinic acid and cobyrinic acid *a,c*-diamide likely have a Co(II) charge due to non-enzymatic reduction from cytosolic flavoproteins (59). In *S. enterica,* CobA (the housekeeping ATP:Co(I)rrinoid adenosyltransferases) adds the *Cob*-adenosyl moiety to Co(I) corrinoids and cobamides (59-61). In the aerobic pathway, cobyrinic acid *a,c*-diamide is adenosylated by CobO (EC 2.1.5.17) (62). In the anaerobic pathway present in *S. enetrica*, CobA (EC 2.1.5.17; PDB 1G5R, 1G5T, 1G64, 4HUT) can adenosylate cobyric acid, cobinamide and cobalamin [(63)]. In *E. coli*, the CobA homologue is known as BtuR (64). CobA has been annotated as being capable of adenosylating cobyrinic acid *a,c*-diamide due to its homology to CobO, but data in support of

that have not been published. The arrest of *de novo* corrin ring biosynthesis in *S. enterica cobA* strains indicates that the final product of this branch of the pathway needs to be adenosylated prior to entering the late steps of the pathway, the branch of the pathway also known as the nucleotide loop assembly pathway (NLA) (63, 65).

In *S. enterica*, CobA facilitates the thermodynamically-unfavorable reduction of the Co ion from its 2+ to its 1+ oxidation state, which is "supernucleophilic" and capable of reacting with bound ATP. *S. enterica* CobA (and its homologue *P. denitrificans* CobO) are also necessary for scavenging cobamide precursors, and they can catalyze the reduction of wide variety of corrinoids (62, 66, 67). The genomes of several organohalide-respiring *D. mccartyi* strains, which cannot synthesize cobalamin *de novo*, contain multiple *cobA* copies, presumably to facilitate efficient corrinoid scavenging (Table A.1). Experimental data demonstrating that *D. mccartyi cobA* genes encode proteins with ATP:Co(I)rrinoid adenosyltransferase activity have not been reported.

The *S. enterica* genome (and those of other prokaryotes) also encodes non-homologous enzymes with CobA-like activity (*i.e.*, PduO and EutT, ECs: 2.1.5.17) (68-70). Three-dimensional crystal structures of several PduO–type enzymes from different prokaryotes have been reported (PDB: 3GAH, 3GAI, 3GAJ,2ZHY,2R6X, 2NT8, 2R6T, 3CI3, 3CI4, 3CI1, 1WVT, 2G2D, 2ZHZ, 3KE4, 3KE5, 1WOZ)(68-70). The structure of EutT-type enzymes has not been solved, but it is known that the *S. enterica* enzyme is a ferroprotein whose activity is oxygen labile (70, 71). PduO and EutT are not involved in the *de novo* biosynthesis of cobamides, but they are necessary to maintain adequate levels of adenosylcobalamin for the degradation of specific diols (*e.g.,* 1,2-propanediol) and alcoholamines (*e.g.,* ethanolamine) (72, 73). Collectively, these enzymes are known as ATP:Co(I)rrinoid adenosyltransferases (ACATs).

PduO and EutT are used in *S. enterica* exclusively in 1,2-propanediol and ethanolamine catabolism (69, 70, 74, 75), respectively. However, certain organisms lacking CobA will use PduO to adenosylate *de novo* or scavenged corrinoids. A bioinformatics study of cobalamin-utilizing prokaryotes identified ACATs in all but two *Clostrida* species and three archaeal species (76), although it was not experimentally determined whether or not these species could bypass the requirement for adenosylated corrinoid precursors. The organohalide-respiring bacterium *S. multivorans* also lacks an ACAT, although it contains an otherwise complete set of cobamide synthesis genes and is capable of synthesizing norpseudocobalamin *de novo* (77). The role of adenosylated corrinoids in *S. multivorans* is unclear. A study in *S. enterica* determined that mutations in *cobU* allowed the strain to utilize non-adenosylated cobamide precursors (78), however these mutations are absent in *S. multivorans cobU*.

Both cob(I) and cob(II)alamin catalyze reductive dehalogenation reactions in the absence of an enzyme and in the absence of an upper ligand (79-84). However, genomics studies indicate that most OHRB contain CobA homologues. Assuming these genes are functional, this information suggests that there is a role for these enzymes in the attachment of the upper ligand. The mechanistic role of the upper ligand has yet to be defined in RDases. Recent RDase crystal structures contained cobamides rather than adenosylcobamides (37, 38), suggesting the adenosyl group is removed prior to binding.

A.5 Corrinoid transport system

Alternative to *de novo* synthesis, many organisms, including OHRB, can import and assimilate corrinoids. This is often advantageous to *de novo* synthesizers as well, due to the resource-intensive process of assembling the corrin ring, an estimated 2% of the *S. enterica*

genome is dedicated to synthesis and metabolism of cobalamin (85). In Gram-negative bacteria, corrinoid uptake is performed by the well-characterized BtuBCDF system (86-88) (PDB 1L7V, 2QI9, 4DBL, 4FL3). BtuB is a TonB-dependent, outer-membrane corrinoid transporter (89, 90). BtuF is a periplasmic binding protein (91), which shuttles the corrinoid from BtuB to the inner membrane ABC transporter, BtuCD (EC 3.6.3.33) (92). Gram-positive bacteria lack the outer-membrane BtuB protein, and it is thought that their homologous BtuF protein is membrane-anchored (93)(94). Although the BtuBFCD system is the only known family of corrinoid transporter, the existence of paralogous copies has been described in *Bacteroides thetaiotamicron* (95), and the proposed function of these multiple copies has been to recognize different types of corrinoids and cobamides. A recent study in *D. mccartyi* showed that the *btuFCD* genes of the standard cobamide transporter were up regulated in cells grown in medium containing phenolyl cobamides plus DMB (96). In addition, a non-homologous, putative iron/cobalamin ABC transporter, DET1174-1176, was up regulated in the presence of exogenous cobalamin and down regulated in its absence. Although it was not shown that this transporter specifically bound cobalamin, these findings raised the intriguing possibility that *D. mccartyi* uses differential transporters to selectively take up cobamides from its environment. It is possible that other OHRB may also use such a strategy. A variety of corrinoids are known to exist in environments such as the human gut (97, 98), but surveys of cobamides at sites contaminated by halogenated organics are lacking. However, Men et al. recently detailed an LC/MS/MS method for differentiating and quantifying cobamides from dehalogenating mixed cultures extracted from two contaminated sites and enriched in the lab (99). These authors found the majority of the cobamides to be cobalamin and *p*-cresol cobamide**,** with trace amounts of

pseudocobalamin (adenylyl-cobamide), 2-methyladenylyl-cobamide, 5-hydroxybenzimidazoyl-cobamide, and 5-methylbenzimidazoyl-cobamide.

Upon import, corrinoids must be adenosylated by an ACAT before further modification can take place (63). This necessitates the removal of inactive upper ligands, such as cyanide. The existence of corrinoid-specific reductases is controversial. One such enzyme, CblC, has been characterized in humans and other animals (100) (EC 1.16.1.5, PDB 3SBY,3SBZ, 3SC0), and recently Warren and co-workers reported detailed studies in support of the bacterial corrinoid reductase CobR as a Co(II) reductase in *Brucella melitensis* (EC 1.14.14.9, PDB 4IRA, 3CBO), which utilizes the aerobic or late Co-insertion pathway (101). In bacteria, reduction of scavenged corrinoids is more likely accomplished by non-enzymatic electron transfer by cytosolic reduced flavoproteins (59) or free dihydroflavins (102). Such nonspecific reductions result in the removal of the native *Cob* ligand of the corrinoid, generating a five-coordinate species that can be acted upon by CobA or PduO (102).

A.6 Assembly of the nucleotide loop

After acquisition of an adenosylated corrinoid, either through *de novo* synthesis or import through the BtuBFCD system, the next step in the pathway is the generation of the nucleotide loop that will ultimately coordinate the cobalt center on the α face of the ring. There are several pathways by which this can occur, for simplicity we will start by discussing the *de novo* pathway for cobalamin synthesis.

In *S. enterica*, CbiB synthesizes adenosylcobinamide-phosphate (AdoCbi-P, EC 6.3.1.10), the first intermediate in the assembly of the nucleotide loop. CbiB catalyzes the addition of aminopropanol phosphate to the *f* propionic acid side chain of adenosylcobyric acid (47, 103). In

S. enterica, it was shown that CbiB could use the alternative substrate, ethanolamine-phosphate, to catalyze the eventual synthesis of nor-cobalamin, i.e. cobalamin lacking the methyl group at C176 (103). The similar molecule norpseudocobalamin, which has an adenine in place of DMB, was isolated from *Sulfurospirillum multivorans* (29). It would not be surprising that, in this organism, the CbiB homologue preferentially uses ethanolamine-phosphate instead of aminopropanol-phosphate.

The multifunctional AdoCbi kinase/AdoCbi-P guanylyltransferase enzyme CobU (characterized in *S. enterica*, (104, 105), EC 2.7.1.156/2.7.7.62 PDB 1C9K, 1CBU) or the homologous CobP in *P. denitrificans* (106) plays two separate roles. It can phosphorylate scavenged AdoCbi, in effect replacing the role CbiB plays in the *de novo* pathway, and it can attach a guanosyl moiety to the aminopropanol-phosphate tail of AdoCbi-P, forming AdoCbi-GDP. The latter is necessary for the addition of the base, which will form a coordination bond with the cobalt ion of the ring. In the case of cobalamin, the base is 5,6-dimethylbenzimidazole, which is activated by CobT to its ribotide form, α-ribazole-phosphate (α-RP) (EC 2.4.2.21, PDB 1L4E, 1L4F, 1L4B), before it can be condensed with AdoCbi-GDP by CobS to yield AdoCbl-5'P (107-109)(EC 2.7.8.26). The phosphate moiety of AdoCbl-5'P is released by CobC to form the final product, AdoCbl (EC 3.1.3.73, PDB 3HJG).

A.7 Synthesis of the lower ligand

The diversity of cobamides found in nature is due to their lower bases. These bases fall into three general categories: benzimidazoles, purines, and phenolics (110). The rationale behind the requirement of different enzymes for different lower bases has yet to be resolved. Several

OHRB incapable of *de novo* synthesis require exogeneous cobalamin, at least one species, *S. multivorans*, has been demonstrated to synthesize norpseudocobalamin (29).

Some enzymes can use alternative corrinoids with minimal loss to activity, yet others are greatly affected by non-optimal corrinoids. For instance, pseudocobalamin, which utilizes adenine instead of DMB as a lower ligand, can support growth of *S. enterica* under all conditions that require cobalamin (111). 5'-Methybenzimidazolyl-cobamide, which is synthesized by some sulfate-reducing bacteria (112, 113) can support PCE dechlorination of *D. mccartyi* even though that bacterium preferentially scavenges cobalamin (114). However, the RDase in crude extracts of *Sulfospirillum multivorans* has 50-fold lower activity when using cobalamin instead of its native norpseudocobalamin (115).

5,6-Dimethylbenzimidazole is the most studied of the cobamide lower ligands, yet many questions remain about how DMB is synthesized. DMB can be synthesized by one of two pathways. An oxygen-dependent mechanism has been reported in *Pseudomonas shermanii*, in which isotopic labeling experiments revealed that DMB was synthesized from the flavin group of flavin mononucleotide (116, 117). The enzyme that catalyzes this $FMNH_2$-dependent synthesis, BluB, was characterized in *Rhodospirillum rubrum* and *Sinorhizobium meliloti* (118, 119). The enzymes catalyzing the anaerobic route of DMB synthesis have not been identified, although the process had been described *Eubacterium limosum* using isotopic labeling (120). It was determined that formate, erythrose, glutamine, glycine and methionine make up the component carbon and nitrogen sources for DMB synthesis.

There is little known about the synthesis of benzimidazole bases other than DMB. Glycine was shown to be incorporated into the same positions of 5-hydroxybenzimidazole (121) and 5-methoxybenzimidazole (122) as in DMB, suggesting a partially shared pathway as DMB

synthesis. However, differences have been identified as well, such as the inability to use erythrose in 5-hydroxybenzimidazole (123) or methionine in 5-methylbenzimidazole synthesis (124).

Crofts et al. recently described a high-throughput bioassay for detection of free benzimidazoles and derivatives from environmental samples (125). The authors detected picomolar amounts of benzimidazole, but not DMB, from two geographically different soil samples. The availability of free benzimidazole in the environment is an intriguing potential source of lower ligands for organisms that synthesize or scavenge cobamides.

Purines, particularly adenine, are another type of lower ligand often found in cobamides. The source of purine ligands in wild-type cells is unknown, although it has been proposed that adenine, hypoxanthine, and guanine are redirected to corrinoid synthesis directly from the purine biosynthetic pathway, which assumes the existence of an appropriate glycosidase to convert the 5'-nucleotides from that pathway to free bases (110). Anderson and coworkers isolated several mutant strains in *S. enterica* that increased the intercellular concentrations of free adenine in a DMB-free environment, which resulted in pseudocobalamin synthesis. The synthesis of pseudocobalamin was reverted to cobalamin by adding exogenous DMB (67).

Phenolic lower bases also exist in the environment, produced most notably by *Sporomusa ovata* (4, 126, 127). Tyrosine degradation has been identified as the source of the *p*-cresol base in *S. ovata*, and has been suggested to be the source of the phenol base as well (126, 127). The phenolic lower bases lack the nitrogen moiety that coordinates the central cobalt ion, and it is unable to support Cbl-dependent growth of *S. enterica* under conditions that require one-electron, AdoCbl chemistry.

The lower ligand must be activated to an α-nucleotide form before it can be attached to AdoCbi-GDP. In the case of DMB, this process involves the catabolism of an existing nucleotide, namely nicotinate mononucleotide, to attach the ribosyl-P moiety of NaMN to DMB resulting in an unusual α-*N*-glycosidic linkage yielding α-ribazole-phosphate (α-RP). In *S. enterica*, this reaction is performed by CobT (128). The CobT enzyme also phosphoribosylates DMB using nicotinamide adenine dinucleotide (NAD^+), forming the α-DMB-adenine dinucleotide intermediate called α-DAD (129). It is thought that α-DAD is converted to α-RP through an unidentified hydrolase, yet the identity of this putative hydrolase remains unknown. In the case of pseudocobalamin, it was proposed that adenine is activated to an a-nucleoside by the same enzymes, CobU, S, T and C, that are responsible for activating DMB in *S. enterica* (67), although biochemical evidence to support this idea has not been reported to date.

Sporomusa ovata uses the CobT homologues ArsAB (EC 2.4.2.21/2.4.2.55), which, unlike CobT, form a heterodimer capable of activating phenolic lower bases, such as *p*-cresol and phenol (5) (PDB 4HDM, 4HDN, 4HDR, 4HDS). However, ArsAB is not specific for phenolics. The enzyme can also activate DMB and purines, despite a clear preference for phenolic substrates (130). Notably, when *S. ovata* is grown with excess benzimidazoles in the medium, it incorporates them into cobamides at the expense of phenolic groups, resulting in growth inhibition (131), suggesting that the enzyme may have high *in vivo* affinity for benzimidazole and its derivatives. ArsAB can support growth of a *S. enterica cobT*$^-$ strain in the presence of cobinamide and DMB at nearly the same doubling time as a *cobT*$^+$ strain.(132)

Like the *S. ovata* ArsAB enzyme, *S. multivorans* CobT uses exogenous DMB at the expense of its native lower ligand base. Micromolar amounts of DMB added to *S. multivorans* growth medium on PCE inhibit growth and produces nor-cobalamin instead of the native cofactor,

norpseudocobalamin. Addition of *p*-cresol to the growth medium had no effect on the growth rate (115).

Listeria innocua lacks CobT, and instead makes α-RP through the non-homologous CblT and CblS enzymes (133). CblT transports a-R from the environment, and CblS phosphorylates it to α-RP (EC: 2.7.1.-), suggesting that a-R may be environmentally available to some organisms. Recently, CblT and S were identified in *Desulfitobacterium hafniense*. However, unlike *L. innocua*, *D. hafniense* also contains CobT (134)

The precursor of the RDase PceA in *Desulfitobacterium hafniense* strain Y51 was shown to aggregate in the absence of cobalamin, which is necessary to complete folding of PceA and subsequent membrane translocation (34). PrePceA aggregates contain CobT among other enzymes. It is an intriguing possibility that the final steps of cobamide synthesis are taking place near the membrane to efficiently reconstitute and translocate PceA. It has been shown that CobS is a membrane-bound protein in *S. enterica* and *Methanobacterium thermoautotrophicum* (109) and it is possible that other Cob enzymes are components of a macromolecular complex.

A.8 Lower ligand remodeling

Cobamide-scavenging organisms may not always encounter the exact cobamide they require, or the cobamide may be incomplete. Such organisms must be able to remove the lower ligand and replace it. In *Salmonella enterica*, the kinase activity associated with CobU is needed to salvage cobinamide from the environment. The first step after translocation of Cbi into the cell is its conversion to AdoCbi by the housekeeping adenosyltransferase CobA (63). Once AdoCbi is available, CobU uses it to generate AdoCbi-P. The final step in the activation of Cbi is the conversion of AdoCbi-P to AdoCbi-GDP also by CobU (104-106, 135). A non-orthologous

replacement for CobU was found in archaea (136). The archaeal non-orthologous CobU replacement was named CobY, and it should be noted that, while it retains the CobU-like guanylyltransferase activity, it is devoid of AdoCbi kinase activity. To make up for the latter activity, archaea evolved a different strategy for the assimilation of Cbi from the environment. Archaea possess an amidohydrolase, CbiZ (EC 3.5.1.90) that hydrolyzes the amide bond in the nucleotide tail of AdoCbi, generating Ado-cobyric acid (AdoCby) (Fig. A4 (137, 138)). Surprisingly, *cbiZ* can be found in some bacteria. For example, it is known that the genome of *Rhodobacter sphaeroides* encodes a *cbiZ* homologue that encodes a functional enzyme (139-141). In *R. sphaeroides*, cobinamide and cobamides such as pseudocobalamin are substrates of CbiZ. In sharp contrast, CbiZ in this bacterium had no hydrolytic activity when either cyano-cobalamin or adenosyl-cobalamin was the substrate (140). The CbiZ reaction results in AdoCby, the substrate for CbiB. The resulting AdoCbi-P product then enters the late steps of the pathway that assemble the nucleotide loop.

When *D. mccartyi* strain 195 is grown under conditions requiring it to scavenge phenolic cobamides from a co-culture strain, a microarray analysis indicated *cbiZ* transcription is up regulated (96). Also up regulated are the *cbiB* and *cobD* genes, which synthesize AdoCbi-P from Cby generated by CbiZ, which subsequently is channeled into the nucleotide-loop assembly pathway. Together, these data indicate a dependence on CbiZ activity under simulated environmental conditions.

A.9 Cobalamin Riboswitches

AdoCbl-binding riboswitches are important regulators of corrinoid metabolism in many organisms. For instance, expression of cobalamin-synthesizing genes in *S. enterica* is repressed

by a riboswitch in the 5' leader of the *cob* operon mRNA, and expression of cobalamin transporters in *S. enterica* and *E. coli* is also repressed by a riboswitch in the 5' un-translated region of the *btuB* gene (142-145). Recently, several riboswitches have been characterized in *D. hafniense* strains Y51, DCB-2 and TCE1 (134). Eighteen riboswitches were described in total, with predicted functions primarily to regulate *de novo* corrinoid synthesis and corrinoid transporter genes. Additionally, corrinoid-dependent transcriptional repression was observed for the transporter *btuF*, the phosphoribosyltransferase *cobT* and the precorrin methyltransferase *cbiET*.

Reinhold and coworkers observed that adding cobalamin to the growth medium of *D. hafniense* stabilized the dechlorinating *pceA* gene (34). When cobalamin was absent from the PCE-free medium, *pceA* was lost after eight passages. When cobalamin was present in PCE-free medium, *pceA* levels were detectable for 60 passages. Whether this effect is due to direct or indirect interactions between cobalamin and *pceA* is unknown.

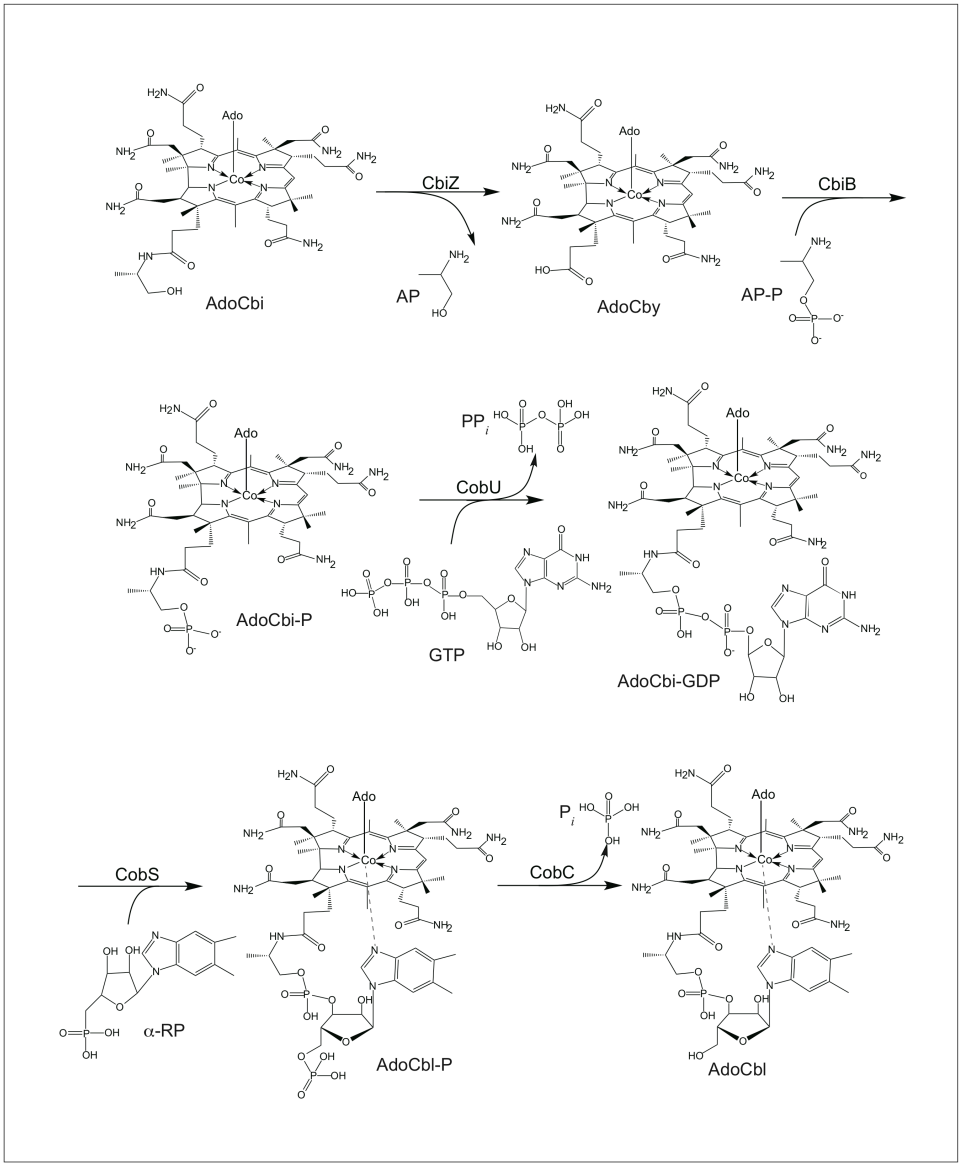

Figure A4. Pathway for the synthesis of adenosylcobalamin via CbiZ-mediated salvaging of adenosylcobinamide. Abbreviations: Ado, adenosyl group; AdoCbi, adenosylcobinamide; AP, aminopropanol; AdoCby, adenosylcobyric acid; AP-P, aminopropanol-phosphate; GTP, guanosine triphosphate; PP, pyrophosphate; AdoCbi-GTP, adenosylcobinamide-guanosine diphosphate; a-RP, alpha-ribazole phosphate; AdoCbl-P, adenosylcobalamin-phosphate; P, phosphate; AdoCbl, adenosylcobalamin.

A.10 Environmental supply of cobalamin

A study by Guerrero-Barajas and co-workers indicated that supplying the corrin-ring precursor porphobilinogen to carbon tetrachloride-dehalogenating sludge enhanced the dehalogenation rate by several-fold over controls in a concentration-dependent manner (146). Similar, although smaller effects were also observed with the addition of other precursors, including methionine, adenine, threonine, and d-aminolevulinic acid, although these effects may have been unrelated to cobamide synthesis. Overall the results indicated that corrin ring synthesis is a limiting factor for reductive dechlorination among certain consortia.

Although almost all OHRB require corrinoids to utilize halogenated compounds as electron acceptors, not all are capable of *de novo* corrin ring biosynthesis. For instance, a comparative genomics study of cobalamin utilization pathways identified 15 species out of 539 analyzed that contain genes for corrinoid-dependent RDases (147). Of these, six species lacked genes for *de novo* corrin ring biosynthesis. Given that many are dependent on organohalides for respiration, it is of interest to learn how corrinoid auxotrophs acquire their cobamides.

As of this writing, no protein capable of exporting corrinoids has been defined, and thus the method by which corrinoids enter the environment is unclear. Some corrinoids are presumably released via cell lysis, but co-culture experiments suggest "cross-feeding" of cobalamin between mutualistic strains (148). A number of studies have defined interactions among the cobalamin-dependent, organohalide-respiring *D. mccartyi* and strains in its biome (96, 149, 150). *D. mccartyi* lacks the genes for *de novo* cobalamin synthesis. *Geobacter lovleyi,* a cobalamin-synthesizing species capable of organohalide respiration with tetrachloroethene (PCE) and trichloroethene (TCE) (151), could support growth of *D. mccartyi* in cobalamin-free media,

indicating *D. mccartyi* feeds off cobalamin produced by *G. lovleyi* (149). *Geobacter sulfurreducens*, a non-dehalogenating species producing an unspecified cobamide, could only support growth of *D. mccartyi* when exogenous DMB was provided. This indicates that either *G. sulfurreducens* is incorporating DMB into its cobamide, or that *D. mccartyi* is utilizing CbiZ to remodel an unusable cobamide into cobalamin. Another study had determined that pure culture *D. mccartyi* could also incorporate benzimidazole, 5-methylbenzimidazole and 5-methoxybenzimidazole into a cobamide to support growth on halogenated compounds (114). *G. lovleyi* respires PCE to *cis*-dichloroethene (*cis*-DCE) (152) whereas some *D. mccartyi* strains can dechlorinate *cis*-DCE and vinyl chloride (VC). It was proposed that the co-occurrence of these organisms at sites contaminated by PCE would be beneficial to *D. mccartyi*, as *G. lovleyi* could supply both *cis*-DCE and cobalamin.

Additional co-culture experiments between *D. mccartyi* strains and *Methanosarcina barkeri*, *S. ovata* and *Sporomusa* sp. strain KB-1 produced similar results (150). Production of Factor III (*Co*α-5-hydroxybenzimidazolyl-cobamide) from *M. barkeri* or phenol and *p*-cresol cobamide from the *Sporomusa* strains did not support cobalamin-dependent growth of *D. mccartyi* on PCE. Exogenous DMB supported growth under these co-culture conditions, as was the case with *G. sulfurreducens*, providing further evidence that *D. mccartyi* is remodeling cobamides into cobalamin using exogenous DMB.

Recently, a defined consortium of three species was shown to be capable of supporting *D. mccartyi* growth when supplied lactate, PCE and DMB (96). *Desulfovibrio vulgaris* Hildenborough and *Pelosinus fermentans* R7 fermented lactate and supplied acetate to *D. mccartyi*. Additionally, *D. vulgaris* supplied H_2, the electron donor for the reductive dechlorination of PCE, while *P. fermentans* supplied corrinoids, either phenyl cobamide or *p*-

cresol cobamide. It was assumed that *D. mccartyi* was supplying fermentable products to the co-culture species to complete the cycle. *D. mccartyi* significantly up regulated *cbiZ* in response to cobamide exposure, indicating that it was importing and remodeling the inactive cobamide into cobalamin through the CbiZ pathway.

A.11 Outlook

Much remains unknown about the metabolism of corrinoids in microbial reductive dechlorination process. Genome sequencing efforts have expanded our knowledge of the potential for cobamide synthesis in OHRB, however the lack of tractable genetic systems in these organisms has made it difficult to tease apart the pathways in the *de novo* synthesizers. Thus the possibility that organohalide-respiring bacteria might be making novel corrinoids, such as the norpseudocobalamin of *S. multivorans*, remains largely unexplored.

The diversity of lower bases figures foremost in many of the questions regarding cobamides in organohalide-respiring bacteria as it does in the wider study of cobalamin. We have a limited understanding of what drives the preference of one base over the other. Although we know that bacteria can remodel cobamides using the CbiZ system to use a different base, we do not know how diverse or available cobamides are in the environment of OHRB. Likewise, we are only beginning to understand the source of the cobamides in the environment, and whether or not dehalogenating communities share corrinoids to metabolize available resources.

A.12 Acknowledgements. This work was supported by USPHS grant R37 GM040313 from the National Institutes of General Medical Sciences to J.C.E.-S.

A.13 References

1. Battersby, A. R. (2000) Tetrapyrroles: the pigments of life, *Nat. Prod. Rep.* **17**, 507-526.

2. Eirich, L. D., Vogels, G. D., and Wolfe, R. S. (1978) Proposed structure for coenzyme F420 from Methanobacterium, *Biochemistry* **17**, 4583-4593.

3. van Beelen, P., Stassen, A. P., Bosch, J. W., Vogels, G. D., Guijt, W., and Haasnoot, C. A. (1984) Elucidation of the structure of methanopterin, a coenzyme from *Methanobacterium thermoautotrophicum*, using two-dimensional nuclear-magnetic-resonance techniques, *Eur. J. Biochem.* **138**, 563-571.

4. Stupperich, E., Eisinger, H. J., and Kräutler, B. (1989) Identification of phenolyl cobamide from the homoacetogenic bacterium *Sporomusa ovata*, *Eur. J. Biochem.* **186**, 657-661.

5. Chan, C. H., and Escalante-Semerena, J. C. (2011) ArsAB, a novel enzyme from Sporomusa ovata activates phenolic bases for adenosylcobamide biosynthesis, *Mol Microbiol.* **81**, 952-967.

6. Abend, A., Bandarian, V., Nitsche, R., Stupperich, E., Retey, J., and Reed, G. H. (1999) Ethanolamine ammonia-lyase has a "base-on" binding mode for coenzyme B12, *Arch Biochem. Biophys.* **370**, 138-141.

7. Yamanishi, M., Yunoki, M., Tobimatsu, T., Sato, H., Matsui, J., Dokiya, A., Iuchi, Y., Oe, K., Suto, K., Shibata, N., Morimoto, Y., Yasuoka, N., and Toraya, T. (2002) The crystal structure of coenzyme B12-dependent glycerol dehydratase in complex with cobalamin and propane-1,2-diol, *Eur. J. Biochem.* **269**, 4484-4494.

8. Lawrence, J. G., and Roth, J. R. (1995) The cobalamin (coenzyme B12) biosynthetic genes of *Escherichia coli*, *J. Bacteriol.* **177**, 6371-6380.

9. Roth, J. R., Lawrence, J. G., and Bobik, T. A. (1996) Cobalamin (coenzyme B12): synthesis and biological significance, *Annu. Rev. Microbiol.* **50**, 137-181.

10. Warren, M. J., Raux, E., Schubert, H. L., and Escalante-Semerena, J. C. (2002) The biosynthesis of adenosylcobalamin (vitamin B12), *Nat. Prod. Rep.* **19**, 390-412.

11. Roessner, C. A., and Scott, A. I. (2006) Fine-tuning our knowledge of the anaerobic route to cobalamin (vitamin B_{12}), *J. Bacteriol.* **188**, 7331-7334.

12. Escalante-Semerena, J. C. (2007) Conversion of cobinamide into adenosylcobamide in bacteria and archaea, *J. Bacteriol.* **189**, 4555-4560.

13. Moore, S. J., and Warren, M. J. (2012) The anaerobic biosynthesis of vitamin B12, *Biochem. Soc. Trans. 40***,** 581-586.

14. Woodward, R. B. (1973) The total synthesis of vitamin B_{12}, *Pure Appl. Chem.* **33**, 145-177.

15. Eschenmoser, A., and Wintner, C. E. (1977) Natural product synthesis and vitamin B_{12}, *Science* **196**, 1410-1420.

16. Eschenmoser, A. (1988) Vitamin B12: experiments concerning the origin of its molecular structure., *Angew. Chem. Int. Ed. Engl.* **27**, 5-40.

17. Lexa, D., and Saveant, J.-M. (1983) The electrochemistry of vitamin B12, *Acc. Chem. Res.* **16**, 235-243.

18. Banerjee, R., and Ragsdale, S. W. (2003) The many faces of vitamin B12: catalysis by cobalamin-dependent enzymes, *Annu. Rev. Biochem.* **72**, 209-247.

19. Brown, K. L. (2005) Chemistry and enzymology of vitamin B_{12}, *Chem. Rev.* **105**, 2075-2149.

20. Randaccio, L., Geremia, S., Demitri, N., and Wuerges, J. (2010) Vitamin B12: unique metalorganic compounds and the most complex vitamins, *Molecules* **15**, 3228-3259.

21. Matthews, R. G. (2001) Cobalamin-dependent methyltransferases, *Acc. Chem. Res.* **34**, 681-689.

22. Matthews, R. G. (2009) Cobalamin- and corrinoid-dependent enzymes, *Metal Ions Life Sci.* **6**, 53-114.

23. Holliger, C., Wohlfarth, G., and Diekert, G. (1998) Reductive dechlorination in the energy metabolism of anaerobic bacteria, *FEMS Microbiol. Rev.* **22**, 383-398.

24. McMurdie, P. J., Behrens, S. F., Muller, J. A., Goke, J., Ritalahti, K. M., Wagner, R., Goltsman, E., Lapidus, A., Holmes, S., Loffler, F. E., and Spormann, A. M. (2009) Localized plasticity in the streamlined genomes of vinyl chloride respiring Dehalococcoides, *PLoS Genet.* **5,** e1000714.

25. Neumann, A., Wohlfarth, G., and Diekert, G. (1998) Tetrachloroethene dehalogenase from *Dehalospirillum multivorans*: Cloning, sequencing of the encoding genes, and expression of the *pceA* gene in *Escherichia coli*, *J. Bacteriol.* **180**, 4140-4145.

26. Miller, E., Wohlfarth, G., and Diekert, G. (1998) Purification and characterization of the tetrachloroethene reductive dehalogenase of strain PCE-S, *Arch. Microbiol.* **169**, 497-502.

27. Maillard, J., Schumacher, W., Vazquez, F., Regeard, C., Hagen, W. R., and Holliger, C. (2003) Characterization of the corrinoid iron-sulfur protein tetrachloroethene reductive dehalogenase of *Dehalobacter restrictus*, *Appl. Environ. Microbiol.* **69**, 4628-4638.

28. Adrian, L., Hansen, S. K., Fung, J. M., Gorisch, H., and Zinder, S. H. (2007) Growth of Dehalococcoides strains with chlorophenols as electron acceptors, *Environ. Sci. Technol.* **41**, 2318-2323.

29. Kräutler, B., Fieber, W., Osterman, S., Fasching, M., Ongania, K.-H., Gruber, K., Kratky, C., Mikl, C., Siebert, A., and Diekert, G. (2003) The cofactor of tetrachloroethene reductive dehalogenase of *Dehalospirillum multivorans* is Norpseudo-B12, a new type of natural corrinoid., *Helv. Chim. Acta* **86**, 3698-3716.

30. Neumann, A., Wohlfarth, G., and Diekert, G. (1995) Properties of tetrachloroethene and trichloroethene dehalogenase of *Dehalospirillum multivorans*. *Arch. Microbiol.* **163**, 276-281.

31. Schumacher, W., Holliger, C., Zehnder, A. J., and Hagen, W. R. (1997) Redox chemistry of cobalamin and iron-sulfur cofactors in the tetrachloroethene reductase of *Dehalobacter restrictus*, *FEBS Lett.* **409**, 421-425.

32. John, M., Schmitz, R. P., Westermann, M., Richter, W., and Diekert, G. (2006) Growth substrate dependent localization of tetrachloroethene reductive dehalogenase in *Sulfurospirillum multivorans*, *Arch. Microbiol.* **186**, 99-106.

33. Palmer, T., Sargent, F., and Berks, B. C. (2005) Export of complex cofactor-containing proteins by the bacterial Tat pathway, *Trends Microbiol.* **13**, 175-180.

34. Reinhold, A., Westermann, M., Seifert, J., von Bergen, M., Schubert, T., and Diekert, G. (2012) Impact of vitamin B12 on formation of the tetrachloroethene reductive dehalogenase in *Desulfitobacterium hafniense* strain Y51, *Appl. Environ. Microbiol.* **78**, 8025-8032.

35. Morita, Y., Futagami, T., Goto, M., and Furukawa, K. (2009) Functional characterization of the trigger factor protein PceT of tetrachloroethene-dechlorinating *Desulfitobacterium hafniense* Y51, *Appl. Microbiol. & Biotechnol.* **83**, 775-781.

36. Maillard, J., Genevaux, P., and Holliger, C. (2011) Redundancy and specificity of multiple trigger factor chaperones in Desulfitobacteria, *Microbiology* **157**, 2410-2421.

37. Bommer, M., Kunze, C., Fesseler, J., Schubert, T., Diekert, G., and Dobbek, H. (2014) Structural basis for organohalide respiration, *Science* **346**, 455-458.

38. Payne, K. A. P., Quezada, C. P., Fisher, K., Dunstan, M. S., Collins, F. A., Sjuts, H., Levy, C., Hay, S., Rigby, S. E. J., and Leys, D. (2014) Reductive dehalogenase structure suggests a mechanism for B12-dependent dehalogenation, *Nature* **517,** 513-516.

39. Cameron, B., Briggs, K., Pridmore, S., Brefort, G., and Crouzet, J. (1989) Cloning and analysis of genes involved in coenzyme B12 biosynthesis in *Pseudomonas denitrificans*, *J. Bacteriol.* **171**, 547-557.

40. Roth, J. R., Lawrence, J. G., Rubenfield, M., Kieffer-Higgins, S., and Church, G. M. (1993) Characterization of the cobalamin (vitamin B_{12}) biosynthetic genes of *Salmonella typhimurium*, *J. Bacteriol.* **175**, 3303-3316.

41. Raux, E., Lanois, A., Warren, M. J., Rambach, A., and Thermes, C. (1998) Cobalamin (vitamin B_{12}) biosynthesis: identification and characterization of a *Bacillus megaterium cobI* operon, *Biochem. J.* **335**, 159-166.

42. Hug, L. A., Maphosa, F., Leys, D., Loffler, F. E., Smidt, H., Edwards, E. A., and Adrian, L. (2013) Overview of organohalide-respiring bacteria and a proposal for a classification system for reductive dehalogenases, *Philos .Trans. R. Soc. Lond. B Biol. Sci.* **368**, 20120322.

43. Bogorad, L., and Granick, S. (1953) The enzymatic synthesis of porphyrins from porphobilinogen, *Proc. Natl. Acad. Sci. U S A* **39**, 1176.

44. Battersby, A. R., McDonald, E., Cornforth, J. W., and Frydman, B. (1976) Biosynthesis of Porphyrins and Corrins [and Discussion], *Phil. Transac. Royal Soc. London. Series B, Biol. Sci.* **273**, 161-180.

45. Leeper, F. J. (1989) The biosynthesis of porphyrins, chlorophylls and vitamin B12., *Nat. Prod. Rep.* **6**, 171-203.

46. Markowitz, V. M., Chen, I. M., Palaniappan, K., Chu, K., Szeto, E., Grechkin, Y., Ratner, A., Jacob, B., Huang, J., Williams, P., Huntemann, M., Anderson, I., Mavromatis, K., Ivanova, N. N., and Kyrpides, N. C. (2012) IMG: the Integrated Microbial Genomes database and comparative analysis system, *Nucleic Acids Res.* **40**, D115-122.

47. Crouzet, J., Levy-Schil, S., Cameron, B., Cauchois, L., Rigault, S., Rouyez, M. C., Blanche, F., Debussche, L., and Thibaut, D. (1991) Nucleotide sequence and genetic analysis of a 13.1-kilobase-pair *Pseudomonas denitrificans* DNA fragment containing five *cob* genes and identification of structural genes encoding Cob(I)alamin adenosyltransferase, cobyric acid synthase, and bifunctional cobinamide kinase-cobinamide phosphate guanylyltransferase, *J. Bacteriol.* **173**, 6074-6087.

48. Debussche, L., Thibaut, D., Cameron, B., Crouzet, J., and Blanche, F. (1993) Biosynthesis of the corrin macrocycle of coenzyme B_{12} in *Pseudomonas denitrificans*, *J. Bacteriol.* **175**, 7430-7440.

49. Thibaut, D., Debussche, L., and Blanche, F. (1990) Biosynthesis of vitamin B12: isolation of precorrin-6x, a metal-free precursor of the corrin macrocycle retaining five S-adenosylmethionine-derived peripheral methyl groups, *Proc. Natl. Acad. Sci. U S A* **87**, 8795-8799.

50. Thibaut, D., Couder, M., Famechon, A., Debussche, L., Cameron, B., Crouzet, J., and Blanche, F. (1992) The final step in the biosynthesis of hydrogenobyrinic acid is catalyzed by the *cobH* gene product with precorrin-8x as the substrate, *J. Bacteriol.* **174**, 1043-1049.

51. Blanche, F., Thibaut, D., Debussche, L., Hertle, R., Zipfel, F., and Muller, G. (1993) Paralleles and decisive differences in vitamin B12 biosynthesis., *Angew. Chem. Int. Ed. Engl.* **32**, 1651-1653.

52. Kruse, T., Maillard, J., Goodwin, L., Woyke, T., Teshima, H., Bruce, D., Detter, C., Tapia, R., Han, C., Huntemann, M., Wei, C. L., Han, J., Chen, A., Kyrpides, N., Szeto, E., Markowitz, V., Ivanova, N., Pagani, I., Pati, A., Pitluck, S., Nolan, M., Holliger, C., and Smidt, H. (2013) Complete genome sequence of Dehalobacter restrictus PER-K23(T.), *Stand. Genom. Sci.* **8**, 375-388.

53. Schipp, C. J., Marco-Urrea, E., Kublik, A., Seifert, J., and Adrian, L. (2013) Organic cofactors in the metabolism of Dehalococcoides mccartyi strains, *Philos. Trans. R. Soc. Lond. B. Biol. Sci.* **368**, 20120321.

54. Raux, E., Thermes, C., Heathcote, P., Rambach, A., and Warren, M. J. (1997) A role for *Salmonella typhimurium cbiK* in cobalamin (vitamin B12) and siroheme biosynthesis, *J. Bacteriol.* **179**, 3202-3212.

55. Moore, S. J., Biedendieck, R., Lawrence, A. D., Deery, E., Howard, M. J., Rigby, S. E., and Warren, M. J. (2013) Characterization of the enzyme CbiH60 involved in anaerobic ring contraction of the cobalamin (vitamin B12) biosynthetic pathway, *J. Biol. Chem.* **288**, 297-305.

56. Moore, S. J., Lawrence, A. D., Biedendieck, R., Deery, E., Frank, S., Howard, M. J., Rigby, S. E., and Warren, M. J. (2013) Elucidation of the anaerobic pathway for the corrin component of cobalamin (vitamin B12), *Proc. Natl. Acad. Sci. U S A* **110**, 14906-14911.

57. Fresquet, V., Williams, L., and Raushel, F. M. (2004) Mechanism of cobyrinic acid *a,c*-diamide synthetase from *Salmonella typhimurium* LT2, *Biochemistry* **43**, 10619-10627.

58. Blanche, F., Couder, M., Debussche, L., Thibaut, D., Cameron, B., and Crouzet, J. (1991) Biosynthesis of vitamin B12: stepwise amidation of carboxyl groups *b, d, e*, and *g* of cobyrinic acid *a,c*-diamide is catalyzed by one enzyme in *Pseudomonas denitrificans.*, *J. Bacteriol.* **173**, 6046-6051.

59. Fonseca, M. V., and Escalante-Semerena, J. C. (2000) Reduction of cob(III)alamin to cob(II)alamin in *Salmonella enterica* Serovar Typhimurium LT2., *J. Bacteriol.* **182**, 4304-4309.

60. Suh, S. J., and Escalante-Semerena, J. C. (1993) Cloning, sequencing and overexpression of *cobA* which encodes ATP:corrinoid adenosyltransferase in *Salmonella typhimurium*, *Gene* **129**, 93-97.

61. Fonseca, M. V., Buan, N. R., Horswill, A. R., Rayment, I., and Escalante-Semerena, J. C. (2002) The ATP:co(I)rrinoid adenosyltransferase (CobA) enzyme of *Salmonella enterica* requires the 2'-OH Group of ATP for function and yields inorganic triphosphate as its reaction byproduct, *J. Biol. Chem.* **277**, 33127-33131.

62. Debussche, L., Couder, M., Thibaut, D., Cameron, B., Crouzet, J., and Blanche, F. (1991) Purification and partial characterization of cob(I)alamin adenosyltransferase from *Pseudomonas denitrificans*, *J. Bacteriol.* **173**, 6300-6302.

63. Escalante-Semerena, J. C., Suh, S. J., and Roth, J. R. (1990) *cobA* function is required for both de novo cobalamin biosynthesis and assimilation of exogenous corrinoids in *Salmonella typhimurium*, *J. Bacteriol.* **172**, 273-280.

64. Lundrigan, M. D., and Kadner, R. J. (1989) Altered cobalamin metabolism in *Escherichia coli btuR* mutants affects *btuB* gene regulation, *J. Bacteriol.* **171**, 154-161.

65. Jeter, R. M., Olivera, B. M., and Roth, J. R. (1984) *Salmonella typhimurium* synthesizes cobalamin (vitamin B_{12}) de novo under anaerobic growth conditions, *J. Bacteriol.* **159**, 206-213.

66. Suh, S., and Escalante-Semerena, J. C. (1995) Purification and initial characterization of the ATP:corrinoid adenosyltransferase encoded by the *cobA* gene of *Salmonella typhimurium*, *J. Bacteriol.* **177**, 921-925.

67. Anderson, P. J., Lango, J., Carkeet, C., Britten, A., Kräutler, B., Hammock, B. D., and Roth, J. R. (2008) One pathway can incorporate either adenine or dimethylbenzimidazole as an alpha-axial ligand of B_{12} cofactors in *Salmonella enterica*, *J. Bacteriol.* **190**, 1160-1171.

68. Johnson, C. L., Pechonick, E., Park, S. D., Havemann, G. D., Leal, N. A., and Bobik, T. A. (2001) Functional genomic, biochemical, and genetic characterization of the *Salmonella pduO* gene, an ATP:cob(I)alamin adenosyltransferase gene, *J. Bacteriol.* **183**, 1577-1584.

69. Buan, N. R., Suh, S. J., and Escalante-Semerena, J. C. (2004) The *eutT* gene of *Salmonella enterica* encodes an oxygen-labile, metal-containing ATP:corrinoid adenosyltransferase enzyme, *J. Bacteriol.* **186**, 5708-5714.

70. Buan, N. R., and Escalante-Semerena, J. C. (2006) Purification and initial biochemical characterization of ATP:Cob(I)alamin adenosyltransferase (EutT) enzyme of *Salmonella enterica*, *J. Biol. Chem.* **281**, 16971-16977.

71. Moore, T. C., Mera, P. E., and Escalante-Semerena, J. C. (2014) the Eutt enzyme of Salmonella enterica is a unique ATP:Cob(I)alamin adenosyltransferase metalloprotein that requires ferrous ions for maximal activity, *J. Bacteriol.* **196**, 903-910.

72. Mera, P. E., and Escalante-Semerena, J. C. (2010) Multiple roles of ATP:cob(I)alamin adenosyltransferases in the conversion of B(12) to coenzyme B (12), *Appl. Microbiol. Biotechnol.* **88**, 41-48.

73. Moore, T. C., Newmister, S. A., Rayment, I., and Escalante-Semerena, J. C. (2012) Structural insights into the mechanism of four-coordinate cob(II)alamin formation in the active site of the *Salmonella enterica* ATP:co(I)rrinoid adenosyltransferase (CobA) enzyme: Critical role of residues Phe91 and Trp93, *Biochemistry* **51**, 9647-9657.

74. Johnson, C. L., Buszko, M. L., and Bobik, T. A. (2004) Purification and initial characterization of the *Salmonella enterica* PduO ATP:Cob(I)alamin adenosyltransferase., *J. Bacteriol.* **186**, 7881-7887.

75. Mera, P. E., Maurice, M. S., Rayment, I., and Escalante-Semerena, J. C. (2007) Structural and functional analyses of the human-type corrinoid adenosyltransferase (PduO) from *Lactobacillus reuter*i, *Biochemistry* **46**, 13829-13836.

76. Rodionov, D. A., Vitreschak, A. G., Mironov, A. A., and Gelfand, M. S. (2003) Comparative genomics of the vitamin B_{12} metabolism and regulation in prokaryotes, *J. Biol. Chem.* **278**, 41148-41159.

77. Goris, T., Schubert, T., Gadkari, J., Wubet, T., Tarkka, M., Buscot, F., Adrian, L., and Diekert, G. (2014) Insights into organohalide respiration and the versatile catabolism of *Sulfurospirillum multivorans* gained from comparative genomics and physiological studies, *Environ. Microbiol.* **16**, 3562-3580.

78. O'Toole, G. A., and Escalante-Semerena, J. C. (1993) *cobU*-dependent assimilation of nonadenosylated cobinamide in cobA mutants of *Salmonella typhimurium*, *J. Bacteriol.* **175**, 6328-6336.

79. Krone, U. E., Thauer, R. K., and Hogenkamp, H. P. C. (1989) Reductive dehalogenation of chlorinated C1-hydrocarbons mediated by corrinoids, *Biochemistry* **28**, 4908-4914.

80. Krone, U. E., Thauer, R. K., Hogenkamp, H. P. C., and Steinbach, K. (1991) Reductive formation of carbon monoxide from carbon tetrachloride and FREONS 11, 12, and 13 catalyzed by corrinoids, *Biochemistry* **30**, 2713-2719.

81. Gantzer, C. J., and Wackett, L. P. (1991) Reductive dechlorination catalyzed by bacterial transition-metal coenzymes, *Environmental science & technology* **25**, 715-722.

82. Assaf-Anid, N., Hayes, K. F., and Vogel, T. M. (1994) Reductive dechlorination of carbon tetrachloride by cobalamin (II) in the presence of dithiotreitol: Mechanistic study, effect of redox potential and pH., *Environ. Sc. Technol.* **28**, 246-252.

83. Chiu, P.-C., and Reinhard, M. (1996) Transformation of carbon tetrachloride by reduced vitamin B12 in aqueous cysteine solution, *Environmental science & technology* **30**, 1882-1889.

84. Lesage, S., Brown, S., and Millar, K. (1998) A different mechanism for the reductive dechlorination of chlorinated ethenes: Kinetic and spectroscopic evidence, *Environmental science & technology* **32**, 2264-2272.

85. Price-Carter, M., Tingey, J., Bobik, T. A., and Roth, J. R. (2001) The alternative electron acceptor tetrathionate supports B12-dependent anaerobic growth of *Salmonella enterica* serovar Typhimurium on ethanolamine or 1,2-propanediol, *J. Bacteriol.* **183**, 2463-2475.

86. DeVeaux, L. C., Clevenson, D. S., Bradbeer, C., and Kadner, R. J. (1986) Identification of the BtuCED polypeptides and evidence for their role in vitamin B12 transport in *Escherichia coli*, *J. Bacteriol.* **167**, 920-927.

87. Cadieux, N., Bradbeer, C., Reeger-Schneider, E., Koster, W., Mohanty, A. K., Wiener, M. C., and Kadner, R. J. (2002) Identification of the periplasmic cobalamin-binding protein BtuF of *Escherichia coli*, *J. Bacteriol.* **184**, 706-717.

88. Rees, D. C., Johnson, E., and Lewinson, O. (2009) ABC transporters: the power to change, *Nat. Rev. Mol. Cell. Biol.* **10**, 218-227.

89. Chimento, D. P., Mohanty, A. K., Kadner, R. J., and Wiener, M. C. (2003) Crystallization and initial X-ray diffraction of BtuB, the integral membrane cobalamin transporter of *Escherichia coli*, *Acta Crystallogr. D Biol. Crystallogr.* **59**, 509-511.

90. Noinaj, N., Guillier, M., Barnard, T. J., and Buchanan, S. K. (2010) TonB-dependent transporters: Regulation, structure, and function, *Annu. Rev. Microbiol.* **64**, 43-60.

91. Borths, E. L., Locher, K. P., Lee, A. T., and Rees, D. C. (2002) The structure of Escherichia coli BtuF and binding to its cognate ATP binding cassette transporter, *Proc. Natl. Acad. Sci. U S A* **99**, 16642-16647.

92. Lewinson, O., Lee, A. T., Locher, K. P., and Rees, D. C. (2010) A distinct mechanism for the ABC transporter BtuCD-BtuF revealed by the dynamics of complex formation, *Nat. Struct. Mol. Biol.* **17**, 332-338.

93. Köster, W. (2001) ABC transporter-mediated uptake of iron, siderophores, heme and vitamin B12, *Res. Microbiol.* **152**, 291-301.

94. Braun, V., and Hantke, K. (2007) *Acquisition of iron by bacteria*, Vol. 6, Springer, Molecular microbiology of heavy metals.

95. Degnan, P. H., Barry, N. A., Mok, K. C., Taga, M. E., and Goodman, A. L. (2014) Human gut microbes use multiple transporters to distinguish vitamin B12 analogs and compete in the gut, *Cell Host Microbe* **15**, 47-57.

96. Men, Y., Seth, E. C., Yi, S., Allen, R. H., Taga, M. E., and Alvarez-Cohen, L. (2014) Sustainable growth of *Dehalococcoides mccartyi* 195 by corrinoid salvaging and remodeling in defined lactate-fermenting consortia, *Appl. Environ. Microbiol.*, In press.

97. Allen, R. H., and Stabler, S. P. (2008) Identification and quantitation of cobalamin and cobalamin analogues in human feces, *Am. J. Clin. Nutr.* **87**, 1324-1335.

98. Girard, C. L., Santschi, D. E., Stabler, S. P., and Allen, R. H. (2009) Apparent ruminal synthesis and intestinal disappearance of vitamin B12 and its analogs in dairy cows, *J. Dairy Sci.* **92**, 4524-4529.

99. Men, Y., Seth, E. C., Yi, S., Crofts, T. S., Allen, R. H., Taga, M. E., and Alvarez-Cohen, L. (2014) Identification of specific corrinoids reveals corrinoid modification in dechlorinating microbial communities, *Environ. Microbiol.*, e12500.

100. Koutmos, M., Gherasim, C., Smith, J. L., and Banerjee, R. (2011) The structural basis of multifunctionality in a vitamin B12-processing enzyme, *J. Biol. Chem.* **286**, 29780-29787.

101. Lawrence, A. D., Taylor, S. L., Scott, A., Rowe, M. L., Johnson, C. M., Rigby, S. E., Geeves, M. A., Pickersgill, R. W., Howard, M. J., and Warren, M. J. (2014) FAD binding, cobinamide binding and active site communication in the corrin reductase CobR, *Biosci. Rep.* **34**, e00120.

102. Mera, P. E., and Escalante-Semerena, J. C. (2010) Dihydroflavin-driven adenosylation of 4-coordinate Co(II) corrinoids: are cobalamin reductases enzymes or electron transfer proteins? *J. Biol. Chem.* **285**, 2911-2917.

103. Zayas, C. L., Claas, K., and Escalante-Semerena, J. C. (2007) The CbiB protein of *Salmonella enterica* is an integral membrane protein involved in the last step of the de novo corrin ring biosynthetic pathway, *J. Bacteriol.* **189**, 7697-7708.

104. Thompson, T. B., Thomas, M. G., Escalante-Semerena, J. C., and Rayment, I. (1999) Three-dimensional structure of adenosylcobinamide kinase/adenosylcobinamide phosphate guanylyltransferase (CobU) complexed with GMP: evidence for a substrate-induced transferase active site, *Biochemistry* **38**, 12995-13005.

105. Thomas, M. G., Thompson, T. B., Rayment, I., and Escalante-Semerena, J. C. (2000) Analysis of the adenosylcobinamide kinase/adenosylcobinamide-phosphate guanylyltransferase (CobU) enzyme of Salmonella typhimurium LT2. Identification of residue His-46 as the site of guanylylation, *J. Biol. Chem.* **275**, 27576-27586.

106. Blanche, F., Debussche, L., Famechon, A., Thibaut, D., Cameron, B., and Crouzet, J. (1991) A bifunctional protein from *Pseudomonas denitrificans* carries cobinamide kinase and cobinamide phosphate guanylyltransferase activities, *J. Bacteriol.* **173**, 6052-6057.

107. O'Toole, G. A., Rondon, M. R., and Escalante-Semerena, J. C. (1993) Analysis of mutants of defective in the synthesis of the nucleotide loop of cobalamin, *J. Bacteriol.* **175**, 3317-3326.

108. Maggio-Hall, L. A., and Escalante-Semerena, J. C. (1999) In vitro synthesis of the nucleotide loop of cobalamin by *Salmonella typhimurium* enzymes, *Proc. Natl. Acad. Sci. U S A* **96**, 11798-11803.

109. Maggio-Hall, L. A., Claas, K. R., and Escalante-Semerena, J. C. (2004) The last step in coenzyme B(12) synthesis is localized to the cell membrane in bacteria and archaea, *Microbiology* **150**, 1385-1395.

110. Renz, P. (1999) Biosynthesis of the 5,6-dimethylbenzimidazole moiety of cobalamin and of other bases found in natural corrinoids, In *Chemistry and Biochemistry of B12.* (Banerjee, R., Ed.), pp 557-575, John Wiley & Sons, Inc., New York.

111. Trzebiatowski, J. R., and Escalante-Semerena, J. C. (1997) Purification and characterization of CobT, the nicotinate-mononucleotide:5,6-dimethylbenzimidazole phosphoribosyltransferase enzyme from *Salmonella typhimurium* LT2, *J. Biol. Chem.* **272**, 17662-17667.

112. Kräutler, B., Kohler, H. P., and Stupperich, E. (1988) 5'-Methylbenzimidazolyl-cobamides are the corrinoids from some sulfate-reducing and sulfur-metabolizing bacteria, *Eur. J. Biochem.* **176**, 461-469.

113. Aaron, M., Charbon, G., Lam, H., Schwarz, H., Vollmer, W., and Jacobs-Wagner, C. (2007) The tubulin homologue FtsZ contributes to cell elongation by guiding cell wall precursor synthesis in *Caulobacter crescentus*, *Mol. Microbiol.* **64**, 938-952.

114. Yi, S., Seth, E. C., Men, Y. J., Stabler, S. P., Allen, R. H., Alvarez-Cohen, L., and Taga, M. E. (2012) Versatility in corrinoid salvaging and remodeling pathways supports corrinoid-dependent metabolism in Dehalococcoides mccartyi, *Appl. Environ. Microbiol.* **78**, 7745-7752.

115. Keller, S., Ruetz, M., Kunze, C., Krautler, B., Diekert, G., and Schubert, T. (2013) Exogenous 5,6-dimethylbenzimidazole caused production of a non-functional tetrachloroethene reductive dehalogenase in *Sulfurospirillum multivorans*, *Environ. Microbiol.* **16**, 3361-3369.

116. Horig, J. A., and Renz, P. (1980) Biosynthesis of vitamin B12. Some properties of the 5,6-dimethylbenzimidazole-forming system of *Propionibacterium freudenreichii* and *Propionibacterium shermanii*, *Eur. J. Biochem.* **105**, 587-592.

117. Kolonko, B., Hörig, J. A., and Renz, P. (1992) Transformation of tritiated (5') riboflavin into 5,6-dimethylbenzimidazole., *Zeits. fuer Naturf. Sect. C. Biosc.* **47**, 171-176.

118. Gray, M. J., and Escalante-Semerena, J. C. (2007) Single-enzyme conversion of $FMNH_2$ to 5,6-dimethylbenzimidazole, the lower ligand of B_{12}, *Proc. Natl. Acad. Sci. U S A* **104**, 2921-2926.

119. Taga, M. E., Larsen, N. A., Howard-Jones, A. R., Walsh, C. T., and Walker, G. C. (2007) BluB cannibalizes flavin to form the lower ligand of vitamin B12, *Nature* **446**, 449-453.

120. Lamm, L., Heckmann, G., and Renz, P. (1982) Biosynthesis of vitamin B12 in anaerobic bacteria. Mode of incorporation of glycine into the 5,6-dimethylbenzimidazole moiety in *Eubacterium limosum*, *Eur. J. Biochem.* **122**, 569-571.

121. Scherer, P., Höllriegl, V., Krug, C., Bokel, M., and Renz, P. (1984) On the biosynthesis of 5-hydroxybenzimidazolylcobamide (vitamin B12-factor III) in *Methanosarcina barkeri*, *Arch. Microbiol.* **138**, 354-359.

122. Hollriegl, V., Lamm, L., Rowold, J., Horig, J., and Renz, P. (1982) Biosynthesis of vitamin B12. Different pathways in some aerobic and anaerobic microorganisms, *Arch. Microbiol.* **132**, 155-158.

123. Eisenreich, W., and Bacher, A. (1991) Biosynthesis of 5-hydroxybenzimidazolylcobamid (factor III) in Methanobacterium thermoautotrophicum., *J. Biol. Chem.* **266**, 23840-23849.

124. Endres, B. (1997) *Untersuchungen zur biosynthese des Basenteils von Vitamin B12 bei Eubacterium limosum und von 5-methylbenzimidazolylcobamid bei Desulfobulbus propionicus*.

125. Crofts, T. S., Men, Y., Alvarez-Cohen, L., and Taga, M. E. (2014) A bioassay for the detection of benzimidazoles reveals their presence in a range of environmental samples, *Front. Microbiol.* **5**, 592.

126. Stupperich, E., and Eisinger, H. J. (1989) Biosynthesis of *para*-cresolyl cobamide in *Sporomusa ovata*, *Arch. Microbiol.* **151**, 372-377.

127. Stupperich, E., and Eisinger, H. J. (1989) Function and the biosynthesis of unusual corrinoids by a novel activation mechanism of aromatic compounds in anaerobic bacteria., *Adv. Space Res.* **9**, 117-125.

128. Trzebiatowski, J. R., O'Toole, G. A., and Escalante-Semerena, J. C. (1994) The *cobT* gene of *Salmonella typhimurium* encodes the NaMN: 5,6-dimethylbenzimidazole phosphoribosyltransferase responsible for the synthesis of N^1-(5-phospho-alpha-D-ribosyl)-5,6-dimethylbenzimidazole, an intermediate in the synthesis of the nucleotide loop of cobalamin, *J. Bacteriol.* **176**, 3568-3575.

129. Maggio-Hall, L. A., and Escalante-Semerena, J. C. (2003) Alpha-5,6-Dimethylbenzimidazole adenine dinucleotide (alpha-DAD), a putative new intermediate of coenzyme B12 biosynthesis in *Salmonella typhimurium*, *Microbiology* **149**, 983-990.

130. Newmister, S. A., Chan, C. H., Escalante-Semerena, J. C., and Rayment, I. (2012) Structural insights into the function of the nicotinate mononucleotide:phenol/p-cresol phosphoribosyltransferase (ArsAB) enzyme from Sporomusa ovata, *Biochemistry* **51**, 8571-8582.

131. Mok, K. C., and Taga, M. E. (2013) Growth inhibition of *Sporomusa ovata* by incorporation of benzimidazole bases into cobamides, *J. Bacteriol.* **195**, 1902-1911.

132. Chan, C. H., Newmister, S. A., Talyor, K., Claas, K. R., Rayment, I., and Escalante-Semerena, J. C. (2014) Dissecting cobamide diversity through structural and functional analyses of the base-activating CobT enzyme of *Salmonella enterica*, *Biochim. Biophys. Acta* **1840**, 464-475.

133. Gray, M. J., and Escalante-Semerena, J. C. (2010) A new pathway for the synthesis of alpha-ribazole-phosphate in *Listeria innocua*, *Mol. Microbiol.* **77**, 1429-1438.

134. Choudhary, P. K., Duret, A., Rohrbach-Brandt, E., Holliger, C., Sigel, R. K., and Maillard, J. (2013) Diversity of cobalamin riboswitches in the corrinoid-producing organohalide respirer *Desulfitobacterium hafniense*, *J. Bacteriol.* **195**, 5186-5195.

135. O'Toole, G. A., and Escalante-Semerena, J. C. (1995) Purification and characterization of the bifunctional CobU enzyme of *Salmonella typhimurium* LT2. Evidence for a CobU-GMP intermediate, *J. Biol. Chem.* **270**, 23560-23569.

136. Thomas, M. G., and Escalante-Semerena, J. C. (2000) Identification of an alternative nucleoside triphosphate: 5'- deoxyadenosylcobinamide phosphate nucleotidyltransferase in *Methanobacterium thermoautotrophicum* ΔH, *J. Bacteriol.* **182**, 4227-4233.

137. Woodson, J. D., Zayas, C. L., and Escalante-Semerena, J. C. (2003) A new pathway for salvaging the coenzyme B_{12} precursor cobinamide in archaea requires cobinamide-phosphate synthase (CbiB) enzyme activity, *J. Bacteriol. 185*, 7193-7201.

138. Woodson, J. D., and Escalante-Semerena, J. C. (2004) CbiZ, an amidohydrolase enzyme required for salvaging the coenzyme B_{12} precursor cobinamide in archaea, *Proc. Natl. Acad. Sci. USA* **101**, 3591-3596.

139. Gray, M. J., Tavares, N. K., and Escalante-Semerena, J. C. (2008) The genome of *Rhodobacter sphaeroides* strain 2.4.1 encodes functional cobinamide salvaging systems of archaeal and bacterial origins, *Mol. Microbiol.* **70**, 824-836.

140. Gray, M. J., and Escalante-Semerena, J. C. (2009) The cobinamide amidohydrolase (cobyric acid-forming) CbiZ enzyme: a critical activity of the cobamide remodelling system of *Rhodobacter sphaeroides*, *Mol. Microbiol.* **74**, 1198-1210.

141. Gray, M. J., and Escalante-Semerena, J. C. (2009) In vivo analysis of cobinamide salvaging in *Rhodobacter sphaeroides* strain 2.4.1, *J. Bacteriol.* **191**, 3842-3851.

142. Richter-Dahlfors, A. A., and Andersson, D. I. (1992) Cobalamin (vitamin B12) repression of the Cob operon in *Salmonella typhimurium* requires sequences within the leader and the first translated open reading frame, *Mol. Microbiol.* **6,** 743-749.

143. Richter-Dahlfors, A. A., Ravnum, S., and Andersson, D. I. (1994) Vitamin B12 repression of the *cob* operon in *Salmonella typhimurium*: translational control of the *cbiA* gene, *Mol. Microbiol.* **13**, 541-553.

144. Ravnum, S., and Andersson, D. I. (1997) Vitamin B12 repression of the *btuB* gene in *Salmonella typhimurium* is mediated via a translational control which requires leader and coding sequences, *Mol. Microbiol.* **23**, 35-42.

145. Nahvi, A., Barrick, J. E., and Breaker, R. R. (2004) Coenzyme B12 riboswitches are widespread genetic control elements in prokaryotes, *Nucl. Acids Res.* **32**, 143-150.

146. Guerrero-Barajas, C., and Field, J. (2006) Enhanced anaerobic biotransformation of carbon tetrachloride with precursors of vitamin B12 biosynthesis, *Biodegradation* **17**, 317-329.

147. Zhang, Y., Rodionov, D. A., Gelfand, M. S., and Gladyshev, V. N. (2009) Comparative genomic analyses of nickel, cobalt and vitamin B12 utilization, *BMC Genomics 10*, 78.

148. Seth, E. C., and Taga, M. E. (2014) Nutrient cross-feeding in the microbial world, *Front. Microbiol.* **5,** 350.

149. Yan, J., Ritalahti, K. M., Wagner, D. D., and Loffler, F. E. (2012) Unexpected specificity of interspecies cobamide transfer from Geobacter spp. to organohalide-respiring *Dehalococcoides mccartyi* strains, *Appl. Environ. Microbiol.* **78**, 6630-6636.

150. Yan, J., Im, J., Yang, Y., and Loffler, F. E. (2013) Guided cobalamin biosynthesis supports Dehalococcoides mccartyi reductive dechlorination activity, *Philos. Trans. R. Soc. Lond. B Biol. Sci.* **368**, 20120320.

151. Wagner, D. D., Hug, L. A., Hatt, J. K., Spitzmiller, M. R., Padilla-Crespo, E., Ritalahti, K. M., Edwards, E. A., Konstantinidis, K. T., and Löffler, F. E. (2012) Genomic determinants of organohalide-respiration in *Geobacter lovleyi*, an unusual member of the Geobacteraceae, *BMC genomics* **13**, 200.

152. Sung, Y., Fletcher, K. E., Ritalahti, K. M., Apkarian, R. P., Ramos-Hernández, N., Sanford, R. A., Mesbah, N. M., and Löffler, F. E. (2006) Geobacter lovleyi sp. nov. strain SZ, a novel metal-reducing and tetrachloroethene-dechlorinating bacterium, *Appl. Environ. Microbiol.* **72**, 2775-2782.

153. Overbeek, R., Begley, T., Butler, R. M., Choudhuri, J. V., Chuang, H. Y., Cohoon, M., de Crecy-Lagard, V., Diaz, N., Disz, T., Edwards, R., Fonstein, M., Frank, E. D., Gerdes, S., Glass, E. M., Goesmann, A., Hanson, A., Iwata-Reuyl, D., Jensen, R., Jamshidi, N., Krause, L., Kubal, M., Larsen, N., Linke, B., McHardy, A. C., Meyer, F., Neuweger, H., Olsen, G., Olson, R., Osterman, A., Portnoy, V., Pusch, G. D., Rodionov, D. A., Ruckert, C., Steiner, J., Stevens, R., Thiele, I., Vassieva, O., Ye, Y., Zagnitko, O., and Vonstein, V. (2005) The subsystems approach to genome annotation and its use in the project to annotate 1000 genomes, *Nucleic Acids Res* **33**, 5691-5702.

154. Altschul, S. F., Gish, W., Miller, W., and Myers, E. W. (1990) Basic local alignment search tool., *J. Mol. Biol.* **215**, 403-410.